Stomoxys calcitrans influence the outcome of lumpy skin disease virus inoculation in bovine experimental models

A thesis submitted for the degree of

Doctor of Philosophy



Charlotte Cook

Worcester College

University of Oxford

Sir William Dunn School of Pathology

Michaelmas Term 2022

Abstract

The poxvirus lumpy skin disease virus (LSDV) is the etiological agent of lumpy skin disease (LSD), a severe, systemic transboundary disease of cattle and water buffalo. LSD is a rapidly emerging disease, spreading into and across the Middle East, eastern Europe, and Asia in the past decade, and which is now threatening bovine inventories in Australia. The disease presents as cutaneous lesions that can become necrotic, as well as pyrexia and reduction in milk and meat yields, causing substantial production and economic losses in rural communities.

LSDV is mechanically transmitted by haematophagous arthropods including stable flies (*Stomoxys calcitrans*). Cutaneous host responses to arthropod feeding activity have been shown to influence disease pathogenesis following inoculation with a range of biologically transmitted viruses including dengue and West Nile virus. This thesis examined whether this was also true for mechanically transmitted pathogens by studying the impact of secreted *S. calcitrans* saliva on LSDV in a bovine primary skin cell model and on an in vivo experimental bovine model of LSD.

A secreted saliva collection methodology using a modified artificial membrane feeding system was first optimised for use with laboratory reared *S. calcitrans*, before the virus was exposed to the saliva and titrated on MDBK cells. This showed no enhancement of LSDV replication. A more representative primary skin cell model was constructed by isolating primary fibroblasts from bovine ear pinnae. The replication of LSDV in this model was characterised, and when co-inoculated with secreted fly saliva, no impact on the replication kinetics was seen. However, in vitro models lack the systemic immune responses of an in vivo model, which could be influenced by the insect's saliva and thus affect pathogenesis. Therefore, three groups of ten cattle were inoculated intradermally

with 1×10^6 pfu of LSDV via multiple intradermal microdoses that aimed to mimic the biting action of flies in the field. Group 1 received virus alone, group 2 received virus mixed with *S. calcitrans* secreted saliva, and group 3 received virus inoculated immediately after *S. calcitrans* spot-feeding. Fewer animals in group 2 developed clinical disease compared to group 1, suggesting a suppressive effect of *S. calcitrans* saliva on disease development. In contrast, the animals in group 3 displayed disease with different kinetics and severity when compared to group 1. Cutaneous lesions appeared in significantly greater numbers in group 3 compared to group 1, accompanied by an earlier viraemia and accelerated antibody response.

The central question in this thesis asked if mechanical vectors of disease, such as *S. calcitrans* for the poxvirus LSDV, were able to alter the infectivity of viruses like biological vectors can. By using in vitro skin cell models and novel in vivo models, it was shown that *S. calcitrans* are more than a simple means for deposition of virus into the skin of a cow. Through co-incident bite trauma and/or saliva deposition, *S. calcitrans* are able to influence the resultant disease. This not only increases understanding of LSDV pathogenesis, but also highlights the overlooked importance of mechanical vectors in virus transmission.

Acknowledgements

I used to title this project in seminars as “Blood, Spit and Tears”- I think this is an accurate analysis of this DPhil! This thesis is the culmination of what feels like more than four years of work, and it would not have come to fruition without the support, care, and love of so many people.

I’d firstly like to thank my supervisor Dr Pip Beard for her enthusiasm, can-do attitude, and unwavering understanding. When I met you for the first time, I knew instantly that I wanted to do my PhD in your lab, and I have never been disappointed. It has been a total joy. I only hope I can take the non-academic skills and guidance you have given me and pass them onto any future people I ever lead.

I would also like to thank Dr Karin Darpel, for her wisdom, kindness, and pastoral care. I never felt like I had no one to go to for support, because I knew you were there.

To PoxWorld- the funniest, smartest group I could have wished to join, thank you. Your support, help with any question I had, large or small. Long and frustrating days in the lab would have been much more demoralising without your jokes, singing and humour. In particular, Petra, thank you for being an unofficial mentor and perpetual cheerleader.

I would like to thank my PhD Girl Gang: Lizzie, Abi, Gerry and Becky- your love, care and puns keep me going, and the experience wouldn’t have been the same without you. To my VLA crew- escaping into our fantasy world from the perils of academia most weeks kept me sane, and you are all incredible.

Mum, Dad, Harriet – you are my north stars when I am lost and low, and I am the person I am because of you. Thank you for asking questions, making me think about my work from a different perspective, and for your unconditional love. To Alex- thank you for being my rock and helping me to see the bigger picture. I love you in every universe.

And finally, a reminder to myself. You completed this journey despite mental health issues, a global pandemic, political turmoil, multiple family bereavements and severe illnesses, and an anxious brain constantly questioning if you were good enough.

You did this.

You can do anything.

This thesis is dedicated to Doreen Carter (1935-2022), who was the proudest Grandma.

Impact of COVID-19

I was in my second year of study when the COVID-19 pandemic reached the UK. On Monday 23rd March 2020, the Pirbright Institute site was closed to all but essential research in order to maintain the Institutes role as a government diagnostic capability. I worked from home until Thursday 21st May 2020 with no access to the laboratory, which delayed many of the experiments in Chapters 3 and 4. This caused us to pivot from the construction of a 3D bovine skin cell model to focus on the role of *S. calcitrans* saliva.

Additionally, the animal experiment that had been planned for summer 2020 was delayed, meaning that the two replicates of 15 cattle had to be run back-to-back in 2021. This did not allow for optimisation of sampling strategies and some of the animal tissue samples were not able to be analysed before the end of my DPhil.

Overall, I was lucky that my project was largely unaffected by laboratory shutdowns due to the pandemic, but it has taken a toll on my wellbeing.

Declaration

This statement is to certify that the content of this thesis is my own work unless otherwise stated. This thesis has not been submitted for any degree or other purposes at this or any other university. All assistance received in preparing this thesis and sources herein have been acknowledged.

Charlotte Cook

Worcester College

September 2022

Statement of Contributions

I gratefully acknowledge the following who contributed to the research presented in this thesis:

Chapter 3

Mass spectrometry data was generated by Dr Stuart Armstrong, University of Liverpool

Chapter 4

The Pirbright Bioimaging facility and support through the Core Capability Grant BBS/E/I/00007039

Chapter 5

The Pirbright Animal Services Unit for assistance with the animal experiments

Blood PCR data was generated by the Non-Vesicular Reference Laboratory, The Pirbright Institute

Skin PCR data was generated by Dr Henry Munyanduki

Chapter 6

The Pirbright Flow Cytometry facility and support through the Core Capability Grant BBS/E/I/00007039

FVNT data was generated by Dr Petra Fay

Dissemination

Publications

FAY, P. C., **COOK, C. G**., WIJESIRIWARDANA, N., TORE, G., COMTET, L., CARPENTIER, A., SHIH, B., FREIMANIS, G., HAGA, I. R. & BEARD, P. M. 2020. Madin-Darby bovine kidney (MDBK) cells are a suitable cell line for the propagation and study of the bovine poxvirus lumpy skin disease virus. *Journal of Virological Methods,* 285**,** 113943.

Conference Presentations

5-6 September 2019 **International Meeting on Arboviruses and Their Vectors (Poster)**

Lumpy skin disease virus does not replicate productively in insect cell lines

4-7 April 2022 **Microbiology Society Annual Conference (Presentation)**

Not just a 'dirty needle': the influence of *Stomoxys calcitrans* on lumpy skin disease

18-20 May 2022 **EPIZONE Annual Conference (Presentation)**

Stomoxys calcitrans feeding activity influences the kinetics of lumpy skin disease

List of Abbreviations

Ag-5	Antigen 5
APHA	Animal and Plant Health Agency
ATP	Adenosine triphosphate
BCA	bicinchoninic acid assay
BPF	Bovine primary fibroblasts
BPK	Bovine primary keratinocytes
BTV	Bluetongue virus
CAPV	Capripoxvirus
CEV	Cell associated enveloped virus
CMI	Cell mediated immunity
CPE	Cytopathic effect
Ct	Cycle threshold
CTL	Cytotoxic T lymphocytes
DEFRA	Department for Environment, Food and Rural Affairs
DENV	Dengue virus
DMEM	Dulbecco's Modified Eagle Medium
DNA	Deoxyribonucleic acid
dpi	Days post infection
ECTV	Ectromelia virus
EEV	Extracellular enveloped virus
ELISA	Enzyme-linked immunosorbent assay
FBS	Foetal bovine serum
FVNT	Fluorescent virus neutralisation test
GALT	Gut-associated lymphoid tissue
GTPV	Goatpox virus
ID	Intradermal
IEV	Intracellular enveloped virus
IFN	Interferon
IL	Interleukin
IMV	Intracellular mature virus
IRF	Interferon regulatory factors

IV	Intravenous
kDa	Kilodalton
LC	Liquid chromatography
LPS	Lipopolysaccharide
LSD	Lumpy skin disease
LSDV	Lumpy skin disease virus
MALT	Mucosa-associated lymphoid tissue
MDBK	Madin-Darby Bovine Kidney cells
MFS	Membrane feeding system
MOI	Multiplicity of infection
MS	Mass spectrometry
OIE	Office International des Epizooties
ORF	Open reading frame
PBMC	Peripheral blood mononuclear cells
PBS	Phosphate buffered saline
PCR	Polymerase chain reaction
PFU	Plaque forming units
PKR	Protein kinase R
ppm	Parts per million
SALT	Skin-associated lymphoid tissue
SDS-PAGE	Sodium dodecyl-sulphate polyacrylamide gel electrophoresis
SEM	Standard error of the mean
SFV	Semliki Forest virus
SGE	Salivary gland extract
SPPV	Sheeppox virus
TLR	Toll-like receptor
UV	Ultra-violet
VACV	Vaccinia virus
VARV	Variola virus
VNT	Virus neutralisation test
WNV	West Nile virus
WOAH	World Organisation for Animal Health

Table of Contents

Abstract ..... **ii**
Acknowledgements ..... **iv**
Impact of COVID-19 ..... **v**
Declaration ..... **vi**
Statement of Contributions ..... **vii**
Dissemination ..... **viii**
List of Abbreviations ..... **ix**
Introduction **14**
1.1 A Brief Introduction to Lumpy Skin Disease Virus 14
1.2 The History and Geographic Distribution of LSD 15
1.3 Clinical signs and pathology of Lumpy Skin Disease 17
1.4 Pathogenesis 17
1.5 Lumpy Skin Disease Virus: Molecular Details 18
1.5.1 Taxonomy of LSDV 18
1.5.2 Genome of LSDV 19
1.5.3 Morphology of LSDV 21
1.5.4 Replication cycle of poxviruses 22
1.6 The Immune Response 26
1.6.1 The host immune response to viruses 26
1.6.2 The immune response to LSDV 30
1.7 Transmission of Lumpy Skin Disease 31
1.7.1 The Sequence of Transmission 32
1.7.2 Alternative transmission routes 33
1.7.3 *Stomoxys calcitrans* 33
1.8 The Role of Arthropod Vectors 36
1.9 Current Methods of LSD Control 41
1.10 The Impacts of Lumpy Skin Disease 44
1.11 Aims and central hypothesis 45
Materials and Methods **47**
2.1 Cells 47
2.1.1 Continuous cell line culture and maintenance 47
2.1.2 Isolating bovine primary cells methodology 47
2.2 Viruses 49
2.2.1 Production of LSDV stocks 49
2.2.2 Sucrose purification of LSDV stocks 50

2.2.3 LSDV titration 50
2.2.4 LSDV growth curves in MDBK and primary cells 51
2.3 Western blotting of cell lysates 52
2.4 Immunofluorescent confocal imaging 54
2.5 *Stomoxys calcitrans* 55
2.5.1 *S. calcitrans* maintenance. 55
2.5.2 *S. calcitrans* saliva collection 55
2.5.3 *S. calcitrans* saliva concentration. 55
2.5.4 Sample analysis of *S. calcitrans* saliva via silver stain. 56
2.5.5 BCA assay for saliva protein quantification. 57
2.5.6 Coomassie gels for mass spectrometry 57
2.5.7 Proteomic analysis of *S. calcitrans* saliva 57
2.5.8 *S. calcitrans* in vitro impact assay 59
2.5.9 *S. calcitrans* saliva in LSDV growth kinetics 60
2.6 In vivo animal studies 61
2.6.1 CIVS 1 and 2 study design 61
2.6.2 Ethical approval, housing, and husbandry 63
2.6.3 Histopathology 64
2.6.4 PCR of blood 64
2.6.5 Quantification of LSDV in skin via qPCR 64
2.6.6 Flow cytometry 65
2.6.7 Serum ELISA 66
2.6.8 IFN-γ release assay 66
2.6.9 Fluorescent virus neutralisation test (FVNT) 67
2.7 Statistical analysis 68
Collection and characterisation of *Stomoxys calcitrans* secreted saliva 69
3.1 Introduction 69
3.2 Results 72
3.2.1 Optimising a membrane feeding system for the collection of *S. calcitrans* secreted saliva. 72
3.2.2 Quantification and visualisation of secreted *S. calcitrans* saliva 76
3.2.3 *S. calcitrans* saliva contains a variety of proteins, including those with immunoreactive properties 78
3.2.4 Assessing the impact of *S. calcitrans* secreted saliva on LSDV in an MDBK cell line .. 87
3.3 Discussion 88
3.4 Summary 94
Characterising LSDV replication in primary bovine fibroblasts and keratinocytes 95
4.1 Introduction 95

4.2 Results 97
4.2.1 Isolation of bovine primary skin cells 97
4.2.2 LSDV infection of bovine primary fibroblasts 99
4.2.3 The impact of *S. calcitrans* saliva on LSDV kinetics 109
4.2.4 LSDV infection of bovine primary keratinocytes 110
4.3 Discussion 113
4.4 Summary 117
The effect of *S. calcitrans* on the clinical outcome of LSDV infection 118
5.1 Introduction 118
5.2 Results 120
5.2.1 Successful establishment of a new in vivo LSDV infection model 120
5.2.2 The impact of inoculation model on clinical lumpy skin disease 130
5.2.3 LSDV replication and disease establishment in the three models 145
5.3 Discussion 151
5.4 Summary 157
Immune responses to *S. calcitrans* interactions with the host and LSDV infection 159
6.1 Introduction 159
6.2 Results 161
6.2.1 Blood cell population changes in response to LSDV inoculation 161
6.2.2 Inoculation route and clinical outcome are not correlated with a cell-mediated IFN-γ dependent immune response, as measured by a whole blood interferon-gamma assay 168
6.2.3 LSDV antibody production by LSDV challenged animals does not pass threshold levels 170
6.2.4 Fly-fed and inoculation animals produced antibodies much more rapidly 172
6.3 Discussion 174
6.4 Summary 178
Conclusions 179
Appendix 183
Bibliography 186

1

Introduction

1.1 A Brief Introduction to Lumpy Skin Disease Virus

Lumpy skin disease (LSD) is an emerging, high consequence, transboundary viral disease. The causative agent is lumpy skin disease virus (LSDV), a double-stranded DNA capripoxvirus (in the *Poxviridae* family) that exclusively infects cattle and water buffalo. The virus is thought to be transmitted predominantly by haematophagous arthropod vectors mechanically, and there is no known reservoir host. The disease is characterised by multifocal cutaneous nodules, fever, anorexia, and skin oedema, and can result in death of the infected animal. The disease is listed as a notifiable disease (OIE, 2021) by the World Organisation for Animal Health (WOAH, previously known as OIE) as well as the United Kingdom. As such any suspected cases of LSD must be reported immediately to the Animal and Plant Health Agency (APHA) to avoid further spread (DEFRA, 2014).

As a neglected pathogen, there is much left to understand about LSDV, particularly about its vector-borne transmission and early interactions with the host.

1.2 The History and Geographic Distribution of LSD

LSD is commonly accepted to have been first described as pseudo-urticaria of cattle in Zambia (then referred to as Northern Rhodesia) in 1929. After this, the disease spread across southern Africa gradually, being reported in Botswana in 1943 and then South Africa in 1944 (as Ngamiland cattle disease), where it was noted with great prescience that the economic loss this disease caused was significant and concerning (Von Backstrom, 1945). It then spread to the northeast into Kenya in 1957 (Davies, 1982). By the end of the 20th century, epizootics of LSDV had been reported across most of sub-Saharan Africa, and into Nigeria, Mali, Cameroon (OIE, 2017a), Sudan (Ali and Obeid, 1977) and Egypt (House et al., 1990). Its presence was established outside the continent for the first time in unconfirmed cases in Kuwait in 1986-1988 and in Israel in 1989 (Yeruham et al., 1995), possibly via the movement of infected *Stomoxys calcitrans* flies from Egypt. LSDV remained circulating in the Middle East until 2013-2016, when there was a huge surge of outbreaks resulting in the disease penetrating into Turkey (Sevik and Dogan, 2017), Greece (Tasioudi et al., 2016), the Balkans (Vidanovic et al., 2016), and Russia (Sprygin et al., 2018a) for the first time. It has been postulated that the sudden spread of disease into countries that had never reported LSDV before was catalysed by the Syrian civil war (Alkhamis and VanderWaal, 2016, Wainwright et al., 2013). This could have caused underreporting of disease and mass displacement of people and their animals into neighbouring nations, though these theories require further investigation. While outbreaks in these regions were swiftly controlled, in 2019 LSD was reported in Asia for the very first time. The expansion into the continent was swift, with waves of cases into Bangladesh (first reported in July 2019), China (August 2019), India (August 2019), Nepal (June 2020), Taiwan (July 2020), Sri Lanka (September 2020), Bhutan, (September 2020) Hong Kong (October 2020), Vietnam (October 2020),

Myanmar (November 2020), Thailand (March 2021), Malaysia (May 2021), Laos (May 2021), Cambodia (May 2021), Mongolia (August 2021), Pakistan (October 2021), Indonesia (February 2022) and Singapore (March 2022) (WAHIS, 2022).

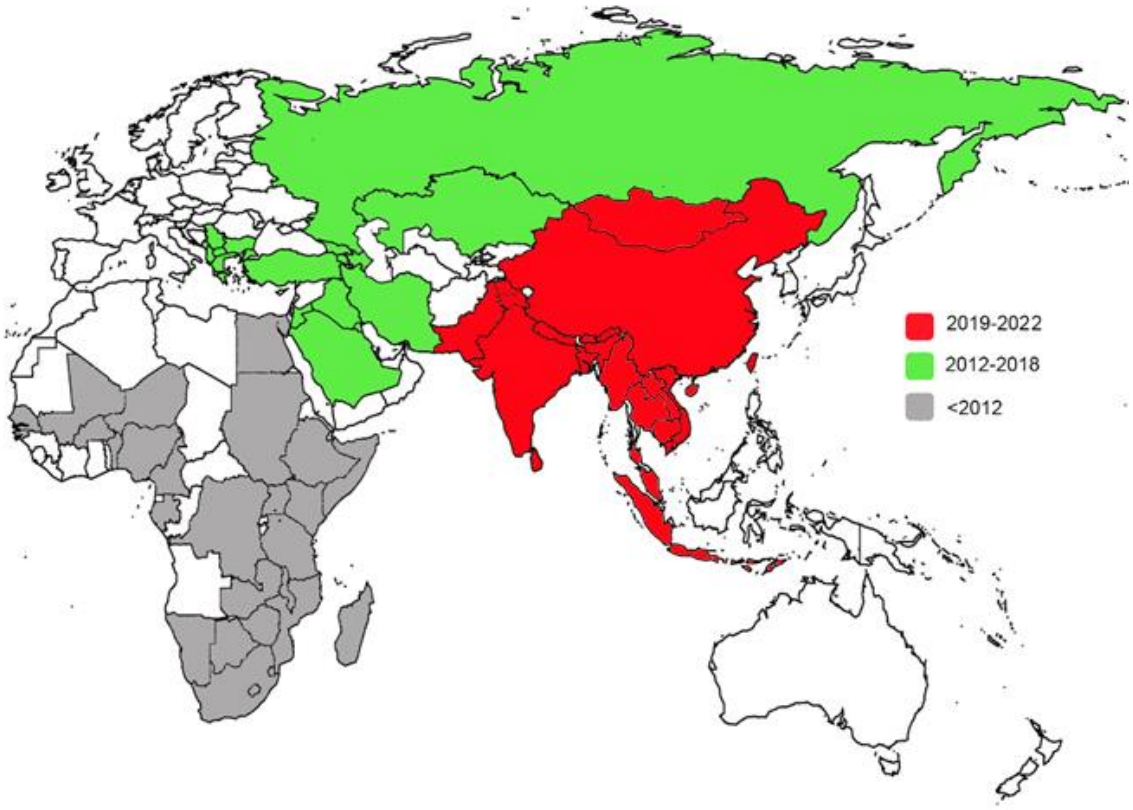


Figure 1.1: Geographic distribution and expansion of LSD

LSD was endemic to much of Africa before 2012 (shown in grey) before expanding into the Middle East and Europe (in green). Since 2019, the disease has spread rapidly into and across Asia (in red). Image created by Prof. Pip Beard.

The swift spread of the disease eastwards had provoked concern in Australasia about the potential for outbreaks in the Australian subcontinent, with the Inspector-General of Biosecurity of the Australian Government stating that an incursion of LSD into Australia would have "significant consequences for our beef, water buffalo, and dairy cattle industries." (Inspector General of Biosecurity, 2022)

1.3 Clinical signs and pathology of Lumpy Skin Disease

LSD has a relatively low morbidity and mortality, with recent outbreaks in Europe ranging from 8.7% to 12.3% morbidity, and 0.4% to 6.4% mortality (Beard, 2016). LSDV shows a strong tropism to the skin, with clinically affected animals developing multifocal raised cutaneous nodules between 0.5-5cm in diameter (Sanz-Bernardo et al., 2020). These skin lesions are the disease's characteristic clinical sign, and can become necrotic, predisposing cattle to secondary bacterial infections. Accompanying symptoms include: fever; lethargy; oral, nasal, and ocular discharge; anorexia; reduction in milk production and fertility, with a rise in abortions in pregnant stock (OIE, 2017a).

The histopathology is characterised by ballooning degeneration of the epidermis, spongiosis, and intracytoplasmic inclusion bodies within degenerate keratinocytes. The dermis is infiltrated by histiocytes. In necrotic lesions, the epidermis is replaced by wedge-shaped infarcts of necrotic tissue. The key feature of LSDV and capripoxviruses in comparison to other poxvirus genera, is the necrotising vasculitis of blood vessels in the dermis which leads to the infarct formation (Sanz-Bernardo et al., 2020). This histopathology is evident both in experimentally infected animals and in clinical animals in the field (Mathewos et al., 2022).

1.4 Pathogenesis

Pathogenesis is the process by which a disease develops. In LSD, the virus is initially inoculated into the skin by an arthropod vector. The subsequent interactions between the virus and the skin are unclear. In other poxviruses (for example ectromelia virus (ECTV)) within a few hours the virus spreads to the popliteal lymph node (Sigal, 2016) and then into

the bloodstream, causing a primary viraemia (Fenner et al., 1987). From the blood, the virus is deposited back in the skin, via a “homing” mechanism which is still unclear. Once in the skin the virus causes inflammation of the epidermis and dermis, including inflammation and necrosis of blood vessels which leads to infarction (Sanz-Bernardo et al., 2020). The lesions that form contain a very high amount of virus which facilitates onward transmission.

In in vivo experimental models, challenged animals may develop clinical disease, characterised by the development of skin nodules and the pathologies described in section 1.3, but approximately 50% of challenged animals will not develop skin nodules. These two outcomes are referred to as clinical and nonclinical respectively and, to date, the factors determining whether an animal has a clinical or nonclinical outcome following challenge are unknown. The role of the nonclinical animals is particularly intriguing but poorly understood. Viral DNA can be detected in the blood and skin of some of these nonclinical animals intermittently and at low levels during the post-challenge period, leading some researchers to refer to them as subclinical. Nonclinical/subclinical disease in the field has not been well studied, therefore the role these animals play in the epidemiology of LSD is unknown.

1.5 Lumpy Skin Disease Virus: Molecular Details

1.5.1 Taxonomy of LSDV

Lumpy skin disease virus is a member of the Poxviridae family, in the Capripoxvirus genus. There are only three members of the genus - lumpy skin disease virus (LSDV), sheeppox

virus (SPPV) and goatpox virus (GTPV). The genomes of the three viruses are highly conserved, sharing 97% nucleotide identity (Tulman et al., 2002).

Capripoxviruses have very narrow host ranges. Lumpy skin disease virus infects cattle and water buffalo only, while SPPV and GTPV respectively infect sheep and goats only. Some reports have suggested LSDV can infect other ruminants including eland (*Taurotragus oryx*) (Molini et al., 2021), giraffe (*Giraffa camelopardalis*) (Dao et al.) and impala (*Aepyceros melampus*)(Barnard, 1997). These findings have been determined by variable antibody responses, sporadic swab PCR tests, or cases in single (likely inbred) zoo animals, making evidence for widespread LSDV infection in wildlife unconvincing.

1.5.2 Genome of LSDV

LSDV has a double-stranded DNA genome, with 150,773 base pairs (Tulman et al., 2001) and hairpin ends. Like other poxviruses, it has a central coding region sandwiched between two inverted terminal repeat regions, which each have at least 2,418 base pairs. LSDV encodes 156 putative genes, a large proportion of which are conserved in other poxviruses and code for replication machinery (the core genome) or are homologues of genes used for replication in other Chordopoxviruses. Other conserved genes encode proteins for protein processing, virion structure and assembly, and viral virulence and host range. LSDV strains contain five genes that are disrupted by mutations in the other capripoxviruses GTPV and SPPV, typical of the widely accepted consensus that poxviruses evolve via gene loss (Biswas et al., 2020). The core genome is very similar to that of the sub-family, with high amino acid identity and collinearity (Gershon et al., 1989a). The terminal regions are less similar to other poxvirus homologues at the amino acid level, which is unsurprising since this region contains genes coding for proteins involved in virulence, immune evasion and host range. LSDV encodes one protein that lacks homology to other known poxviral

proteins, LSDV132 (LSDV022 now has a homologue in deerpox virus) (Tulman et al., 2001, Afonso et al., 2005).

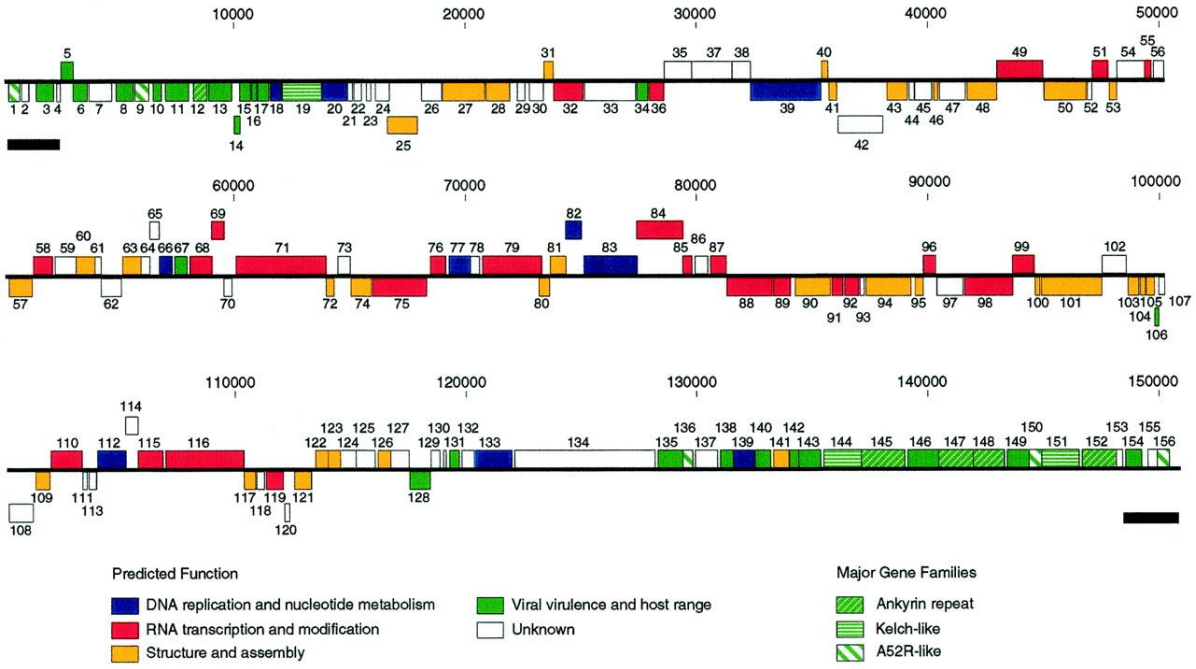


Figure 1.2: Annotated linear map of the LSDV genome

Open reading frames (ORFs) are numbered from left to right based on the position of the methionine initiation codon, with the number of base pairs displayed above the map. Above the line are ORFs transcribed to the right of the initiation codon and ORFs transcribed to the left are below. Genes with similar functions and members of gene families are coloured according to the figure key. Inverted terminal repeats are shown as black bars below the map. Image sourced from Tulman et al., 2001.

Poxviruses are able to recombine, though until the 1980s there was no published evidence of poxvirus recombinants arising through natural transmission (Gershon et al., 1989b). From 2017 recombinant strains of LSDV were isolated from field cases of LSD in Kazakhstan, Russia (Sprygin et al., 2018b), Hong Kong (Flannery et al.), and northern China (Lu et al., 2021). Further investigation has found that these recombinants likely arose during seed production of a particular vaccine that contained a mixture of capripoxviruses (Vandenbussche et al., 2022).

1.5.3 Morphology of LSDV

Capripoxvirus virions have a classic and distinct brick-like shape, with a length of 293–299nm and a width of 262–273nm (OIE, 2017a). When studied using electron microscopy (Figure 1.3), the LSDV virions have a similar structure to that of other poxviruses (Figure 1.4), with a biconcave core positioned between two lateral bodies, within an outer lipoprotein bilayer membrane envelope. LSDV virions likely go through morphogenesis in a process similar to orthopoxviruses, beginning as immature virions (IVs) that become intracellular mature virus (IMV) in the viral factory in the cell cytoplasm. The IMVs then gain a double membrane in the Golgi apparatus or via early endosomes to become intracellular enveloped virus (IEV). IEVs that reach the cell surface and are displayed there are referred to as cell-associated enveloped virus (CEV). Extracellular enveloped virus (EEV) are IEVs that have been released from the cell. EEVs and CEVs are therefore identical, but have one more membrane than IMVs (Smith et al., 2002). The changing morphology that the virions pass through enable the virus to utilise different avenues of dissemination, and are forms of disguise to avoid the host immune response (Bidgood and Mercer, 2015).

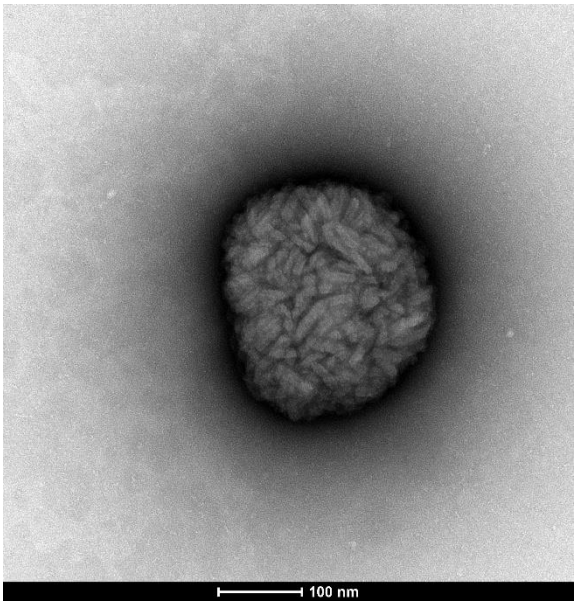


Figure 1.3: Representative image of the outer structure of a LSDV virion

Image taken using electron microscopy, by Dr P. Fay and Prof. P Hawes, The Pirbright Institute

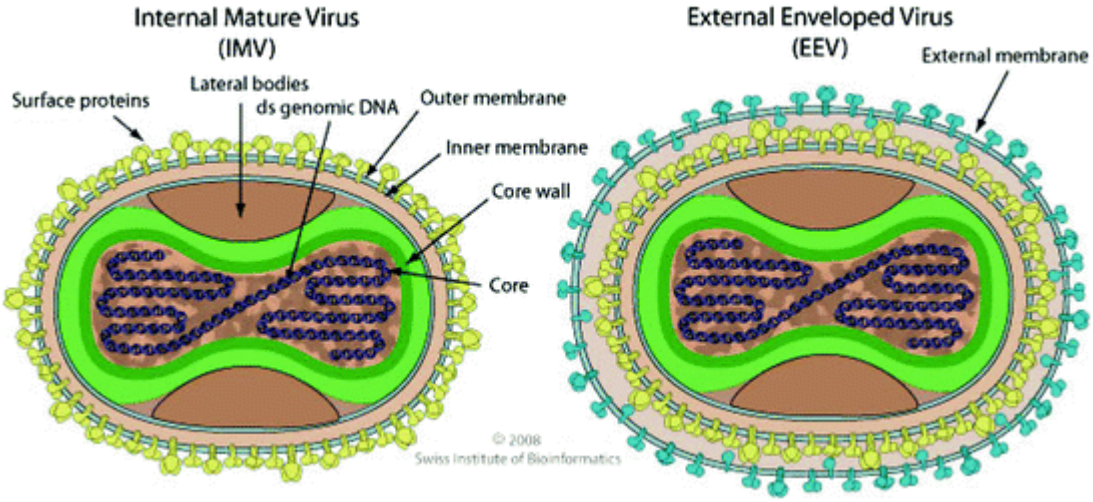


Figure 1.4: Schematic of poxvirus structure

Image sourced from the Swiss Institute of Bioinformatics, 2008.

1.5.4 Replication cycle of poxviruses

Most double-stranded DNA viruses replicate in the nucleus of host cells, generally by hijacking the host's replication machinery. In contrast, LSDV and other poxviruses replicate entirely in the cytoplasm of cells. The following descriptions of poxviral entry, replication and exit are based on observations of the prototype poxvirus, Vaccinia virus. As a neglected virus, the replication cycle of LSDV has not been fully investigated and described. However, the LSDV genome shares most genes for replication with other poxviruses, so it is likely that it follows the traditional poxvirus replication cycle.

1.5.4.1 Entry

The IMV virion can pass the nucleoprotein core into the cytoplasm either at a neutral pH via fusion at the plasma membrane or via an endocytic pathway at low pH after micropinocytosis (Schmidt et al., 2011), which appears to be the primary method for most orthopoxviruses (Roberts and Smith, 2008) (Figure 1.5). Poxviruses have a set of four proteins for attachment to the host cell, and a conserved set of eleven proteins that form the Entry Fusion Complex (Moss, 2012). This complex is embedded in the membrane of the

mature virion, and all eleven proteins are then required for core entry (Moss, 2016). As described above, EEVs have two lipid envelopes surrounding the virus core and not just one like IMVs. Therefore, a single fusion event will not result in the core of an EEV entering the cytoplasm. This problem has been overcome by the virus by the outer viral membrane of EEVs being disrupted by a ligand-induced nonfusogenic reaction, which then enables the inner viral membrane to fuse with the plasma membrane and release the virus core into the cytoplasm (Law et al., 2006). Extracellular virions (CEV's and EEV's) have been observed to fuse faster and more efficiently with the plasma membrane (Doms et al., 1990).

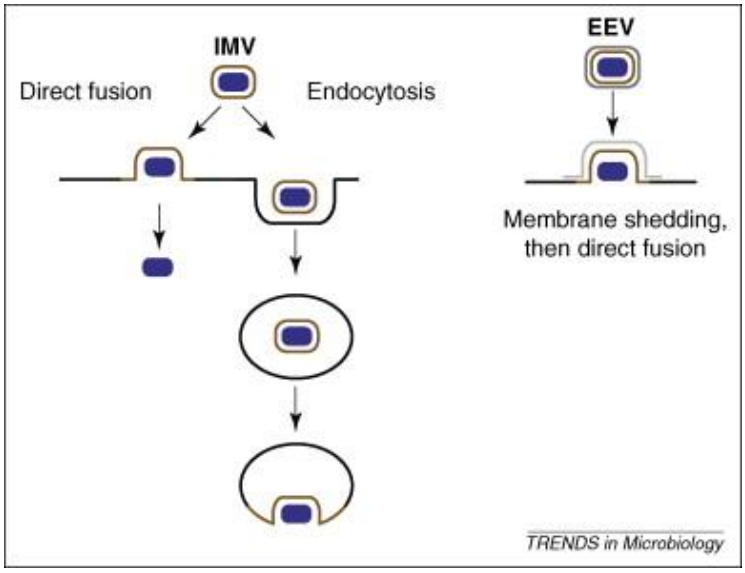


Figure 1.5: IMV and EEV entry

This diagram shows the possible entry mechanisms for IMV and EEV virions. IMVs enter either via direct fusion or endocytosis after micropinocytosis. EEVs enter via direct fusion after the outer membrane has been disrupted. Image sourced from Roberts and Smith, 2008.

1.5.4.2 Gene expression and replication

Once within the cell, poxviruses begin replication in the cytoplasm in viral factories, a result of the endoplasmic reticulum of the host cell being remodelled by the virus (Tolonen et al., 2001). Poxviruses are able to replicate in the cytoplasm due to their large genome encoding all the machinery required for self-sufficient transcription and DNA replication. By pre-preparing early expression factors late in infection, poxviruses are able to rapidly uncoat

as soon as they enter the host cell and begin replication (Walsh, 2017). However, they do still require host ribosomes to translate the mRNA produced. To deceive the host ribosomes, poxvirus kinases are able to phosphorylate ribosome residues, selecting for translation of viral mRNAs and conferring an advantage to the virus (Jha et al., 2017). Additionally, poxviruses have engaged in an arms race with the cell's antiviral response, developing "gene accordions" via specific gene amplifications to swiftly adapt to protein kinase R (which is a host enzyme that prevents viral protein synthesis by phosphorylating viral translation initiation factors) (Elde et al., 2012). They are also able to decap host mRNA to suppress host translation and promote viral translation, by encoding their own decapping enzymes (Cantu et al., 2020). Poxviruses then exhibit ATP-dependent Type III packaging of the replicated genome into the waiting new capsid, concluding the assembly of a new virion (Chelikani et al., 2014).

1.5.4.3 Exit and dissemination

Once the virion is mature, there are several pathways via which exit can occur (Smith and Law, 2004). The simplest is the non-specific release of virus via lysis of the host cell after cell death, which is how IMVs (which make up the majority of the viral progeny) exit the cell. Prior to cell lysis, some IMV virions are transported via microtubules to the viral wrapping centre near the microtubule organising centre where they are enveloped in a double membrane (derived from the Golgi network or from endosomes) and become IEVs. Some of these IEVs are then moved to the surface of the cell via microtubules again, where through the outer membrane fusing with the cell surface membrane, the virion is able to be displayed on the cell surface as a CEV or released as an EEV. Release vs retention seems to depend on the host cell type and on viral strain. EEVs are key to long range dissemination

of virus, whereas CEV are more important in cell to cell transmission and provoke the formation of actin tails to springboard the virion further.

Actin tails have been observed in cells infected with orthopoxviruses such as vaccinia virus (VACV), monkeypox virus and variola virus (the etiological agent of smallpox). The process of actin tail formation has been most clearly studied in VACV. Actin is induced into polymerising into filaments underneath a CEV at the surface of the infected cell (Cudmore et al., 1995) by the viral A36 protein. The A36 protein (shown in dark blue in Figure 1.6) is found in the outer membrane of the IEV. When the outer membrane of the IEV fuses with the plasma membrane during virion exit, A36 is deposited in the plasma membrane (van Eijl et al., 2000, Bidgood and Mercer, 2015). A36 then potentiates the polymerisation of cellular actin into protrusions via phosphorylation of A36 by Src and Abl family kinases (Newsome et al., 2006), followed by recruitment of adaptors Nck and Grb2 (Scaplehorn et al., 2002), and finally N-WASP (Frischknecht et al., 1999), via WIP, to activate the Arp2/3 actin polymerisation complex (Donnelly et al., 2013).

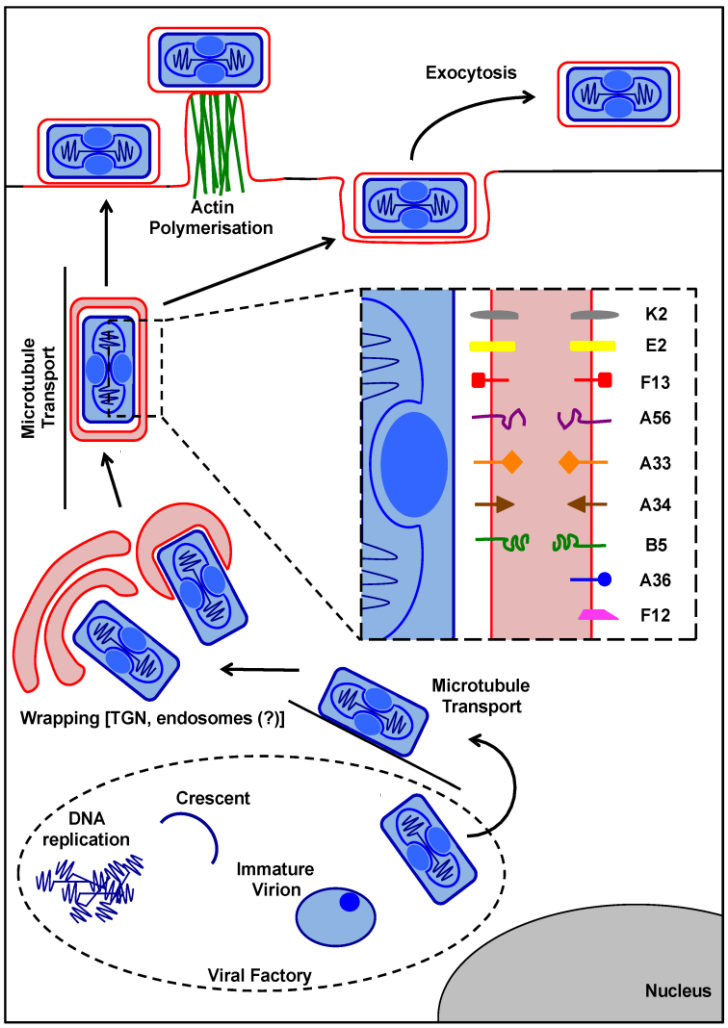


Figure 1.6 Exit routes of LSDV virion types

Diagram to show the different ways LSDV can exit the host cell. IMVs are transported by microtubules from the viral factory from where they either leave via host cell lysis or via a posited budding mechanism. IMVs can also be wrapped in more membranes sourced from the trans-Golgi network (TGN) or possibly early endosomes, becoming IEVs. These are then moved via microtubules to the cell surface membrane where they become CEVs and eventually EEVs or stimulate actin tail formation to be propelled away to neighbouring cells. Image sourced from Bidgood and Mercer, 2015.

1.6 The Immune Response

1.6.1 The host immune response to viruses

The first response to a virus entering the host is their recognition commonly by the host's pattern-recognition receptors (PRRs), which then trigger the activation of the innate immune response, and from that, the adaptive immune response. The innate immune system's purpose is to prevent or reduce initial infection, to shield cells from infection, and to clear any cells that have already become infected. It begins with the initial physical barrier of the epithelial surfaces, including the outer barrier of the skin, which prevents the entry of most pathogens. Once within the barrier, the innate immune response includes the complement system, defensins and their chemotactic properties, and cytokines. Its key

cellular protagonists are neutrophils, monocytes, macrophages, eosinophils, and mast cells.

In the skin, cells form a complex and unique immune system, where all cell types participate in the immune response. Some people have even suggested this system be formally known as the skin-associated lymphoid tissue (SALT), similar to the recognised mucosa-associated lymphoid tissue (MALT) and gut-associated lymphoid tissue (GALT). However, it has also been shown that the lymphoid properties of SALT are likely to be transient and inducible (Kogame et al., 2021), and the concept remains controversial. Dendritic cells, mast cells, T and B cells and keratinocytes work together across the epidermis and dermis to detect pathogens and initiate innate immune responses (Nestle et al., 2009). Keratinocytes display toll-like receptors (TLRs) including TLR1, TLR2, TLR4, TLR5, and TLR6 on their cell surface. Activation of these PRRs is often a key starting point for the dermal immune response, resulting in the activation of the type 1 interferon pathway (Lai and Gallo, 2008), triggering cytokine maturation and activating a variety of transcription factors including NF-κB and interferon regulatory factors (IRFs) (Newton and Dixit, 2012). Keratinocytes can also participate in the innate immune response by producing cytokines such as IL-1, IL-6, IL-10, IL-17, IL-18, IL-22, and tumour necrosis factor alpha (TNF-α) (Quaresma, 2019). Keratinocytes can be stimulated to produce antimicrobial peptides (AMPs) when activated by IL-17 and IL-22. Cytokines are then able to go on and activate immune cells, like the pleotropic cytokine IL-1. This molecule can then induce a wide variety of biological effects, including T helper cell and dendritic cell activation and B cell maturation and clonal expansion (Arend et al., 2008).

Fibroblasts make up a large part of the dermis, and also contribute to the immune response. They have been shown to express ten different TLRs (Yao et al., 2015) and can

produce defensins which are able to enhance phagocytosis (Tecle et al., 2007) and regulate interleukin secretion (Shi et al., 2007). Additionally, as sentinels, they also release proinflammatory cytokines that alert and prime the rest of the immune system (Van Linthout et al., 2014).

Dendritic cells are professional antigen-presenting cells found predominantly in the dermis, able to capture pathogens and infected cells, present the antigens, and migrate to the lymph nodes to activate T lymphocytes (Klechevsky, 2015). Langerhans cells are another form of tissue-specific macrophage (resident in the epidermis) and were once thought to be the prototype for dendritic cells (Malissen et al., 2014). However, Langerhans cells are much longer lived and are locally self-maintained whereas dendritic cells need to be continuously replenished and are derived from the bone marrow rather than an embryonic origin (Doebel et al., 2017, Clayton et al., 2017). Other key immune cells in the skin include neutrophils, which are often the first circulating cells to respond to tissue wounding and acute inflammation (Fine et al., 2020), eosinophils which infiltrate the skin in response to infection and release toxic granule proteins (Radonjic-Hoesli et al., 2021), and mast cells whose degranulation has been shown to protect mice from VACV (Wang et al., 2012).

The next level of host defence after the innate immune response is the adaptive immune system. The adaptive immune response can be further subdivided into humoral and cell mediated. Humoral immunity focuses on memory and effector B cells that produce antigen specific antibodies that bind to the surface of a pathogen or an infected cell. These are then able to bind to antigens, to neutralise virus, aid opsonisation and phagocytosis, or activate of the complement cascade. Cell mediated immunity to viruses is generally driven by T cells, macrophages, and cytokine release. Once activated, T cells can secrete interferon

gamma (IFN-γ), a pleiotropic cytokine that can regulate genes to control apoptosis, production of inflammatory signalling molecules, and much more. T cells, once activated, proliferate, and differentiate into effector cells. Differentiation of these T cells is guided by antigen-presenting cells, cytokines, and costimulatory molecules (Mescher et al., 2006). These differentiated effector cells then spread throughout the whole body in the blood and lymph, but do not stay activated for long (Mueller and Rouse, 2008). Some become memory cells, which provide protection in the event that the virus enters the host again and is recognised. Some become cytotoxic T lymphocytes (CTLs). The primary function of CTLs is to recognise virus infected cells, and to induce apoptosis via perforins and cytotoxic granules. CD4 T cells also participate in defence against virus, as "helpers" to the CD8 T cell response and as a form of viral memory. CD4 cells are not as cytotoxic as CD8 cells, but do produce cytokines after encountering antibody, further accentuating the immune response. Effector memory T cells also have tissue homing capabilities, enabling them to wait in tissues like the skin, where they can respond more quickly (Tufail et al., 2013).

The bovine immune response is not as well studied as the human immune response. Though similar to that of other mammals, there are some unique differences. For example, γδ T cells make up an unusually high proportion of the lymphocyte populations of young calves and are thus a crucial regulatory T cell subset (Guzman et al., 2014). Additionally, cattle are known to have limited Ig gene segment diversity and achieve variability through recombination. In terms of the immune response in the skin, cathelicidins are secreted by skin cells in response to pathogen exposure, and act to recruit neutrophils. Humans and mice both express one cathelicidin. In contrast, cattle express at least 7 cathelicidin genes (Young-Speirs et al., 2018).

1.6.2 The immune response to LSDV

The immune response to LSDV has not been fully explored, with many areas still poorly characterised. For example, very little is known about the innate immune response to capripoxviruses, with one study showing that infection of peripheral blood mononuclear cells of sheep with SPPV resulted in the upregulation of RIG-1 PRRs (Chibssa et al., 2021). Histopathology of LSDV infected bovine skin nodules shows that the dermis becomes infiltrated by neutrophils and histiocytic cells, which are known to be important effectors of the inflammatory response and in the activation of the adaptive immune response (Mantovani et al., 2011).

Poxviruses evade antiviral responses via a number of different strategies, including encoding antagonists that inhibit the PKR signalling pathway (Romano et al., 1998), interfering with the DNA-PK dimer to reduce the numbers of cytokines and chemokines produced (Peters et al., 2013), and producing enzymes that prevent dsRNA from accumulating and activating innate immune responses (Liu et al., 2015). Poxviruses are known to produce proteins that can bind to IFN- γ, suppressing the immune response and resulting in greater pathogenesis in vivo (Alcami and Smith, 1996).

Knowledge of the adaptive immune response to LSDV is also limited. Vaccination studies have demonstrated that cattle produce a humoral and cell-mediated immune response to challenge with live attenuated LSDV vaccine strains (Muller et al., 2019, Milovanovic et al., 2019). In terms of a humoral response, neutralising and binding antibodies were produced in varying titres in response to vaccination (Samojlovic et al., 2019, Kitching et al., 1987). Neutralising antibodies against sheeppox were also shown to be detected over 200 days post inoculation in vaccinated sheep and goats (Fay et al., 2022a). A recent study of LSD showed that clinical cattle developed an antibody response more rapidly (Fay et al., 2022b)

and more strongly (Sanz-Bernardo et al., 2021) than non-clinical animals, who also developed a partially neutralising antibody response.

Even less is known about the cell-mediated immune response to LSDV. The CMI response is coordinated and communicated by cytokines, including interleukins and interferons (IFN), in particular the key indicator IFN-γ. Past studies have quantified the amount of IFN-γ produced by vaccinated and/or challenged cattle (Haegeman et al., 2021, Kara et al., 2018), showing a high responsiveness to vaccine challenge and LSDV knockout viruses. More recently, work has shown that cattle challenged with LSDV via virus-positive arthropods developed different CMI immune signatures and kinetics of immune responses than those challenged via needle-inoculation (Fay et al., 2022b). This highlights the lack of knowledge around the influence of arthropod inoculation on LSDV pathogenesis, the most relevant route of LSDV transmission.

1.7 Transmission of Lumpy Skin Disease

LSDV is the only poxvirus known to be entirely transmitted by arthropods, with little if any role played by direct transmission. This emphasises the importance of mechanical vector-borne transmission for LSDV. A number of other poxviruses are also vector borne: myxoma virus can be transmitted by fleas and mosquitoes between rabbits (Brugman et al., 2015, Mead-Briggs and Vaughan, 1975), and mosquitoes transmit fowlpox amongst poultry (Yeo et al., 2019). *S. calcitrans* flies transmit other capripoxviruses, goatpox and sheeppox (Kitching and Mellor, 1986, Mellor et al., 1987).

LSDV has been successfully transmitted from a clinical to naïve animal under experimental conditions by *Aedes aegypti* mosquitoes (Chihota et al., 2001), *Amblyomma hebraeum* and

Rhipicephalus appendiculatus ticks (Lubinga et al., 2015, Tuppurainen et al., 2013), and *S. calcitrans* flies (Sohier et al., 2019).

1.7.1 The Sequence of Transmission

1.7.1.1 LSDV Acquisition

Studies on the acquisition of LSDV by hematophagous arthropods showed that *S. calcitrans*, *A. aegypti*, *Culex quinquefasciatus* and *Culicoides nubeculosus* acquire the virus at the same rate (Sanz-Bernardo et al., 2021).

More detailed experiments have found that "sub-clinical" animals (animals that have been challenged with LSDV, and have LSDV detected in samples but do not present with cutaneous lesions) are much less important than clinical animals in arthropod transmission- insects are 97% less likely to acquire LSDV from a subclinical animal than from skin nodules on a clinical one (Sanz-Bernardo et al., 2021).

Vectors also were more likely to acquire LSDV from a lesion than from infected blood or non-nodular skin, showing the importance of the cutaneous lesions to promoting virus transmission (Sanz-Bernardo et al., 2022). It's possible that the development of necrotic lesions as part of the disease pathogenesis is a transmission strategy by LSDV, since stable flies locate feeding sites via chemosensory inputs and host volatiles (Jeanbourquin and Guerin, 2007), and wounded necrosing tissue is known to express many volatiles (Thomas et al., 2010).

1.7.1.2 LSDV Retention

After feeding on nodules of a clinical animal, *A. aegypti* and *S. calcitrans* retained LSDV for up to 8 days, with data suggesting that virus remained on the mouthparts for longer than

on the body (Sanz-Bernardo et al., 2022). Evidence supports the theory that LSDV is transmitted mechanically, similarly to myxoma virus, with no evidence for viral replication within the insect (Sanz-Bernardo et al., 2021, Chihota et al., 2001, Sohier et al., 2019).

1.7.1.3 LSDV Deposition

The most poorly understood part of the LSDV transmission cycle is deposition. Very little work has been conducted on the deposition of LSDV from virus positive arthropods.

1.7.2 Alternative transmission routes

With the recent swift spread of LSDV across Asia, it has been posited that LSDV could be being transmitted via alternative routes. Direct transmission has been investigated under experimental conditions. Naïve cattle living in close contact with infected animals for over a month did not develop disease (Carn and Kitching, 1995a). In addition, epidemiological modelling of an infected large dairy herd showed that the infection dynamics could not be explained by a direct contact route within a large herd (Magori-Cohen et al., 2012). Recent work on the recombinant LSDV strain from Russia has suggested that it may be more effective at direct transmission, with five of ten naïve cows tethered next to infected animals developing clinical disease (Aleksandr et al., 2020). This is a very unusual finding and has not been replicated by other researchers.

1.7.3 *Stomoxys calcitrans*

S. calcitrans, also known as stable flies, are telmophagous filth flies that are a common arthropod pest. The male and female flies are both obligate blood feeders, and a serious pest of agricultural animals, particularly cattle. They are pool feeders, with coarse labellar teeth (Figure 1.7) (Zumpt, 1973) that create a haematoma in the skin that they feed from (Lavoipierre, 1965).

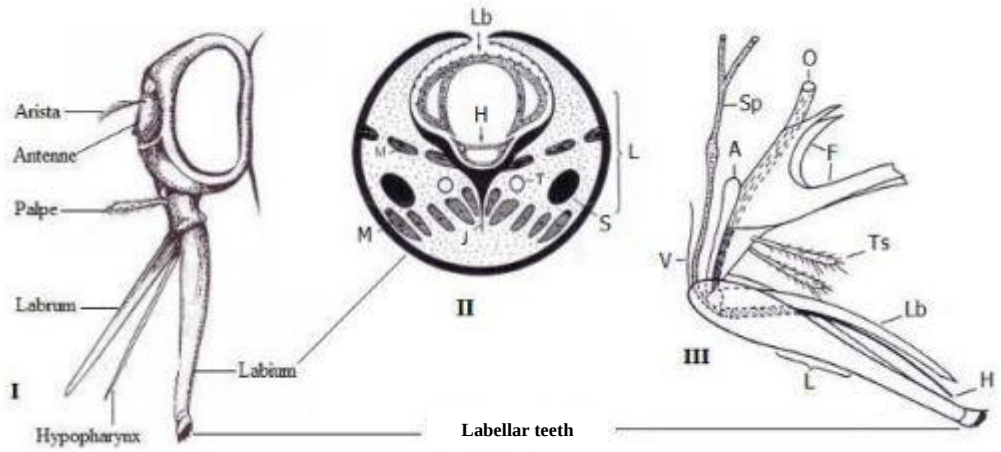


Figure 1.7 Diagram of *Stomoxys calcitrans* stable fly mouthparts

The diagram shows the (I) head in profile, (II) proboscis in cross section, and (III) mouthparts in lateral view. It also shows in more detail the: (L) labium, (H) hypopharynx, (Lb) labrum, (Ts) palps, (V) membrane between proboscis and head capsule, (A) apodema, (F) fulcrum, (Sp) salivary gland, (O) oesophagus, (T) trachea, (J) endoskeleton, (S) labellum tendon, (M) muscles. Image sourced from Zumpt, 1973.

Flies tend to bite on the legs and below the hocks of animals (likely due to the shorter hair and absence of swishing tail), but can move to the sides and back if populations are large and feeding sites are crowded (Foil and Hogsette, 1994). Stable flies are some of the most widely distributed of the nuisance flies, and are found across the world (Foil and Hogsette, 1994). Stable fly abundance and activity seems to be linked to spring rainfall (Mullens and Peterson, 2005), with studies in California (Mullens and Meyer, 1987), Alberta (Lysyk, 1993), and south-west England (Parravani et al., 2019) suggesting that flies are active from spring to mid-autumn, with populations peaking in summer. Flies tend to live for a week or two in the field, but up to 35 days in laboratory conditions. Though *S. calcitrans* tend to remain in areas with a high concentration of cattle to feed on, research has shown that they have the capacity for long range flight, with marked flies flying 225 km from marking sites (Hogsette and Ruff, 1985).

S. calcitrans tend to feed quickly, engorging after 3-4 minutes of feeding, though feeds are often interrupted by flies changing position (Showler and Osbrink, 2015). Adult male flies

require blood meals to reach sexual maturity, and adult female flies need blood to produce eggs, which they lay in oviposition medium (which must contain decaying vegetation matter, including cattle dung), producing 60-130 eggs per laying cycle (Foil and Hogsette, 1994). Eggs hatch after 2-5 days at 26°C into emergent larvae, which move down in the substrate to prevent desiccation. After 14-26 days at 26°C, the third instar larvae then enter pupation. Young flies hatch from the pupae most commonly between 9-13 days (James and Harwood, 1970) (Figure 1.8). Mating then begins at 3-5 days old, and egg laying at 5-8 days old (Foil and Hogsette, 1994).

Due to their interrupted feeding and refeeding behaviour, *S. calcitrans* are ideal vectors for pathogen transmission. Both male and female flies are known to be involved in the transmission of equine infectious anaemia (Issel et al., 1988) and West Nile virus (Doyle et al., 2011), as well as trypanosomes (Odeniran et al., 2019). They are also suspected to be carriers of Rift Valley fever virus (Hoch et al., 1985) and bovine herpes virus (Gibbs et al., 1973). *S. calcitrans* have also long been suspected to transmit lumpy skin disease virus due to the seasonality of epidemics and high abundance of flies around outbreaks (Kahana-Sutin et al., 2017). Reproduction number modelling suggested that stable flies were one of the most competent vectors of LSDV (Gubbins, 2019) but it had not been experimentally proven until recently (Sohier et al., 2019).



Figure 1.8 Image of an adult *Stomoxys calcitrans* stable fly

Stable flies look very similar to house flies (*Musca domestica*) apart from the sharp proboscis. They are 4-7mm long, grey in colour, with black stripes on their thorax and a checkered abdomen. Picture sourced from Infravec2, fly sourced from The Pirbright Institute colony.

1.8 The Role of Arthropod Vectors

Arthropods are known to be important vectors of many pathogens, including the etiological agents of malaria and Lyme disease, and many viruses such as dengue virus, chikungunya virus and West Nile virus. Vectors can transmit pathogens mechanically or biologically. Mechanical vectors transmit pathogens without becoming infected themselves, whereas in biological transmission the vector is host to part of the replication cycle of the pathogen before onward transmission. Some examples of biologically transmitted viruses include Crimean-Congo haemorrhagic fever and Zika virus, which both replicate in their insect vectors before infecting their next hosts. Mechanical transmission via the aphid's needle-like stylet is common amongst plant viruses, including potyviruses (Gadhave et al., 2020) but also has been demonstrated in the transmission of fowlpox virus (Yeo et al., 2019) and myxoma virus (Fenner and Woodroofe, 1953). Arthropod vectors can

have an impact on the host and on the virus in a number of different ways, through their bite, saliva or even microbiome. As such, they are a key and often overlooked part of viral pathogenesis.

The bite of an arthropod vector breaks the skin barrier, inevitably causing trauma to the organ. Mosquitoes are known to use their needle-like proboscises to probe for capillaries, causing local tissue damage (Choumet et al., 2012). *Culicoides* midges, like *S. calcitrans*, are telmophagous and cause laceration of the skin to blood feed. Ticks also cause mechanical damage to the epidermis and dermal blood vessels when their chelicerae and mouthparts slice the skin to allow for feeding (Richter et al., 2013). These penetrations into the skin by arthropods produce an initial innate and inflammatory immune response which is aimed at preventing infection of the wound and removing injured and necrotic cells (Reinke and Sorg, 2012). The bite of a haematophagous arthropod works in tandem with the vector's saliva. The saliva of many insects is a cocktail of compounds which are thought to aid arthropods in taking an uninterrupted blood meal. *A. aegypti* saliva contains sialokinin, which acts as a vasodilator and elongates the insect's probing time (Martin-Martin et al., 2022). Arthropod saliva is also known to contain anti-coagulants to prevent blood clotting and disruption of feeding (Gao et al., 2011, Kawahori et al., 2022). Saliva with an anaesthetic effect has also been reported in the saliva of triatomine bugs, possibly to evade host notice to prolong the feed (Dan et al., 1999). These components of saliva aid the arthropod but are molecules foreign to the host, which the host's immune response will respond to, possibly aiding transmission of any pathogen carried by the arthropod.

Insect vector saliva and bites can impact the host immune response, and thus arbovirus/host interactions, often in ways favourable to the pathogen.

Table 1.1 – The impact of arthropod secreted saliva, SGE or direct feeding on pathogen infections in mammalian cells or hosts

Pathogen	In vitro/ in vivo	Host/ cell type	Salivary origin	Effect of vector saliva on virus infection or disease compared to virus infection only	Potential mechanisms	Reference
Mosquito-borne pathogens						
West Nile Virus	In vivo	Mice	Bite of infected mosquito (BIM)	Higher viraemia Faster neuroinvasion	Not determined (ND)	(Styer et al., 2011)
	In vivo	Mice	SGE	Higher viraemia	ND	(Styer et al., 2011)
	In vivo	Mice	SGE	Increased disease and mortality	ND	(Schneider et al., 2006)
	In vivo	Mice	BIM	Higher WNV RNA levels in skin and draining lymph node	Enhancement of IL-10 expression Reduced T-lymphocyte levels	(Schneider et al., 2010)
	In vitro	Human primary keratinocytes	Secreted saliva	Decrease in viral load at 24hpi, significant increase in virus replication at 48hpi	At 24hpi, ↓ IL-28A, IFIT2, CXCL10, CCL20	(Garcia et al., 2018)
Dengue virus	In vivo	Mice	BIM	Higher, sustained viraemia, erythema, thrombocytopenia	IFN-γ, sIL-2Rα	(Cox et al., 2012)
	In vivo	Mice	SGE	Increased viral titres in skin Exacerbates pathogenesis	↑infection of dermal dendritic cells and macrophages ↑ recruitment neutrophils and monocytes to dermis Disruption of endothelial barrier	(Schmid et al., 2016)
	In vitro	Mouse embryonic fibroblasts	SGE	Increase in virus RNA	Serine protease activity	(Conway et al., 2014)

	In vivo	Mice	SGE	100-fold increase in virus RNA in lymph nodes	Serine protease activity	(Conway et al., 2014)
	In vivo	Rhesus macaques	BIM	Longer viraemia, higher viral titres	Elevated IL-10, IL-4, IL-5, IL-1β expression	(McCracken et al., 2020)
Semliki Forest virus	In vivo	Mice	Secreted saliva	Increase in viral titre and virus RNA levels Reduced survival rate	Reduction in blood vessel barrier function due to sialokinin	(Lefteri et al., 2022)
	In vivo	Mice	Uninfected mosquito bite, then virus inoculation by needle (UMNI)	Increased viral RNA in draining lymph node, brain and skin, increased mortality	↑IL-10 protein expression in skin and serum, ↑ IFN-γ gene expression in skin	(Pingen et al., 2016)
Chikungunya virus	In vivo	Mice	UMNI	Reduced survival rate, severe dermal haemorrhage, 10-fold higher viraemia	↓ TLR-3, IL-2, IFN-γ, TNF-α, IFN-β gene expression ↑ IL-4, IL-10 gene expression	(Agarwal et al., 2016)
	In vitro	Human skin fibroblasts	Secreted saliva	Increased virus replication	Decreased expression of type 1 IFN-induced genes	(Wichit et al., 2017)
Rift Valley Fever virus	In vivo	Mice	UMNI	Increased mortality rates, increased viraemia and viral load in liver and brain	ND	(Le Coupanec et al., 2013)
Bunyamwera virus	In vivo	Mice	UMNI	Higher virus replication, higher viral load in skin and spleen	ND	(Pingen et al., 2016)
Zika virus	In vivo	Rhesus macaques	BIM	Delayed time to peak viral load Altered tissue tropism	ND	(Dudley et al., 2017)
***Culicoides*-borne pathogens**						

Bluetongue virus	In vivo	Sheep	Infected *C. nubeculosus* bite	Enhanced viraemia Higher clinical scores	↑ MX1 and CXCL-10 gene expression	(Pages et al., 2014)
Bluetongue virus	In vivo	Sheep	Secreted saliva	More severe and prolonged clinical signs	ND	(Drolet et al., 2015)
Tick-borne pathogens						
Powassan virus	In vivo	Mice	SGE	At lower virus loads, SGE enhances clinical signs and disease	Upregulation of IL-1β, IL-4, IL-6, IL-10, TNF-α	(Hermance and Thangamani, 2015)
Powassan virus	In vivo	Mice	SGE	Facilitates neuroinvasion by virus Accelerated disease progression Decreased survival times.	ND	(Santos et al., 2021)
African swine fever virus	In vivo	Pigs	SGE	Greater hyperthermia, delay in local virus spread	Macrophage recruitment	(Bernard et al., 2016)

Inoculation of arboviruses alongside vector saliva has been investigated for many important pathogens (summarised in Table 1.1). Inoculation of West Nile virus mixed with *Culex tarsalis* salivary gland extract (SGE) resulted in higher viraemia in mice (Styer et al., 2011). This could be due to an inhibitory effect of vector saliva on the keratinocyte inflammatory response (Garcia et al., 2018). Saliva, SGE and spot-feeding by *Ae. aegypti* has been shown to have an impact alongside several viruses: increasing oedema in Semliki Forest virus inoculation sites and preventing free virus drainage and encouraging infection of cutaneous cells (Pingen et al., 2017); increasing dengue severity, endothelial cell permeability and vascular leakage in mice, likely due to the action of sialokinin (Lefteri et al., 2022), allowing the virus to move further faster (Schmid et al., 2016); and downregulation of inflammatory genes coding and upregulation of anti-inflammatory genes in chikungunya infected mice, as well as a higher viraemia and organ degeneration (Agarwal et al., 2016). *Culicoides* saliva promotes bluetongue viraemia, infection and expression of clinical signs by delaying IFN-induced host gene expression and the neutralising antibody response (Pages et al., 2014). These studies highlight that insect vector saliva might be able to indirectly (through local and/or systemic immune modulation) influence viral dissemination, replication and ultimately virulence.

1.9 Current Methods of LSD Control

Lumpy skin disease is controlled in a number of ways, which vary by geopolitical location and by the specific outbreak situation. The methods used include movement restrictions, slaughter of infected or in-contact cattle, vaccination, and vector control.

Movement restrictions involve prevention of cattle movement, with animals kept on farms in quarantine. Recommendations suggest that animals should not be allowed to move, with slaughter taking place in restricted zones (Tuppurainen et al., 2017). In addition, trade restrictions are put in place. These trade restrictions can be severe: entire countries can be banned from trading live animals or animal products e.g., Russia banned the import of cattle and associated products from Sri Lanka, Vietnam and Thailand in April and May 2021, and Thailand issued a temporary ban on import of cattle products from Myanmar in May 2021 (World Trade Organisation, 2021).

Commonly, slaughter of LSD infected animals and those in-contact with them is carried out, a process known as “stamping out”. This is often a government mandated action, to try to limit the spread of disease but also as a response to trade restrictions. However, stamping out is economically costly to affected farmers and to the government who should provide compensation. Furthermore, if carried out in an epidemic situation where many farms have already been infected, stamping out will not be as effective. Finally, stamping out can be socially damaging, and can provoke distrust in government and veterinary services, and possibly result in under reporting. When a model was made of transmission between infected farms in Bulgaria and Greece, it was shown that vaccination had a greater impact on reducing LSDV spread than any stamping out policy (Miranda et al., 2016).

The best control strategy for prevention of LSD is vaccination. The vaccines on the market today are predominantly live attenuated virus strains based on LSDV, GTPV, or SPPV. Most live attenuated homologous vaccines are composed of the LSDV Neethling strain, which was attenuated via high numbers of passage from the very first disease outbreaks in South Africa. These homologous vaccines have been shown to be efficacious in the field during the LSD outbreaks in south eastern Europe in 2016-2017 (Calistri et al., 2020), and were

evaluated well in an experimental setting (Haegeman et al., 2021), protecting against nodule formation with vaccinated animals showing no viraemia after challenge. Heterologous vaccines based on goatpox virus and sheeppox virus can also be used for protecting against LSDV.

A disadvantage of live attenuated vaccines is that there is the potential for vaccine virus shedding, transmission of vaccine virus, or recombination with field strains. Inactivated vaccines would be a safer alternative, since they cannot replicate, recombine or revert to virulence. Some inactivated vaccines for capripoxviruses have been developed, but they lack long term protection and could prevent serological surveillance (this is key for declaring disease free status) (OIE, 2017a). However, studies have shown that this methodology could still be a useful and effective option in the control repertoire (Wolff et al., 2021).

Since LSDV is transmitted by haematophagous insect vectors, it is logical that vector surveillance and control might be useful in the toolkit. Insecticides and repellents were employed by Greece, Bulgaria, Russia and North Macedonia during the European outbreak of 2016 (European Food Safety Authority, 2017). The use of pesticides is a difficult strategy to widely implement without disrupting important biodiversity and ecological networks. However, the use of pesticides locally preceding an anticipated rise in insect vectors could be successful. Since *S. calcitrans* flies oviposit and pupate in manure and rotting straw, vector control in a barn or housed situation might consist of regular cleaning and maintenance to eliminate vector breeding sites. This would not, however, work in a pasture or nomadic situation. Using confined housing, nets and insect traps to protect the cattle from insects is also a possibility, but is likely to be expensive. Integrated vector control that

employs a mixture of strategies would likely be the most effective option, but so far, there is no evidence for the effectiveness of vector control on the epidemiology of LSDV.

1.10 The Impacts of Lumpy Skin Disease

In regions where LSD has historically been endemic, cattle are often relied on for multiple purposes. As the global population increases and the climate crisis continues, food security becomes an increasingly important issue, as 9.8% of the global population are estimated to be undernourished (FAO et al., 2022). Cattle are a key source of protein, important nutrients and essential amino acids through their meat and milk, which may not be accessible in the same quantities from other ruminants (Tona, 2021). Additionally, in some populations of southern Africa, cattle are seen as "living currency", and are used as a symbol of wealth, and for trade, gifts, dowries, and as payment (Shava and Masuku, 2019). Finally, it has been estimated that 30% of farming land was prepared by draught animals (FAO, 2003), which include cattle and water buffalo. Draught power can also help people, especially women, to leave the backbreaking work of manual tillage (Smith et al., 2013). Therefore, as well as causing animal suffering, the disease contributes to rural poverty, economically impacting farmers and smallholders (ICPALD, 2013). In Ethiopia, where the livestock subsector contributes 40% to the agricultural gross domestic product (Gari et al., 2010), the median total economic loss of an outbreak in a single herd was USD 1,176 (Molla et al., 2017), a sizeable amount when the GNI (gross national income) per capita of Ethiopia in 2018 was USD 790 (The World Bank, 2020).

In countries where the disease is not endemic, declaring an outbreak can result in trade embargoes (OIE, 2018) and movement restrictions, with the favoured outbreak control

policy in Europe being “stamping out” whole herds (Council Directive, 17 December 1992), compounding economic problems. This cost the countries of Albania, Bulgaria, and North Macedonia a combined 20.9 million Euro (Casal et al., 2018). The spread of LSD into Asia is of great concern, since China, Bangladesh and India have some of the largest cattle populations globally. The estimated costs of direct losses of livestock and production on South, East and Southeast Asian countries was estimated by the FAO to be USD 1.45 billion (Roche et al., 2021).

1.11 Aims and central hypothesis

LSDV is transmitted by several haematophagous arthropods including *S. calcitrans* in a mechanical fashion. The role of the arthropod vector in LSDV pathogenesis is poorly understood. For example, the saliva and bite of arthropods has been shown to have an impact on the pathogenesis of biologically transmitted viruses, but this has not been investigated for mechanically transmitted viruses such as LSDV. Understanding the influence of the inoculating vector on the outcome of infection could enable more effective disease control strategies to be developed, potentially aimed at disrupting virus transmission.

The main aim of this thesis was to investigate the role of *S. calcitrans* on the pathogenesis of LSDV and the impact on clinical outcome of LSD. The central hypothesis was that:

“LSDV pathogenesis and clinical outcome is influenced by the interaction of *S. calcitrans* with the host”

This hypothesis was investigated through the following research aims:

- To optimise an adapted artificial membrane feeding system for the collection of *S. calcitrans* secreted saliva from laboratory reared flies, and characterise the composition of the secreted saliva.
- To optimise a protocol for the isolation of bovine primary fibroblasts and keratinocytes and characterisation of a bovine skin in vitro model.
- To determine if *S. calcitrans* saliva impacts LSDV replication and pathogenesis in vitro.
- To carry out in vivo experiments to explore the effect of *S. calcitrans* saliva and feeding on the pathogenesis and clinical outcome of LSD.

2

Materials and Methods

2.1 Cells

2.1.1 Continuous cell line culture and maintenance

Madin-Darby bovine kidney (MDBK) cells (ATCC code CCL-22) were cultured in vented 175cm^2 flasks (Fisher Scientific) at 37°C, in a 5% CO_2 atmosphere in Dulbecco's Modified Eagle's Medium (DMEM) (Life Technologies) supplemented with 10% Foetal Bovine Serum (FBS) (Life Technologies) and 1% penicillin-streptomycin (100 units/ml penicillin and 100µg/ml streptomycin) (Sigma). They were passaged weekly by aspirating off the media, and the cells were gently washed with 7ml of phosphate buffered saline (PBS). 4ml of 0.25% Trypsin-EDTA (Life Technologies) was added to the cells and the flask was returned to the incubator until the cells rounded off and detached from the flask. 6ml maintenance medium was added (as detailed in Table 2.1) to prevent further trypsin action and resuspend the cells. Cells were passaged at 1:20 to 1:30.

2.1.2 Isolating bovine primary cells methodology

A 3cm^2 square of tissue was cut from the distal ear pinna or inguinal area of 6-12 month old cattle and cleaned three times in sterile water. The sample was shaved, and the skin excised from the cartilage. The skin was cut into 5mm strips and treated with 10mg/ml Dispase (Sigma) overnight at 4°C to dissociate the epidermis and dermis. These two layers

were gently pulled apart with sterile disposable tweezers and sterile rat-toothed forceps following incubation.

Bovine primary fibroblasts (BPF): The dermis strips were cut into 5mm^2 squares. Each piece was dipped into media (as detailed in Table 2.1) and placed directly into tissue culture plates, upper side down. 10-15 pieces were placed in each 100mm dish. 1-2 drops of the BPF media were placed onto each piece of tissue. These were incubated at 37°C, in 5% CO_2 atmosphere overnight. 8ml of BPF media was added, and any floating skin pieces removed. The BPF media was replaced after 48h, with the remaining skin pieces removed a further 48h later. When adherent fibroblast colonies were seen, the cells were washed with PBS and removed from the dish using 2ml 0.25% Trypsin-EDTA until cells dissociated, then centrifuged at 200 g for 5 minutes (min) and resuspended in 10ml BPF media. The cells were seeded into cell culture vessels and grown at 37°C, 5% CO_2. BPFs were grown to 90% confluency and passaged at a ratio of 1:5 using 0.25% Trypsin-EDTA.

Bovine primary keratinocytes (BPK): The epidermis strips were macerated using sterile disposable scalpels, then placed into a 50ml tube with 10ml 0.25% Trypsin-EDTA, and incubated at 37°C for 10 min, mixing the samples gently every 5 min. 25ml of BPK media (detailed in Table 2.1) was added and the solution was mixed then filtered through 70µm cell strainers, then centrifuged at 200 g for 5 min at 6-8°C. The pellet was resuspended in 10ml media then seeded into a 100mm tissue culture plate coated with Coating Matrix (Thermo Fisher Scientific) and incubated at 37°C, 5% CO_2 for approximately a week with regular media changes. It took on average 10d for small colonies of keratinocytes to form, with larger colonies forming at 17d.

Table 2.1: Cell culture maintenance media and supplements

Cell line	Base media	Supplements
MDBK	500ml 1×DMEM without NaPyr (Life Technologies)	10% FBS, 1% penicillin-streptomycin (100 units/ml penicillin and 100µg/ml streptomycin)
Bovine primary fibroblasts	500ml 1×DMEM without NaPyr (Life Technologies)	10% FBS, 2% penicillin-streptomycin, 5 µg/ml amphotericin B (Sigma)
Bovine primary keratinocytes	KGM2 BulletKit (Lonza)	All those included in the kit, 1% penicillin-streptomycin, 2.5 µg/ml amphotericin B (Sigma)
For infection with virus, FBS supplement in media is reduced to 2.5%		

2.2 Viruses

2.2.1 Production of LSDV stocks

Work with LSDV was carried out in high containment facilities and in line with Specified Animal Pathogens Order 3 (SAPO3) regulations. Disinfection of workspaces used the validated disinfectant FAM30 at a 1:200 dilution. 10-20 175cm^2 flasks of confluent MDBK cells were infected with LSDV at a multiplicity of infection (MOI) of 0.01. Cultures were incubated at 37°C, in a 5% CO_2 atmosphere for 5-7 days until cytopathic effect (CPE) was seen in every flask. The cells were scraped down into the media using a cell scraper, and the cell/media mix collected in 50ml falcon tubes. The cells were then spun in a centrifuge at 1500 × g for 10 min at room temperature (RT). The supernatant was discarded, and the pellets resuspended in PBS to give a 50ml resuspension in one falcon tube. The tube was spun again as before, and the supernatant discarded. The pellets were then frozen at -80°C or taken forward for sucrose purification (section 2.2.2).

2.2.2 Sucrose purification of LSDV stocks

The cell pellets described in section 2.2.1 were resuspended in 10ml of ice cold 10mM Tris-Cl pH 9. The resuspended cells were incubated on ice for 15 min. The cell suspension was transferred to a sterile 15-20ml Dounce homogeniser (preferably cooled on ice). The piston was gently raised and pushed down 25 times, pausing after each set of 5 cycles. The solution was then transferred to a 50ml tube and spun at 750 × g for 5 min. 18ml of 36% sucrose (w/v) in Tris-HCl (10mM) pH 9 was added to S28/S32 OptiSeal ultracentrifuge tubes (Beckman Coulter). The spun supernatant was collected and trickled down the side of the ultracentrifuge tube so that it formed a layer on top of the sucrose solution. The pellet was discarded. The tubes were balanced to the nearest 0.1g with 10mM Tris-HCl pH 9. The tubes were spun in an Optima XL-90 ultracentrifuge (Beckman Coulter) using a SW32 rotor, at 13,500 rpm for 80 min. The supernatant was then aspirated off and discarded, and the pellet resuspended in 1ml Tris-HCl pH 9 and stored at -80°C.

2.2.3 LSDV titration

Titres of LSDV stocks and samples from LSDV infected cells were quantified using plaque assays. MDBK cells were cultured in six-well plates until they reached a 95% confluent monolayer. Viral stocks and samples were defrosted and sonicated for 30 seconds (sec) at 20-30 kHz on a Misonix 3000 sonicator. Ten-fold serial dilutions were made in infection cell culture medium (DMEM, 1% penicillin-streptomycin, 2.5% FBS). Overlying MDBK media was removed from the six-well plates, and 1ml of the dilutions inoculated into separate wells and incubated at 37°C in 5% CO_2 for 1 hour (h). Control wells were inoculated with 1ml of uninfected media. After this, the inoculum was aspirated from each well and replaced with 2ml of semi-solid overlay made of 1ml 3% carboxymethylcellulose (CMC) (Sigma) and 1ml 2×DMEM media (SLM-202-B, Merck) supplemented with 5 % FBS (Life

Technologies), 2 % penicillin-streptomycin (Sigma), 10ml 100 mM sodium pyruvate, and 25ml sodium bicarbonate solution (Merck). The plates were incubated for a week at 37°C, 5% CO_2. The overlay was removed, and the plates were stained with 2ml crystal violet solution (0.1.% (w/v) crystal violet (Sigma) in 15% methanol) in each well. After incubation for 1h at RT, plates were washed with water and air dried. The foci were counted and the titre of the virus determined. The protocol for titrating whole blood samples was the same apart from the substitution of DMEM with calcium free DMEM (Gibco™; 11380037) supplemented with 1% penicillin-streptomycin and 2.5% FBS.

Table 2.2: LSDV strains used and their source

Virus strain (LSDV)	Source*
Cameroon	Non-vesicular research laboratory (NVRL), The Pirbright Institute
Eastern Europe	NVRL, The Pirbright Institute
Neethling (lab adapted)	NVRL, The Pirbright Institute
eGFP-095-LSDV	Dr Gessica Tore, a postdoc in Dr Pip Beard's group

* Viruses used have not been published and do not have ID numbers.

2.2.4 LSDV growth curves in MDBK and primary cells

Cells to be infected were grown to confluency in 6-well tissue culture plates. The overlying media was removed, and cells were infected with LSDV at a high MOI of 5, low MOI of 0.01, or mock infected with 1ml infection maintenance media per well. The virus was incubated on the cells for 1h at 37°C in 5% CO_2. The inoculum was removed and washed twice with 2ml of maintenance media, before a final 2ml was added. Samples were then taken at various timepoints up to 7 days post infection (dpi) by scraping cells into the surrounding supernatant using a cell scraper, and pipetting the mix into a 2ml Eppendorf. Samples were stored at -80°C until they were titrated.

2.3 Western blotting of cell lysates

Cell lysates were collected for protein analysis by Western blot. Supernatant of cells a 6 well plate was removed and 100µl radioimmunoprecipitation (RIPA) buffer with protease inhibitors (1 protease inhibitor tablet (Roche) in 10ml RIPA solution (Fisher Scientific)) added, followed by incubation for 20 min at room temperature. The cells and RIPA buffer were then scraped together and put in a pre-chilled Eppendorf. This was then spun for 15 min, 12,000 rpm, 4°C. Samples were stored at -80°C before analysis. 12µl of cell lysate was mixed with 4µl DTT and heated to 95°C for 5 min. SDS-polyacrylamide gel electrophoresis (SDS-PAGE) using a 12.5% resolving and 5.5% stacking gel was used to separate viral proteins by size. The resolving gels were made by mixing (per gel) 2ml of acrylamide/bisacrylamide 30% solution (Sigma), with 50µl 10% SDS, 1ml resolving gel buffer (BioRad), 2ml sterile water, 50µl 10% ammonium persulfate (AMPS)(Sigma), and 4µl tetramethylethylenediamine (TEMED)(Sigma). The mixture was poured into gel casts and overlaid with 500µl sterile water. Once the gel had set, the water was poured off. The stacking gel was then poured on top of the resolving gel, and a 10-well comb inserted into the gel cast. The stacking gel was made up of 0.68ml acrylamide/bisacrylamide 30% solution (Sigma), 40µl 10% SDS, 0.4ml stacking gel buffer (BioRad), 2.5ml sterile water, 40µl 10% ammonium persulfate (AMPS)(Sigma), and 4µl tetramethylethylenediamine (TEMED)(Sigma). Set gels were removed from the casting equipment and transferred into BioRad Mini Protean vertical electrophoresis cell. Running buffer (1:9, 10x concentrate Tris-Glycine-SDS buffer: sterile water) was added to fully submerge the gels and generously cover the bottom of the gel casts. The comb was removed, and 20µl of each sample were loaded. The Li-Cor Chameleon Pre-stained Protein Ladder was used to give a reference for

protein size. Electrophoresis was carried out at 120V until the dye front was 5mm from the end of the resolving gel (1-2h).

The gel was then read via semi-dry transfer. The gel was extracted carefully from the cast and “flopped” into a tray of buffer. Extra thick blot filter paper and PVDF membrane (Merck Millipore) were cut to the size of the gel. The membrane was activated in methanol before being washed in sterile water. On the Trans-Blot ® SD Semi-Dry Transfer Cell (BioRad), the parts were assembled in this order: filter paper soaked in transfer buffer, the activated PVDF membrane, the gel, then another transfer buffer soaked filter paper. The electrode was attached and the transfer was run for 45 min at 18V. The membrane was removed and blocked for 1h at room temperature on a roller in a 1:1 mix of PBS and Odyssey® Blocking Buffer (Li-Cor). The membrane was then incubated overnight at 4°C on a roller with rabbit polyclonal antibody directed towards LSDV E3 protein (generated for Dr Pip Beard’s lab by Antibody Production Services, Life Service Group, targeting LSDV034) and mouse monoclonal antibody directed towards actin (Cell Signalling, Cat#4970). The antibodies were at 1:1000 dilutions in 2.5ml PBS and 2.5ml Odyssey® Blocking Buffer (Li-Cor). The membrane was then washed three times in PBS containing 0.1% Tween (PBS-T) on a roller, for 10 min each time. Secondary antibodies were then incubated with the membranes for 1h on a roller at room temperature. These were anti-E3 (Anti-rabbit IgG, AlexaFluor 680, Jackson ImmunoResearch, Cat#111-625-144) and anti-actin (Anti-mouse IgG, AlexaFluor 790, Jackson ImmunoResearch, Cat#115-655-146), at 1:15000 in 2.5ml PBS and 2.5ml Odyssey® Blocking Buffer. After probing, the membrane was washed three times again in PBS-T for 10 min each time, on a room temperature roller. Enhanced chemiluminescence (ECL) (Thermo Scientific) was then performed on the membrane according to

manufacturer's instructions. Visualisation of detected protein bands was carried out on Syngene G:Box.

2.4 Immunofluorescent confocal imaging

Cells were seeded at 1×10^5/well onto sterile square glass coverslips in 6-well tissue culture plates and then infected with LSDV and incubated for an appropriate time. The media was aspirated off and cells fixed in 4% paraformaldehyde for 40 min at RT. Cells were washed twice gently in PBS at RT, and if necessary, were stored in PBS at 4°C for a maximum of a week. Cells were permeabilised with 1ml per well of 0.2% Triton-×100 diluted in PBS for 15 min at RT and washed twice again in PBS. Cells were then blocked with 1ml per well of blocking buffer (2% FBS in PBS), and incubated in the buffer for 1h at RT. Cells were incubated with phalloidin label (1µl/coverslip, in 100µl blocking buffer) in a covered humidity chamber for 1h. Cells were then incubated with 100µl DAPI label per coverslip (1µl of 5mg/ml DAPI stock solution diluted to 1:10000 in 10ml deionised water) for 5 min at RT in a covered humidity chamber. The cells were then washed twice in PBS and once in deionised water. Coverslips were mounted on glass slides using Vectashield and allowed to set for 1h at RT before the edges were sealed with clear polish. Mounted slides were stored at 4°C, and observed on a confocal laser-scanning microscope, Leica TCS SP5. Slides were visualised using 405, 488, and 640nm laser lines for the appropriate dyes and a 63× oil immersion objective lens. Images were acquired using Leica Application Suite X (LAS-X) software.

2.5 *Stomoxys calcitrans*

2.5.1 *S. calcitrans* maintenance.

The *S. calcitrans* flies were sourced from the colony maintained at the Pirbright Institute, established in 2011 from a parent colony maintained by the United States Department of Agriculture. The colony was maintained at approximately 26°C and 60-70% humidity. The flies were fed daily on defibrinated horse blood (catalogue item HB029 from TCS Biosciences) by saturating cotton wool in blood in plastic weighing boats. New generations of flies were created by harvesting eggs from the cotton wool feeding pads, via gentle washing and cleaning. The viable eggs were collected in a pipette and were seeded in beakers full of moist larval medium (for two 500ml larval containers, mix 500ml powdered grass meal, 150ml cornmeal, a teaspoon of dry yeast and approximately 400ml of water). It took approximately 12-15 days for adult flies to first emerge.

2.5.2 *S. calcitrans* saliva collection

The method of collection and its optimisation is detailed in Chapter 3 of this thesis.

2.5.3 *S. calcitrans* saliva concentration.

Once saliva collection from the flies was completed (it is not known exactly how many of the flies fed on the membranes salivated), the Durapore® PVDF 0.2 µm membranes (Millipore) (that had been stored in PBS at 4°C) were cut into four irregular pieces and returned into their storage PBS. The membranes were washed in PBS at 4°C overnight under constant rotation. The eluted proteins were then concentrated to a smaller volume, for a more representative and useful concentration to use in further work. The solution was sterilised by passing it through a 0.2 µm filter (Merck Millipore), then dispensed into a

3kDa Vivaspin 20 centrifugal concentrator column (Sartorius) and spun at 1950g and 10°C to give a final volume of approximately 1000µl.

2.5.4 Sample analysis of *S. calcitrans* saliva via silver stain.

Samples were prepared by adding sample buffer (made with SDS sample buffer and dithiothreitol (DTT)) to the sample in the volumes described in Table 3, then heating the samples for 5 mins at 95°C.

Table 2.3: Sample preparation for silver stain protocol

	Amount of sample (µl)	Amount of sample buffer (µl)
Saliva collection	15	5
ATP and dH2O	15	5
Bovine serum albumin (BSA)	2	2

The SDS-PAGE gel was used to separate *S. calcitrans* salivary proteins by size to enable the proteins to be visualised clearly by silver staining. 15% resolving gels of 1mm thickness were used, with 5.5% stacking gels overlaid on them. The resolving gels were made by mixing (per gel) 2.5ml of acrylamide/bisacrylamide 30% solution (Sigma), with 50µl 10% SDS, 1ml resolving gel buffer (BioRad), 1.5ml sterile water, 50µl 10% ammonium persulfate (AMPS)(Sigma), and 4µl tetramethylethylenediamine (TEMED)(Sigma). The gels were then made as described above in section 2.3. The Page Ruler™ Plus Pre-stained Protein Ladder was loaded first to give a reference for protein size, then the saliva sample and ATP sample, then BSA as a positive control. Electrophoresis was carried out at 120 volts until the dye front was 5mm from the end of the resolving gel. After electrophoresis, the gel was

removed and was tested for presence of proteins through silver staining, using the Pierce™ Silver Stain Kit (ThermoFisher Scientific) according to manufacturer's instructions.

2.5.5 BCA assay for saliva protein quantification.

The concentration of protein in the concentrated saliva was tested by using the Pierce™ BCA Protein Assay Kit (ThermoFisher Scientific). The enhanced manufacturers protocol was used for a working range of 5-250µg/ml, and the standards and samples were measured on a NanoDrop spectrophotometer. The zero reference of the standard was used to blank the instrument rather than water. The absorbance of the standards and samples were measured, then the protein concentration of the samples by interpolating from the standard curve.

2.5.6 Coomassie gels for mass spectrometry

The concentrated secreted saliva was separated via SDS-PAGE as described in 2.5.3 but after electrophoresis, the gel was rinsed three times for 5 min with 100ml deionised water. The gel was placed in a tray and covered with 20ml SimplyBlue™ SafeStain (Fisher Scientific) and incubated for 1h at RT on a laboratory rocker. The stain was discarded after incubation and the gel was washed in 100ml deionised water for 1h. The water was replaced, and the gel was washed for another hour. Specific pieces of the gel were excised and stored in deionised water before being sent for analysis by mass spectrometry.

2.5.7 Proteomic analysis of *S. calcitrans* saliva

Proteomic analysis and mass spectrometry was carried out at the University of Liverpool by Dr Stuart Armstrong.

<u>Sample digestion</u>

In-gel digestion was essentially as described by Shevchenko et al. (2006). Pre -excised and stained bands were cut into smaller pieces (approx. $1mm^3$). Gel pieces were then de-stained and in gel digestion performed as described below.

Slices were de-stained with 25mM ammonium bicarbonate/ 50 % acetonitrile (v/v). Proteins were reduced for 10 minutes at 60°C with 10 mM dithiothreitol (Sigma) in 25 mM ammonium bicarbonate and then alkylated with 55 mM iodoacetamide (Sigma) in 50 mM ammonium bicarbonate for 30 minutes in the dark at room temperature. Gel pieces were washed for 15 minutes in 50 mM ammonium bicarbonate and then dehydrated with 100% acetonitrile. Acetonitrile was removed and the gel plugs rehydrated with 0.01 µg/µL proteomic grade trypsin (Thermo Fisher Scientific) in 25 mM ammonium bicarbonate. Digestion was performed overnight at 37°C. Peptides were extracted with 50% (v/v) acetonitrile, 0.1% trifluoroacetic acid (TFA) (v/v) and the extracts were reduced to dryness using a centrifugal vacuum concentrator (Eppendorf) and re-suspended in 3 % (v/v) methanol, 0.1 % (v/v) TFA for analysis by MS.

Mass spectrometry

LC-MS/MS analysis was similar to that described by Aljabr et al. (2019). Peptides were analysed by on-line nanoflow LC using the Ultimate 3000 nano system (Dionex/Thermo Fisher Scientific). Samples were loaded onto a trap column (Acclaim PepMap 100, 2 cm × 75 µm inner diameter, C18, 3 µm, 100 Å) at 9µl /min with an aqueous solution containing 0.1 % (v/v) TFA and 2% (v/v) acetonitrile. After 3 min, the trap column was set in-line an analytical column (Easy-Spray PepMap® RSLC 50 cm × 75 µm inner diameter, C18, 2 µm, 100 Å) fused to a silica nano-electrospray emitter (Dionex). The column was operated at a constant temperature of 35°C and the LC system coupled to a Q-Exactive mass spectrometer (Thermo Fisher Scientific). Chromatography was performed with a buffer

system consisting of 0.1 % formic acid (buffer A) and 80 % acetonitrile in 0.1 % formic acid (buffer B). The peptides were separated by a linear gradient of 3.8 – 50 % buffer B over 30 minutes at a flow rate of 300 nl/min. The Q-Exactive was operated in data-dependent mode with survey scans acquired at a resolution of 70,000 at m/z 200. Scan range was 300 to 2000m/z. Up to the top 10 most abundant isotope patterns with charge states +2 to +5 from the survey scan were selected with an isolation window of 2.0Th and fragmented by higher energy collisional dissociation with normalized collision energies of 30. The maximum ion injection times for the survey scan and the MS/MS scans were 250 and 50ms, respectively, and the ion target value was set to 1E6 for survey scans and 1E4 for the MS/MS scans. MS/MS events were acquired at a resolution of 17,500. Repetitive sequencing of peptides was minimized through dynamic exclusion of the sequenced peptides for 20s.

Protein Identification

Spectral data were analysed using the PEAKS studio X+ software (Bioinformatics Solutions Inc., Waterloo, ON, Canada, (Ma et al., 2003)). Tandem MS data were searched against the Stomoxys calcitrans protein database (UniProt) and a contaminant database (cRAP, GPMDB, 2012). Search parameters were as follows; precursor mass tolerance set to 15 ppm and fragment mass tolerance set to 0.02 Da. Trypsin, was set as the protease. Two missed cleavage events were permitted. Carbamidomethylation (C) was set as a fixed modification. Oxidation (M) and acetylation (N-term) were set as variable modifications. The search was specific. The false discovery rate was set at 1%.

2.5.8 *S. calcitrans* in vitro impact assay

The secreted saliva was removed from storage at -80°C and defrosted. Neat secreted saliva (120µl of collection 1 and 105 µl of collection two) was decanted into Tube A. Then a 5-fold

dilutions series of four was created, resulting in five tubes of saliva concentrations: 1 (neat), 1:5, 1:25, 1:125, 1:625. Six tubes containing 60µl of LSDV Cameroon were prepared and sonicated. 60µl of each dilution were added to the virus tubes, with 60µl PBS added to the sixth viral tube as a positive control. The mixes were left for 4h at room temperature. After this incubation, 100µl of each sample (including the control) was diluted in 900µl titration media (2.5% DMEM with 1% penicillin-streptomycin) to give a dilution of 10^{-1}. 200µl of this solution was then diluted in 1.8ml titration media to give a dilution of 10^{-2}, with the dilution series continuing until a dilution of 10^{-7} was reached. 1ml of each dilution for each sample was inoculated onto wells of MDBK monolayers and incubated at 37°C for 1h. The inoculum was then removed and replaced with an overlay made of 3% CMC/2×DMEM. This was left on for a week at 37°C. The overlay was removed, and the plates were stained with 2ml crystal violet in each well. The foci were counted and the titre of the virus in that sample determined.

2.5.9 *S. calcitrans* saliva in LSDV growth kinetics

BPFs were grown to 90% confluency in 6-well tissue culture plates at 37°C in a 5% CO_2 atmosphere. Per culture plate, 3.6µl secreted saliva (0.6µl per well, calculated via extrapolating from the volume of saliva secreted from a single *Ae. aegypti* mosquito) was mixed with LSDV Cameroon at an MOI of 5, with 3.6µl PBS mixed with the same volume of virus as a control. The mixes were incubated for 2h. 6ml DMEM with 2.5% FBS and 1% penicillin-streptomycin was then added to each mix. Media was aspirated from confluent BPFs, and each well was then infected with the inoculum, and the control in parallel. The subsequent growth curve and titration of samples was carried out as described in 2.2.3 and 2.2.4.

2.6 In vivo animal studies

2.6.1 CIVS 1 and 2 study design

The CIVS study aimed to explore the effect of *S. calcitrans* saliva and bite on the pathogenesis of LSD, and was funded by the BBSRC In Vivo Skills Award. Thirty male Holstein-Friesian calves 4-6 months old (weight range 133- 167kg) were included in the study, which was carried out as two replicates of 15 animals. In each replicate, animals were stratified according to weight, and then randomly assigned to the three treatment groups, resulting in 5 animals in each group. Investigators could not be blinded to animal group allocation due to the in vivo skills training requirements of the grant. Animals were acclimatised to The Pirbright Institute's high containment animal units for 10 days prior to the start of the experiments.

Challenge

Group 1. Animals were inoculated with 1×10^6 pfu LSDV intradermally (1ml in both of the craniodorsal flanks of each animal, delivered as ten 100 µl microdoses).

Group 2. Each animal was challenged with 1×10^6 pfu LSDV mixed with 10µg salivary proteins. Inoculum was delivered as in Group 1.

Group 3. Per animal, two pots containing flies were placed with the netting contacting the skin on each craniodorsal flank for 5 min, giving 10 min of feeding time overall. Each animal was then challenged with 1×10^6 pfu LSDV. Inoculum was delivered as in Group 1.

Virus isolates

The LSDV strain used was sourced from the OIE Capripoxvirus Reference Laboratory at The Pirbright Institute and originated from the skin of an LSD-affected bovine in eastern Europe in 2016. The virus was grown on MDBK cells in high-glucose Dulbecco's modified Eagle's

medium supplemented with HEPES (Life Technologies) supplemented with 2.5% foetal bovine serum, and 1% penicillin-streptomycin at 37°C in a 5% CO_2 atmosphere. Infectious virus titre (number of plaque-forming units/millilitre, pfu/ml) was determined by plaque assay on MDBK cells.

Flies

S. calcitrans were sourced from The Pirbright Institute colony (colony established in 2011 from individuals kindly provided by the Mosquito and Fly Research Unit, USDA Florida). Insects were reared under the following conditions: approximately 200 eggs per pot, incubated for ~16 days in larval pots containing a ratio of 3:2:1 (powdered grass meal, water, and corn meal) and a flat tablespoon of baker's yeast. They were maintained in BugDorms in insectaries at 27 ± 2°C, 70% RH, with a 16:8 light/dark cycle. Insects were fed daily using defibrinated horse blood. 20-25 insects were aspirated into plastic containers covered by mesh the day before feeding. No blood was provided for approximately 18 h before feeding.

Monitoring of clinical signs in animals

Physical and clinical parameters were collected throughout the duration of the trial: heart rate, temperature, respiratory rate, swelling at inoculation site, number of nodules (and their locations), anorexia, lameness, behavioural changes (including isolation, lethargy, abnormal posture), and lymph node size. Heart and respiratory rates were recorded every 2-3 days. Rectal temperature was recorded daily. Palpations of the lymph nodes and inoculation sites were conducted daily, as was behavioural monitoring. Nodule appearance was monitored by shaving the hair from the calves and conducting a touch assessment daily. The experiments lasted 28 days after inoculation of animals, and was concluded by euthanasia via captive bolt or intravenous barbiturate overdose. Animals were euthanised

before 28 dpi if they reached humane or scientific endpoints. Humane endpoints were scored by: a) temperature of 1.5°C above baseline for 4 consecutive days (having not responded to appropriate drugs), b) if the animal is not eating at the beginning of the 3rd consecutive day, or c) if an animal showed consistent signs of isolation, exhibition of delayed responses, lethargy and abnormal posture for 4 consecutive days.

Sample collection

The following samples were collected for each animal. 10ml EDTA blood samples were collected at -2, 3, 5, 7, 9, 11, 13, 16, 19, 23, and 27 dpi for PCR analysis and virus titration. Skin microbiopsies were collected at 5, 11, and 16 dpi for PCR analysis. 20ml serum samples were collected for ELISA at -2, 5, 7, 9, 11, 13, 16, and 19 dpi. 10ml heparinised blood samples were collected for flow cytometry and interferon gamma release assays (IGRA) at -2, 3, 5, 7, 9, 11, 16, 19, 23, and 27 dpi. At post-mortem, lesions were collected for histopathology.

2.6.2 Ethical approval, housing, and husbandry

The experimental studies were conducted under the project licence P2137C5B approved by the UK Home Office in line with the Animals (Scientific Procedures) Act 1986. The studies were approved by The Pirbright Institute Animal Welfare and Ethical Review Board (authorisation numbers AR001176 and AR001177). The animals were sourced from a commercial high health herd and confirmed as negative for BVDV via PCR prior to the study. The animals were housed in rooms ($22m^2$) in the primary high-containment (SAPO4, Biosafety Level 3 Agriculture) animal facility at the Pirbright Institute. Bedding material was provided (https://www.mayofarmsystems.co.uk/mayo-mattress-stable-mat/), light/dark cycle was 12:12 h, temperature was held between 10°C to 24°C, and humidity 40% to 70%. Animals were fed concentrated rations twice daily and given ad lib access to hay and water.

Environmental enrichment was provided, including rubber toys and a hollow ball stuffed with hay.

2.6.3 Histopathology

Samples were excised from the skin post-mortem using sterile equipment and immediately stored in 10% sterile buffered formalin in sealed plastic containers. Tissues were then processed to paraffin wax blocks at the Easter Bush Veterinary Pathology department, Royal (Dick) School of Veterinary Studies, sectioned at 4 µm, and stained with haematoxylin and eosin (H&E) following standard protocols.

2.6.4 PCR of blood

DNA was extracted and PCR was conducted by the Non-Vesicular Reference Laboratory at The Pirbright Institute. The real-time PCR assay for CaPV targeted an 89 bp region within the LSDV074 ORF. Each assay used a dual labelled fluorogenic (TaqMan®) probe that allowed the assay to be performed in a closed-tube format minimising the potential for cross-contamination of post-PCR products. Marek's disease virus was used as an extraction control.

2.6.5 Quantification of LSDV in skin via qPCR

DNA was extracted from the defrosted 2mm skin punch biopsies using the Digestion Workflow from the MagMAX™ CORE Nucleic Acid Purification Kit (Applied Biosystems). The experiment was performed according to manufacturer's instructions using a KingFisher Flex magnetic particle processor (Applied Biosystems). In brief, plasmids containing LSDV ORF068 (19AEL6VP; Invitrogen) and bovine cytochrome B (19AEL7QP; Invitrogen) were linearised and used to generate standards. The biopsies were digested by adding 90µL of proteinase K buffer (4489111, Life Technologies) and 10µL proteinase K (25530049, Life

Technologies) to the skin biopsy. The sample was incubated for 2 h at 55°C. Tubes were lightly vortexed during incubation and centrifuged briefly at the end of incubation. 20µL of MagMAX Core magnetic beads (Applied Biosystems) were added to the lysate and mixed by pipetting. 100µL of the bead and lysate mixture was transferred to the KingFisher deep well plates (Life Technologies) containing 350µL of lysis solution and 350µL of binding solution. Extraction was done as outlined in the MagMAX core extraction kit and the MagMAX_CORE_No_Heat protocol was used to extract DNA from the samples. DNA was eluted in 50µL of elution buffer. A TaqMan multiplex PCR assay designed to amplify LSDV068 using forward and reverse primers 5' GGCGATGTCCATTCCCTG 3' and 5' AGCATTTCATTTCCGTGAGGA 3' respectively and a probe - ABY 5' CAA TGG GTA AAA GAT TTC TA3' QSY was used to detect LSDV. A forward primer – GTAGACAAAGCAACCCTTAC and a reverse primer -GGAGGAATAGTAGGTGGAC for bovine Cytochrome B and a probe - FAM 5'TTA TCA TCA TAG CAA TTG CC 3' MGBNQF was used for the detection of bovine cytochrome B. TaqMan Multiplex master mix (4461884, Life Technologies) was used with MUSTANG PURPLE as the passive reference dye. In brief, the reaction setup was as follows; 5µL of template was used in a total of 20µL reaction. Final primer concentrations were 500nM and 250nM for probes. An initial denaturation at 95°C for 20 sec was carried out and 50 cycles of denaturation at 95°C for 15 sec, annealing and signal acquisition at 58°C for 1 min were done. Viremia was analysed in duplicate, and results presented as mean copies per 2mm biopsy.

qPCR data for skin from the CIVS studies were generated by Dr. Henry Munyanduki.

2.6.6 Flow cytometry

Antibody cocktails were prepared in an MBSC, using 0.5% bovine serum albumin (BSA)/PBS. 100µl heparinised whole blood from each animal was aliquoted in triplicate into

empty FACS tubes and mixed with 30µl antibody cocktail, made of CD3 (MM1a) conjugated with AF488 (Alexa Fluor™ 488 Antibody Labeling Kit), CD14 (CC-G33, BioRad) conjugated with AF647 (Alexa Fluor™ 647 Antibody Labeling Kit), CD40 (IL-A158, Immunological Toolbox) conjugated with PE (Lightning Link, Novus Biologics), and γδ TCR (GB21a, Washington State University) conjugated with PB (Pacific Blue Antibody Labeling Kit). Blood from CV1 and CV6 cattle were used as single colour (SC), fluorescence minus one (FMO) and unlabelled controls. The blood samples and antibodies were incubated for 30 min at RT in the dark. 2ml eBioscience™ Fix/Lyse Solution (10×) diluted 1:10 in sterile water was added to each tube to lyse the red blood cells. The tubes were incubated at RT for 30 min in the dark. 100µl of vortexed Invitrogen™ 123count eBeads™ (Fisher Scientific) were added to each tube (excluding SC and FMOs). Samples were read on the LSR Fortessa. Compensation was run on single colour controls. Data was analysed in FCS Express 7 (De Novo software).

2.6.7 Serum ELISA

Serum samples from CIVS were analysed using a commercially available kit, ID Screen Capripox Double Antigen ELISA (IDVet, Montpellier, France). The ELISA was carried out according to the manufacturer's instructions. Samples with an S/P% ratio of ≥ 30% were defined as positive.

2.6.8 IFN-γ release assay

200µl whole heparinised blood from each animal was stimulated with either the positive controls (pokeweed mitogen (PWM) or negative controls (PBS) or LSDV Neethling (MOI 1). These cells were incubated overnight at 37°C after which the blood was centrifuged at 300 × g for 10 min and the supernatants were harvested and stored at -80^{o}C.

ELISA plates were coated with 50 µl/well of 5 µg/mL of mouse anti-bovine IFN-γ antibody (MCA2112, Bio-Rad Antibodies) by overnight incubation at 4°C. Plates were washed five times with washing buffer (PBS and 0.05% Tween20 [Thermo Fisher Scientific]). 100µl/well of blocking buffer (PBS, 0.05% Tween 20, 0.5% BSA) were added and plates incubated for 1h at 37°C. Blocking buffer was removed and 100 µl/well of samples and IFN-γ standards (recombinant bovine IFN-γ; BioRad Antibodies) starting at 300 ng/mL followed by two-fold dilutions added. Samples were diluted at 1:2 in carrier buffer (PBS, 0.05% Tween 20, 0.5% BSA). Plates were incubated for 1h at 37°C, then washed five times with washing buffer. Biotinylated mouse anti-bovine IFN-γ antibody (MCA1783B; Bio-Rad Antibodies) diluted to 0.5 µg/mL in carrier buffer was added (50µl/well) and plates incubated for 1 h at 37°C. After five washes with washing buffer, streptavidin-HRP conjugate (N-100, Thermo Fisher Scientific) diluted 1:1500 in carrier buffer was added (50 µl/well) and incubated for 30 min at 37°C. After five final washes, 50 µl/well of 3,3',5,5'-tetramethylbenzidine (TMB) substrate (Thermo Fisher Scientific) was added and incubated at RT for 5 min. Substrate development was followed by the addition of stop solution (1N H_2S0_4). Optical densities were immediately read in a spectrophotometer at 450 nm.

2.6.9 Fluorescent virus neutralisation test (FVNT)

MDBK cells were seeded (3×10^5/ml) in 96 well plates and incubated overnight at 37°C in a 5% CO_2 atmosphere and used at 80-90% confluency. All sera samples, positive (LIMT Calf 5) and negative (NVRL, M008) controls were heat-inactivated on a heat block at 56°C for 30 min. Serum samples were diluted 1:10 in cell culture medium (DMEM, 2.5% heat-inactivated FBS, 100 units/ml penicillin, and 100µg/ml streptomycin). Two-fold serial dilutions from 1:10 to 1:1280 were prepared from the test sera and all samples received an equal volume (110µl) of recombinant EGFP-095-LSDV Neethling virus (7×10^2 pfu/ml)

and were incubated for 1h at 37°C in a 5% CO2 atmosphere. A mock (media) control was included which did not receive any sample or virus and a virus-only control was added to samples. All samples and controls were tested in duplicate. FVNT data were generated by Dr Petra Fay.

In corresponding wells, 150µl of the controls and serum samples were added to the prepared MDBK cells in 50µl of cell culture medium (DMEM, 2.5% heat-inactivated FBS, 100 units/ml penicillin, and 100µg/ml streptomycin). Plates were incubated at 37°C in a 5% CO2 atmosphere for 5 days. To interpret the results, fluorescent foci were counted using a fluorescent UV light microscope (Olympus CKX53). The complete neutralising antibody titre was calculated as the highest dilution at which no foci were identified.

2.7 Statistical analysis

GraphPad Prism 8.3.0 (GraphPad Software, San Diego, USA) was used for graphical and statistical analysis of data. Tests including T-tests and mixed effects models were conducted to determine statistical significance in data sets analysed. p-values < 0.05 were considered to be statistically significant.

3

Collection and characterisation of *Stomoxys calcitrans* secreted saliva

3.1 Introduction

The saliva of blood-feeding arthropods has been shown to facilitate the acquisition of a blood meal by the arthropod, and to influence the transmission, dissemination and/ or disease manifestation of co-administered pathogens. Much of the work in the field of insect saliva has focused on mosquitoes, with other blood-feeding arthropods such as flies and *Culicoides* biting midges less well studied. This chapter examines the composition of the mechanical vector *Stomoxys calcitrans* (stable fly) saliva, and its impact on the infectivity and replication of lumpy skin disease virus (LSDV).

When haematophagous arthropods attempt to acquire a blood meal from a host they face a number of challenges. These include the activation of the host's immune response against the breaching of the skin barrier, blood clotting at the feeding site, and triggering of the pain response, thus alerting the host to the feeding activity resulting in displacement of the arthropod from the host. Saliva of blood feeding arthropods has been demonstrated to circumvent these challenges by containing a cocktail of anti-coagulants, anaesthetics, and other pharmacologically active compounds (Fontaine et al., 2011). In addition to assisting the arthropods feeding activity, saliva has been demonstrated to enhance infectivity of arthropod-transmitted viruses, such as WNV (Styer et al., 2011), DENV

(Schmid et al., 2016), SFV (Pingen et al., 2017), and BTV (Pages et al., 2014). Viruses are transmitted by insect vectors biologically (where part of the replication cycle of the virus occurs within the vector) or mechanically (where the vector just carried the virus from one host to another). The impact of vector saliva on biologically transmitted viruses has been widely researched, but very little is known about the role of insect saliva on the transmission and disease manifestation of mechanically transmitted viruses. Components of saliva known to influence viral disease outcome vary between insects. Examples of these proteins include *Aedes aegypti* venom allergen-1, that enhance viral replication in macrophages and dendritic cells (Sun et al., 2020), and *Aedes* sialokinin, which increases blood vessel permeability and availability of virus permissive cells (Lefteri et al., 2022). This indirect modulation of the local host immune response is a mechanism which could be equally relevant to mechanically transmitted viruses.

A reliable method for collecting arthropod saliva which minimises contamination is crucial for research into the role of salivary components. A common method used to collect secreted mosquito saliva is stimulated salivation into capillary tubes filled with media or oils (Anderson et al., 2010). However, this process is time consuming, with low yields of salivary proteins gained for the time expended on collection. As an alternative to secreted saliva, some studies have used salivary gland extract (SGE) instead. This involves the careful dissection of the salivary glands from insects before the glands are macerated and the mixture filtered to remove cellular debris. SGE of *S. calcitrans* has been used as a substitute for pure secreted salivary proteins to study the proteome and transcriptome (Wang et al., 2009) of the salivary gland of the fly, in addition to the effect of the components of SGE on the bovine immune response (Swist et al., 2002, Ameri et al., 2008). The unavoidable issue with SGE, however, is that the final product is highly likely to be contaminated with non-

secreted or structural fly proteins. Additionally, dissecting the salivary glands from the insects requires an investment of considerable amount of time, knowledge of the anatomy of the arthropod at hand, skill, and dexterity for the return of low salivary protein yields. A methodology that collects large quantities of secreted saliva proteins from *S. calcitrans* would be invaluable for research into the interactions between the vector, their hosts, and pathogens they can transmit.

Previous work on *Culicoides* midges (well-known biological vectors) developed a method for the consistent collection of large amounts of secreted salivary proteins through the adaption of a heated membrane feeding system (Langner et al., 2007, Cooke, 2018). The 2007 system used 10% sucrose soaked Durapore membranes enclosed between Parafilm™ on top of an inner glass chamber filled with horse blood, warmed to 37°C by warm water circulation in the outer glass chamber. 5000 *Culicoides nubeculosus* midges were fed on the filters over 3 days, for 20-30 minutes at a time, with rest periods in between. In contrast, the protocol from 2018 replaced the glass-chamber system heated by water circulation with a Hemotek system and added additional layers of Parafilm™ to prevent perforation of the lower fluid reservoir, aiming to reduce potential for contamination of the secreted saliva sample whilst leaving midge feeding efficiency unchanged. Furthermore, endotoxin free water was used to fill the fluid reservoir of the heated feeding system and soak the Durapore™ membrane instead of heparinised horse blood and 10% sucrose respectively. Similar numbers of *Culicoides sonorensis* per pot were then fed on the membranes, but for 12 minutes per pot. Both methods resulted in successful collection of secreted midge salivary proteins.

The aims of this chapter were to adapt the artificial membrane feeding system from 2018 to collect *S. calcitrans* secreted saliva, to identify and quantify the proteins present in *S.*

calcitrans secreted saliva, and to compare this sialome to that previously described for other blood-feeding arthropods. The last aim was to assess the impact of *S. calcitrans* secreted saliva on LSDV in vitro.

3.2 Results

3.2.1 Optimising a membrane feeding system for the collection of *S. calcitrans* secreted saliva.

A method for collecting *S. calcitrans* secreted saliva was developed by modifying the previously described membrane feeding system based method used for the collection of secreted saliva from *Culicoides* midges (Cooke 2018). A Hemotek membrane feeding system (MFS) was used as the basis for the *S. calcitrans* saliva collection method. These MFSs are widely used in research settings to enable haematophagous arthropods to feed and to maintain colonies without using live animals, but are not the feeding method of choice for colonised *S. calcitrans*. The Hemotek MFS consists of a reservoir, usually containing defibrinated blood or sucrose solution, sealed with Parafilm™, which acts as a skin substitute, and attached to a heating source to enable the blood to be warmed to 37°C. Plastic pots covered with fine mesh and containing arthropods are then placed on the Parafilm™ covering the reservoir, enabling feeding to take place.

Initially the propensity for *S. calcitrans* flies to feed on the Hemotek™ MFS was examined, since this methodology is not used for maintenance feeding of this species. Approximately 20 laboratory-reared male and female *S. calcitrans* at an average of 14.5 days post-eclosion (range: 10-19 days) were starved the previous day then collected via an aspirator and transferred to a plastic pot (53mm diameter) and closed with fine mesh. The flies were

then placed on an MFS containing defibrinated horse blood for 15 minutes. Flies were then examined visually for swollen and reddened abdomens, indicating feeding had taken place. The thin layer of Parafilm™ was also examined for perforations created by the flies' proboscises. Approximately 75% of flies had reddened abdomens and successfully fed, indicating they were capable of feeding on an MFS.

In order to collect secreted salivary proteins, they must be captured on a hydrophilic Durapore™ membrane. The capability of the flies to feed on the MFS with the membrane included was examined. When the fly pots were placed on the reservoir containing the membrane, as demonstrated in Figure 3.1, they seemed to be drawn down by the heat of the reservoir, and when feeding occurred it happened in small areas, with flies grouping together. When the overlying layers of Parafilm™ were removed and carefully stretched, small circular perforations were clearly seen in clusters, matching the feeding behaviour observed. This showed that *S. calcitrans* were capable of feeding on a fully assembled MFS that could collate their salivary proteins.

With successful feeding of potted flies on Durapore® membranes confirmed, the system was then optimised to maximise the yield of saliva. A vital way to ensure the collection of high yields of salivary protein is to stimulate repeat feeding by the flies, therefore adaptations to the system were trialled to achieve this. The feeding reservoirs were prepared according to the standard methodology by securing an unstretched layer of Parafilm™ with a rubber ring (Figure 3.2.A-C), sealing the inner chamber before the reservoir was filled with endotoxin free water (Fisher Scientific) (Figure 3.2.D). This was followed by a Durapore™ PVDF 0.2 μm membrane (Millipore) overlaid with two thinly stretched layers of Parafilm™ to allow for penetration by the proboscis and feeding without contamination of the membrane by non-salivary proteins (Figure 3.2.E). Excess Parafilm™

was trimmed away from the completed reservoir insert (Figure 3.2.F) before it was screwed into the main Hemotek™ apparatus and allowed to warm to 37°C (Figure 3.2.G). Feeding flies for 15 minutes using Durapore™ membranes that had been soaked in distilled water before assembly of the MFS was trialled but did not prompt repeat feeding, with only one perforation recorded. ATP stimulates the probing and engorging response in mosquitoes (Klun et al., 2013) (Luo, 2014) and in *S. calcitrans* (Ascoli-Christensen et al., 2008), prompting trials of a methodology that soaked the Durapore™ membrane in 1mM ATP/endotoxin free water solution by dipping the membrane in the solution briefly. This resulted in successful repeat feeding behaviour by the flies over the 15 minutes, shown by the increase in perforations of the Parafilm™.

Once repeat-feeding behaviour had been stimulated in the flies, the number and frequency of feeds was optimised. Maintaining flies in the plastic pots between feeds was compared to returning the flies to the large BugDorms in between feeding session, which required repeated aspirator collection. After three days of the pot-maintained flies being fed on blood via Hemotek daily, there were only 11/27 flies alive. Two days later, all were dead. Saliva collections take at least 10 days to conduct, so keeping the flies in pots was not a viable methodology. The process that resulted in the most feeding behaviour and least mortality was when the flies were starved the day before in the cage, captured into the small pots, exposed to the membrane, then released back into the cage to rest and blood feed. In order not to overstress the flies, this process was conducted in a rotating fashion on three separate cages of similarly aged flies i.e., on any given day, one cage was being used for saliva collection, one was starved in preparation for collection the next day, and one was blood fed.

The final optimised methodology consisted of flies being starved the day before the potted flies were placed onto the MFS for approximately 15 minutes per pot. After the MFS was fed on 3-4 times by a pot of flies, a sterile needle and forceps were used to remove the Parafilm™ covering the membrane layer, being careful not to pierce the lower Parafilm™ layer (Figure 3.2.J-K). The fed-on Durapore™ membranes were placed into PBS using sterile forceps and stored at 4°C.

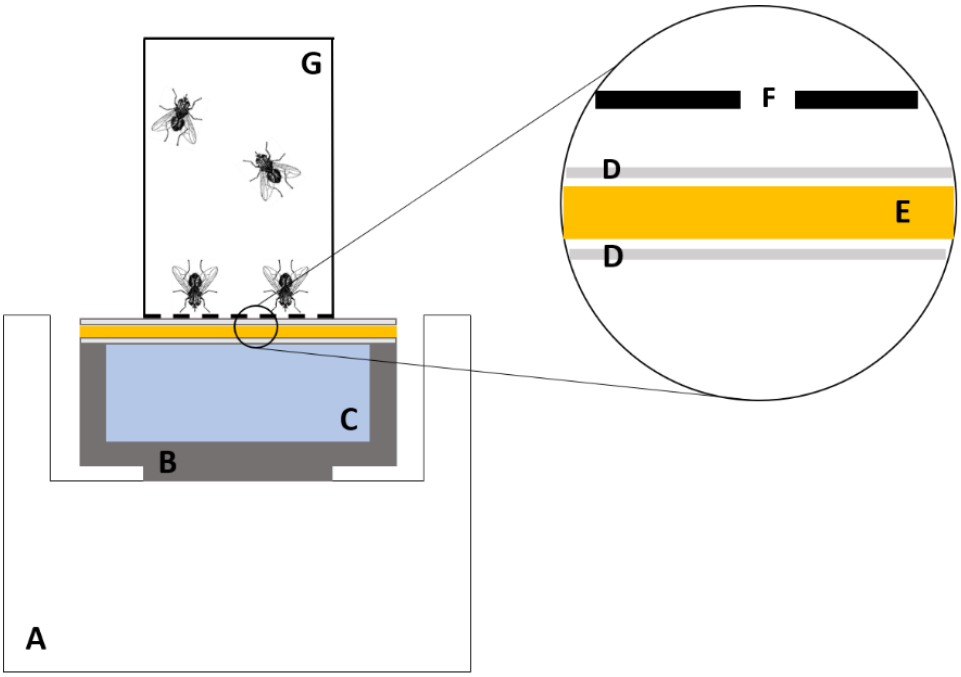


Figure 3.1- *S. calcitrans* saliva collection system

A: Hemotek™ base- heats the system to 37°C; B: screw in reservoir; C: distilled water- to conduct heat to the membrane; D: Parafilm™ – prevents contamination of the membrane with non-salivary proteins and seals water in the reservoir; E: Durapore PVDF 0.2 µm membrane soaked in ATP solution; F: fine netting to allow fly feeding; G: transparent 4cm diameter pot containing *S. calcitrans* flies

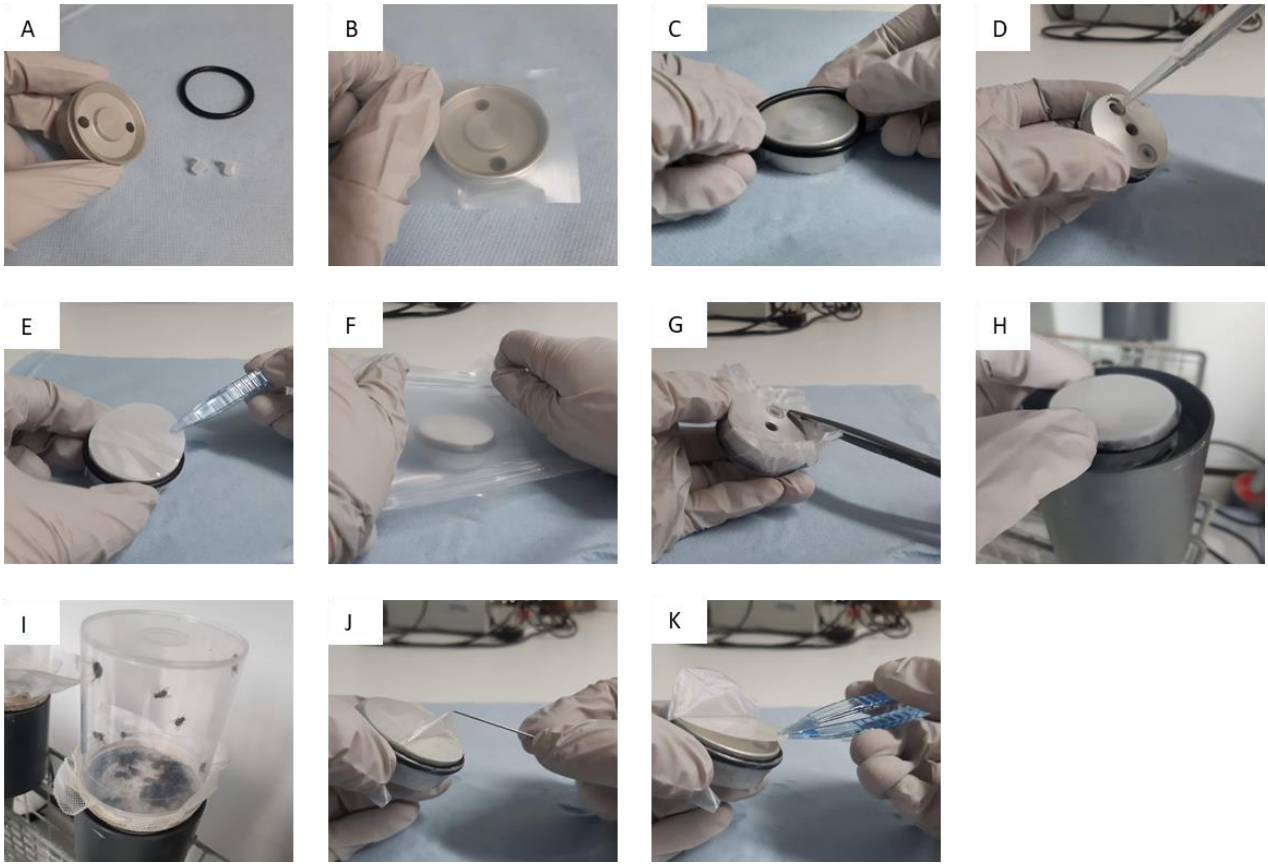


Figure 3.2- Constructing the *S. calcitrans* saliva collection system

The pictures show the order of construction of the Hemotek reservoir to collect salivary proteins, and the dismantling of the system to collect the membrane holding the protein deposits. The components required are a metal reservoir, a black rubber O-ring and two plastic plugs (A). An unstretched piece of Parafilm™ is then placed on the top (B) and secured with the O-ring (C). One of the plugs is put into place before the reservoir is filled with distilled water and the second plug inserted (D). The Durapore™ membrane was dipped in 1mM ATP/dH2O using sterile tweezers and placed on the unstretched Parafilm™ (E). Two layers of thinly stretched Parafilm™ were wrapped over the top (F), avoiding air bubbles, and the excess was trimmed away from the reservoir (G). The completed reservoir was screwed into the FU1 feeder and power pack (H), and the potted flies were placed net side down and allowed to feed (I). After feeding, the stretched Parafilm™ was removed using a sterile syringe needle (J). The fed on Durapore™ membrane was retrieved using sterile tweezers and placed in a Falcon tube ahead of salivary protein collection and concentration (K).

3.2.2 Quantification and visualisation of secreted *S. calcitrans* saliva

Saliva collection from *S. calcitrans* was carried out using this methodology. The collection occurred over 9 days, and 38 Durapore™ membranes were fed on. After collection, the saliva sample was concentrated to approximately 1000 µl using Vivaspin 20 centrifugal concentrators with a 3kDa cut-off and the proteins quantified using the Pierce™ BCA

Protein Assay Kit (ThermoFisher Scientific) according to manufacturers' instructions. The first collection contained 186 µg/ml protein (Table 3.1).

Secreted saliva collection from *S. calcitrans* has not been reported previously. To determine if secreted saliva had been successfully collected, 15µl of concentrated sample from the first collection was separated on a 15% SDS-PAGE gel and the protein profile was visualised by silver staining (Figure 3.3.A). Several proteins of varying sizes were detectable within the material collected from the membrane feeding system. This indicated that this novel methodology to collect *S. calcitrans* saliva was able to obtain proteins secreted during insect feeding.

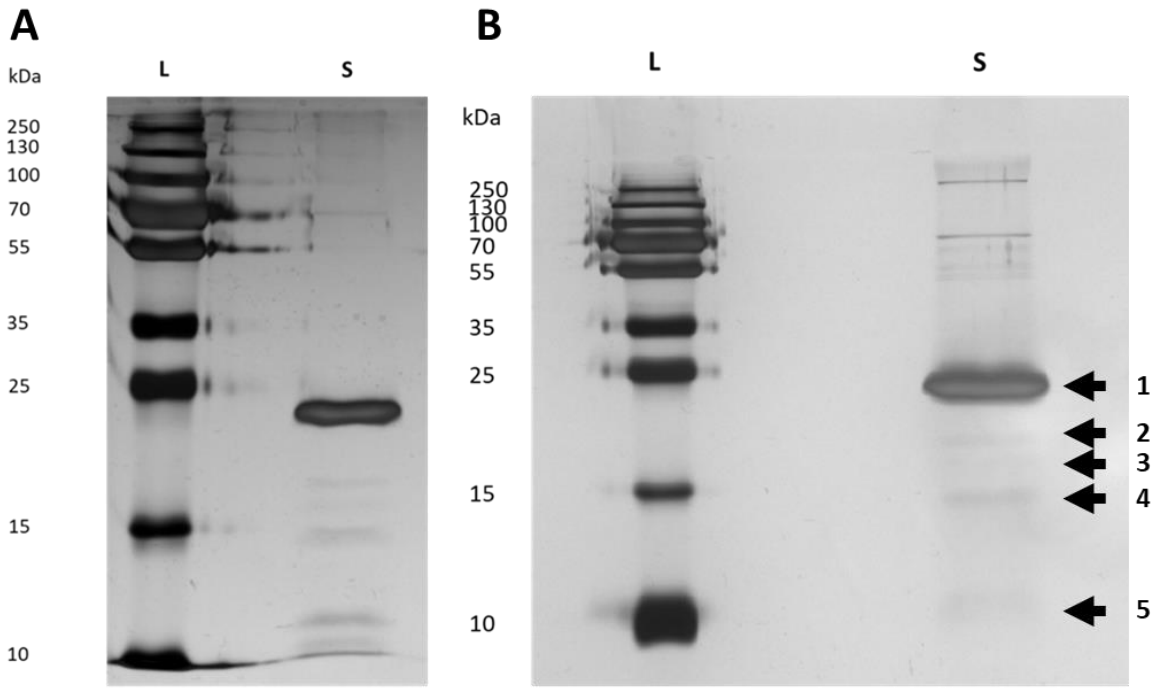


Figure 3.3: The protein profile of proteins in *S. calcitrans* saliva

Secreted saliva (S) was collected and concentrated from *S. calcitrans* (A is the first collection, B is representative of the three collections) and was analysed on 15% SDS/PAGE gel before being visualised by silver staining. PageRuler Plus was used as the ladder (L).

Collections were then repeated twice more to increase the amount of secreted saliva proteins (details in Table 3.1). Saliva collection 3 was used for the in vivo work presented in this thesis (Chapter 5).

Over the three collections, a minimum of 5 salivary protein bands were consistently and clearly visible, shown in the representative profile in Figure 3.3.B. The most abundant protein was detected at 23-24kDa. Four additional clusters of proteins detected with molecular weights between 11-13 kDa, 15-19 kDa, 50-70 kDa, and about 250 kDa were present at lower quantities.

Table 3.1 – *S. calcitrans* secreted salivary protein quantification

Collection number	Number of membranes collected	Number of feeding episodes (times pots of ~25 flies of mixed sex were fed on membranes)	Total protein quantification (µg per approx. 1ml final volume of saliva sample)
1	38	124	186
2	~50	min. 252	107
3	144	260	380

3.2.3 *S. calcitrans* saliva contains a variety of proteins, including those with immunoreactive properties

The protein bands present on the polyacrylamide gel of the first collection suggested that secreted saliva had been successfully collected using the MFS methodology. In order to identify the proteins present within the collected material, mass spectrometry was used to analyse whole *S. calcitrans* saliva from the first collection. When this was returned

successfully, subsequent collections were also sent for mass spectrometry, as whole saliva and as slices of Coomassie gels. The proteins identified in the whole saliva are listed in Table 3.2, and their presence or absence in each saliva collection is noted. The top ten most abundant proteins (defined by count of spectra) present in every collection were further annotated with their putative function (Table 3.3). The analysis showed the presence of proteins with immunoreactive potential such as Antigen-5, as well as many *S. calcitrans* proteins of unknown function.

Table 3.2: *S. calcitrans* salivary proteins

Protein Accession Number	Protein description	Presence in saliva collection
tr|Q7Z0B5|Q7Z0B5_STOCA	Antigen 5	1, 2, 3
tr|A0A1I8PC31|A0A1I8PC31_STOCA	SCP domain-containing protein	1, 2, 3
tr|A0A1I8Q1A7|A0A1I8Q1A7_STOCA	Uncharacterized *Stomoxys calcitrans* protein	1, 2, 3
tr|A0A1I8PUN2|A0A1I8PUN2_STOCA	Uncharacterized *Stomoxys calcitrans* protein	1, 2, 3
tr|A0A1I8Q6W6|A0A1I8Q6W6_STOCA	Alpha-amylase	1, 2, 3
tr|A0A1I8PV60|A0A1I8PV60_STOCA	Uncharacterized *Stomoxys calcitrans* protein	1, 2, 3
tr|A0A1I8PU36|A0A1I8PU36_STOCA	Peptidase S1 domain-containing protein	1, 2, 3
tr|A0A1I8P7C1|A0A1I8P7C1_STOCA	Carboxylic ester hydrolase	1, 2, 3
tr|A0A1I8PSA1|A0A1I8PSA1_STOCA	Lipocln_cytosolic_FA-bd_dom domain-containing protein	1, 2, 3
tr|A5WXR7|A5WXR7_STOCA	Putative 13.7 kDa secreted salivary gland protein	1, 2, 3
tr|A5WXR8|A5WXR8_STOCA	Putative 15.6 kDa secreted salivary gland protein	1, 2, 3
tr|A0A1I8PGD9|A0A1I8PGD9_STOCA	Uncharacterized *Stomoxys calcitrans* protein	1, 2, 3
tr|A0A1I8Q114|A0A1I8Q114_STOCA	Carboxylic ester hydrolase	1, 2, 3
tr|A0A1I8NQD5|A0A1I8NQD5_STOCA	C-type lectin domain-containing protein	1, 2, 3
tr|A0A1I8PI66|A0A1I8PI66_STOCA	Uncharacterized *Stomoxys calcitrans* protein	1, 2, 3
tr|A0A1I8NWI4|A0A1I8NWI4_STOCA	Uncharacterized *Stomoxys calcitrans* protein	1, 2, 3
tr|A0A1I8Q544|A0A1I8Q544_STOCA	Peptidase S1 domain-containing protein	1, 2, 3
tr|A0A1I8QE72|A0A1I8QE72_STOCA	Endonuclease_NS domain-containing protein	1, 2, 3

tr|A0A1I8Q0V7|A0A1I8Q0V7_STOCA	Lipase domain-containing protein	1, 2, 3
tr|A0A1I8PQD6|A0A1I8PQD6_STOCA	Uncharacterized *Stomoxys calcitrans* protein	1, 2, 3
tr|A0A1I8PQI3|A0A1I8PQI3_STOCA	Uncharacterized *Stomoxys calcitrans* protein	1, 2, 3
tr|A0A1I8Q1H9|A0A1I8Q1H9_STOCA	P/Homo B domain-containing protein	1, 2, 3
tr|A0A1I8Q1I4|A0A1I8Q1I4_STOCA	P/Homo B domain-containing protein	1, 2, 3
tr|A0A1I8PZ42|A0A1I8PZ42_STOCA	Uncharacterized *Stomoxys calcitrans* protein	1, 2, 3
tr|A0A1I8PZ57|A0A1I8PZ57_STOCA	Uncharacterized *Stomoxys calcitrans* protein	1, 2, 3
tr|A0A1I8P1G4|A0A1I8P1G4_STOCA	Peptidase S1 domain-containing protein	1, 2, 3
tr|A0A1I8PR12|A0A1I8PR12_STOCA	Transferrin	2, 3
tr|A0A1I8NR78|A0A1I8NR78_STOCA	Uncharacterized *Stomoxys calcitrans* protein	2, 3
tr|A0A1I8NTR2|A0A1I8NTR2_STOCA	Peptidase S1 domain-containing protein	2, 3
tr|A0A1I8PUP6|A0A1I8PUP6_STOCA	C-type lectin domain-containing protein	2, 3
tr|A0A1I8PU39|A0A1I8PU39_STOCA	Uncharacterized *Stomoxys calcitrans* protein	1, 3
tr|A0A1I8PLP5|A0A1I8PLP5_STOCA	Uncharacterized *Stomoxys calcitrans* protein	1, 3
tr|A0A1I8PLL7|A0A1I8PLL7_STOCA	Uncharacterized *Stomoxys calcitrans* protein	1, 3
tr|A0A1I8PLH0|A0A1I8PLH0_STOCA	Uncharacterized *Stomoxys calcitrans* protein	1, 3
tr|A0A1I8PLN8|A0A1I8PLN8_STOCA	Uncharacterized *Stomoxys calcitrans* protein	1, 3
tr|A0A1I8PQL1|A0A1I8PQL1_STOCA	Uncharacterized *Stomoxys calcitrans* protein	2, 3
tr|A0A1I8PQF4|A0A1I8PQF4_STOCA	Uncharacterized *Stomoxys calcitrans* protein	2, 3
tr|A0A1I8Q5Q1|A0A1I8Q5Q1_STOCA	Uncharacterized *Stomoxys calcitrans* protein	1, 3
tr|A0A1I8PL64|A0A1I8PL64_STOCA	Uncharacterized *Stomoxys calcitrans* protein	1, 2
tr|A0A1I8P4Z0|A0A1I8P4Z0_STOCA	Uncharacterized *Stomoxys calcitrans* protein	1, 2
tr|A0A1I8P599|A0A1I8P599_STOCA	Peptidase S1 domain-containing protein	1, 2
tr|A0A1I8Q0V1|A0A1I8Q0V1_STOCA	Uncharacterized *Stomoxys calcitrans* protein	1, 2
tr|A0A1I8NQQ2|A0A1I8NQQ2_STOCA	C-type lectin domain-containing protein	3
tr|A0A1I8Q1D6|A0A1I8Q1D6_STOCA	Histone H4	3
tr|A0A1I8PLR9|A0A1I8PLR9_STOCA	Histone H4	3
tr|C4N1A2|C4N1A2_STOCA	Histone H3	3
tr|A0A1I8PWA9|A0A1I8PWA9_STOCA	Histone H4	3
tr|A0A1I8NZL0|A0A1I8NZL0_STOCA	Histone H4	3
tr|A0A1I8P6I8|A0A1I8P6I8_STOCA	Peptidase S1 domain-containing protein	3
tr|A0A1I8NWH3|A0A1I8NWH3_STOCA	Peptidase S1 domain-containing protein	3
tr|A0A1I8PKN3|A0A1I8PKN3_STOCA	Uncharacterized *Stomoxys calcitrans* protein	3
tr|A0A1I8Q8X9|A0A1I8Q8X9_STOCA	Uncharacterized *Stomoxys calcitrans* protein	3

tr|A0A1I8PZ44|A0A1I8PZ44_STOCA	Uncharacterized *Stomoxys calcitrans* protein	3
tr|A0A1I8Q4R8|A0A1I8Q4R8_STOCA	Uncharacterized *Stomoxys calcitrans* protein	3
tr|A0A1I8P6C4|A0A1I8P6C4_STOCA	Histone H4	3
tr|A0A1I8QB12|A0A1I8QB12_STOCA	Histone H4	3
tr|A0A1I8PQ52|A0A1I8PQ52_STOCA	Peptidase S1 domain-containing protein	3
tr|A0A1I8P0B4|A0A1I8P0B4_STOCA	Peptidase S1 domain-containing protein	3
tr|A0A1I8PCV8|A0A1I8PCV8_STOCA	Peptidase S1 domain-containing protein	3
tr|A0A1I8NMV9|A0A1I8NMV9_STOCA	Tubulin beta chain	3
tr|A0A1I8QCE9|A0A1I8QCE9_STOCA	Peptidase S1 domain-containing protein	3
tr|A0A1I8P1D1|A0A1I8P1D1_STOCA	SCP domain-containing protein	3
tr|A0A1I8PYF3|A0A1I8PYF3_STOCA	Uncharacterized *Stomoxys calcitrans* protein	3
tr|A0A1I8PYB6|A0A1I8PYB6_STOCA	Uncharacterized *Stomoxys calcitrans* protein	3
tr|A0A1I8PYB8|A0A1I8PYB8_STOCA	Uncharacterized *Stomoxys calcitrans* protein	3
tr|A0A1I8PYD2|A0A1I8PYD2_STOCA	Uncharacterized *Stomoxys calcitrans* protein	3
tr|A0A1I8PYE7|A0A1I8PYE7_STOCA	Uncharacterized *Stomoxys calcitrans* protein	3
tr|A0A1I8PYB0|A0A1I8PYB0_STOCA	Uncharacterized *Stomoxys calcitrans* protein	3
tr|A0A1I8PYE2|A0A1I8PYE2_STOCA	Uncharacterized *Stomoxys calcitrans* protein	3
tr|A0A1I8NXY3|A0A1I8NXY3_STOCA	Uncharacterized *Stomoxys calcitrans* protein	3
tr|A0A1I8Q721|A0A1I8Q721_STOCA	Tubulin alpha chain	3
tr|A0A1I8PKP1|A0A1I8PKP1_STOCA	Tubulin alpha chain	3
tr|A0A1I8PD30|A0A1I8PD30_STOCA	Peptidase S1 domain-containing protein	3
tr|A0A1I8NWE6|A0A1I8NWE6_STOCA	Uncharacterized *Stomoxys calcitrans* protein	3
tr|A0A1I8PSG7|A0A1I8PSG7_STOCA	Uncharacterized *Stomoxys calcitrans* protein	1
tr|A0A1I8NRI3|A0A1I8NRI3_STOCA	Ubiquitin-like domain-containing protein	1
tr|A0A1I8P8W3|A0A1I8P8W3_STOCA	Ubiquitin-like domain-containing protein	1
tr|A0A1I8Q6F5|A0A1I8Q6F5_STOCA	Uncharacterized *Stomoxys calcitrans* protein	1
tr|A0A1I8Q5E1|A0A1I8Q5E1_STOCA	Uncharacterized *Stomoxys calcitrans* protein	2
tr|A0A1I8QBI3|A0A1I8QBI3_STOCA	Beta-galactosidase	2

Table 3.3 The putative function of the top 10 most abundant salivary proteins over the three collections in secreted *S. calcitrans* saliva

Abundance (Count of spectra in collection 1, 2, 3)	**Protein identification**	**Putative function**
209, 321, 792	Antigen 5	In cattle, shown to bind to Fc and F(ab')2 parts of bovine IgG (Ameri et al., 2008).
208, 331, 789	SCP domain-containing protein	Antigen 5 derivative (see above).
44, 63, 64	Uncharacterized *S. calcitrans* protein	Domains are transferrin like. Transferrin binds iron, and transports iron to eggs in some insects. It can also function to reduce oxidative stress (Geiser and Winzerling, 2012).
55, 28, 55	Uncharacterized *S. calcitrans* protein	Domains are peptidase and trypsin like. Peptidases are enzymes that cleave small peptides and trypsin is a serine protease that hydrolyses proteins, found in a wide variety of insects (Lazarevic and Jankovic-Tomanic, 2015).
22, 30, 33	Alpha-amylase	Endohydrolysis of (1->4)-alpha-D-glucosidic linkages in polysaccharides containing three or more (1->4)-alpha-linked D-glucose units (Da Lage, 2018).
31, 20, 16	Uncharacterized *S. calcitrans* protein	Domains are endonuclease like. Endonucleases are enzymes, which were suggested to lower the viscosity of the skin when found in *Culex* saliva (Calvo and Ribeiro, 2006).
21, 11, 11	Putative 15.6 kDa secreted salivary gland protein	Protein has 50% identity to Hematobin secreted by the horn fly (*Haematobia irritans*), which inhibits inflammatory response in macrophages in mice (Breijo et al., 2018).
16, 11, 6	Peptidase S1 domain-containing protein	90% identity to serine protease, serine-type endopeptidase activity. These enzymes cleave peptide bonds in proteins, and have been suggested to have anticoagulant activity for *Tabanus yao* (Xu et al., 2008).
15, 9, 11	Lipocln_cytosolic_FA-bd_dom domain-containing protein	Pigment binding. Likely an invertebrate colouration protein, possibly from the proboscis.
7, 14, 15	Peptidase S1 domain-containing protein	Serine-type endopeptidase activity (see above).

Coomassie stained SDS-PAGE gels from the third collection were conducted, and particular bands were cut out using sterile scalpels, stored in deionised water, and sent for mass spectrometry to try and identify the proteins present. The Coomassie stain was very pale, and only clearly showed the ladder and most abundant protein. Therefore, the ladder and the silver stain of the same collection was used to determine the location of bands and slices (Figure 3.4). The mass spectrometry identified most of the slices as having Antigen-5 or its derivative as the most abundant protein in the slice (by spectra count) (Table 3.4). This could be due to the overwhelming signal of the protein, as it is by far the most dominant protein on the gel. However, it does give further evidence that Antigen-5 is a significant component of *S. calcitrans* secreted saliva.

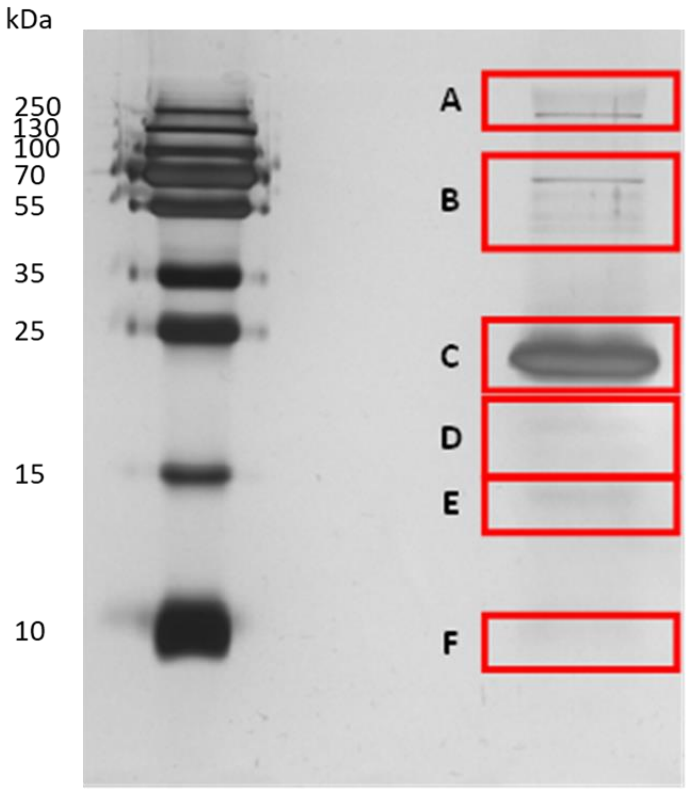


Figure 3.4: Diagram of secreted *S. calcitrans* saliva gel slices sent for mass spectrometry

Secreted saliva (S) was collected and concentrated from *S. calcitrans* and was analysed on 15% SDS/PAGE gel before being stained with Coomassie Blue. PageRuler Plus was used as the ladder (L). The bands were cut out based on a silver stain SDS-PAGE gel of the same collection and sent for analysis.

Table 3.4 Identification of proteins present by band in the *S. calcitrans* SDS-PAGE profile

Gel slice	Protein description	Molecular weight of protein (if identifiable) in kDa (from UniProt)	Abundance (count of spectra)
A	SCP domain-containing protein (Antigen 5 derivative)	29.069	44
	Antigen 5	28.940	41
	Uncharacterized *S. calcitrans* protein (sequences similarities to actin family)	41.822	2
	Uncharacterized *S. calcitrans* protein (sequences similarities to actin family)	41.700	2
	Uncharacterized *S. calcitrans* protein (sequences similarities to actin family)	41.819	2
	Uncharacterized *S. calcitrans* protein (sequences similarities to actin family)	41.818	2
	Uncharacterized *S. calcitrans* protein (sequences similarities to actin family)	41.799	2
B	Uncharacterized *S. calcitrans* protein (transferrin like domain)	142.574	93
	SCP domain-containing protein (Antigen 5 derivative)	29.069	51
	Antigen 5	28.940	51
	Transferrin	71.124	17
	Histone H4	11.381	4
	Histone H4	11.894	4
	Histone H4	11.192	3
	Histone H3	15.328	3
	Histone H4	19.672	2
	Glycerophosphocholine phosphodiesterase	77.514	2

	Glycerophosphocholine phosphodiesterase	77.642	2
	Glycerophosphocholine phosphodiesterase	74.871	2
	Glycerophosphocholine phosphodiesterase	75.000	2
C	SCP domain-containing protein (Antigen 5 derivative)	29.069	453
	Antigen 5	28.940	421
	Uncharacterized *S. calcitrans* protein (likely has serine-type endopeptidase activity)	79.843	17
	Peptidase S1 domain-containing protein (similarity to trypsin domains)	26.684	12
	Peptidase S1 domain-containing protein (similarity to trypsin domains)	28.478	4
D	Antigen 5	28.940	89
	SCP domain-containing protein (Antigen 5 derivative)	29.069	89
	Uncharacterized *S. calcitrans* protein (likely has serine-type endopeptidase activity)	79.843	12
	Lipocln_cytosolic_FA-bd_dom domain-containing protein	21.441	9
	Uncharacterized *S. calcitrans* protein	13.078	3
	Peptidase S1 domain-containing protein (similarity to trypsin domains)	26.684	3
	Uncharacterized *S. calcitrans* protein (with transferrin-like domain)	142.574	2
E	Antigen 5	28.940	77
	SCP domain-containing protein (Antigen 5 derivative)	29.069	72

	Uncharacterized *S. calcitrans* protein	18.501	5
	Uncharacterized *S. calcitrans* protein (likely has serine-type endopeptidase activity)	79.843	2
	C-type lectin domain-containing protein	21.272	2
	C-type lectin domain-containing protein	19.344	2
F	Antigen 5	28.940	47
	SCP domain-containing protein (Antigen 5 derivative)	29.069	44
	Uncharacterized *S. calcitrans* protein (sequences similarities to actin family)	41.700	4
	Uncharacterized *S. calcitrans* protein (sequences similarities to actin family)	41.819	4
	Uncharacterized *S. calcitrans* protein (sequences similarities to actin family)	41.818	4
	Uncharacterized *S. calcitrans* protein (sequences similarities to actin family)	41.799	4
	Uncharacterized *S. calcitrans* protein (sequences similarities to actin family)	41.822	4
	Uncharacterized *S. calcitrans* protein (likely has serine-type endopeptidase activity)	79.843	5
	Peptidase S1 domain-containing protein (similarity to trypsin domains)	27.388	3
	Ubiquitin-60S ribosomal protein L40	14.729	2
	Ubiquitin-like domain-containing protein	17.972	2
	Uncharacterized *S. calcitrans* protein (with a ubiquitin like domain)	60.064	2

3.2.4 Assessing the impact of *S. calcitrans* secreted saliva on LSDV in an MDBK cell line

Arthropod saliva has been shown to influence the infectivity of virus in mammalian cell culture, for example *Culicoides* saliva proteins reduced BTV-1 infectivity for BHK cells 2-6 fold but increased infectivity in KC cells (Darpel et al., 2011). Therefore, the impact of *S. calcitrans* saliva on LSDV infectivity and replication in MDBK cells was assessed in vitro. *S. calcitrans* secreted saliva (11.2 µg salivary protein from each collection) collected as described in section 3.2.2 above, was diluted via fivefold serial dilutions in PBS before being incubated with LSDV for 4 h at room temperature. Each virus / saliva mix was then titrated on MDBK cells. The control (containing the same amount of virus diluted in PBS) with no saliva achieved a titre of 7.7×10^7 pfu/ml (Figure 3.5). The titres of virus incubated with serial dilutions of saliva were all comparable, reaching titres of at least 4×10^7 pfu/ml. This indicates that at the ratios and conditions tested *S. calcitrans* saliva does not affect LSDV infectivity and replication in MDBK cells.

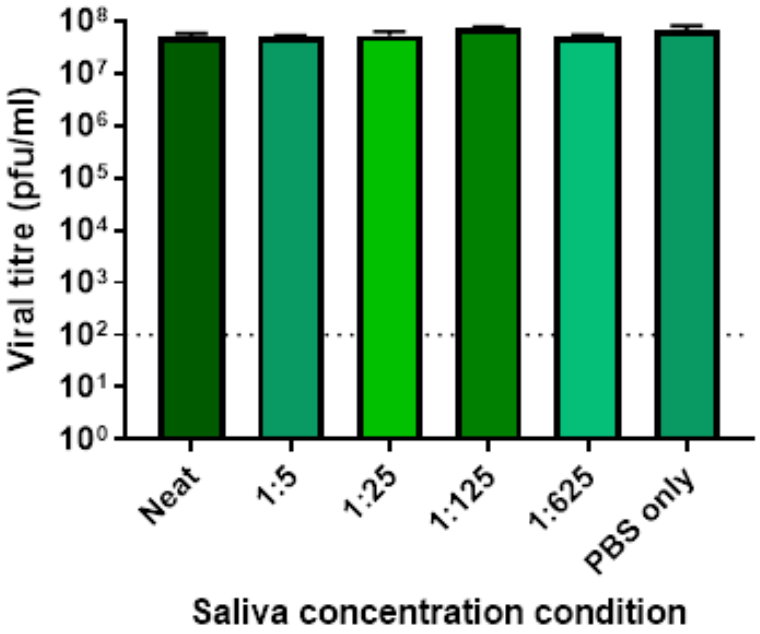


Figure 3.5: *S. calcitrans* saliva does not inhibit LSDV replication in MDBK cells

Neat saliva with the starting amount of approximately 11.2µg protein was diluted in a five-fold dilution series. PBS was used as a negative control. Treatment conditions were incubated with LSDV for 4h before quantifying virus via plaque assay. Data representative of two independent experiments, with saliva from two separate collections.

3.3 Discussion

Previous studies of *S. calcitrans* saliva and its immunoreactive actions have used salivary gland extract as a proxy for secreted saliva (Ameri et al., 2008, Swist et al., 2002). However, homogenated dissected salivary glands very likely contain contaminating non-salivary proteins which may interfere with experimental outcomes. In order to study the influence of *S. calcitrans* saliva on LSDV replication and infectivity, a methodology for collecting high yields of uncontaminated secreted saliva from *S. calcitrans* was needed. A method developed in 2007 used an artificial membrane feeding system to collect the secreted saliva of *Culicoides* midges (Langner et al., 2007), and was later optimised and updated for ease of use, increased yields, and reduction of contamination (Cooke, 2018). Using this protocol as a template, it was optimised for *S. calcitrans* secreted saliva collection, with reprobing by the flies prioritised in order to maximise collection. This was achieved by soaking the membranes in endotoxin free water mixed with ATP, which has been shown to prompt reprobing and refeeding, as well as removing the potentially confounding presence of LPS in the 10% sucrose used in the Langner methodology. There was considerable uncertainty if the methodology of saliva collection could be successfully transferred between highly divergent insect species that differ significantly in size and anatomy of the mouthparts. Stable flies and midges both require feeding on blood to produce eggs, however the primary difference between these insects is that both male and female flies blood feed and blood is their main nutritional source. *S. calcitrans* and *Culicoides* are both telmophages, or “pool feeders”, which means they feed from a blood pool created from blood vessel laceration. However, midges are smaller (creating less trauma to the bitten surface) whereas the larger stable flies have coarse labellar teeth on their proboscis which, upon penetrating the skin, cause a sizeable haematoma which they feed from (Lavoipierre,

1965). The success of this membrane feeding system with two arthropods so different in size and feeding methodology suggests that this saliva collection system could be used for a range of arthropod vectors in order to study the effect of saliva on a wider range of vector-borne pathogens.

Three collections of *S. calcitrans* saliva were successfully made, with a variation in yield due to different numbers of filters used in each collection. After collection via the adapted protocol, the secreted saliva batches were run individually on SDS-PAGE gels and visualised by silver staining for analysis of the protein profile.

Upon collection, concentration and analysis of the saliva using mass spectrometry, multiple proteins known to be found in saliva were identified, such as Antigen-5, peptidase, trypsin, and endonucleases, indicating that we had successfully collected secreted saliva from *S. calcitrans.* This is the first report of secreted saliva collection from *S. calcitrans*. The success of this methodology could allow other researchers who study pathogens transmitted mechanically by *S. calcitrans* including equine infectious anaemia, West Nile fever virus, and Rift Valley fever virus, bovine herpes virus, anthrax, *Anaplasma marginale*, and *Coxiella burnetii,* to explore the role of vector saliva on transmission.

A previous study collected *S. calcitrans* saliva using a salivary gland extract method (Wang et al., 2009). These researchers examined the protein bands using Coomassie blue stained SDS-PAGE gels, which showed approximately 20 clearly visible protein bands including an abundant protein at around 26-27kDa. They also carried out amino terminal sequencing on the excised bands and identified peptides for nine protein bands. Four were identified as being related to thrombostasin, two bands were related to the Antigen-5 family, one was similar to a *Culex* endonuclease, and the last two were a glutamine- rich protein and a protein from the Hyp 16 family. In comparison, the secreted saliva described in this chapter

when run on a silver stained SDS-PAGE gel produced around 11 protein bands. These included an abundant protein at approximately 23-24kDa, and four less abundant clusters of proteins at 11-13 kDa, 15-19 kDa, 50-70 kDa, and about 250 kDa. The greater number of protein bands visible on the SGE gel may be due to contaminating structural debris. When the identities of the protein bands are compared, both had a dominant band at around 23-27 kDa. Amino terminal sequencing established their band to be Antigen-5. In order to confirm the identity of the dominant band in the secreted saliva and ascertain if it was the same as the SGE, and to identify the other proteins present, the secreted saliva was analysed by mass spectrometry.

To identify the proteins present in the secreted saliva collections, whole saliva and gel bands were sent for mass spectrometry analysis by Dr Stuart Armstrong. Genomic experiments have determined that anti-haemostatic and immunomodulatory compounds dominate the sialome of the stable fly (Olafson et al., 2021) and our experimental findings support this, with the secreted saliva containing immunomodulatory proteins such as Antigen-5 and a protein with high identity to hematobin, a protein from horn fly saliva that inhibits the murine inflammatory response (Breijo et al., 2018). The most abundant protein in the whole saliva analysis by far was the protein Antigen-5 and its derivatives. The dominance of Antigen-5 in the secreted saliva mirrored what was seen in the SGE. Antigen-5 (Ag-5) is part of a CAP superfamily that are found in the saliva of many haematophagous arthropods including tsetse flies (Caljon et al., 2009), mosquitoes (Valenzuela et al., 2002, Arca et al., 2007) and sand flies (Lestinova et al., 2017) - as well as in the venom of wasps (Blank et al., 2020). It is also present in the sialome of other haematophagous arthropods like *Tabanus yao* (Ma et al., 2011) and *Culicoides sonorensis* (Lehiy and Drolet, 2014). The function of this family, after remaining undetermined for a long time, is now thought to be

that of copper dependent antioxidant enzymes, that can inhibit oxidative bursts of neutrophils and control platelet aggregation (Assumpcao et al., 2013). Recombinant *S. calcitrans* Ag-5 has been shown to have bovine immunoglobulin binding properties, to be able to bind to the Fc part of IgG, and trigger bovine immune responses by antibodies and memory lymphocytes in calves immunised with Ag-5 (Ameri et al., 2008), and SGE-derived Ag-5 was shown to inhibit proliferation of lymphocytes (Swist et al., 2002). Other proteins with immunoglobulin binding properties found in tick saliva have been suggested to help the tick defend themselves against the host's antibodies and evade the immune system (Wang and Nuttall, 1994). The presence of Antigen-5 could possibly be a factor in the successful dissemination of LSDV on entry into the bovine skin of vaccinated or reinfected individuals by binding to LSDV antibodies and therefore delaying the host immune response. Additionally, suppression of lymphocytes in naïve cattle by Ag-5 in saliva could assist in uninhibited LSDV spread to the lymphatic system and bloodstream.

Other proteins identified in the secreted saliva through mass spectrometry were enzymes: endonucleases, endopeptidases, and carboxylic ester hydrolases (also known as carboxylesterases). The enzymes could aid in blood feeding: for example, endonucleases were suggested to have a feeding matrix viscosity reducing function in *S. calcitrans* (Wang et al., 2009). Proteins with the putative function of serine-type endopeptidases (or serine proteases) have been shown to have anti-clotting actions in *Tabanus* saliva, suggesting a similar action for the *S. calcitrans* enzyme since horse flies and stable flies have a similar life history. Additionally, carboxylic ester hydrolases were heavily implied to be secreted by Asian blue tick larvae into the skin of calves, potentially causing subepidermal capillary dilation and thus increased blood flow (Schleger and Lincoln, 1976). The enzymes could also act to aid transmission of pathogens: an endonuclease in the saliva of sand flies has

been shown to aid in the transmission of leishmania by degrading the extracellular "traps" released by neutrophils at the site of infection (Chagas et al., 2014). Additionally, serine proteases were identified as a component in *Aedes aegypti* saliva that enhanced dengue infectivity in vitro and in vivo via the induction of cell migration (Conway et al., 2014), and in *Culicoides* saliva, that acted to modify the BTV particle directly by cleaving the outer coat protein and generating infectious subviral proteins (Darpel et al., 2011). Therefore, salivary proteins that assist the insect in obtaining a blood meal are utilised by the pathogen to evade the immune response, ensure its transmission, and cause disease. Since similar enzymes and proteins have been found in the secreted *S. calcitrans* saliva, they could also have the potential to achieve these actions. This could mean that the dogma of mechanical delivery of LSDV by *S. calcitrans* could be more nuanced than that of a "dirty needle", as it has historically been assumed to be. However, caution should be taken when comparing salivary component action between vectors, since all vectors have highly specific interactions with their hosts and pathogens, so it cannot be assumed that *S. calcitrans* salivary proteins will have the same actions.

Mass spectrometry analysis also enabled the level of contamination with non-salivary proteins to be observed. A common contaminant of mass spectrometry is keratin, commonly originating from the skin and dust (Hodge et al., 2013). No keratin was present within any of the secreted saliva collections, which suggests that the methodology results in a clean saliva preparation. The presence of transferrin in collections 2 and 3, and proteins with domains similar to those in transferrin could suggest that the saliva sample is contaminated with blood. This would not be unusual finding since the flies had been fed on horse blood, but they had been starved the day before saliva collection. However, the transferrin appeared to be *S. calcitrans* specific, according to UniProt. A homologue of

transferrin has been previously found in insect saliva (Hattori et al., 2015) and could act to transport iron to eggs or to reduce oxidative stress (Geiser and Winzerling, 2012). In the third secreted saliva collection, tubulins and histones were identified, cellular components that would not be unexpected to find in secreted saliva. Collection via secretion rather than maceration of salivary glands aimed to avoid contamination of the collection by cellular proteins from epithelial cells, however since only the third collection seemed to contain cellular proteins, this methodology does still seem to avoid large contamination. Conversely, *S. calcitrans* salivary gland extract has also been found to contain histones, some cytoskeletal proteins, elongation factors, and many ribosomal proteins (Wang et al., 2009). The cytoplasm of salivary gland cells contains a high abundance of ribosomes if metabolically active (Brogna et al., 2002)- this suggests that the salivary gland extract is more contaminated with non-salivary proteins than secreted saliva, and that the secreted saliva has a more representative protein profile for transmission experiments.

With the *S. calcitrans* secreted saliva successfully collected, concentrated and initially characterised, the next step was to explore any impact on LSDV replication and infectivity in MDBK cells (a continuous bovine cell line). Since it is not known what the ratio of LSDV to *S. calcitrans* saliva is when a fly feeds, a range of ratios and concentrations needed to be tested. Four hours of incubation of LSDV with various concentrations of secreted salivary proteins did not enhance viral replication in MDBK cell lines, even at its most concentrated. The saliva also did not appear to reduce infectivity of the virus, consistent with findings where LSDV recovered from the mouthparts of *S. calcitrans* that fed on infected cattle could be titred on cells (Issimov et al., 2020) and in vivo work that shows that LSDV can be spread from donor to recipient successfully via *S. calcitrans* (Sohier et al., 2019). This could begin to imply that if the saliva of the vector has an effect on LSDV infectivity, it is not via

interactions with the virus itself (unlike BTV). However, BTV is a biologically transmitted virus that replicates within *Culicoides* and has a more prolonged exposure to saliva. LSDV, as a mechanically transmitted virus, likely spends much less time exposed to saliva. The impact of *S. calcitrans* saliva on LSDV replication needs to be investigated in more detail via growth curves on a more representative cell line, ideally from primary cell culture and of bovine dermal origin. This cell line is developed and characterised in chapter 4. Furthermore, the saliva might not influence LSDV in vitro, but may in vivo. These theory is examined in chapters 4 and 5.

3.4 Summary

This chapter presents the findings that secreted saliva can be collected from *S. calcitrans* flies in useable concentrations and quantities using a modified artificial feeding system. The saliva contains proteins typical of haematophagous arthropod sialomes, including the protein Antigen-5 in abundance, which has been described as having a bovine immunomodulatory function. The successful collection of *S. calcitrans* secreted saliva allows more detailed investigation of the impact of vector interaction on LSDV infection in bovine cells and on viral infection and the host immune response in vivo.

4

Characterising LSDV replication in primary bovine fibroblasts and keratinocytes

4.1 Introduction

LSDV is a vector borne virus with a strong tropism for the skin. The virus is mechanically transmitted by hematophagous arthropods between cattle, with the virus deposited into the skin of the bovine host during arthropod feeding activity. Like other poxviruses, LSDV's defining clinical feature is the severe multifocal cutaneous nodules. Pathology has been described on internal organs of clinical animals at post-mortem examination, including the respiratory and gastrointestinal tract (OIE, 2017b), they are not a consistent or major feature of the disease, highlighting the cutaneous tropism of LSDV. Microscopically the virus appears able to infect skin cells in vivo, with viral inclusion bodies being observed in fibroblasts and keratinocytes in sections from the cutaneous lumps of infected cattle (Sanz-Bernardo et al., 2020, Prozesky and Barnard, 1982), as well as histiocytic cells resident in the skin.

Despite the importance of the skin in the manifestation of LSD and the replication cycle of the virus, most research into LSDV in vitro is presently carried out in non-skin continuous cell lines. The most common cell lines used are Madin-Darby bovine kidney cells (MDBK) (Fay et al., 2020) and foetal lamb testis cells (OA3.T) (Babiuk et al., 2007). Neither cell line originates from the skin, and the latter is not from the host that LSDV is adapted to. There

is potential that by using a non-representative immortalised cell line, LSDV in vitro research may not accurately reflect the in vivo situation (Kaur and Dufour, 2012). For example, there is evidence that poxviruses behave differently in continuous cells lines compared to primary cells, with the Vaccinia virus (VACV) protein F17 not influencing viral translation in a transformed monkey kidney cell line (Zhang and Moss, 1991) but influencing it when re-investigated in primary human fibroblasts (Meade et al., 2018).

Furthermore, the cell-associated enveloped virion (CEV) of orthopoxviruses such as vaccinia virus, monkeypox virus and variola virus (the etiological agent of smallpox) polymerises actin into filaments at the surface of the infected cell to promote virion exit and spread (Cudmore et al., 1995). This creates long protruding structures called actin tails, some of which have a virion attached to the end. These actin tails have never been observed in LSDV-infected MBDK or OA3.T cells. This may be because LSDV does not form actin tails, or because MDBK and OA3.T cells do not support the formation of actin tails by LSDV. This limitation restricts the usefulness of these cell lines for studying specific areas of LSDV biology, for example, host/virus interactions in the skin. Primary cells are one way of building a more representative cell-based model. Cells isolated from the species and organ of choice, and not transformed into a continuous state, are likely to be most similar to cells in vivo, and thus represent the LSDV infection more accurately.

In this chapter methods for isolating and propagating bovine primary fibroblasts and bovine primary keratinocytes were developed and used to investigate the influence of *S. calcitrans* secreted saliva on LSDV replication and spread in vitro.

4.2 Results

4.2.1 Isolation of bovine primary skin cells

The protocol for isolation of bovine primary fibroblasts (BPF) was developed from previously published protocols describing the isolation of human and bovine fibroblasts (Aasen and Belmonte, 2010, Evans et al., 2014). Briefly, to generate primary bovine fibroblasts, bovine ear pinnae were sourced from a local abattoir, and dermis and epidermis dissociated using Dispase II (Sigma Aldrich), a protease which cleaves fibronectin and collagen IV (Stenn et al., 1989), overnight (Figure 4.1). The dermis was then cut into small pieces and placed in increasing volumes of fibroblast media (DMEM with 10% FBS and 2% penicillin/streptomycin, and 2% amphotericin B) over two days. Once fibroblasts were observed to be attached to the culture vessel, the dermal tissue was removed from the culture. It took approximately 11 d from receiving ear tissue to obtaining monolayers of primary fibroblasts with a bipolar/multipolar elongated spindle shape, typical of dermal fibroblasts. Isolation of BPFs was successful approximately 55% of the time. The fibroblasts maintained a consistent morphology until ~17 passages.

Isolation of bovine primary keratinocytes (BPK) was more difficult, requiring numerous optimisation steps and was successful only 19% of the time. The protocol built upon methods described by Aasen and Belmonte (2010), and Evans et al. (2014) for human and bovine keratinocyte isolation, especially in selecting the optimal culture media and coating matrix for bovine keratinocytes. The most successful method was when the dermis and epidermis of bovine ear pinnae were separated overnight as described above, and the epidermis then macerated before being trypsinised for 10 minutes at 37°C. The mixture was then filtered to remove undigested tissue, centrifuged, and resuspended in media with

2% penicillin and streptomycin, and 2% amphotericin B. The cells were then put onto plates coated with a matrix.

Three different basal media were trialled, with different amounts of serum and variations in supplements. The serum-free KGM2 BulletKit media from Lonza produced colonies of primary keratinocytes most consistently. Cell adherence to the culture vessels was optimised by trialling different coating matrixes including rat tail collagen and Attachment Factor. Best results were obtained using the Coating Matrix Kit (Fisher Scientific), a type I collagen. The time taken to culture keratinocytes from the arrival of ears to keratinocytes ready to infect was about 1 month. The primary keratinocyte cells lasted fewer passages compared to the primary fibroblasts, declining in number and morphology by passage 2-3.

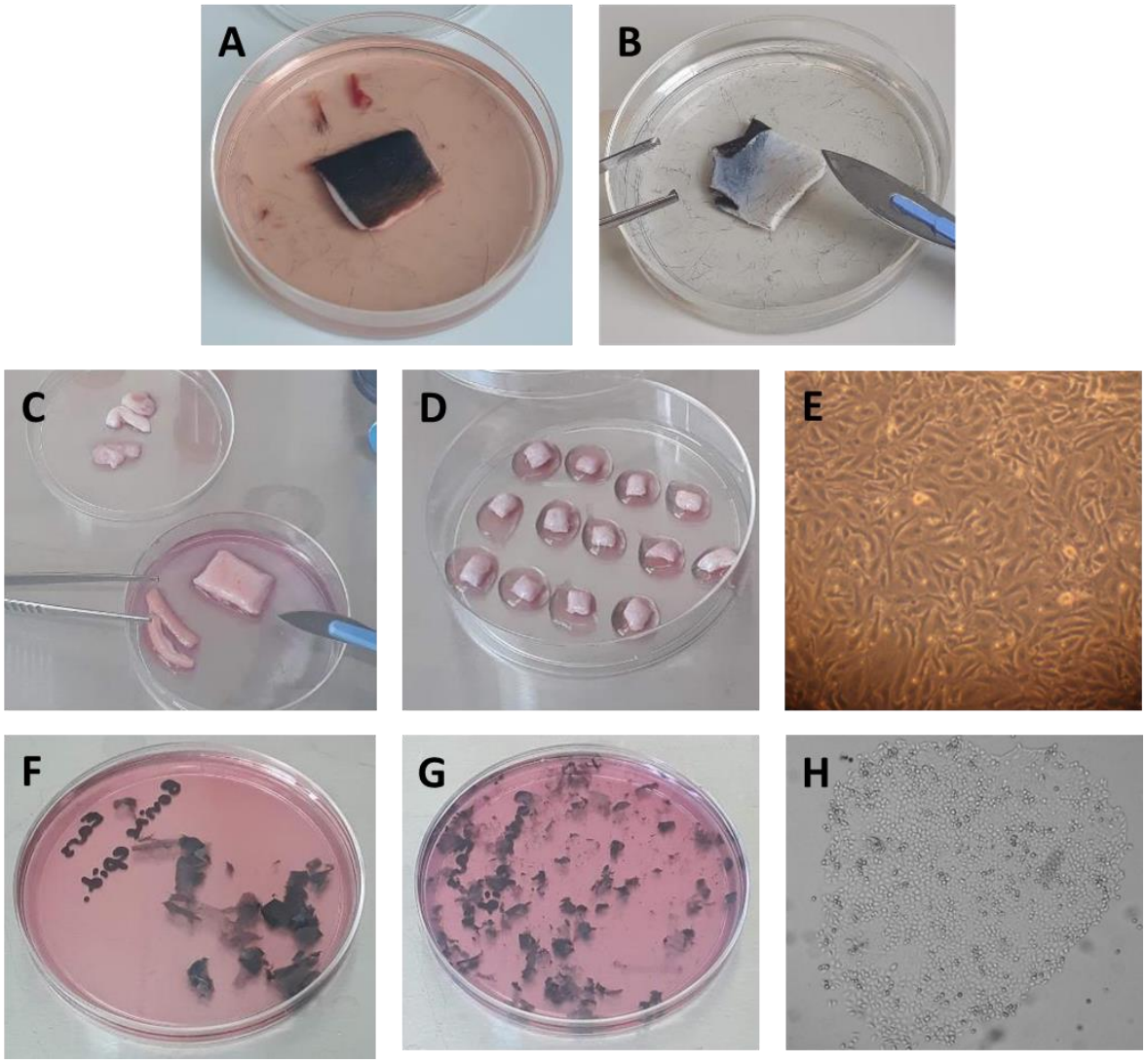


Figure 4.1: Primary fibroblasts and keratinocytes are isolated from bovine ear pinnae

Part of the ear pinnae was cut from the ear (A), before the skin was dissected from ear cartilage (B) then covered in a Dispase II solution overnight before peeling the epidermis away from the dermis. Fibroblasts were prepared by cutting the dermis into strips (C) then small squares, covering with two drops of media (D) and incubating for two days before adding more media and allowing fibroblasts to emerge from the tissue (E). Keratinocytes were isolated by peeling the epidermis away from the dermis (F). The epidermis was then macerated (G) and trypsinised before the undigested tissue was filtered out, and the cell mix was put onto plated tissue culture dishes, allowing colonies to develop (H). E and H were taken on a standard light microscope, at 20x and 4x magnification respectively.

4.2.2 LSDV infection of bovine primary fibroblasts

Once the method for primary fibroblast isolation and growth was optimised, the cells were used to characterise LSDV replication and spread. Cells were infected with LSDV Cameroon strain at an MOI of 5, and subsequent cytopathic effect (CPE) documented. After infection with LSDV the cells began to display typical poxviral cytopathic effect (CPE) after 2 days,

with both rounded and stellate shaped cells visible. (Figure 4.2). By 7 days after infection, the cell monolayer was completely disrupted with many rounded, hyper-refractile cells visible.

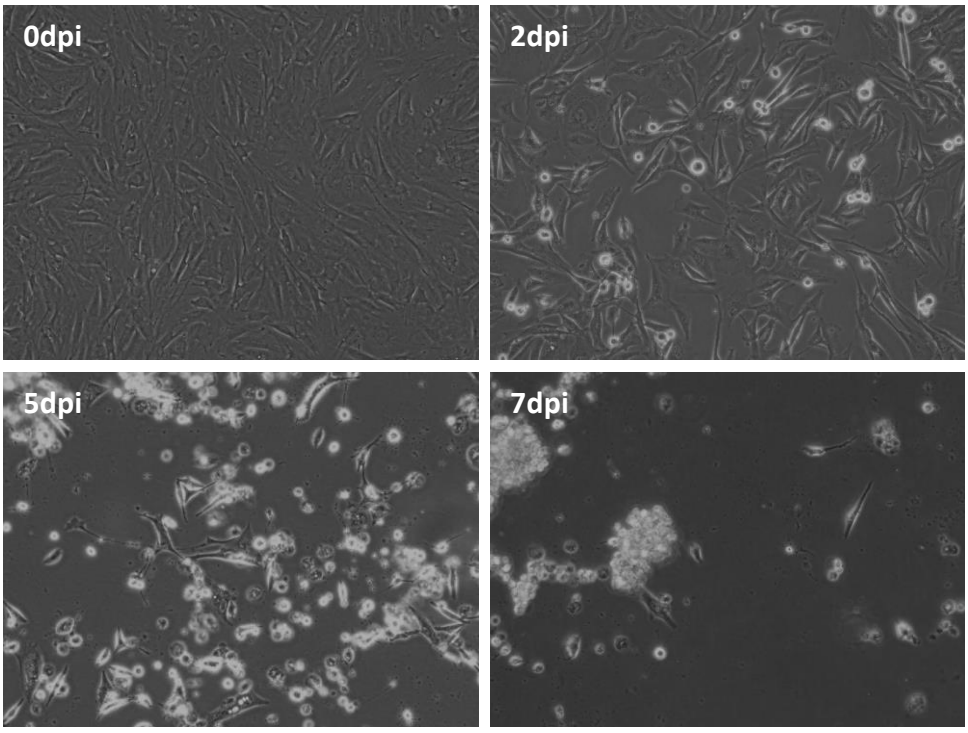


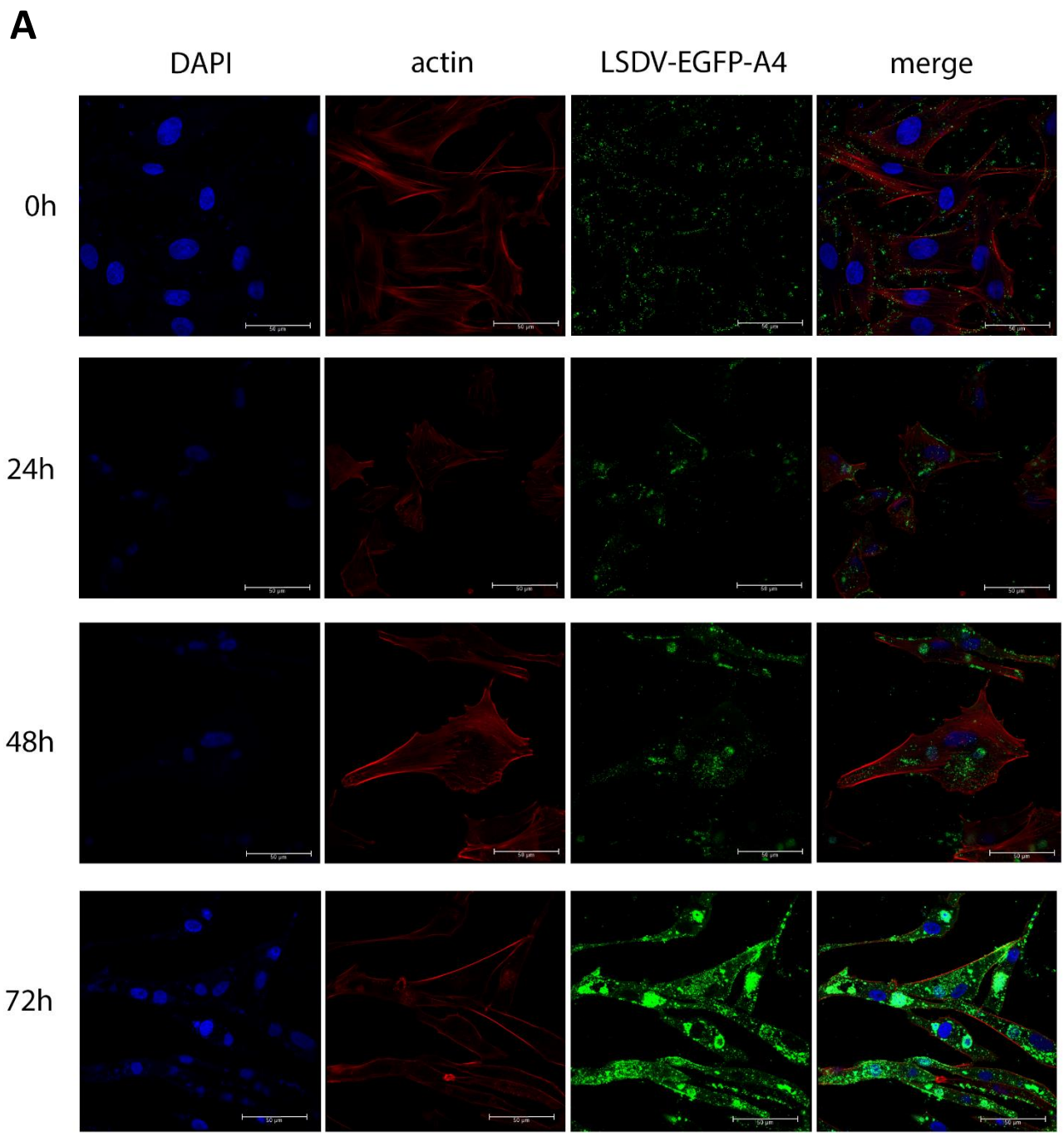
Figure 4.2: Bovine primary fibroblasts display cytopathic effect after infection with LSDV.

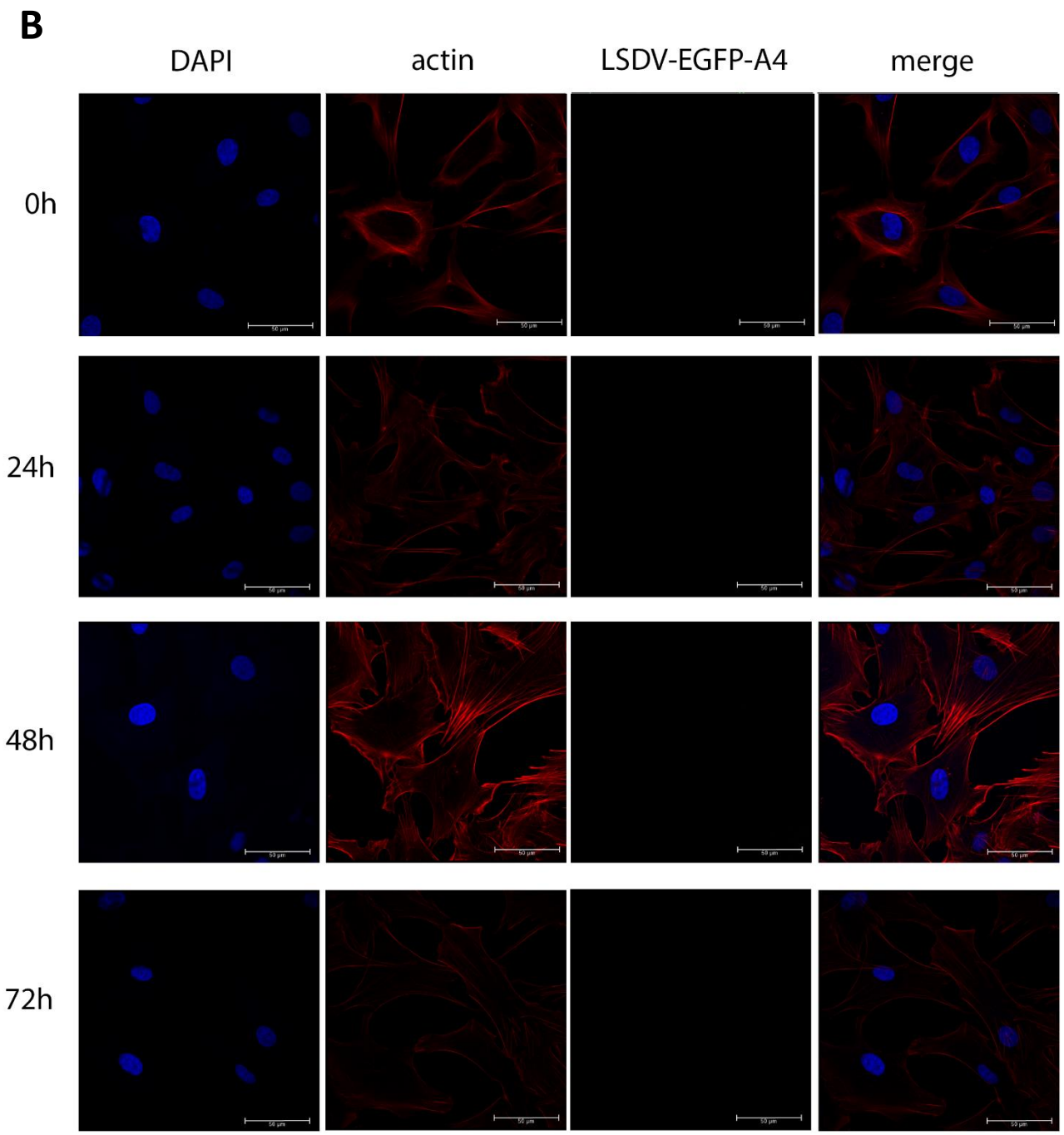
BPF in a confluent monolayer were infected with LSDV Cameroon strain at an MOI of 5, and pictures taken at 0, 2, 5, and 7 days post infection (dpi).

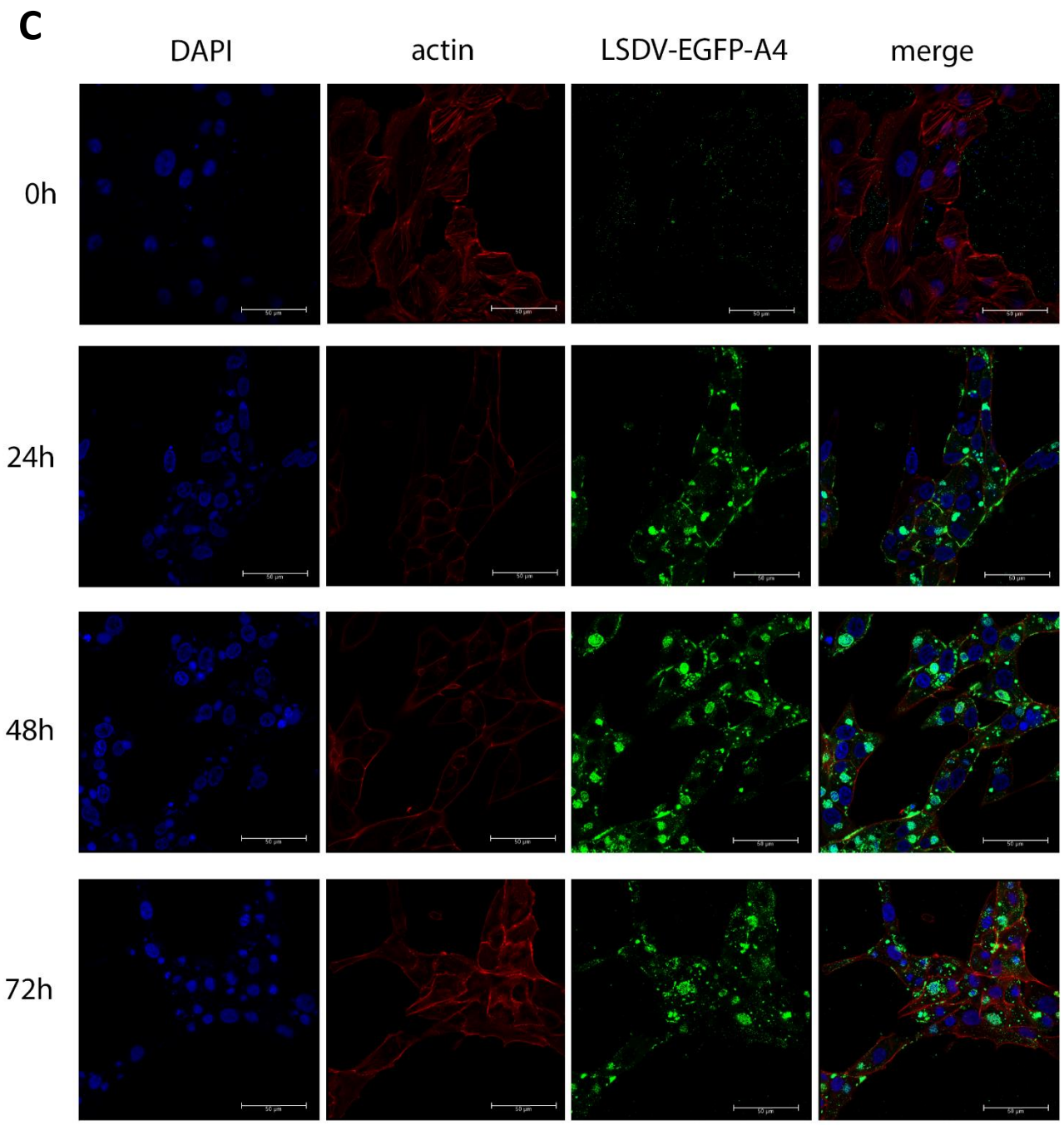
To study the cytopathic effect of LSDV on BPF in more detail, and to track the replication and morphogenesis of LSDV in BPF, confocal microscopy was used. BPFs were infected with an EGFP tagged LSDV Neethling strain (EGFP-095-LSDV Neethling) at an MOI of 1. This strain has been genetically modified to express the enhanced green fluorescent protein (EGFP) marker at the N-terminus of the LSDV ORF095, the orthologue of the A4 protein of VACV. ORF095 is a putative core protein of LSDV, therefore individual virions of the EGFP-095-LSDV Neethling strain are labelled with EGFP (Fay et al., 2022a). Cells were fixed at 0, 24, 48, and 72 hpi, then stained with phalloidin and DAPI before being visualised. From 24 hpi, the cells contained cytoplasmic viral factories, identifiable as perinuclear foci of both DAPI and EGFP fluorescence. In addition, many virions could be seen, as small cytoplasmic

EGFP-labelled punctae, increasing in number over time. In some cells, the virions lined up along the edge of the plasma membrane of the cell (Figure 4.3. A+C), possibly in preparation for exit. Infected cells also showed signs of cytoskeletal rearrangement such as development of filopodial-like projections and some cell membrane ruffling. Actin stress fibres were more pronounced in the mock infected MDBKs than the infected cells, consistent with previously published poxvirus literature (Cudmore et al., 1995, Greseth et al., 2017).

However, of most interest were the possible actin tails seen on infected BPF cells from 24 hpi onwards (Figure 4.3.A, and Figure 4.4). In some of the confocal images, the actin tail-like structures can be seen to have a virion attached to the end (Figure 4.5). Not all infected cells exhibit this modification: from a count of 16 randomly selected sections of each fixed timepoint slide, it was calculated that at 0 hpi no cells were observed to have tails, at 24 hpi 4%, at 48 hpi 8%, and at 72 hpi 3%. Interestingly, actin tails were not observed in the infected MDBK control cells, the in vitro cell line of choice for LSDV study. This suggests that LSDV inoculated into BPFs exhibit additional morphogenic steps compared to MDBKs. BPFs possibly enable LSDV to generate actin tails, unlike MDBKs, and therefore the use of the BPF cell line adds a key piece of information about the life cycle of LDSV.


A
DAPI
actin
LSDV-EGFP-A4
merge
0h
24h
48h
72h


B
DAPI
actin
LSDV-EGFP-A4
merge
0h
24h
48h
72h


C
DAPI
actin
LSDV-EGFP-A4
merge
0h
24h
48h
72h

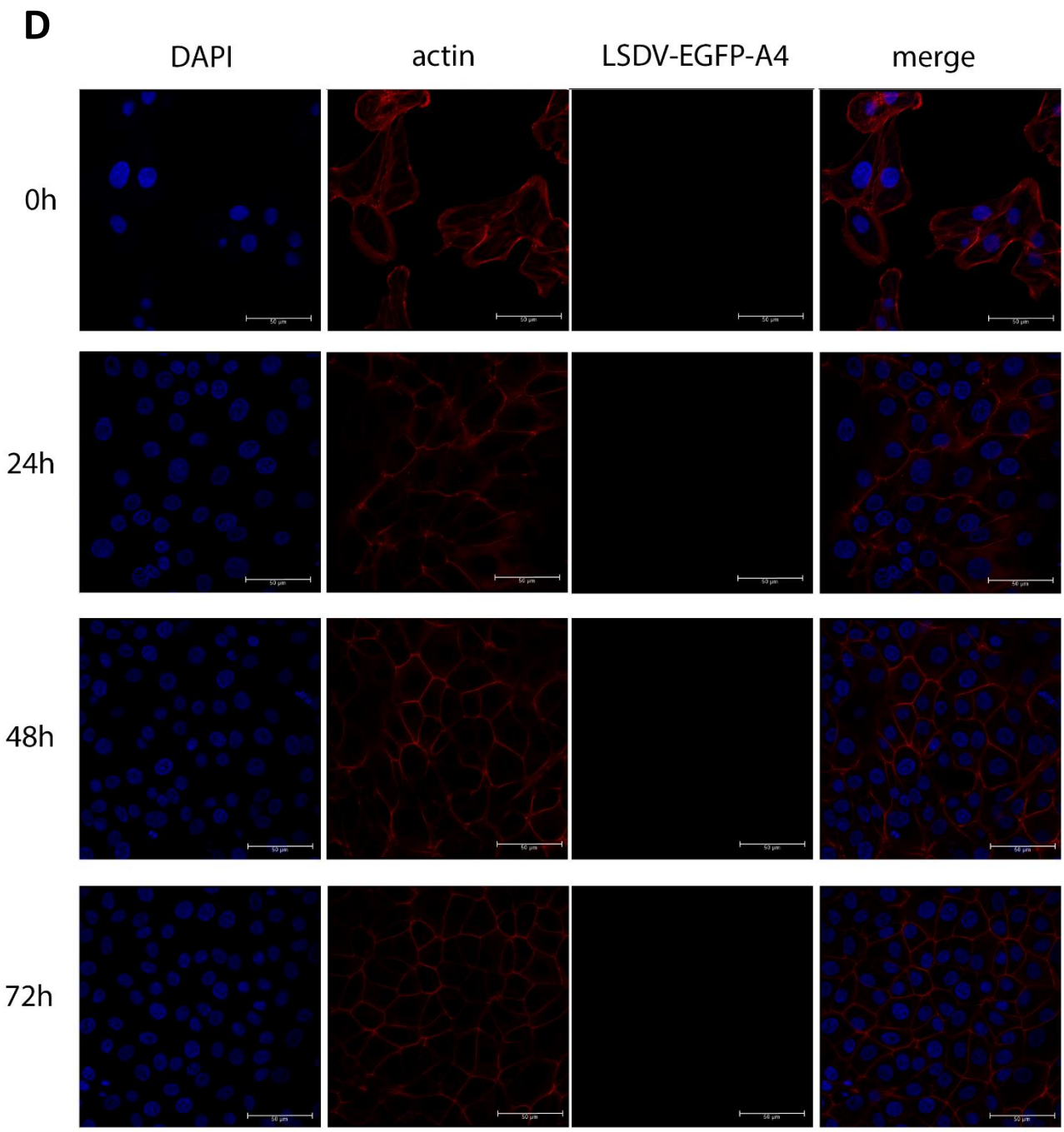


Figure 4.3: LSDV makes viral factories and mobilises along the cell surface membrane in infected BPF

BPF and MDBK cells were seeded onto coverslips and grown to 60-70% confluence at 37C, 5% CO_2. BPF cells were infected with EGFP LSDV Neethling (A). Uninfected BPF cells (B) were used as a negative control. MDBKs cells were used as the positive control, and were infected with EGFP LSDV Neethling (C), with uninfected cells (D) used as a negative control. Cells were fixed at 0, 24, 48, and 72 hpi with 4% paraformaldehyde before being stained with DAPI and phalloidin. Images were all taken at x63 magnification. This figure presents the DAPI channel, the phalloidin channel, and the EGFP virus channel separately, as well as the merged image, for each condition at each time point.

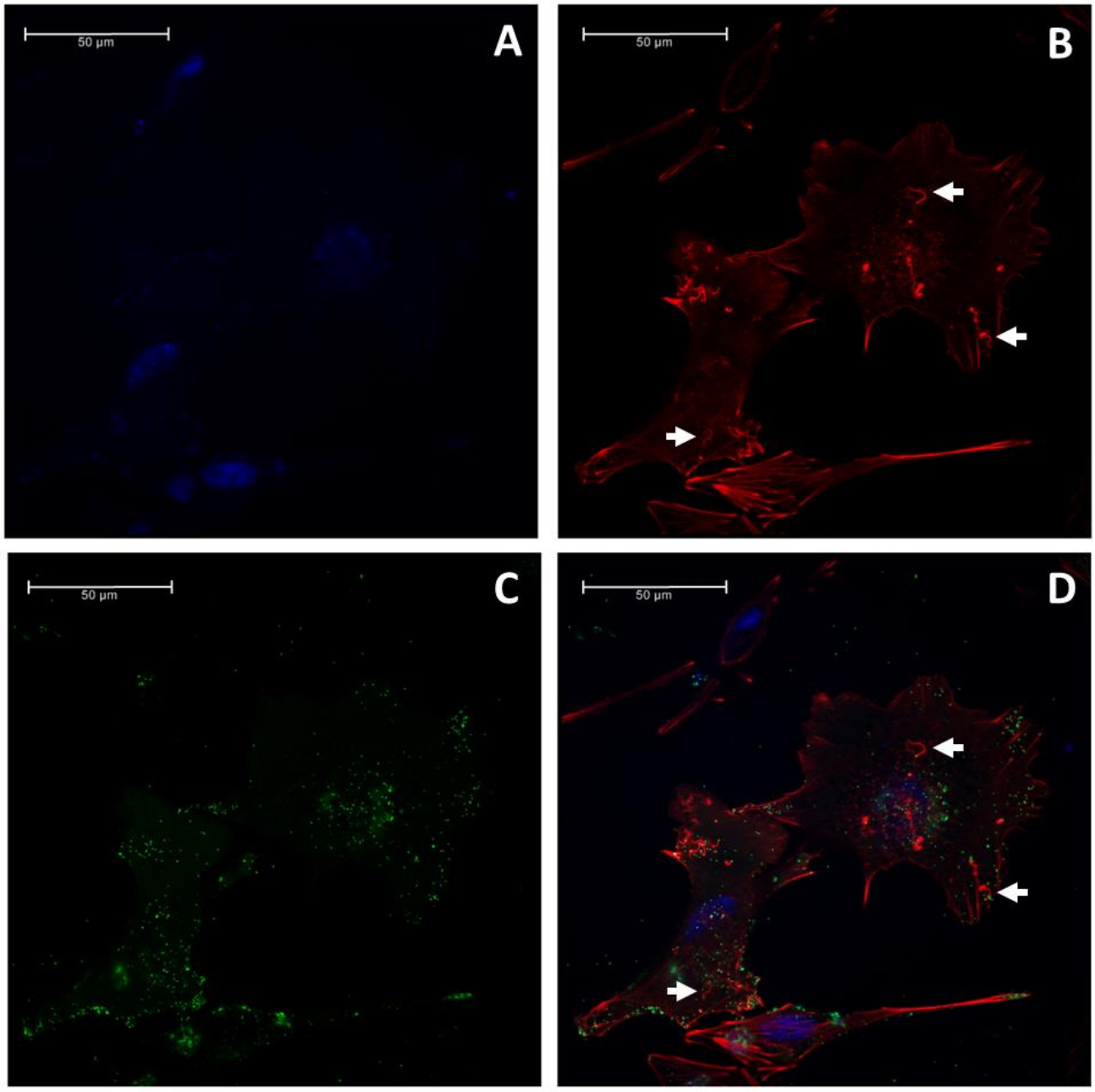


Figure 4.4: A subset of bovine primary fibroblasts seem to exhibit actin tails when infected with LSDV

BPF cells were seeded onto coverslips and grown to 60-70% confluence before infection with EGFP LSDV Neethling (C). Cells were fixed at 48 hpi before being stained with DAPI (A) and phalloidin (B), showing polymerisation of the actin into possible tails (white arrows). The channels were combined to give a merged image (D).

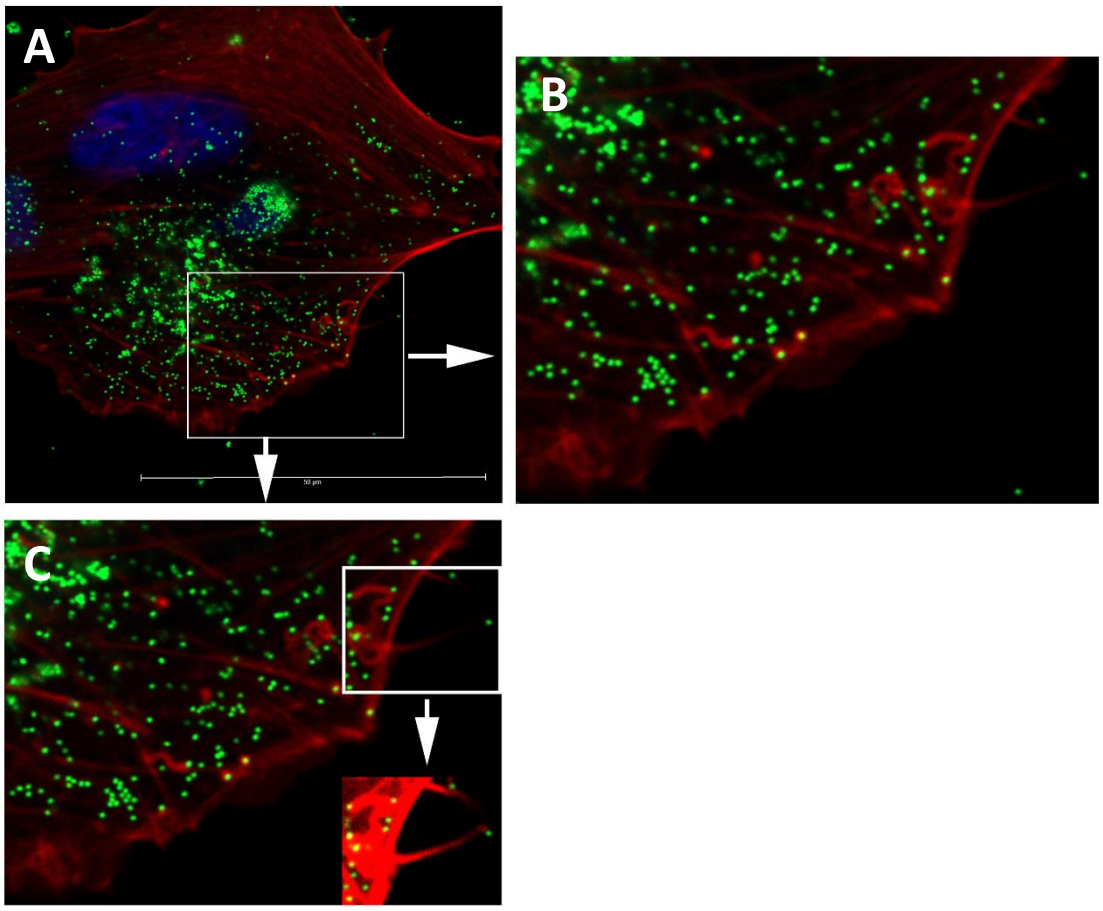


Figure 4.5: Possible actin tails in bovine primary fibroblasts carry LSDV virions

BPF cells were seeded onto coverslips and grown to 60-70% confluence before infection with EGFP LSDV Neethling (C). MDBKs cells were used as the positive control. Cells were fixed at 48 hpi before being stained with DAPI and phalloidin. The channels were combined to give a merged image (A). Adobe Photoshop was used to magnify the image (B and C) and the red channel increased (inset of C) to highlight the possible actin tails.

One-step growth curves were used to further explore the potential for bovine primary fibroblasts as an in vitro model for LSDV infection (Figure 4.6). The impact of passage number (up to passage 10), the site of skin collection, cryostorage, and animal to animal variation on viral titres was investigated. Cells were inoculated with LSDV at an MOI of 5 at 37°C. Cells and supernatant were harvested together at timepoints of 0, 2, 5 and 7 days post infection, and the virus quantified by plaque assay. Titres of virus increased from between 10^4 and 10^5 pfu/ml at 0 dpi to between 10^5 and 10^6 pfu/ml at 2 dpi, with titres

plateauing after this (Figure 4.6.A). Less than 1 log pfu/ml difference in viral titre was noted between the highest and lowest titres of any condition across all time points post infection. This suggests that bovine primary fibroblasts can be cryostored without losing replication potential, and that cells can be sourced from different animals, and from different anatomical locations (such as ear pinna or inguinal region) without substantial variation in LSDV permissiveness. It also suggests that cells passaged up to 10 times do not alter their permissiveness to LSDV.

The growth curves from all infection time-courses in primary fibroblasts and parallel growth curves in MDBK cells were combined (Figure 4.4) to compare LSDV replication. Viral titres in the MDBK control cells rose sharply from 5×10^4 pfu/ml to a steady plateau of just under 10^7 pfu/ml. Viral titres in BPF cells also showed a steep increase until day 2, but settled to a plateau of just above 10^6 pfu/ml (Figure 4.6.B). LSDV titres in BPFs were not significantly different ($p>0.05$) from titres in MDBKs at 0 and 2 dpi. This experiment indicates that LSDV replicates productively in BPF, to similar but slightly lower titres compared to the frequently used MDBK cell line.

To investigate the replication of LSDV in BPF further, the kinetics of viral protein production between BPF and MDBK were compared. BPFs and MDBKs were infected with LSDV and at 0, 2, 4 and 7 dpi whole cell lysates were collected. These lysates were analysed by Western blot to ascertain the presence of E3, a protein encoded by LSDV034 and produced early in the LSDV replication cycle, which would determine when replication began in BPFs. BPFs began producing E3 at 2 dpi, the same time as MDBKs (Figure 4.6.C), but bands became fainter at 7 dpi. This blot shows that early replication kinetics in BPFs are similar to those in MDBKs.

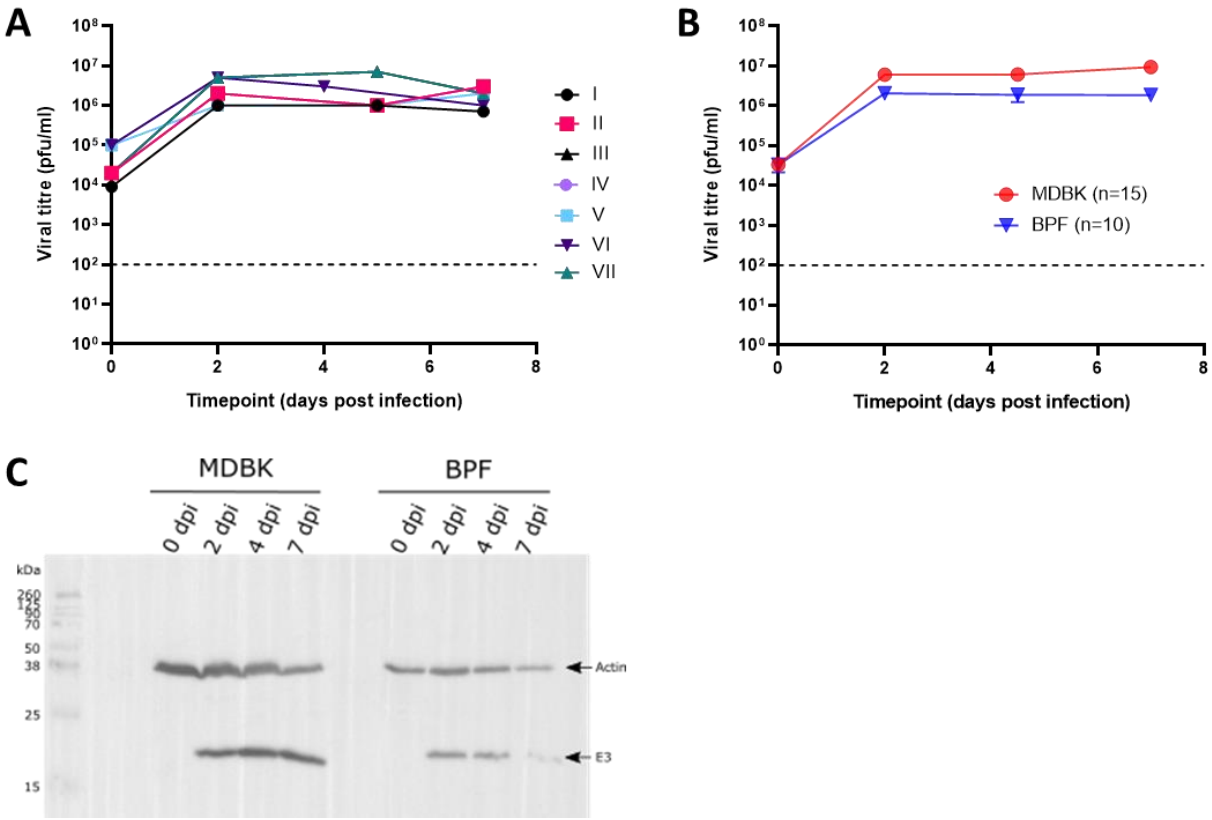


Figure 4.6: Characterising the replication and growth kinetics of LSDV in primary bovine fibroblasts

A) LSDV replication in BPF is unaffected by cell source, passage number, cryostatus or animal to animal variation. Fibroblasts from different conditions and sourced from different animals were infected with LSDV Cameroon at an MOI of 5 and samples collected at the time points shown for viral titration. (I: BPF revived from cryostorage; II: isolated from ear dermis; III: isolated from inguinal dermis; IV: ear sourced fibroblasts infected at passage 6; V: ear sourced fibroblasts infected at passage 10; VI: inguinal sourced fibroblasts infected at passage 6; VII: inguinal sourced fibroblasts infected at passage 10). Cells were infected with LSDV at MOI = 5. Progeny virus was quantified via plaque assay, showing viral titres over time. Data shown as mean ± SEM. B) LSDV Cameroon replicates productively in bovine primary fibroblasts (BPF) and MDBK cells. MDBKs (n=15) and BPFs (n=10) were infected at an MOI of 5 and cells and supernatant collected at the timepoints shown. The dotted line indicates the limit of detection. BPF N=10, includes data presented in A. Data shown as mean ± SEM. C) LSDV E3 protein was expressed from 2 dpi at around 19 kDa, with actin expressed as the loading control at the expected weight of 42 kDa.

4.2.3 The impact of *S. calcitrans* saliva on LSDV kinetics

Once LSDV growth had been characterised in bovine primary fibroblasts, these cells were then used to examine the effect of *S. calcitrans* saliva on LSDV replication in vitro. Secreted *S. calcitrans* saliva (described in chapter 3) was combined with semi-purified LSDV Cameroon, incubated at room temperature for 4h, and then titrated onto MDBK cells. It was shown to have no effect on infectivity (Chapter 3, Figure 3.6). More subtle effects of

secreted *S. calcitrans* saliva were then studied using a one-step growth curve. LSDV Cameroon was mixed with 0.6 µl secreted saliva per well (0.12µg of protein per well for collection 1 and 0.06µg per well for collection 2), incubated for 2 h, and then used to infect bovine primary fibroblasts at a MOI of 5. Cells and supernatant were collected together at 0, 2, 5 and 7 days post infection and titred. The addition of *S. calcitrans* saliva did not result in any difference in the replication of LSDV to the control (Figure 4.7). When compared to BPFs infected with a mixture of LSDV and PBS, titres were very similar, indicating that *S. calcitrans* saliva does not have a detectable effect on LSDV replication in vitro.

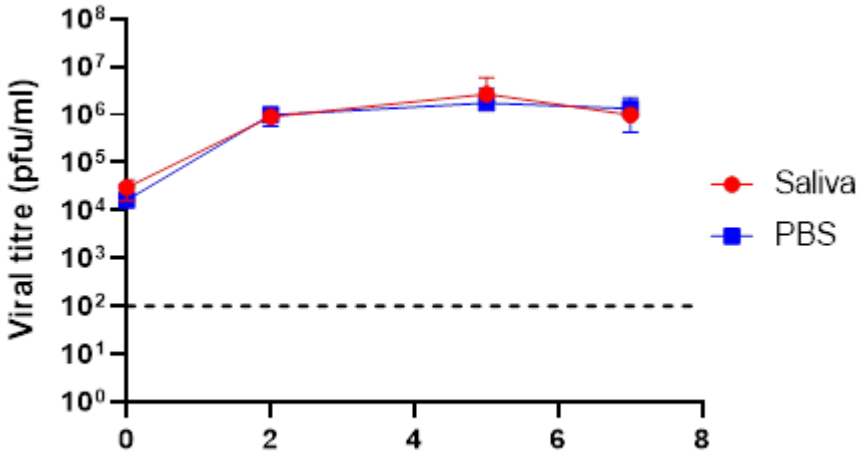


Figure 4.7: Secreted saliva does not impact LSDV kinetics in BPF

Confluent monolayers of BPFs were infected with LSDV Cameroon at an MOI of 5, incubated with 0.6 µl of secreted *S. calcitrans* saliva per infected well, and PBS as the control. Data shown as mean ± SEM, and are representative of two independent experiments, one experiment using saliva from collection 1 and the second using saliva from collection 2.

4.2.4 LSDV infection of bovine primary keratinocytes

Bovine primary keratinocytes (BPKs) were isolated from bovine ear pinnae as described above and evaluated for their permissiveness to LSDV. BPKs were inoculated with LSDV Cameroon strain at an MOI of 5 and examined for CPE. Comparisons of the cellular pathology between infected and uninfected BPK suggest evidence of cytopathic effect,

particularly at day 5 (Figure 4.8). Infected cells are rounded and shrunken, evidence of cytoskeletal rearrangement. Infected and uninfected cells both show some vacuolation.

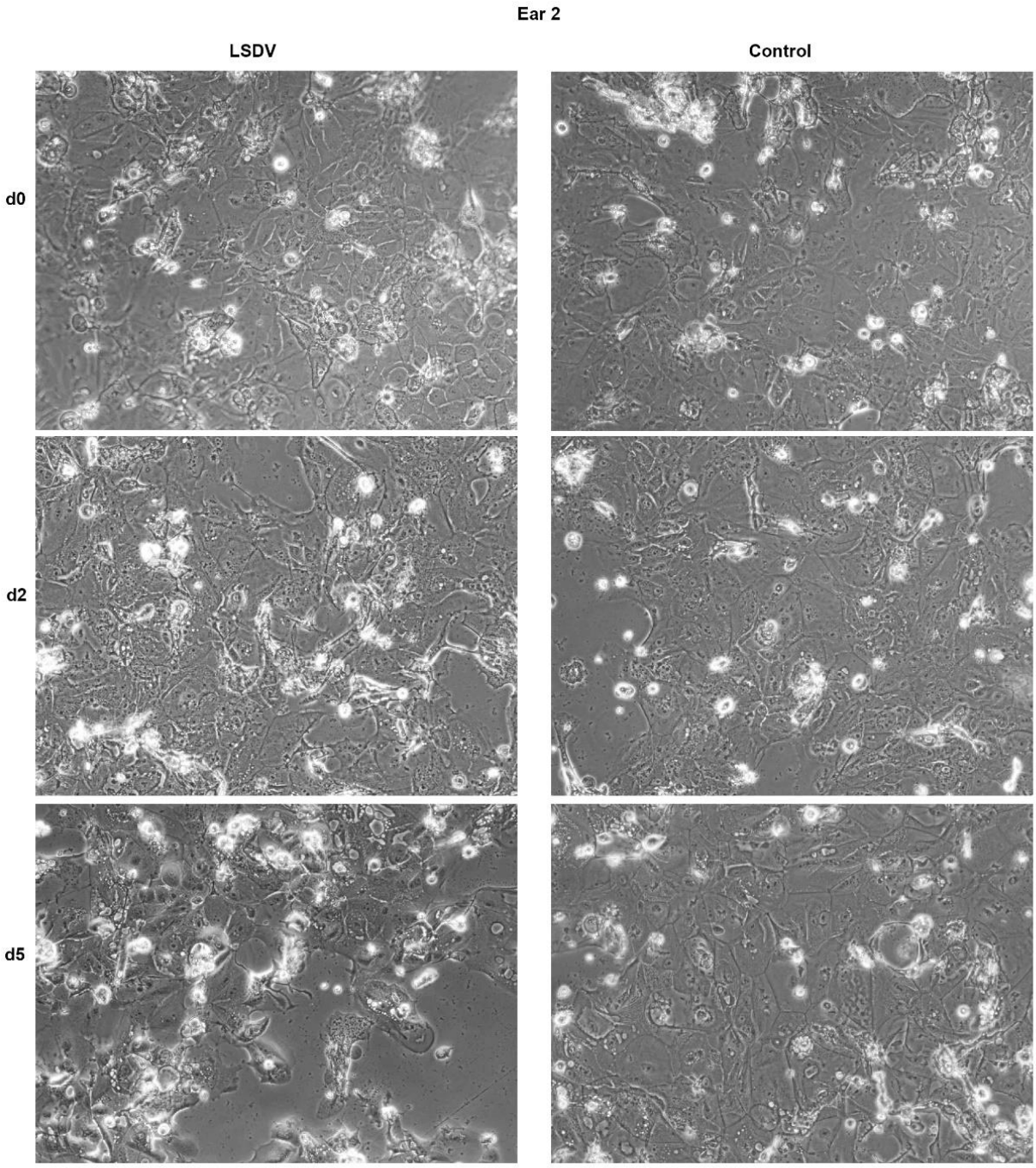


Figure 4.8: LSDV infected BPK cells show cytopathic effect

Cells were infected at MOI=5. Photos were taken on 0, 2 and 5 days after infection. Images are representative of two independent experiments.

A one-step growth curve was then carried out on BPKs to characterise LSDV replication in this cell type. LSDV Cameroon was inoculated at an MOI of 5, at 37°C. Samples (cells and supernatant together) were harvested at 0, 2 and 5 days after infection and titrated by plaque assay to obtain viral titres. The MDBK control cell line reached the usual titre of 10^7 pfu/ml, however the titres in the BPK cells did not rise above 3×10^4 pfu/ml (Figure 4.9), which is less than 1 log pfu/ml difference from 0 dpi. This result indicates that LSDV does not produce infectious virus in BPK cells.

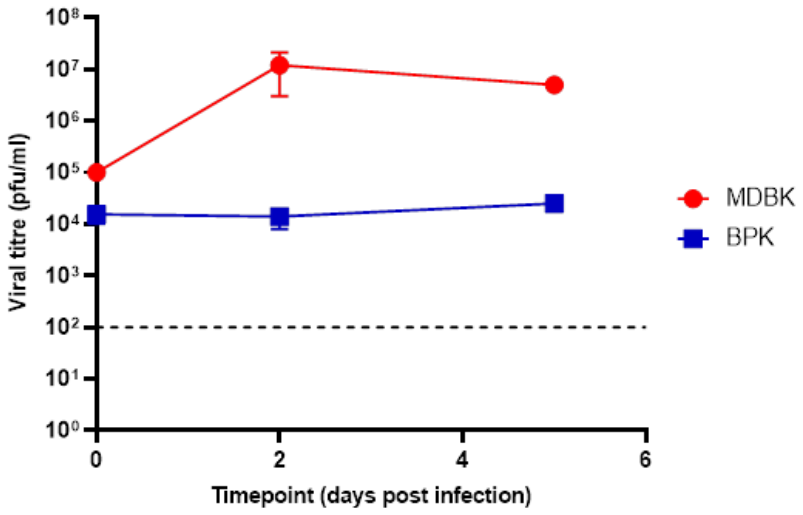


Figure 4.9: LSDV does not replicate productively in primary bovine keratinocytes.

Cells were infected at MOI=5. MDBK used as control. Virus was quantified via plaque assay. Data shown as mean ± SEM, and are representative of two independent experiments.

4.3 Discussion

The work in this chapter shows that bovine primary fibroblasts are a suitable in vitro model for the study of LSDV replication. The growth kinetics of LSDV in this in vitro model were characterised and determined to be comparable to the current lab workhorse cell line, MDBKs. Study of LSDV infection of BPFs demonstrated for the first time that LSDV seems to produce actin tails, like other members of the Poxviridae family such as VACV and ECTV (Cudmore et al., 1995, Duncan et al., 2018). The BPF model was also used to explore the impact of *S. calcitrans* secreted saliva on LSDV replication in vitro. Saliva had no effect on viral replication, which correlates with the finding in chapter 3 that saliva of varying concentrations had no impact on the infectivity of LSDV on MDBKs. Development of a second in vitro primary skin cell model was attempted, using primary bovine keratinocytes. However, these cells were much harder to reliably isolate, which made them difficult to study. The few experiments that were conducted suggested that LSDV could infect these cells, generating CPE, but that it did not replicate productively.

Several continuous cell lines have been used to study LSDV however, they are of non-skin origin which could be producing data that does not accurately represent LSDV infection in cattle skin. For example, MDBKs and OA3.Ts have contributed hugely to the field in terms of capripoxvirus propagation and assay development (Babiuk et al., 2007, Fay et al., 2020), however they may not be the most accurate and therefore most suitable cell line for further study into LSDV replication biology. In contrast, primary cells are the most closely representative environment of the tissue of interest. Past work has used primary cells from lamb testes and lamb kidneys to propagate LSDV, with other studies showing that multiple sources of bovine primary cells can support LSDV replication (Binepal et al., 2001). Primary cell work comes with its own challenges. Primary cells are time consuming to isolate from

the original tissue and easily contaminated by fungi and bacteria. They also have a finite lifespan, meaning that fresh isolations need to occur regularly, or a large stock of cells need to be cryobanked. Additionally, the cells have a limited expansion capacity. There is the risk that with passage, cells will lose similarity to the initial culture, thus potentially rendering them unrepresentative as continuous cell lines. In this chapter, isolation protocols for bovine primary skin cells were developed, and LSDV replication within them characterised. The isolation protocol was consistently successful for bovine primary fibroblasts, producing the cells nearly every time isolation was attempted. However, success was measured at 55% due to fungal contamination of the fibroblast cultures. Infection capability was not altered by cryostorage, tissue source location or cell passage number. When the replication kinetics of BPFs were compared with the laboratory workhorse cell line of MDBKs, replication was very similar. All these data indicate that the primary cell line is a suitable candidate for representative and accurate studies of LSDV replication, and is a useful addition to the toolkit. This has further been confirmed by its use in other projects by lab members (Lewis et al., J Virol under review).

The cells have already proven to be an important asset in the possible discovery of a key poxviral exit mechanism. During the confocal characterisation of LSDV infection in BPFs, actin tails seemed to be observed in a small proportion of infected cells. Poxviral actin tail formation has been best characterised in the prototype poxvirus VACV. The A36 protein of VACV is located in the outer membrane of the intracellular enveloped virus (IEV) virion form and deposited in the plasma membrane during the membrane fusion event associated with exit of the IEV to become a CEV (van Eijl et al., 2000). A36 then potentiates the polymerisation of cellular actin into protrusions via phosphorylation of A36 by Src and Abl family kinases (Newsome et al., 2006), followed by recruitment of adaptors Nck and

Grb2 (Scaplehorn et al., 2002), and finally N-WASP (Frischknecht et al., 1999), via WIP, to activate the Arp2/3 actin polymerisation complex (Donnelly et al., 2013). The actin tails enable the virus to spread more easily, either between neighbouring cells or by repulsion to cells much further away to sidestep the usual limitations of cell-to-cell replication. They are likely an important release and dispersal method for poxviruses but had not been observed before in LSDV infected cells. Infection of BPF isolated via the described methodology with EGFP-LSDV generated actin tails in a maximum of 8% of cells infected. This confirms predictions made from studies of the LSDV protein LSDV126 (Dodding and Way, 2009), a highly divergent functional ortholog of A36 in VACV. When this protein was expressed in cells infected with a A36 knockout Vaccinia virus, actin tail formation was rescued, implying that LSDV is able to produce a protein that triggers the formation of actin tails. However, it is not known why a minority of BPFs produced actin tails, and why there appears to be a specificity to the cell types able to produce actin tails when infected with LSDV. LSDV is very specific in its host range so this could be a related phenomenon. Alternatively, there could be a specificity to actin tail production in skin cells, which would explain the lack of tails seen in OA3.T and MDBK cells. Poxviruses can exit infected cells in different ways, as cell-associated enveloped virus on actin tails, or as intracellular mature virus via cell lysis or exocytosis (Smith and Law, 2004). It could be that LSDV favours the IMV exit mechanism, which is why a minority of BPFs produced actin tails. However, the different methods of virion exit from cells can't be measured presently due to the lack of neutralising antibody for intracellular mature virus, which are the infectious poxvirus particles produced within the cytoplasm.

Primary bovine keratinocytes were isolated alongside the fibroblasts, to further explore LSDV replication potential in bovine skin. These cells were more challenging to isolate and

optimise, with 19% success in isolation. Those that were isolated and infected with LSDV did show evidence of cytopathic effect, which suggests that the virus was able to enter the cells. However, when the replication kinetics of LSDV were evaluated, there was no productive replication of progeny virus by LSDV detected in BPKs. The lack of replication in keratinocytes led us to return to the literature. Some viruses are known to replicate in keratinocytes, for example herpes simplex virus (HSV) type 1 (Nicola et al., 2005), and human papillomavirus (HPV) type 1 (Egawa et al., 2015), but the evidence for poxvirus replication in primary keratinocytes is unconvincing. There is no cell culture system that can support molluscum contagiosum virus (MOCV) replication in vitro - any replication detected is exclusively in human basal keratinocytes in vivo (McFadden, 2005). Limited replication by Vaccinia virus has been observed in human keratinocytes (Liu et al., 2005), with infected keratinocytes only producing 21.8 pfu virus particles per cell, 10 times less than the yields in dermal fibroblasts. VACV infected keratinocytes also underwent rapid programmed cell death (He et al., 2014). Replication of other epitheliotropic viruses in keratinocytes has been studied, and the level of keratinocyte differentiation may be a key factor in the permissiveness of keratinocytes for infection by HSV and adenovirus type 2 (Taichman et al., 1983). It is possible that the primary keratinocytes isolated from the bovine skin in this protocol were at the wrong differentiation stage, and therefore were not permissive to replication. Since isolating any keratinocytes was challenging, perhaps an alternative system like an ex vivo biopsy model or an organoid model would be better suited for the study of LSDV replication in these cell types.

In chapter 3, *S. calcitrans* secreted saliva had been collected, and an infection assay of mixed virus and saliva carried out on MDBKs. This showed no impact on the ability of virus to infect and replicate in cells. The lack of effect of secreted saliva on LSDV replication

kinetics was confirmed in this chapter by using the bovine primary fibroblasts. This further suggests that *S. calcitrans* saliva does not impact the infectivity of virus through interactions with the virus itself, unlike the cleaving effect of *Culicoides* saliva on BTV (Darpel et al., 2011). There is potential that, despite BPFs being a more representative in vitro model, any effect by the saliva will only be observed in vivo. Work on the impact of *Aedes* saliva on infection by the biologically transmitted pathogen Semliki Forest Virus (SFV) showed a disparity in infection phenotype between in vitro and in vivo results (Lefteri et al., 2022), prompting a hypothesis that if saliva does have an impact on the pathogenesis of LSDV, that it might require processes absent ex vivo. To test this hypothesis, an in vivo experiment using cattle was designed to explore the impact of *S. calcitrans* and their saliva on LSDV pathogenesis, as described in the next chapter.

4.4 Summary

This chapter details the isolation of bovine primary fibroblasts and the characterisation of their infection by LSDV. BPFs are a useful in vitro model for the study of LSDV, and possibly more representative than MDBKs, since they seem to produce actin tails – a classic poxvirus exit mechanism that has not been seen before for LSDV. Bovine primary keratinocytes were also isolated and no productive LSDV replication was seen, suggesting that these cells play a different role from BPFs in LSDV infection. When secreted saliva collected as detailed in Chapter 3 was infected alongside LSDV onto BPFs, no impact was observed on viral replication kinetics. It is unlikely that saliva impacts the virus directly, and could instead act on the host immune response, an impact which may be observed in vivo.

5

The effect of *S. calcitrans* on the clinical outcome of LSDV infection

5.1 Introduction

This chapter investigates the impact of *S. calcitrans* saliva and feeding mechanism on LSDV infection in cattle. Previous work described in this thesis showed that secreted *S. calcitrans* saliva did not influence the infectivity of LSDV in MDBKs (Chapter 3) or LSDV replication and spread in bovine primary fibroblasts (Chapter 4), however the effect of arthropod saliva on viruses in vitro can be entirely different to the effect in vivo. In a study by Lefteri et al, cells infected in the presence of *Ae. aegypti* saliva did not present with the same virus-enhanced phenotype observed in mice, likely due to essential in vivo-specific processes that are necessary for vector saliva to boost viral infection (2022). Therefore, to establish if a mechanical arthropod vector of LSDV affects clinical disease, an in vivo LSDV experiment was carried out in the high containment animal unit at Pirbright.

In vivo experimental models of disease aim to mimic the natural disease seen in the field as accurately as possible. Currently, there are a number of in vivo cattle models of LSDV which vary in inoculation methodology and disease outcome. In the past, cattle have been challenged with LSDV intravenously (Carn and Kitching, 1995b, Irons et al., 2005, Babiuk et al., 2008), intradermally (Carn and Kitching, 1995b, Chihota et al., 2001, Prozesky and Barnard, 1982), subcutaneously (Kitching et al., 1989), into the conjunctiva (Carn and

Kitching, 1995b), and intranasally (Carn and Kitching, 1995b). Combinations of these methods have also been employed: intravenous and intradermal challenge (Sanz-Bernardo et al., 2021), and intradermal and subcutaneous challenge (Prozesky and Barnard, 1982). A problem with all these models is the low percentage of cattle that develop clinical disease after challenge, usually around 40-50% (Table 5.1). This variability in disease outcome makes LSD in vivo experiments more challenging to design, requiring higher numbers of cattle in each group. It is not known why some cattle are resistant and some susceptible to LSDV infection in experimental models.

Table 5.1 – Clinical outcomes in experimental LSDV models

Published paper	Inoculation method	LSDV strain	Clinical LSD outcome	Percentage success (%)
Carn and Kitching 1995	Intradermal	Neethling	4/25	16.0
	Intravenous		8/11	72.7
	Conjunctival		0/2	0.0
	Intranasal		1/2	50.0
Irons et al., 2005	Intravenous	V248/93	2/6	33.3
Babiuk et al., 2008	Intravenous	Neethling	6/8	75.0
Prozesky and Barnard, 1982	Intradermal/subcutaneous	Unknown field isolate	3/7	42.9
Chihota et al., 2001	Intradermal	Field isolate, Egypt 1989	2/2	100.0
Kitching et al., 1989	Subcutaneous	Neethling	1/4	25.0
		Kenya LSD B507	2/5	40.0
		Nigeria LSD	2/3	66.7
Sanz-Bernardo et al., 2021	Intravenous/intradermal	Eastern Europe field isolate	3/8	37.5
			Average of all models:	46.6

The inoculation methodology used previously by the Beard lab involved an intravenous (IV) bolus of LSDV suspension containing 10^6 pfu virus being injected into the jugular vein, and two intradermal (ID) injections of the same viral suspension on the left and right sides of

the neck. The aim of this high titre viral challenge via two different inoculation routes was to increase the probability that the inoculated animal would develop clinical disease. However, even with this "double inoculation route" the model did not result in less variability, with only 7/17 challenged cattle developing LSD (and only 4 became severe cases) (Sanz-Bernardo et al., 2021, Sanz-Bernardo et al., 2022). None of the experimental models previously described consider the role of the vector during virus inoculation. It would be beneficial from both a scientific and welfare refinement position to develop a new in vivo model of LSDV that addresses these shortcomings.

The aim of this chapter is to establish a new in vivo bovine model for the study of LSD, and to investigate the interplay between the mechanical vector *S. calcitrans*, the virus and the bovine host in the pathogenesis of clinical lumpy skin disease.

5.2 Results

5.2.1 Successful establishment of a new in vivo LSDV infection model

5.2.1.1 Inoculation methodologies

To unpick the interactions between the vector, the virus, and the bovine host, three novel inoculation methods were used to challenge cattle with LSDV. All three inoculation methods incorporated multiple 100µL "microdoses" of LSDV to imitate insect inoculation during natural transmission more closely. The first method (CV) inoculated 1×10^6 pfu LSDV intradermally into the skin in a total of 20 microdoses of 100µL of virus. 10 microdoses were injected into the left craniodorsal flank and 10 into the right craniodorsal flank, just caudal to the scapula (Figure 5.1A). The second method (CS) studied the influence of *S. calcitrans* secreted saliva on experimental LSD by mixing 10µg of *S. calcitrans* secreted

salivary protein with 1×10^6 pfu LSDV, before being delivered in a total of 2ml in the same 20 × 100 µL intradermal microdose format (Figure 5.1B). The third delivery method (CF) studied the influence of *S. calcitrans* feeding on experimental LSD by feeding two pots of ~25 adult virus-negative, laboratory reared *S. calcitrans* flies on the left and right craniodorsal flanks for 5 minutes each (Figure 5.1C), before 1×10^6 pfu LSDV was immediately inoculated in 10 microdoses into the feeding sites on each flank, identical to the CV group (Figure 5.1F). This technique has been used in other studies of vector-borne pathogens and is known as "spot-feeding" (Styer et al., 2011, Schneider et al., 2006)

The study was designed in collaboration with a specialist statistician (Dr Simon Gubbins). A power calculation was carried out to determine the group sizes required. Assuming 50% of calves develop disease in group CV and 100% of calves develop disease in groups CS and CF, a group size of 10 will be able to detect a significant difference with 87% power and 95% confidence (one-sided test) in the proportion of animals developing clinical disease. A total of 30 Holstein-Friesian male calves were therefore recruited to the study. At the time of challenge, calves were between 120-190 days old, and had arrival body weights of 151.5 ± 2kg (mean ± SEM) (see Appendix Table 8.1). In order to maximise sample collection and analysis, the experiment was divided into two identical replicates of 15 cattle (3 groups of 5) and carried out sequentially as experiments CIVS1 and CIVS2.

Physiological and behavioural responses of the calves to the novel inoculation methods was studied. Delivery of inoculum by methods CV and CS formed intradermal "blebs" within the skin which had resolved by 24 hpi. During the 5-minute initial fly feeding in method CF flies could be seen feeding on the skin surface, stimulating intermittent tail swishing, kicking, skin twitching, and general movement in the cattle. Examination of the flies immediately post-feeding revealed at least some flies with reddened abdomens

(Figure 5.1D) consistent with feeding. Fly feeding also resulted in hyperaemia and mild swelling at the site of feeding in some animals (Figure 5.1E).

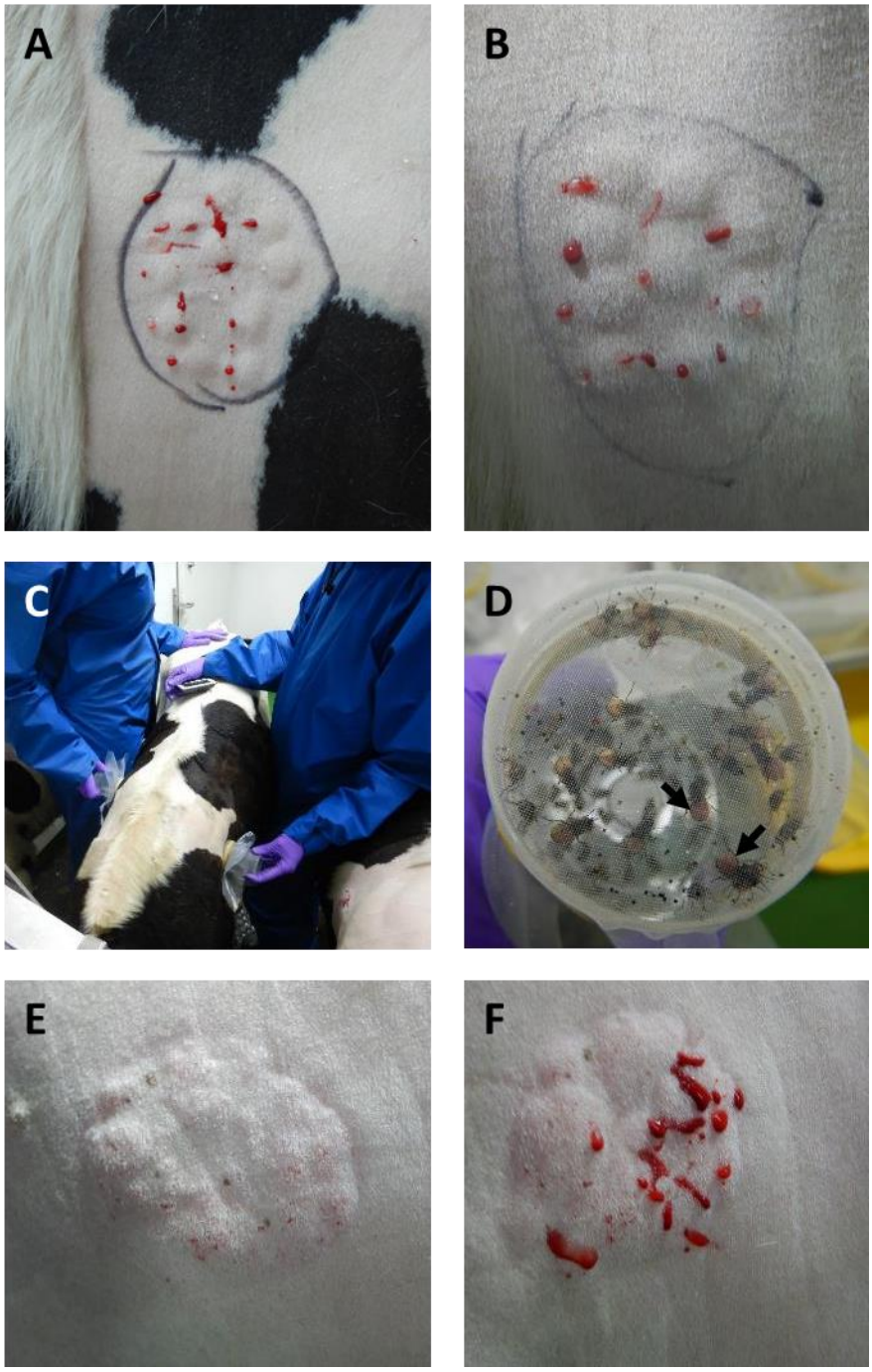


Figure 5.1: Methods of inoculation

Cattle were separated into three groups and inoculated in three ways. Cattle in the first group were inoculated intradermally with 1×10^6 pfu LSDV in 10 microdoses of 100µl per site (A). Cattle in the second group were inoculated intradermally with 1×10^6 pfu LSDV and 10µg *S. calcitrans* salivary proteins, in 10 microdoses of 100µl per site (B). Cattle in the third group were fed on by pots of *S. calcitrans* flies at the chosen site of inoculation (C) and showed evidence of feeding, such as engorged insects (shown with black arrows in D) and skin reactions (E). Then, the cattle were inoculated intradermally with 1×10^6 pfu LSDV in 10 microdoses of 100µl per site (F).

5.2.1.2 Clinical outcomes and gross pathology

Clinical observations were taken each day for 28 days post inoculation, including rectal temperature, heart rate, respiratory rate, and demeanour. The hair on each calf was clipped back early in the experiment and the skin was closely examined each day to detect and count any cutaneous lesions consistent with LSD. Lumpy skin disease manifests as characteristic cutaneous lesions from 0.5 to 5 cm in diameter that develop from macules to papules to nodules and then become necrotic after 3-4 days as a consequence of fibrinonecrotic vasculitis of the deep dermal blood vessels (Sanz-Bernardo et al., 2020). In this study an inoculated animal was classified as clinical once it developed one or more skin nodules at a site distant from inoculation. Six out of ten animals inoculated with virus alone (CV) developed clinical disease, three out of ten animals inoculated with a mixture of virus and saliva (CS) developed clinical disease, and seven out of ten animals spot-fed by flies then inoculated with virus into the feeding site (CF) developed clinical disease (Table 5.2, Figure 5.2).

Table 5.2 – A descriptive table showing the clinical outcomes of challenged animals

Inoculation condition	Disease condition	Experiment CIVS1	Experiment CIVS2	Totals
CV (Virus only)	Clinical	2/5	4/5	6/10
	Non-clinical	3/5	1/5	4/10
CS (Saliva and virus)	Clinical	2/5	1/5	3/10
	Non-clinical	3/5	4/5	7/10
CF (Fly feeding then virus)	Clinical	3/5	4/5	7/10
	Non-clinical	2/5	1/5	3/10

The cutaneous lesions distant from the site of inoculation were first noted on calves between 5-7 dpi (Figure 5.2). The lesions were well defined and initially appeared as slightly raised and reddened areas. Over the following 2-3 days the lesions became dark purple to black, and developed a sunken central region which then developed into a scab. This is consistent with progression from plaque to papule to vesicle to nodule to necrosis to scab. The appearance of new lesions on the skin of the calves continued throughout the course of disease – nodule appearance was not synchronised as has been reported for smallpox (Jahrling et al., 2004).

Skin samples from calves CF2 and CF4 were collected at post-mortem examination (11 dpi), fixed in formalin, processed to paraffin wax blocks and histological sections prepared and stained with haematoxylin and eosin. The histopathological changes identified were consistent with lumpy skin disease, characterised by severe multifocal dermatitis with necrotising fibrinoid vasculitis (Sanz-Bernardo et al., 2020). Intracytoplasmic inclusion bodies, likely representing viral factories, were present particularly in large histiocytic cells in the dermis and subcutaneous tissues of affected regions of skin (Figures 5.3-5.5).



Figure 5.2: Gross pathology of lumpy skin disease delivered via three different methods.

Cattle inoculated with each of the three methods tested developed clinical disease, defined as cutaneous nodules distant from the inoculation sites. An example of the gross cutaneous pathology from each group at different time points post infection is shown (CV1 9 dpi, A), (CS5 7 dpi, B), (CF3 7 dpi, C; CF9 11 dpi, D).

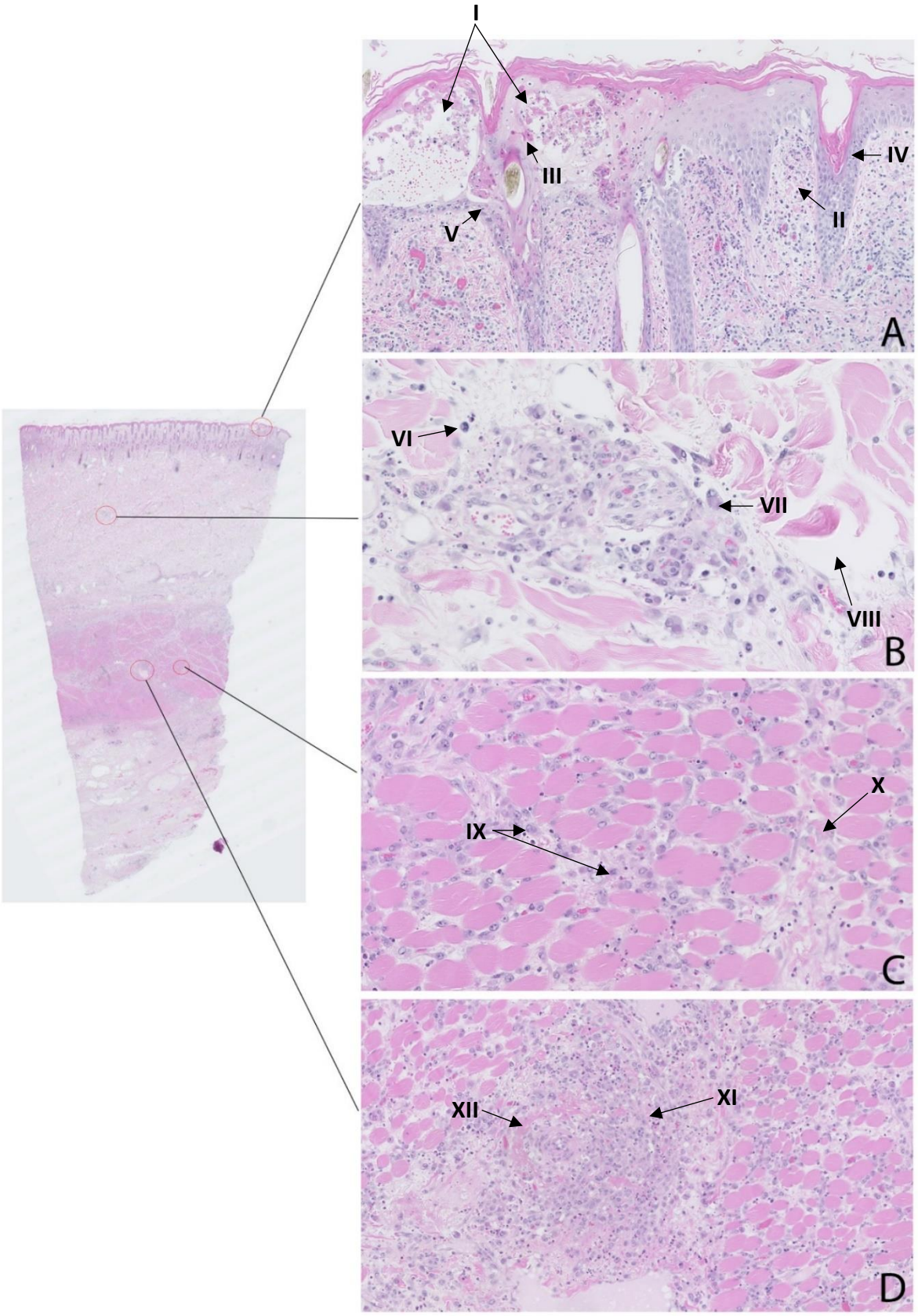

I
III
IV
V
II
A
VI
VII
VIII
B
X
IX
C
XII
XI
D

Figure 5.3 Section of haired skin (cutaneous lesion) taken at post-mortem examination from calf CF2 11DPI.

Extensive and marked inflammatory and degenerative changes are present through all layers of skin.

The epidermis (A) contains intraepidermal microvesicles containing cellular debris (I). The epidermis is moderately hyperplastic with spongiosis change present (II). Keratinocytes are hypertrophic and display ballooning degeneration (III). There are scattered necrotic keratinocytes. Epithelial cells lining hair follicles also affected (IV). There are occasional intracytoplasmic inclusion bodies within keratinocytes (V).

The dermis (B) is extensively infiltrated with inflammatory cells, mainly histiocytes (often with marginated chromatin) (VI), with fewer lymphocytes, plasma cells and neutrophils too. Many of the histiocytes have prominent intracytoplasmic inclusion bodies (VII). There is congestion, hyperaemia and oedema (VIII), and abundant cell debris.

The underlying musculature (C) is widely invaded by cords of histiocytic cells (IX), fewer lymphocytes and neutrophils. There is mild scattered muscle fibre degeneration (X). There is prominent perivascular inflammation (D) with fibrinoid necrosis of the blood vessel wall (vasculitis).

Interpretation of these histopathological images was kindly provided by Dr Pip Beard.

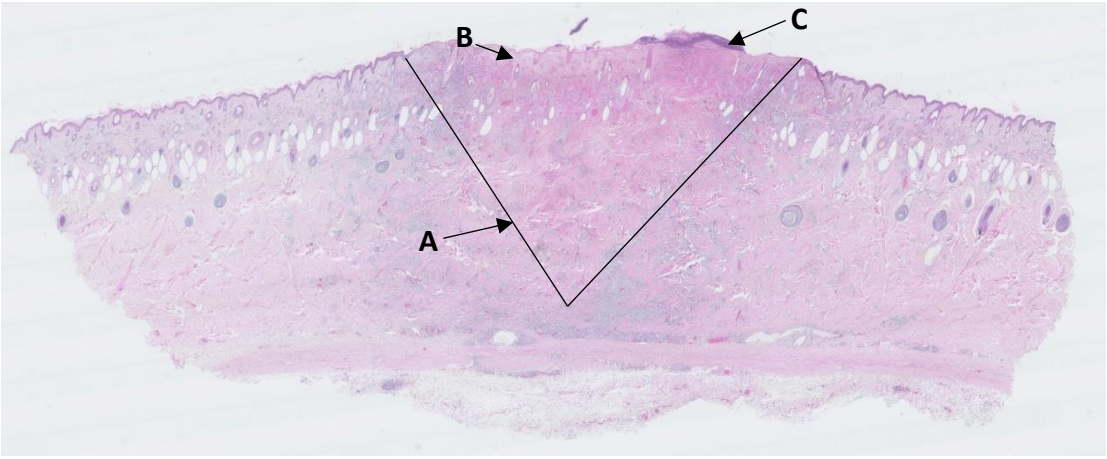


Figure 5.4 Section of haired skin from calf CF4 11DPI.

An early infarct is visible (A), characterised by a focally extensive section of necrotic epidermis (B), with overlying exudate containing cell debris (C). Cells within the infarct, extending the full thickness of the skin, are pale staining and beginning to lose cellular detail.

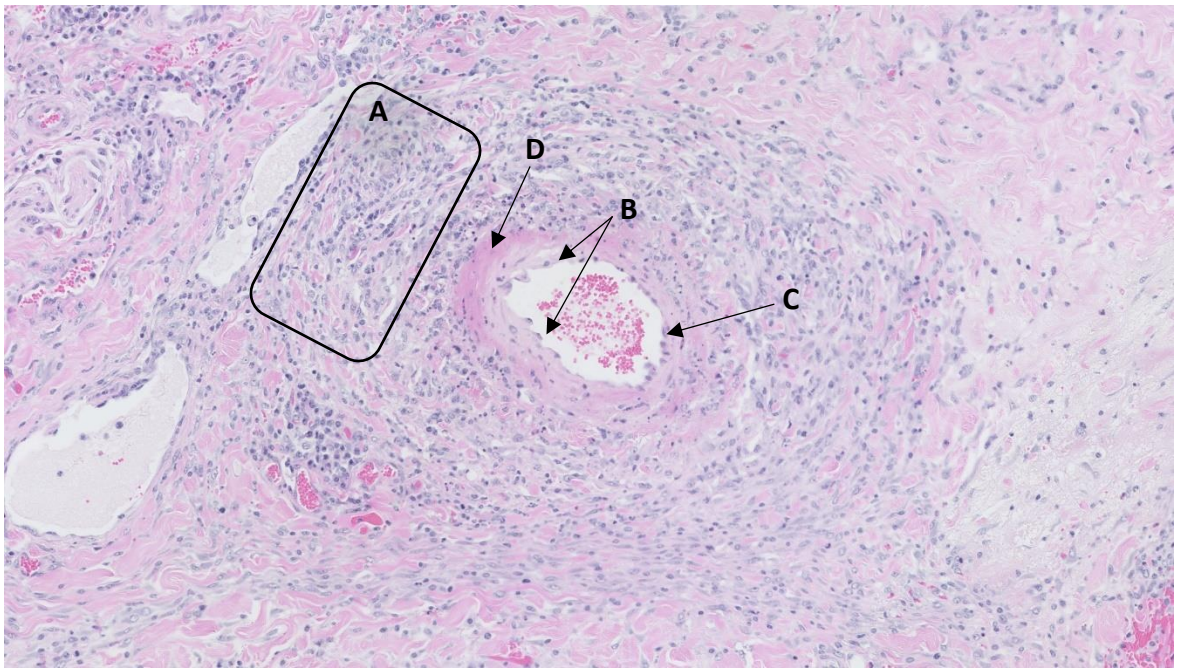


Figure 5.5 Calf CF2 11DPI, section of haired skin, displaying fibrinoid vasculitis.

There is marked accumulation of perivascular inflammatory cells (A). Endothelial cells lining the blood vessel are plump (B). Inflammatory cells can be seen invading the wall of the blood vessel (C), with accumulation of fibrin (necrosis) (D).

In accordance with the ethical requirements of this moderate protocol experiment and the project licence, clinical animals that developed pyrexia (a temperature of 1.5°C above the individuals' baseline), anorexia or abnormal behaviour for three consecutive days were euthanised via an appropriate method. This resulted in some clinical animals being euthanised early in the experiment, and on different days, as shown in the Kaplan-Meier graph (Figure 5.6). Survival was not significantly different between the three groups (log-rank test, for virus only vs flies and virus p=0.5710, for virus only vs virus and saliva p=0.1593, and for flies and virus vs virus and saliva p= 0.0561).

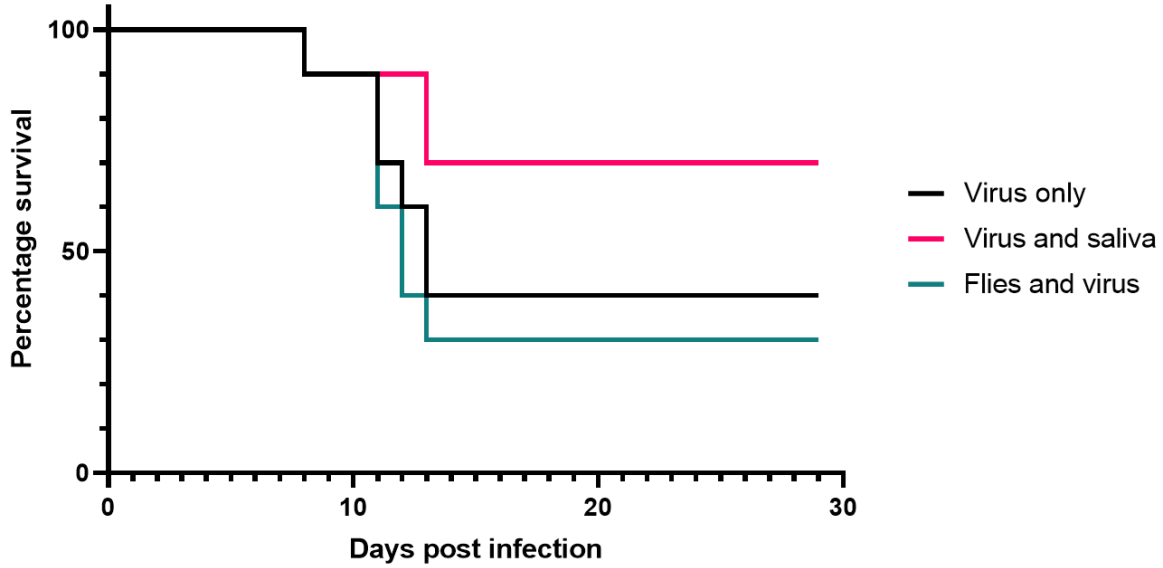


Figure 5.6 Survival of cattle varied between groups

The humane endpoint (euthanasia) of each animal was coded as a death on the Kaplan-Meier survival graph. N=10 for each inoculation group. The difference in survival was not significantly different when tested by the log-rank test.

There were three co-morbidities present in the calves – ringworm, bronchopneumonia, and orchitis and epididymitis secondary to castration. Most of the calves demonstrated multifocal, mild, chronic dermatophytosis (ringworm), which was present on arrival and did not change during the study. During the study a subset of the calves were treated with Imaverol for ringworm according to clinical need. One animal (CF1) arrived with moderate

to marked bronchopneumonia, including increased respiration rate and effort, and increased lung sounds on auscultation, particularly on the right cranioventral area. This calf (CV1) was given intensive treatment for bronchopneumonia including Naxcel, Bisolvon, Ventipulmin and Dexadreson. A subset of calves were given terramycin for scrotal infections secondary to castration pre-arrival. Calves with marked pyrexia secondary to LSD were given the non-steroidal anti-inflammatory drug Metacam. In addition, all calves were given Nuflor on arrival to prevent shipping fever. Treatments for all animals are detailed in Table 8.2 in the appendix.

Altogether the initial clinical findings showed that LSDV intradermal inoculation using a microdose challenge method can cause clinical disease in between 30 and 70% of inoculated cattle.

5.2.2 The impact of inoculation model on clinical lumpy skin disease

The three new challenge methodologies were all able to produce clinical lumpy skin disease. However, the aim of the experiment was to determine if the addition of the vector saliva or spot feeding with the vector itself accentuated the infectivity of LSDV or altered the pathogenesis of the disease. The clinical data was examined in detail to determine the influence of method of inoculation.

5.2.2.1. Lymphadenopathy is more severe in the clinical cattle

Increased size of superficial lymph nodes (lymphadenopathy) was noted in all 30 inoculated calves. By 3 dpi the pre-scapular and pre-femoral lymph nodes were mildly increased in size and firm to palpate (Figure 5.7). The lymph nodes continued to increase in size in the

clinical animals until 13 dpi with no clear differences between the three treatment groups (apart from at 5dpi where the fly fed and virus challenged group had a significantly higher lymph node score than the virus only group, p=0.0208 when tested by mixed-effects analysis), whereas the lymph node scores of non-clinical animals peaked between 5-9 dpi and reached far lower scores on average (Figure 5.7).

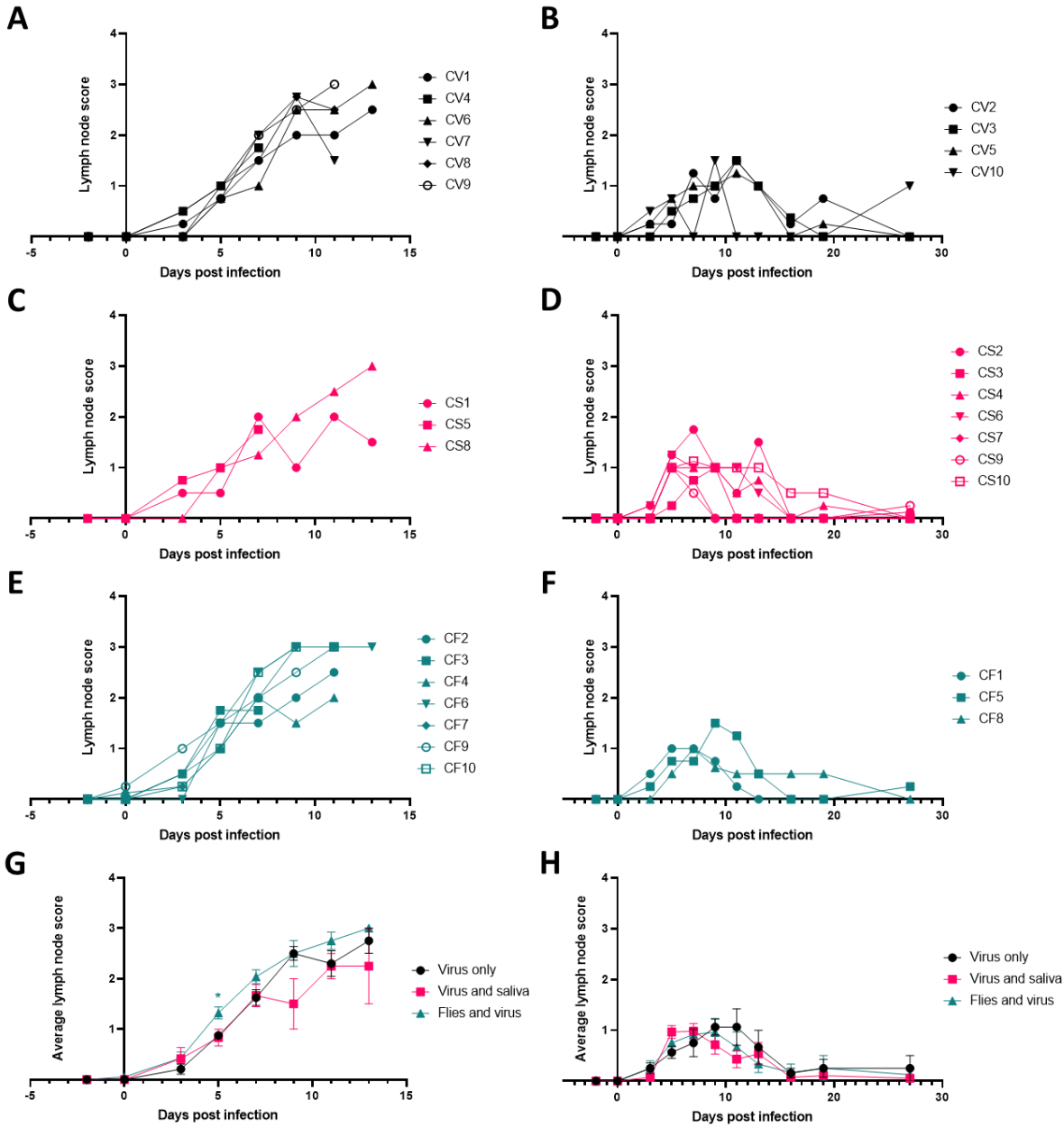


Figure 5.7: Trends in lymph nodes swelling in clinical and non-clinical animals

The swelling of lymph nodes was monitored regularly from two days before infection until the conclusion of the experiment at 28 dpi. Left and right pre-scapular and pre-femoral lymph nodes were palpated, scored, and averaged across the individual animal. Scores from the virus only challenge group were divided into clinical (A) and non-clinical (B) animals, as were the clinical (C) and non-clinical (D) animals from the saliva and virus challenged group, and the fly fed and virus challenged group (E and F). The data were then grouped into each condition group (black for virus only, pink for saliva and virus, and blue for fly fed) and averaged, for clinical (G) and non-clinical animals (H). Data shown as mean ± SEM. Treatment groups within G and H were compared using mixed-effects analysis. * denotes $p<0.05$.

5.2.2.2 Rectal temperature is higher and more enduring in clinical compared to non-clinical animals

Temperatures were taken rectally every day from each animal, and adjusted to each animal's baseline temperature, which was determined by averaging rectal temperatures taken in the four days prior to challenge. When temperatures for clinical animals were averaged (Figure 5.8.G), all three treatment groups showed a temperature spike at 4 dpi, with temperatures then maintained above the baseline between 6 and 13 dpi. There are some differences in the temperature of clinical animals between treatment groups - the three animals in the saliva and virus treated group (CS) did not experience a reduction in temperature after the spike at 4 dpi (Figure 5.8.C) and significantly dropped (mixed-effect analysis, $p= 0.0015$) compared to the fly fed group at 10dpi (though this is likely an artefact of a two calf average). The temperature spike in the fly fed then virus challenged group (CF) was slightly higher above the baseline than the other groups, with one animal reaching 2°C higher (Figure 5.8.E). The virus only challenged group (CV) experienced a deeper reduction in temperature post-spike than the fly-fed group at 5 dpi (Figure 5.8.A). However, these differences between the groups were not significant when tested via a mixed effects model.

In comparison, the average temperatures of non-clinical animals compared to the baseline demonstrated a lower increase for a shorter time compared to the clinical animals. The temperatures of the non-clinical calves in all three treatment groups increased at 8-9 dpi, then reduced to below the baseline for the rest of the experiment (Figure 5.8.H). Non-clinical animals from the saliva and virus challenged group demonstrated an earlier and higher temperature difference from the baseline than the other two treatment groups,

though this was not statistically significant. Temperature correlating with clinical outcome suggests this is a key clinical sign to monitor and use in a clinical scoring system.

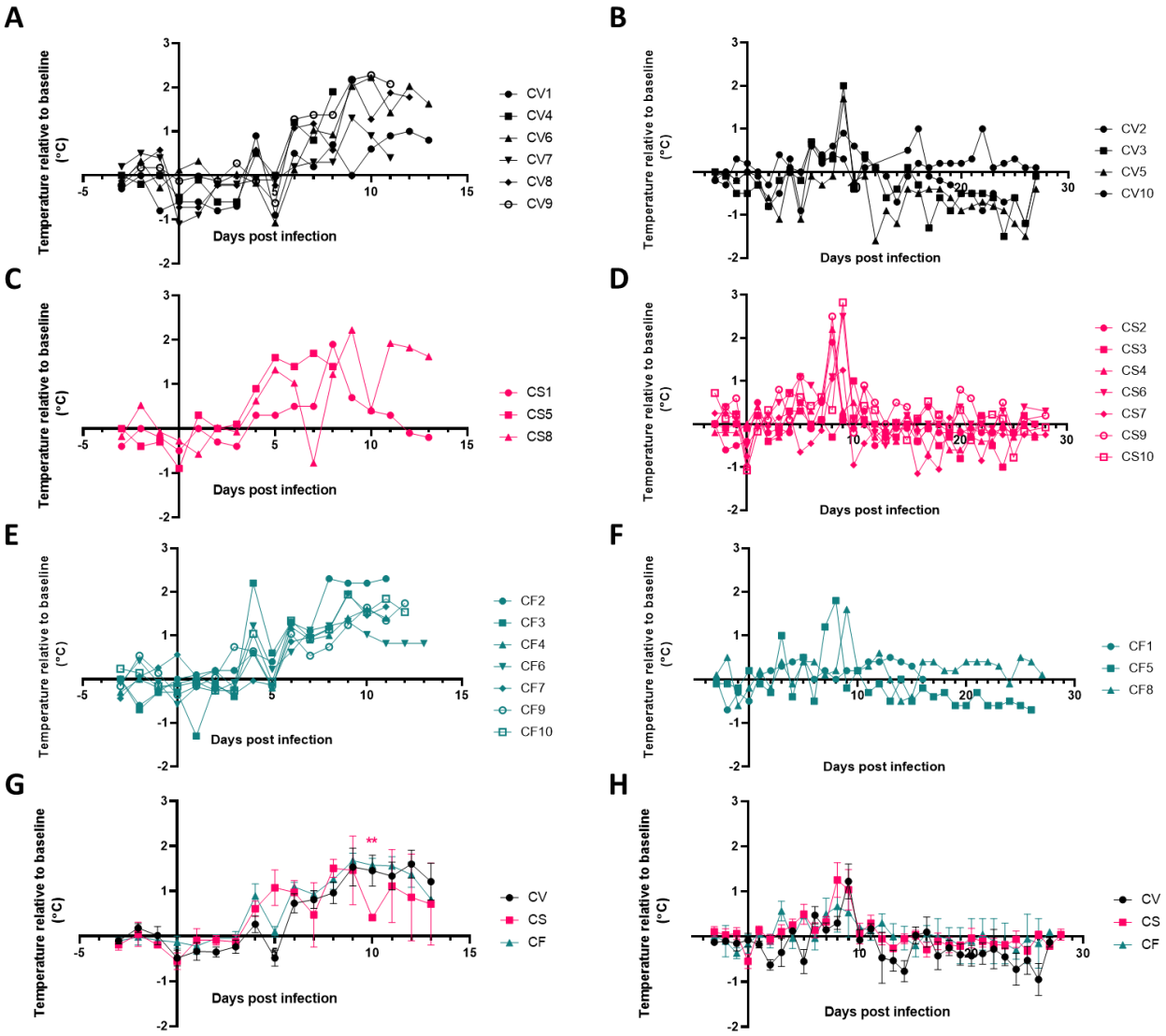


Figure 5.8: Trends in rectal temperatures in clinical and non-clinical animals

Temperatures were taken rectally every day from three days before infection until the conclusion of the experiment at 28 dpi. These were adjusted to each animals' individual temperature baseline. Temperatures from the virus only challenged group were divided into clinical (A) and non-clinical (B) animals, as were the clinical (C) and non-clinical (D) animals from the saliva and virus challenged group, and the fly fed and virus challenged group (E and F). The data were then grouped into each condition group (black for virus only, pink for saliva and virus, and blue for fly fed) and averaged, for clinical (G) and non-clinical animals (H). Data shown as mean ± SEM. Treatment groups within G and H were compared using mixed-effects analysis. ** denotes $p<0.01$.

5.2.2.3 Heart rates display different patterns for clinical and non-clinical outcomes, but respiratory rates do not.

Increased heart rates and respiratory rates can be indicators of pain and stress in cattle (Kovacs et al., 2014), and thus potential correlates of disease severity. When the heart rates of clinical animals were plotted (Figure 5.9.G), there was a pattern of a steady increase in heart rate from 0 dpi to 11 dpi in the virus inoculated (CV) and fly-fed (CF) groups (Figure 5.9.A and E). Heart rate patterns in clinical animals in the saliva and virus inoculated group (CS) were more difficult to study since there were only three animals in this category, and one was euthanised at 9 dpi. Overall, the heart rates of the three clinical animals in the saliva and virus inoculated group (CS) were more varied and had a higher average rate at 5 dpi than the other groups (Figure 5.9.C). Heart rates then dropped to 11 dpi rather than rising as in the other two groups.

In non-clinical animals, heart rates changed over a longer period, rising to their respective peaks between 7-9 dpi before decreasing to averages of 51-56 bpm at 19 dpi, before rising again towards pre-challenge rates (Figure 5.9.H). Animal CF1 had marked bronchopneumonia, leading to respiratory distress and a higher heart rate (Figure 5.9.F, pale blue line), and was excluded from the averaged data. Infection with LSDV clearly affects the heart rate of animals, and this clinical sign should be included in a scoring system.

When respiratory rates were compared, they show that there is variation in respiratory rates between challenged animals, but that there is a largely similar trend between clinical and non-clinical animals across all three treatment groups (Figure 5.10.G and H). Animal CF1 had marked bronchopneumonia, leading to a higher respiratory rate (Figure 5.9.F, pale blue line), and was excluded from the averaged data. All treatment groups, for clinical and

non-clinical animals, show a peak at about 9 dpi, which correlates with peaks in heart rates and temperature. Respiratory rates are unlikely to be a key factor in a clinical scoring system for LSDV, though it would still be useful to monitor these as part of animal welfare.

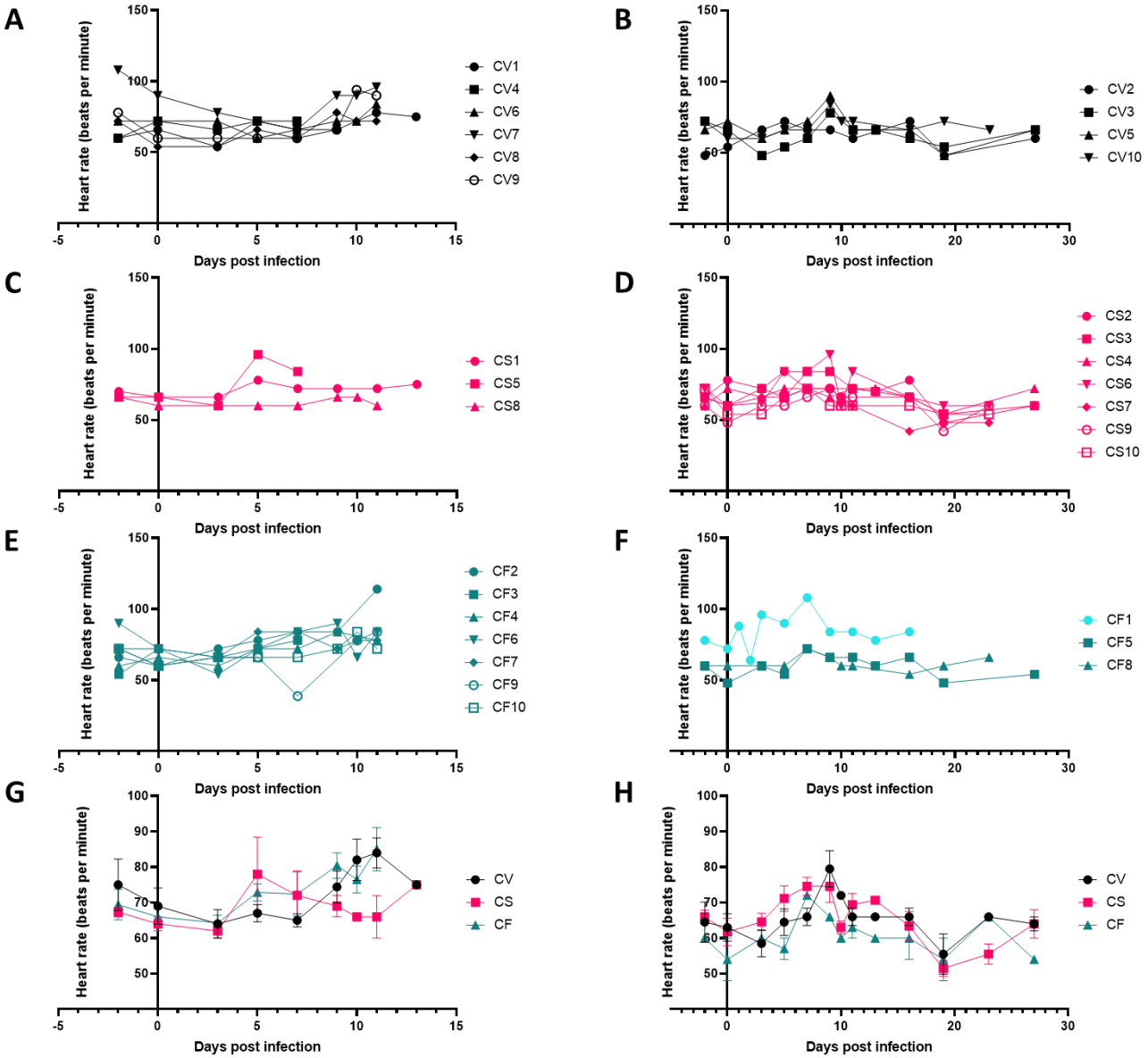


Figure 5.9- Trends in heart rates over the course of the study

Heart rates were measured by manual examination from two days before infection until the conclusion of the experiment at 28 dpi. Heart rates from the virus only challenged group were divided into clinical (A) and non-clinical (B) animals, as were the clinical (C) and non-clinical (D) animals from the saliva and virus challenged group, and the fly fed and virus challenged group (E and F). The data were then grouped into each condition group (black for virus only, pink for saliva and virus, and blue for fly fed) and averaged, for clinical (G) and non-clinical animals (H). CF1 (shown in pale blue) was excluded as the animal had respiratory distress. Data shown as mean ± SEM. Treatment groups within G and H were compared using mixed-effects analysis.

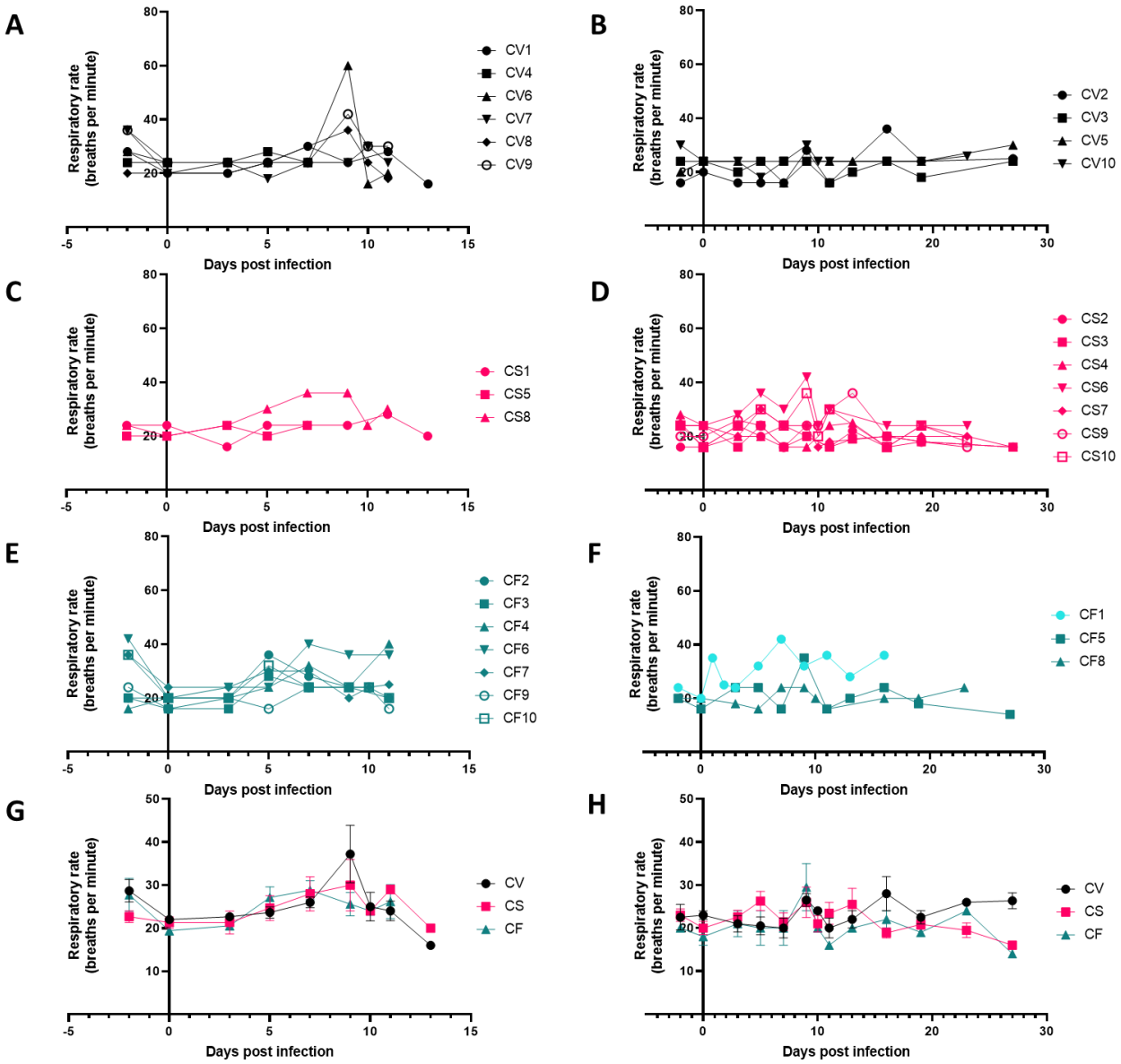


Figure 5.10- Trends in respiratory rates over the course of the study

Respiratory rates were measured by manual examination from two days before infection until the conclusion of the experiment at 28 dpi. Respiratory rates from the virus only challenged group were divided into clinical (A) and non-clinical (B) animals, as were the clinical (C) and non-clinical (D) animals from the saliva and virus challenged group, and the fly fed and virus challenged group (E and F). The data were then grouped into each condition group (black for virus only, pink for saliva and virus, and blue for fly fed) and averaged, for clinical (G) and non-clinical animals (H). CF1 (shown in pale blue) was excluded as the animal had respiratory distress. Data shown as mean ± SEM. Treatment groups within G and H were compared using mixed-effects analysis.

5.2.2.4 Cutaneous nodules appeared faster and in significantly more numbers in the fly spot-fed group

The number of cutaneous nodules were counted carefully on each animal across the face, neck, flanks, and hindquarters. Counting had an upper limit of 100 nodules per animal per day. No nodules were detected at any timepoint on non-clinical animals (Figure 5.11, right panel). On clinical animals, all nodules were similar in manifestation (red and raised, and of a similar size, as seen in Figure 5.2), however differences were noted when the number of nodules was tracked over time. Cutaneous nodules were first noted at 5 dpi in group CS, 6 dpi in group CF, and 7 dpi in group CV. The number of nodules on the calves in the CF group rose rapidly, so that by 7 dpi there were significantly more nodules per clinical animal in the fly fed and virus challenged group (CF) than on clinical animals in the group that was inoculated with just virus (CV) (mixed effects model, p=0.0130, Figure 5.11.G). This difference is more apparent when the data is viewed as a heatmap (Figure 5.12), showing the number of clinical animals in the CF group that had lesions by 7 dpi (7/7) compared to only 2/6 clinical calves in group CV. This suggests that fly feeding before inoculation has an impact on the pathogenesis of lumpy skin disease.

The low number of clinical calves in group CS (3) and the variation in the number of nodules across these three animals resulted in large error bars (Figure 5.11.C) and no statistical difference in the number of nodules between this group and CF or CV groups.

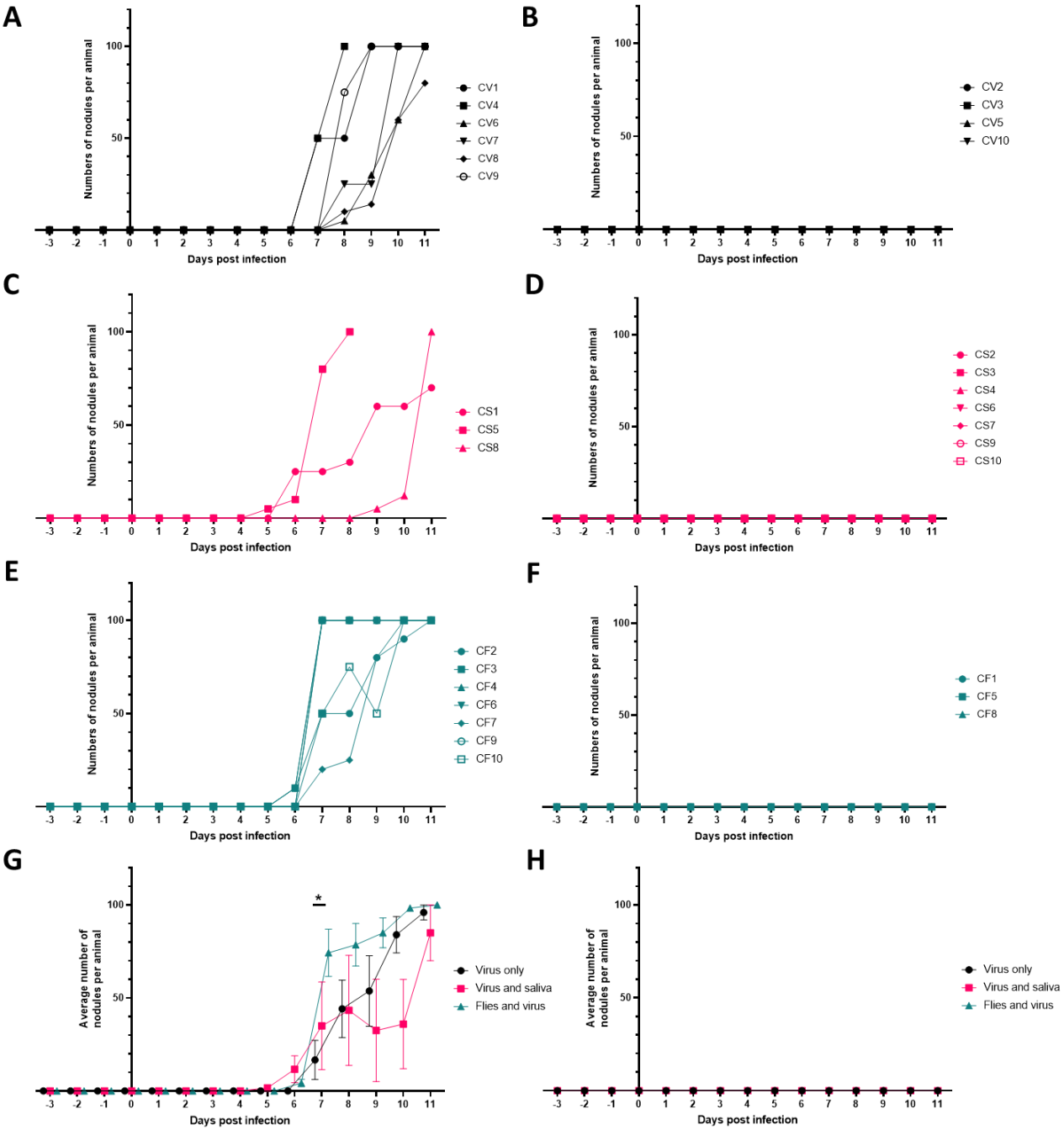


Figure 5.11 – Average number of nodules per animal compared between treatment groups

Nodules were counted during manual examination of each animal. Nodule numbers from the virus only challenged group were divided into clinical (A) and non-clinical (B) animals, as were the clinical (C) and non-clinical (D) animals from the saliva and virus challenged group, and the fly fed and virus challenged group (E and F). The data were then grouped into each condition group (black for virus only, pink for saliva and virus, and blue for fly fed) and averaged, for clinical (G) and non-clinical animals (H). Graph shows data collected from -3 dpi to 11 dpi. Data shown as mean ± SEM. Treatment groups within G and H were compared using mixed-effects analysis.

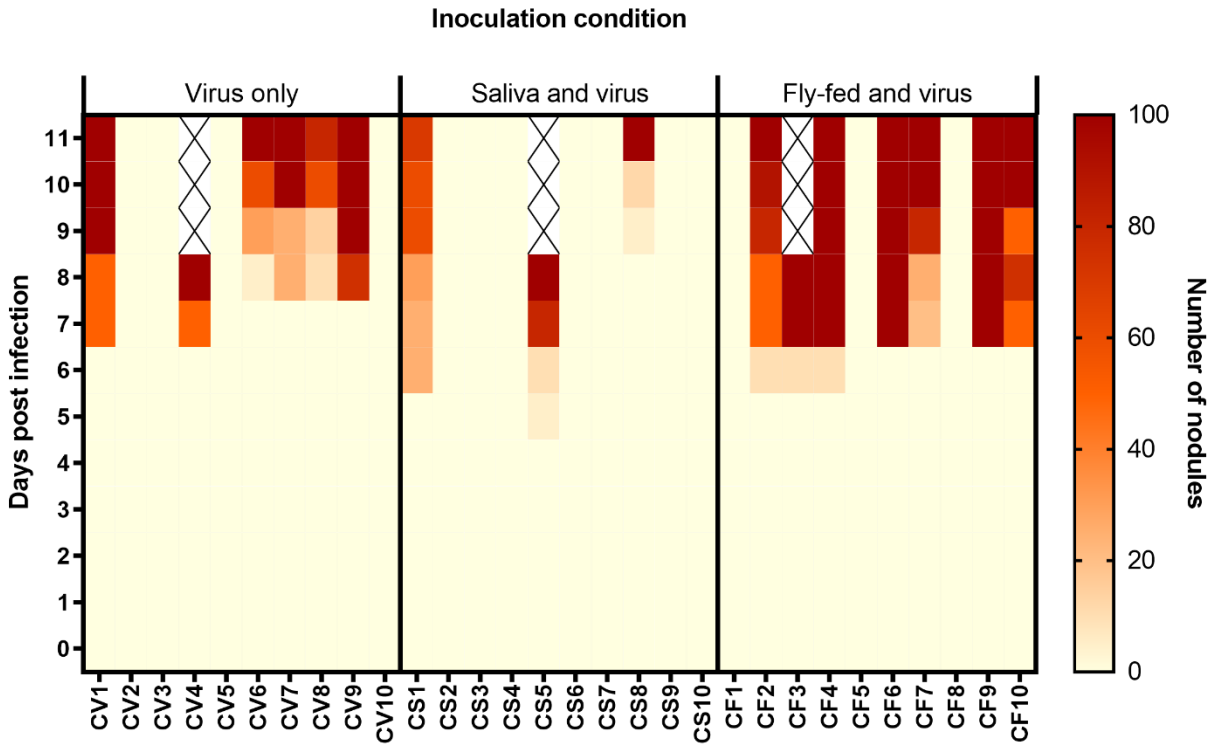


Figure 5.12– Nodules develop in more numbers more rapidly in the fly-fed (CF) group

Nodules were counted by manual examination of each animal in each treatment group. A double gradient was used to show nodule number development. Boxes with a cross indicate that an animal had been euthanised prior to this time point.

5.2.2.5 Development of a clinical scoring system for experimental lumpy skin disease

Clinical scoring systems are designed to systematically quantify observations of subjects in order to predict outcomes, estimate disease severity, and determine possible treatments. They have been used in human and in veterinary medicine, for example for evaluation of skin conditions like canine demodicosis (Dengler et al., 2021) and monitoring bovine respiratory disease in dairy calves (Maier et al., 2019). A previous scoring system for experimental LSD was developed by Carn and Kitching (1995b) and later modified by other LSD researchers (Wolff et al., 2020). It has been a useful tool for quantifying the progress of clinical lumpy skin disease. However, even the modified rubric does not consider the full range of LSD clinical signs. To make a more comprehensive and holistic comparison of LSD severity between animals, the current LSD scoring system was further optimised by using

the 30 calves in the CIVS1 and CIVS2 studies. Multiple factors that are commonly presented by animals with clinical LSD were included: number of cutaneous nodules, enlargement of lymph nodes, temperature, unusual behaviour, anorexia, oedema and lameness, and ocular/nasal discharge and salivation. These criteria were then weighted differently, to account for severity of some clinical signs (Table 5.3). Each animals' total score was then combined and compared.

As expected, there was a clear distinction between the clinical score of the clinical and non-clinical animals, with the clinical cases scoring much higher, with maximum scores of between 10 and 15 points, compared to the nonclinical animals which had maximum scores of around 5 (Figure 5.13). This difference was significant (using a mixed effects model for analysis) between the clinical and non-clinical animals in the virus inoculated groups (CV) at 7 dpi and 11 dpi ($p= 0.0146$ and $p<0.0001$ respectively) and between the clinical and non-clinical animals in the fly spot-fed and virus inoculated group (CF) at 7 dpi and 11 dpi ($p=0.0003$ and $p=0.0001$ respectively) (Figure 5.14).

The scores of the clinical animals were then compared across the three treatment groups. The maximum scores of the clinical animals were similar in all treatment groups, however the scores rose faster in the fly fed and virus inoculated group (CF) when compared to the virus only (CV) and virus and saliva inoculated (CS) groups (Figure 5.14). The clinical animals in the fly fed group (CF) reached a higher severity score more quickly than the other groups and was significantly higher than the virus inoculated group (CV) at 7 dpi ($p=0.0104$, mixed effects model). The clinical animals in the virus and saliva group (CS) had a lower severity overall over the course of the experiment, but the variation within the three clinical cattle prevented any statistical significance from being reached (Figure 5.14). The scoring system was able to differentiate significantly between clinical outcomes in two of the three

inoculation methodologies. It also showed clearly that fly feeding impacts pathogenesis, resulting in significantly greater disease severity developing earlier post infection.

Table 5.3 – A new system to score the severity of lumpy skin disease in experimentally infected animals

Clinical sign	Score
Nodules	
0	0
1-20	1
21-40	2
41-60	3
61-80	4
80+	5
Lymph nodes	
Average of all lymph nodes rounded to nearest whole number	
0	0
>0-1	1
>1-2	2
>2-3	3
Temperature	
At or below baseline	0
>0 to 0.5 above baseline	1
>0.5 to 1 above baseline	2
>1 to 1.5 above baseline	3
>1.5 above baseline	4
Behaviour (isolation/slow/lethargic/abnormal posture)	
No abnormal behaviour	0
Animal exhibits one abnormal behaviour	1
Animal exhibits multiple abnormal behaviours	2
Anorexia	
No anorexia	0
Animal not eating	2
Oedema/lameness	
No oedema	0
Oedema in one area	1
Oedema in two areas	2
Ocular/nasal discharge/salivation	
No discharge	0
Discharge	1

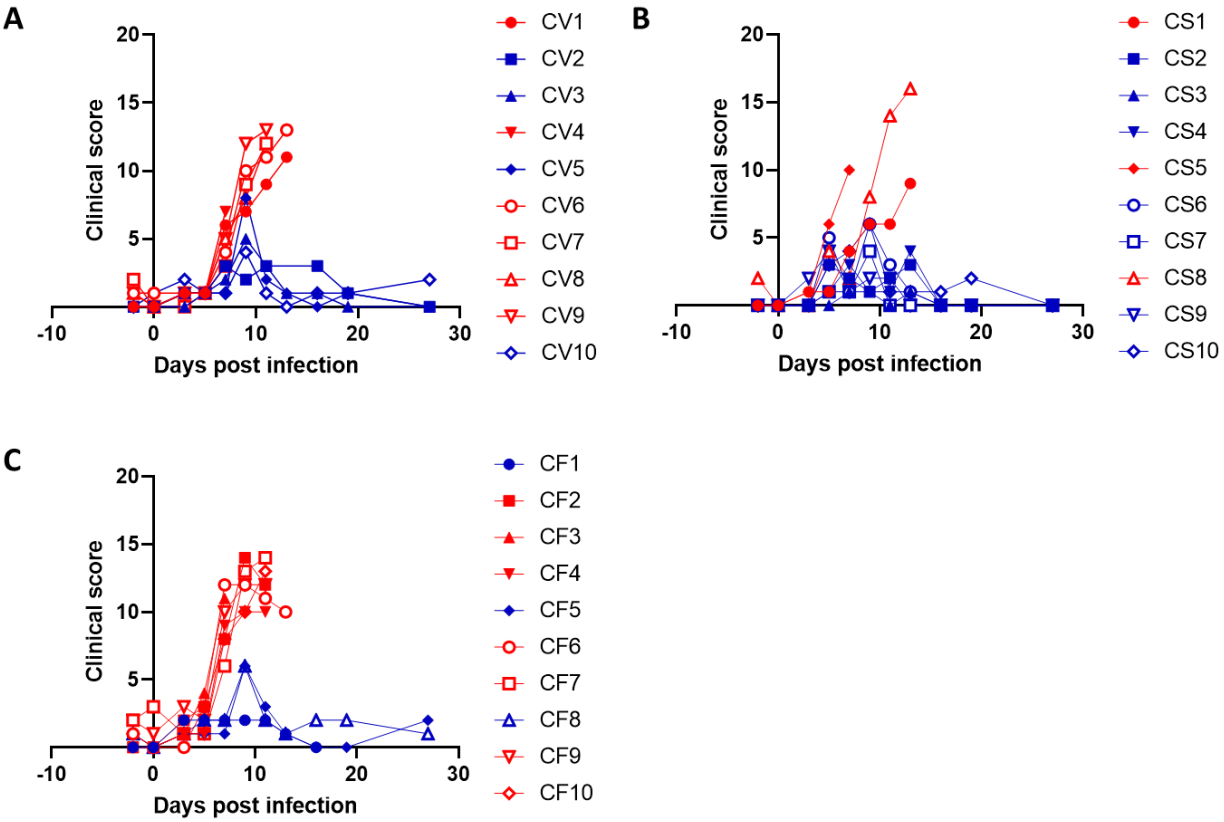


Figure 5.13 – Severity of disease in LSDV challenged animals

Using a new scoring system, virus (A), virus and saliva (B), and fly fed and virus (C) challenged animals were assigned clinical severity scores based on their clinical signs. Animals who presented with a clinical outcome are shown in red, and with a non-clinical outcome in blue.

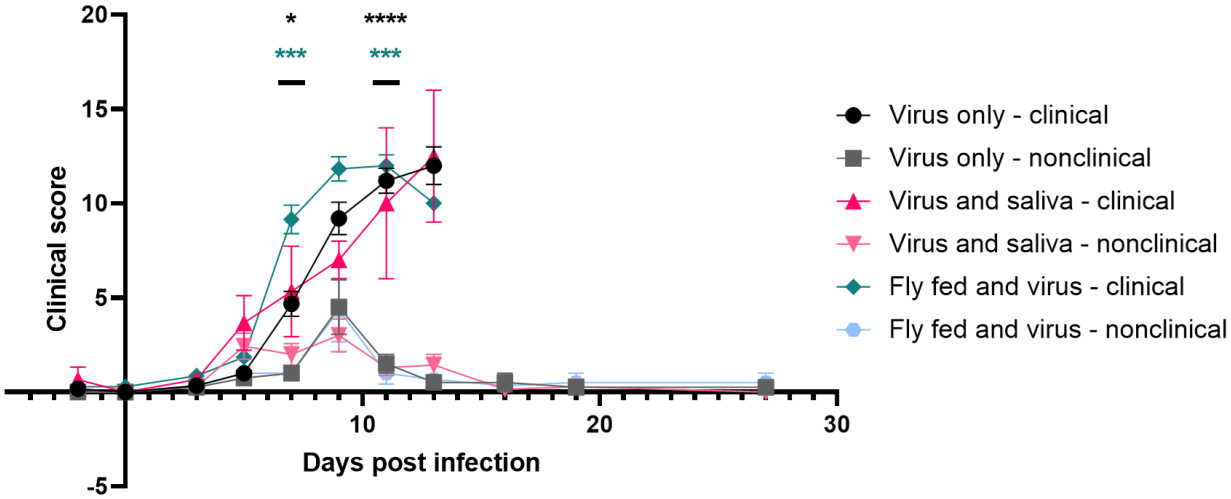


Figure 5.14 – Comparison of treatment group disease severity as assessed by novel scoring system

Scores for each animal were pooled into treatment groups depending on clinical outcome and averaged. Data shown as mean ± SEM. Data shown to 13 dpi for clinical animals and 27 dpi for non-clinical animals. A significant difference was shown between clinical and non- clinical animals in the virus inoculated group (black stars) and clinical and non-clinical animals in the fly spot-fed groups (blue stars) at 7 dpi and 11 dpi. Significance was determined by a mixed effects model.

5.2.3 LSDV replication and disease establishment in the three models

Analysis of the clinical data from the study revealed that inoculation of saliva alongside virus seemed to have a suppressive effect on development of clinical disease. However, fly feeding before inoculation of LSDV hastened and potentiated the disease pathogenesis with cutaneous nodules appearing faster and in significantly higher numbers than in the other treatment groups, and clinical animals developing higher clinical scores. To explore if these differences correlated with LSDV replication in the infected animals, quantification of the virus both systemically and locally was conducted.

The amount of viral DNA present in the blood of calves in each treatment group was determined by using a PCR assay targeting the LSDV074 ORF (also known as the P32 gene) of capripoxviruses. These PCR assays were carried out by the Non-Vesicular Reference Laboratory (NVRL) at the Pirbright Institute. The limit of detection was set at 42 cycles. All clinical animals developed a classic viraemia, with increasing amount of viral DNA detected in the blood up to 11 dpi (inferred by decreasing cycle threshold numbers). Viral DNA was occasionally detected in the blood of non-clinical animals, but the Ct value was high and intermittent (Figure 5.15).

On comparison between the treatment groups, the data mirrored the results from the clinical findings with viraemia detected slightly earlier in the fly fed group than in the other two groups, and at a lower Ct value, indicating higher amounts of viral DNA (Figure 5.16). The earlier viraemia in fly fed animals is more clear in Figure 5.17, with viral DNA detected in the blood of 5 calves in the CF group at 5 dpi, compared to only 1 calf in the CS group and 0 calves in the CV group. After 5 dpi the Ct values of the fly fed group and the virus only group continue to increase, however after 9 dpi in the saliva and virus inoculated group the Ct value plateaus. This echoes the average nodule number data for this group.

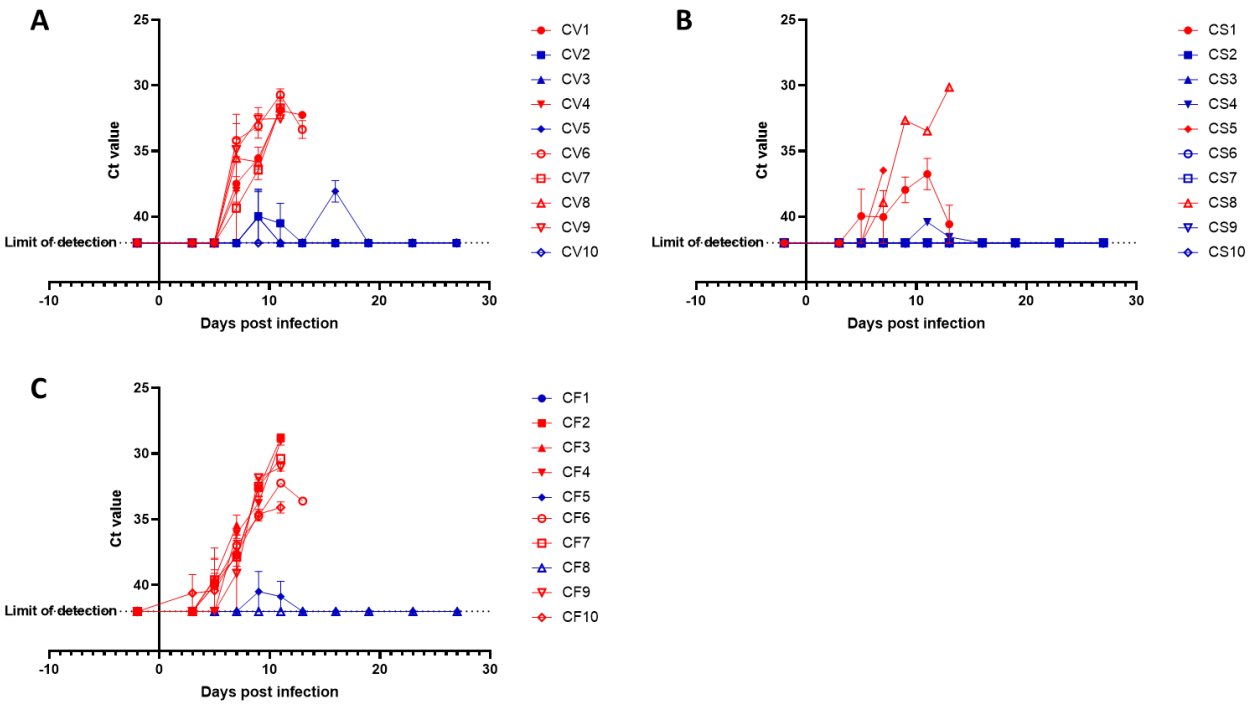


Figure 5.15 – Viraemia of individual infected animals

Viral DNA was detected in duplicate in EDTA blood samples from infected animals, using an established PCR assay targeting LSDV074. Animals who presented with a clinical outcome are shown in red, and with a non-clinical outcome in blue. Data shown as mean ± SEM. The PCR was carried out by the NVRL, Pirbright.

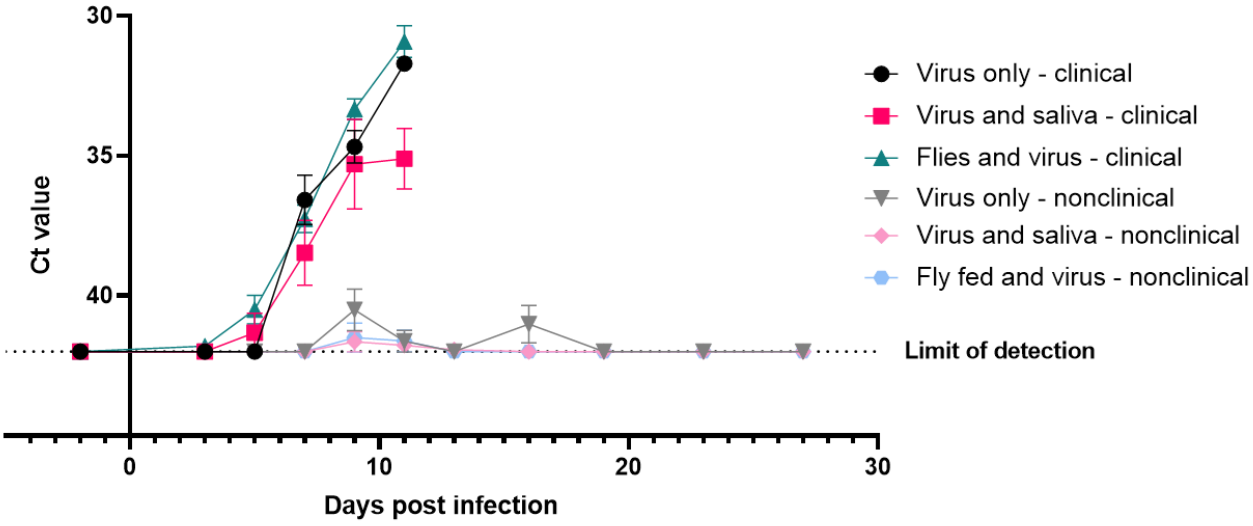


Figure 5.16 – Clinical animals develop a higher viraemia than non-clinical animals across all inoculation groups

Viral DNA was detected in duplicate in EDTA blood samples from infected animals, using an established PCR assay targeting LSDV074. They were then pooled into treatment groups and averaged. Data are shown from -2 dpi to 11 dpi. Data shown as mean ± SEM. The PCR was carried out by the NVRL, Pirbright.

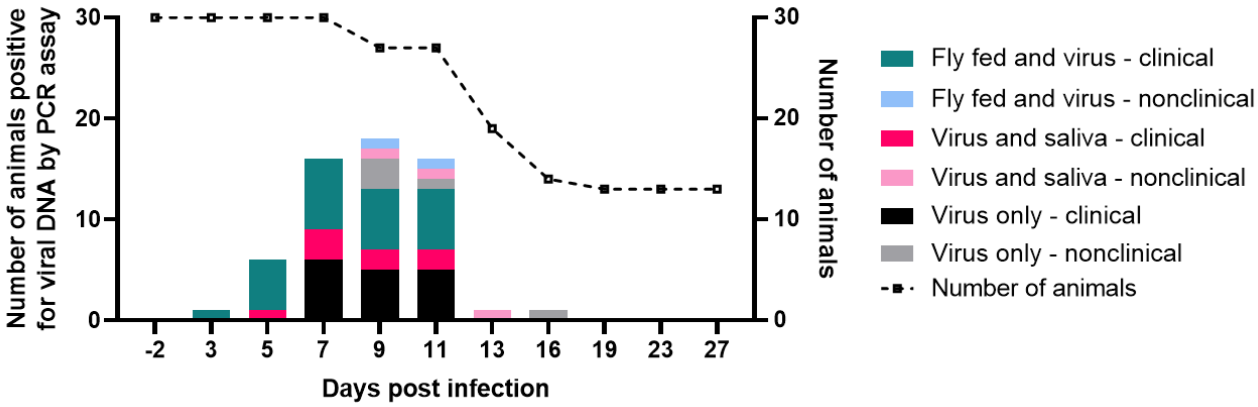


Figure 5.17 – Clinical animals in the fly spot-fed group develop a viraemia faster

Viral DNA was detected in duplicate on EDTA blood samples from infected animals, using an established PCR assay targeting LSDV074. The number of animals with any Ct value below 42 were then pooled into clinical outcomes within treatment groups. The number of animals present in the experiment was also tracked on the same graph. The PCR was carried out by the NVRL, Pirbright.

PCR assays detect viral DNA, including that from dead viral particles and viral debris, but does not quantify the amount of infectious virus present. To quantify the amount of infectious virus present in the blood of the inoculated calves, plaque assays were carried out on blood samples with a positive PCR result. Samples were titrated on a confluent monolayer of MDBK cells using calcium-free media and stained with crystal violet after 1 week.

In total 63 blood samples were titrated, 52 from clinical calves and 11 from nonclinical calves. Live virus was detected in eighteen samples, all from clinical animals (animals marked (C) in Figure 5.18). Titres of virus in the clinical animals was low, ranging from 10-1000 pfu/ml. No live virus was detected in the blood of a nonclinical animal. Ten of the samples containing live virus came from animals in the CF group, and only four from the CV and four from the CS groups. Live virus was detected in blood samples from 6/7 of the clinical calves in group CF, but only 2/6 of the clinical CV calves, and 2/3 of the clinical CS calves. In addition, animals in the fly fed and virus challenged treatment group had the

highest viral titres measured in their blood (1000 pfu/ml at 11 dpi). This finding aligns with animals in the fly fed group having the most severe disease scores.

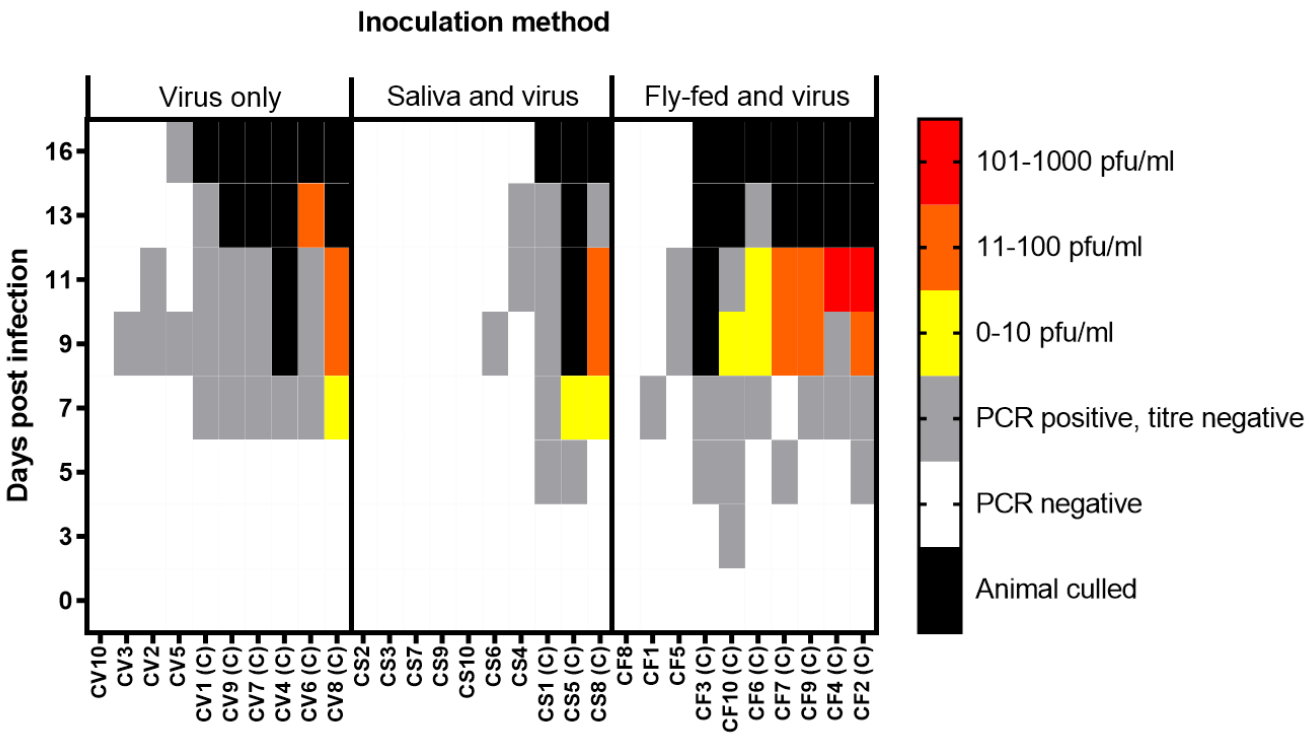


Figure 5.18 – Productive virus quantification of PCR positive blood samples

Blood samples that were NVRL PCR test positive were tested via MDBK plaque assay and stained after 7 days. Plaques were counted manually. (C) denotes a clinical animal.

To explore the amount of virus present in the skin of the calves during infection, 2mm skin microbiopsies were taken from nodules of clinical animals or normal skin of nonclinical animals at 5, 11 and 16 dpi. DNA was extracted from the biopsy and viral DNA quantified using a qPCR targeting the 068 ORF of LSDV. This PCR incorporated a standard curve to enable quantification of the amount of viral DNA present in each 2mm skin sample. Each sample was run in duplicate, and the limit of detection was set at 38 cycles. The PCR was carried out by Dr Henry Munyanduki from the PoxWorld team.

No viral DNA was detected in any of the skin samples collected at 5 dpi, with the exception of trace amounts detected in only one of the two duplicate PCRs from DNA extracted from

the skin of two preclinical calves in the CF group. In contrast, all samples taken from the nodules of clinical calves at 11 dpi were positive (5/5 clinical animals in the virus only inoculated group, 2/2 clinical animals in the saliva and virus inoculated group, and 6/6 clinical animals in the fly-fed and virus inoculated group (Figure 5.19). The viral genome copy numbers present in each microbiopsy at 11 dpi were similar between inoculation groups (Figure 5.20), with the exception of CV7. This suggests that the amount of viral DNA in the nodules of clinical animals is not impacted by inoculation method.

Only trace amounts of viral DNA (less than 1392 copies per biopsy on average) were detected in the skin samples taken from nonclinical calves (Figure 5.19, shown in yellow). Small amounts of DNA were detected in only one of the two duplicate PCRs from nonclinical calves CV2, CV10, CS2 and CS3 at 11 dpi. These trace amounts were detected at cycle thresholds above 38, which was much closer to the limit of detection, making the findings of lower confidence. Slightly more convincingly, trace amounts of DNA were detected in both duplicate PCRs from nonclinical calves CF1 and CF8. However, these findings should still be interpreted with caution. Despite the trace amounts detected in duplicate in the CF1 and CF8, it would be presumptuous to assume that these animals were PCR positive.

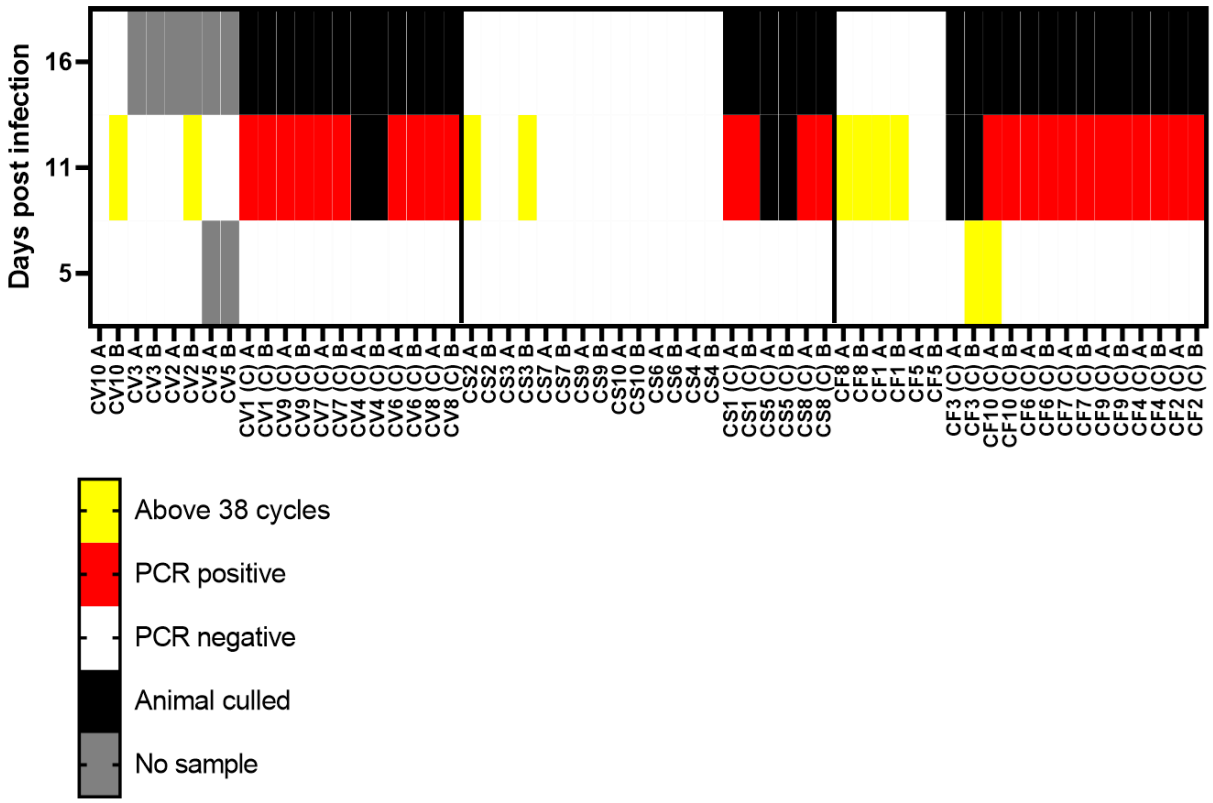


Figure 5.19 – Virus is detected in the skin of clinical calves at 11 dpi but not in non-clinical calves

Using 2mm biopsy punches, skin samples were taken from all animals at 5 dpi, 11 dpi and 16 dpi. Viral DNA was extracted from the tissue and quantified using qPCR in duplicate. (C) denotes a clinical animal. The PCR was carried out by Dr Henry Munyanduki.

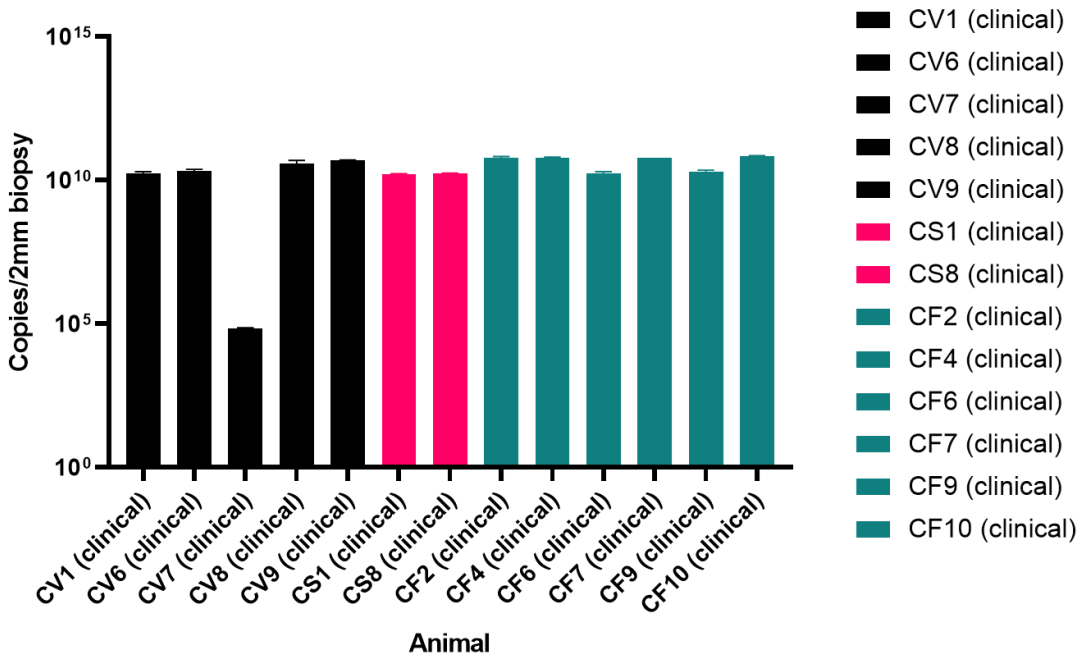


Figure 5.20 – Virus is produced in higher amounts in the skin of clinical animals at 11 dpi

Using 2mm biopsy punches, skin samples were taken from all animals at 5 dpi, 11 dpi and 16 dpi. Viral DNA was extracted from the tissue and quantified using qPCR in duplicate. Only samples from 11 dpi were positive and were shown here. Data shown as mean ± SEM. The PCR was carried out by Dr Henry Munyanduki.

5.3 Discussion

In vivo experimental models of LSD suffer from two major failings - they do not produce clinical disease consistently, and not include any components of arthropod vectors as would be present during natural transmission. During this project, three new in vivo models were developed that explored these challenges and questions.

The method of virus inoculation, by 10 microdoses at each inoculation site for every treatment group, was designed to mimic the feeding action of LSDV-positive flies during natural transmission. This was very different to previously described inoculation models, and there was uncertainty that this novel methodology would produce any disease, considering the smaller volumes of virus being used. In fact, this method of viral inoculation produced disease more consistently than in previous studies. Of the 17 cattle infected in previous transmission studies at Pirbright using a large intravenous bolus of virus alongside intradermal inoculations, 7 calves (41%) developed clinical disease, with only 4 (23%) progressing to severe disease (Sanz-Bernardo et al., 2021, Sanz-Bernardo et al., 2022). In the virus only microinoculated group in this experiment (CV), 60% of calves developed severe disease, more than twice the number in the previous studies. This increase in the number of severely affected cattle following inoculation has led to this “microinoculation” model being adopted as the gold-standard for other LSD experimental work at Pirbright, and enabled group sizes to be reduced.

This increase in the number of cattle developing severe disease in the CV group could be due to the use of the multiple microinoculations. Smaller volumes of virus are inoculated which, instead of getting flushed away through lymphatic drainage, may be able to remain in the skin and infect fibroblasts and other skin cells. It is also possible that removing the large intravenous bolus of LSDV could have had an impact- a concentrated amount of

purified virus taken in the bloodstream to the spleen could have driven a more rapid systemic immune response and thus reduced the number of cattle that developed severe disease.

There was a similar clinical outcome in the calves in the fly-fed and virus inoculated group (CF), with 7 out of 10 inoculated calves developing clinical disease, suggesting that spot-feeding by the flies did not impact the number of animals developing clinical disease when compared to the group inoculated by microinoculation of virus alone (CV). However, the saliva and virus inoculation mix (CS group) showed a strong trend for suppression of disease development, with only 30% of animals developing clinical disease. This was opposite to the initial hypothesis, since previous studies of biologically transmitted arboviruses have shown that vector saliva can increase viraemia and tissue titres in murine models of West Nile virus infection (Styer et al., 2011), and increase infectivity in models of dengue virus and Semliki Forest virus in murine hosts (Conway et al., 2014, Lefteri et al., 2022). The suppressive effect of the virus and saliva mix in this model of LSD may be related to the amount of saliva inoculated. It is not known how much saliva is inoculated by *S. calcitrans* when feeding, therefore a standard amount of 10µg of saliva protein was used in the CS inoculation. This is most likely a higher amount of saliva than would be inoculated by flies in the field. As stated in Chapter 3, *S. calcitrans* secreted saliva contains Antigen-5, which has been shown to have immunomodulatory properties, and other active substances such as salivary enzymes. The inclusion of a high concentration of salivary proteins containing immunomodulators could have provoked a greater immune response which might either have been able to eliminate the virus or may have created an environment less conducive for viral establishment. There could be a “Goldilocks” level of saliva that is not too little and not too much, but just right to be able to modulate the local immune response to enable

LSDV to survive long enough to replicate, or even invoke the presence of immune cells that the virus can infect and hijack.

These models developed in this chapter needed to be able to produce clinical disease that was representative of disease observed in cattle following natural LSDV transmission in the field. All clinical animals produced raised cutaneous nodules comparable in appearance and presentation to that seen previously, as well as a fever. With disease confirmed, the differences in disease presentation between the three treatment groups was examined using clinical data. Several key clinical signs were measured over the course of the experiment, including rectal temperature, heart rate, respiratory rate, and pre-scapular and pre-femoral lymphadenopathy. In terms of temperature, there was a difference between the clinical and non-clinical animals in all inoculation groups. Clinical animals in all groups experienced a higher initial temperature spike at 5 dpi, before rising again to a sustained high temperature. This pattern was not recapitulated in the non-clinical calves, who experienced a similar but much more transient peak in rectal temperature at 9-10 dpi. This temperature spike across all inoculated animals, clinical and non-clinical, has been recorded in previous experimental models. Fever in animals with a systemic poxvirus disease is not unexpected. That it is seen in non-clinical animals is more unusual, and suggests that these animals are also experiencing a detectable systemic response. It has been noted that fever can result in increased expression of cell membrane molecules that enhanced lymphocyte movement (“homing”) into the lymphatic system (Chen et al., 2006) and an increase in neutrophil recruitment to local sites of infection (Rice et al., 2005). However, organisms that developed more than a mild fever in response to viral infections often had worse outcomes, in part due to the metabolic cost, heat stress to cells, and organ

dysfunction (Belon et al., 2021). This could explain how despite all challenged animals developing a fever, some animals resolved infection, and some went on to become clinical.

Differences between the three groups were most obvious when the cutaneous nodules were counted and analysed. The cutaneous nodules are the defining clinical feature of LSD, and in past experimental models, their numbers on each animal have been used as a proxy for disease severity (Sanz-Bernardo et al., 2021). When analysed, nodules on the clinical animals in the fly-fed and virus challenged group (CF) appeared in significantly higher numbers than the virus only challenged group (CV) at 7 dpi. Nodule numbers in the mixed saliva and virus inoculated group (CS) varied between the three clinical calves, making comparisons with this group more difficult. Discovering that nodules were developing earlier and in significantly higher numbers in fly-fed animals is important: it demonstrates that the fly vector alters the pathogenesis of the disease, and that inoculating with LSDV alone is perhaps not the best experimental infection model for studying pathogenesis and the early immune response in the skin.

The differential timing of nodule development could be due to the trauma of the fly bite, and/or the inoculation of fly saliva. These factors could alter the immune environment into which the virus was then inoculated. Since nodules in the skin of saliva and virus inoculated animals (group CS) were more variable, it is tempting to say that the saliva of the vector is not the deciding factor, however, it should be reiterated that this group was most likely inoculated with a higher concentration of salivary proteins than flies feeding would normally inoculate. *S. calcitrans* are telmophagous flies which use coarse labellar teeth to lacerate tissues to create pools of blood, or haematomas, to feed from (Lavoipierre, 1965). This causes a lot of damage to the skin and could recruit inflammatory cells to the site to then be infected, or cause oedema and thus heighten the lymph flow, and transport of

virions systemically. The importance of the local immune environment to poxviruses has been highlighted previously by work on scarification for vaccinia virus vaccine delivery, which has been shown to induce a robust T cell and non-specific immune response (Liu et al., 2010, Rice et al., 2014). The findings from the CF group in our experiment is consistent with this, suggesting that the vector alters the dermal microenvironment, thereby acts as a catalyst for disease development.

Studies to quantify virus also gave interesting results that mirrored the findings of the clinical observations. PCR assays and viral titrations were used to measure the presence of viral DNA and quantity of infectious virus in blood samples from all experimental animals. The presence of viral DNA in longitudinal blood samples of infected cattle was first investigated using a PCR assay, which showed that it was present in all clinical animals and only transiently in non-clinical animals, at low levels. This is consistent with previous models of experimental LSDV infection in cattle (Sanz-Bernardo et al., 2021, Aerts et al., 2021). Ct values detected were very similar between the virus only inoculated (CV) clinical animals and the fly-fed and virus inoculated (CF) animals across all timepoints post infection, with divergence in Ct values for the saliva and virus inoculated (CS) animals at 11 dpi to higher values, implying less viral DNA in the blood at that timepoint. However, there were only two clinical animals in the CS group at 11 dpi which could bias the data. These results also showed that LSDV DNA was detected earlier in the fly-fed group (CF) than in the other groups, first noted at 3 dpi. This implies that the virus became systemic within the bloodstream more quickly than in the other inoculation groups, suggesting that the insect bite and/or saliva could be assisting in viral evasion of the immune response in the skin, accelerating the movement of virus to the lymph nodes. However, presence of DNA does not always correlate with infectious virus. Therefore, titrations of the whole blood

were undertaken and showed that higher titres of virus were detected in more animals in the fly-fed inoculation group (CF) than in the other groups. Altogether, this suggests that fly-fed and virus inoculated animals experienced an earlier viraemia at 3 and 5 dpi with more calves with higher titres of productive virus at 9 and 11 dpi when compared to the other groups. These results are consistent with the appearance of nodules in greater numbers, faster, in this group.

The viral titres measured in the blood were very low, however copy numbers of viral DNA were very high in the skin nodules (greater than 10^{10} copies per 2mm biopsy). These findings are consistent with previous work (Sanz-Bernardo et al., 2022) which found low amounts of virus in the blood but very high amounts in the skin nodules. It is possible that the virus spreads in the animal through the blood at low levels and is then seeded out and multiplies to much higher numbers in the skin. Higher amounts of virus in the skin would give a greater chance of mouthpart contamination of arthropod vectors and consequent spread onwards to naïve animals. A more novel finding was that there was no difference in the amount of viral DNA in the skin between the three inoculation groups. The change in pathogenesis that fly feeding causes was seen in early stages of disease manifestation and in blood, but not in the skin (in clinical animals). Fly feeding prior to virus inoculation may cause an increase in the number of nodules, but it does not change their morphology or the amount of virus present in them. An increased number of lesions and thus transmission opportunities could mean that increasing the amount of virus in each lesion is superfluous and risks exposure to the host immune response. Therefore, the fly fed pathogenesis does not evoke an increase in the amount of virus in the skin. To investigate this hypothesis further, future studies could take larger biopsy samples from the skin nodules which would enable titration of live virus.

In previous work, scoring rubrics were compiled that aimed to assess the severity of LSD produced by experimental infection. However, these past scoring systems needed further optimisation, in order to take into account the complete range of clinical signs. Though the number of nodules had been observed to be greater and developed faster in fly fed animals, for a more severe pathogenesis to be decisively attributed to this inoculation methodology, more factors needed to be included in the overall assessment of severity. Additionally, the construction of a more comprehensive scoring system could result in a matrix with predictive capabilities. On compiling a range of recorded clinical signs and weighting them according to the perceived impact on the animal, the scoring system provided better granularity, showing a clear difference in score between clinical and non-clinical animals, which was significant at 7 and 11 dpi in the virus only challenged group and the fly-fed and virus challenged group. The scores were not significantly different between the treatment groups apart from at 7 dpi between clinical scores of fly-fed and virus challenged cattle and virus only inoculated animals. Additionally, the scores were not significantly different before the nodules appeared (the current accepted determinant of a clinical outcome). This shows that the scoring system currently is not predictive of disease but could be useful for monitoring animal welfare and treatment as disease progresses.

5.4 Summary

Experimental cattle infection models of LSDV currently lack inclusion of the vector in their methodologies, and do not produce disease consistently. The novel microinoculation infection model developed here was able to produce disease more reliably, in 60% of calves inoculated. Comparisons of different inoculation methods revealed that vector interaction can affect pathogenesis of LSD. Direct feeding of *S. calcitrans*, a vector thought to

mechanically transmit LSDV, led to the production of more nodules, a higher and earlier viraemia, and a more severe disease than virus inoculated alone. *S. calcitrans* saliva inoculated at this concentration appeared to suppress disease. This vector was more than just a “dirty needle”, but it was still unclear why these outcomes were observed in the animals. The immune response to feeding trauma and salivary proteins could be a key factor in the clinical presentation and altered disease pathogenesis of the infected animals.

6

Immune responses to *S. calcitrans* interactions with the host and LSDV infection

6.1 Introduction

Chapter 5 explored the interactions between LSDV, *S. calcitrans* and the bovine host by comparing the outcome of intradermal inoculation of cattle with (i) LSDV (CV), (ii) LSDV and *S. calcitrans* saliva (CS), or (iii) LSDV inoculated immediately after spot-feeding of *S. calcitrans* (CF). Cattle inoculated with LSDV after fly feeding developed disease more quickly than cattle inoculated with LSDV alone, reached higher clinical scores and had more virus in their blood. In contrast, fewer cattle inoculated with LSDV mixed with *S. calcitrans* saliva (CS) developed disease. To understand the basis for the differences in pathogenesis between the three inoculation methods, the systemic immune responses of the cattle to LSDV inoculation were studied.

A successful immune response detects and identifies a pathogen and clears it without excessive damage to the host. An immune response to viral infection starts with an immediate innate immune response that, if warranted, develops to the more specific adaptive immune response. The bovine immune response to LSDV is poorly understood, and the specific bovine immune responses to the combination of LSDV and the inoculating vector are even less well known.

Haematophagous arthropods elicit local and systemic immune responses when they feed as they cause tissue injury in their pursuit of a blood meal. Some arthropods such as *S. calcitrans* cause more significant trauma and pain due to their feeding methodology and size of proboscis. *S. calcitrans* are telmophagous or "pool feeders": when they feed, they lacerate the tissues of the skin, collecting blood from the resultant haemorrhagic pool. This trauma triggers a swift inflammatory and innate immune response. In addition to the trauma of feeding, arthropod saliva has been demonstrated to have immunomodulatory properties. It contains components that likely evolved to facilitate the blood-feeding of the arthropod, for example to prevent vasoconstriction (Lerner et al., 1991) and aggregation of platelets (Ribeiro et al., 1984). Additionally, to respond to the immune attack invoked by the biting action, saliva of ticks, mosquitoes and sandflies has been shown to stymy innate immune response strategies (Bissonnette et al., 1993, Cavalcante et al., 2003, Gwakisa et al., 2001) and alter adaptive immune responses to hinder the cell-mediated immune response (Theodos and Titus, 1993, Wasserman et al., 2004).

The action of arthropod saliva may aid in the infection and pathogenesis of the virus (Styer et al., 2011, Schmid et al., 2016). Of particular relevance to this study, the saliva of *S. calcitrans* has been shown to suppress bovine lymphocyte proliferation (Swist et al., 2002). The work in this thesis has shown that secreted saliva of *S. calcitrans* contains abundant Antigen-5 (see Chapter 3) which has immunoglobulin binding and therefore potentially immunomodulatory properties (Ameri et al., 2008). It is therefore possible that the bite trauma or the saliva of *S. calcitrans*, or a combination of the two, could have an immunomodulatory impact and therefore influence the development of LSD in vivo.

The aim of this chapter was to explore the influence of the vector *S. calcitrans* on the immune response of cattle that had been experimentally infected with LSDV.

6.2 Results

6.2.1 Blood cell population changes in response to LSDV inoculation

Poxviral disease is associated with alterations in the haematological profile, including leukopenia (De et al., 2020), lymphopenia (Rehfeld et al., 2013), and neutrophilia (Jeklova et al., 2008). In cattle naturally infected with LSDV, studies of the blood showed an early lymphopenia, and a later macrocytic hypochromic anaemia (Neamat-Allah, 2015). To explore the haematological changes associated with the three inoculation methods of LSDV challenge, the changes in the number of mononuclear leukocytes in the venous blood of cattle intradermally inoculated with LSDV was examined. Due to the high containment nature of the experiment standard haematological analysers could not be used, therefore a flow cytometry panel was designed.

The flow cytometry panel incorporated counting beads to enable quantification of absolute numbers of monocytes, T cells, B cells and gamma-delta T cells present in blood. Briefly, heparinised blood was collected from each animal and mixed with conjugated antibodies before red blood cells were lysed and the counting beads added. Cell populations within samples were then determined by flow cytometry using the BD LSR Fortessa. The gating strategy to identify specific cell populations in the blood is described in Figure 6.1. The number of cells of each subpopulation per µl was then calculated and compared between cattle of the different inoculation groups.

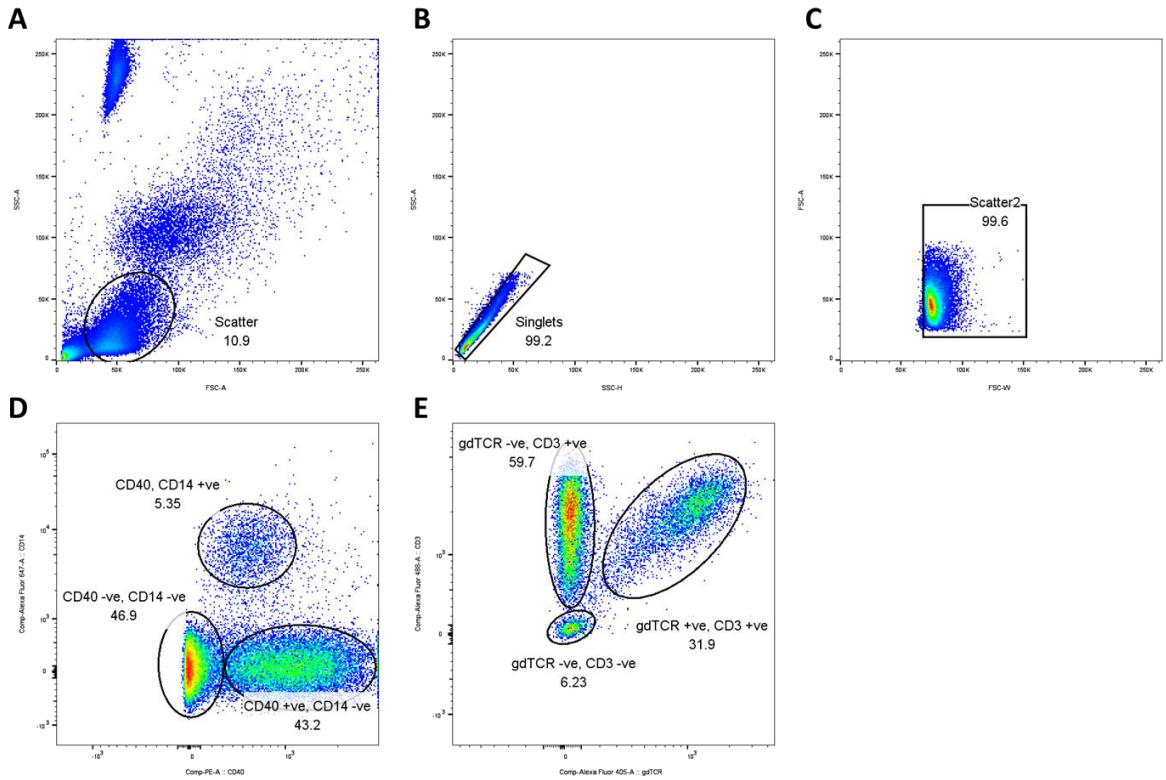


Figure 6.1 – The whole blood flow cytometry panel gating strategy.

Cells were plotted on a forward vs side scatter plot (A) to isolate the mononuclear cell population, then gated to exclude doublets via a side scatter area vs height plot (B). Further debris was excluded by gating on a forward scatter area vs width plot (C). Monocyte (CD14 positive, CD40 negative) and B cell (CD14 negative, CD40 positive) populations were selected by plotting markers for CD14 vs CD40 (D). The CD40/CD14 negative population was plotted on CD3 vs gamma delta T cell receptor (γδ TCR) cell marker plot, to isolate the T cell population (CD3 positive, γδ TCR negative) and gamma delta T cells (CD3 positive, γδ TCR positive) (E).

There was variation in cell numbers between individual animals before challenge (Figure 6.2). For example, animal CV5 (a non-clinical animal) had higher numbers of T cells than the other animals in the virus only inoculated group across the whole experiment, and animal CS9 (also a non-clinical animal) had a higher gamma delta T cell count across the whole experiment. This inter-animal variation in haematologic profiles has been observed in other work on cattle and could be due to factors such as recent activity, hydration, or body condition (Roland et al., 2014). Despite this variation, broad trends present across the animals over time were very similar.

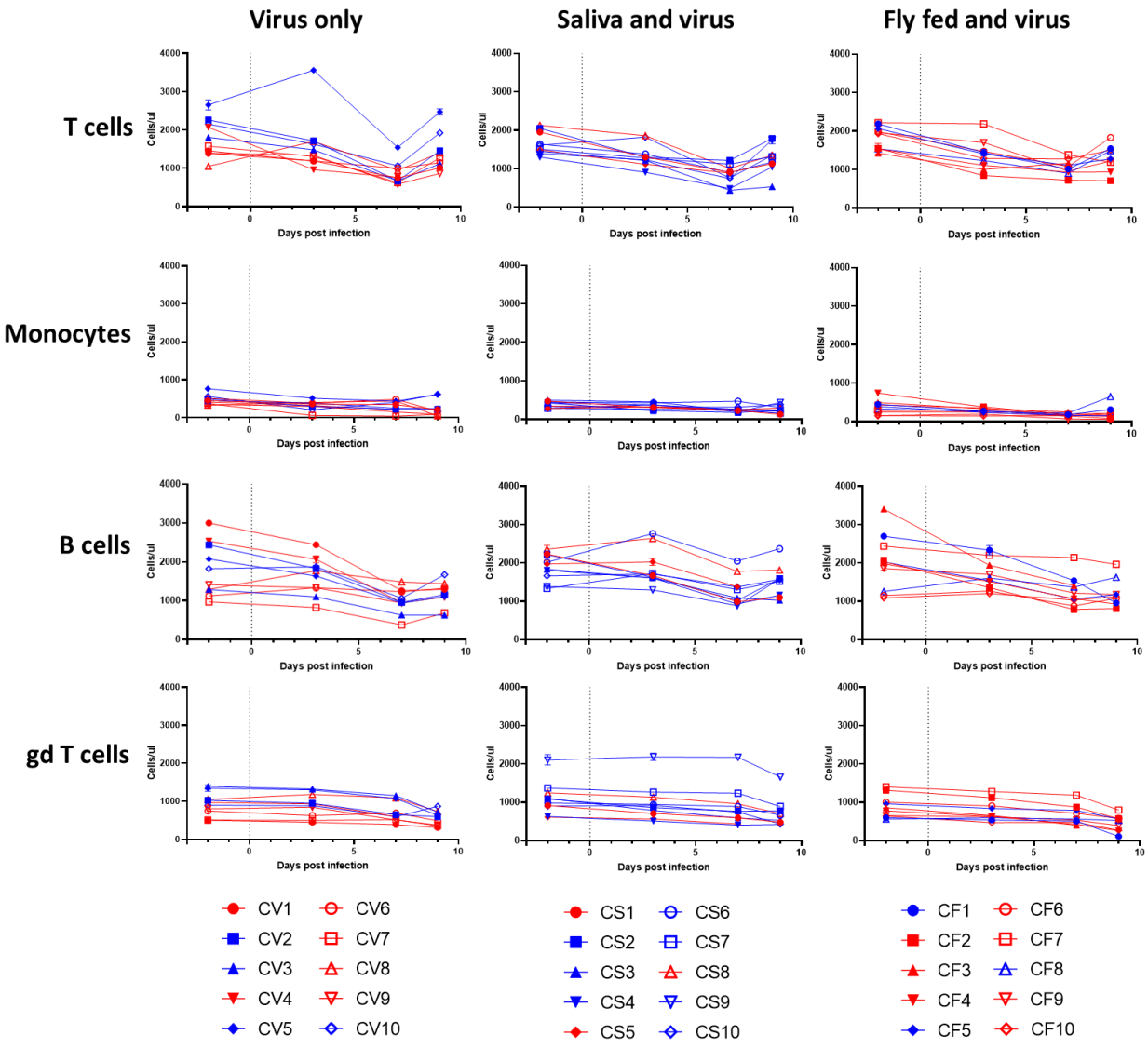


Figure 6.2 – Mononuclear cell population profiles show similar trends in the response to LSDV across treatment groups

Populations of blood mononuclear cells were gated and the absolute count of cells/µl was calculated for each animal and cell type. The dashed line indicates the day of challenge. Animals that became clinical are shown in red, and those that remained non-clinical are shown in blue. The panel was carried out in triplicate. Data shown as mean ± SEM.

To see if the method of inoculation influenced the cellular response to infection, the cell numbers of each cell type for every animal were averaged across the different methodologies (CV, CS and CF) and compared (Figure 6.3, left panel) and shown as a proportion of the baseline at -2 dpi. The panel showed that T cell numbers decreased after challenge until 7 dpi to 50.5% of pre-challenge numbers for the virus only group, 58% for

the fly-fed group, and 51.2% for the virus and saliva inoculated group. Numbers of T cells then increased sharply between 7 and 9 dpi, recovering to 81.8% of pre-challenge numbers in the virus only challenged group, 69.2% in the fly-fed group, and 77.0% in the virus and saliva inoculated group.

Following LSDV inoculation the proportion of monocytes reduced substantially to 7 dpi for all three groups to a mean of 64.1% of the pre-challenge numbers for the virus only group, 52.1% for the fly-fed group and 71.1% for the virus and saliva inoculated group. Monocyte numbers then dropped further at 9 dpi in the virus only group, increased in the fly-fed group, and remained consistent in the virus and saliva inoculated group.

γδ T cells in all three treatment groups followed a similar trend. At 3 dpi, all groups showed numbers of 87.7 to 96.8% of pre-challenge. There was then a reduction of cell numbers by 7 dpi to 74.8-79.4%. At 9 dpi numbers reduced again, with the virus only group and the saliva and virus group experiencing very similar declines in cell proportion, of 16.3% and 15.1% respectively. The fly-fed group experienced a larger reduction of 23.1% to 51.7% of pre-challenge numbers.

B cell numbers stayed at pre-challenge levels for the virus only challenged group until 3 dpi before reducing by 33.8% between 3 and 7 dpi, and then rising to an average of 73.5% at 9 dpi. Mean cell number proportions for the fly-fed and virus challenged groups reduced more slowly after challenge, with a reduction to 89.4% from the pre-challenge average by 3 dpi, and to 67.7% by 7 dpi. This group only exhibited a small recovery in cell numbers at 9 dpi, to 72.3% of pre-challenge numbers. The saliva and virus challenged group followed a similar trend to the virus only group, plateauing until 3 dpi before dropping to 69.2% of pre-challenge levels at 7 dpi and rising again by 15.0% at 9 dpi to 84.2%.

The data were then analysed to determine if there was a correlation between changes in the haematological profile and clinical outcome. The 30 cattle were grouped into clinical (n=16) and non-clinical (n=14) outcomes, and the change in cell number proportions relative to pre-challenge numbers analysed (Figure 6.3, right panel). Both clinical and non-clinical animals developed a marked lymphopenia at 7 dpi, with the average number of T cells dropping to 56.6% of pre-challenge numbers at 7 dpi in the clinical calves and to 49.3% in the non-clinical calves over the same time period, and B cells dropping to 66.2% at 7 dpi in the clinical calves and to 65.2% in the non-clinical calves. A consistent decrease in cell number proportions was also seen in monocytes in clinical and non-clinical calves. The average proportion of monocytes in clinical animals reduced by 37.7% by 7 dpi, and by 37.4% in non-clinical animals. Between pre-challenge and 7 dpi, γδ T cell numbers also decreased in both clinical and non-clinical animals. In clinical calves, average cell numbers dropped to 74.7%, and to 79.7% in non-clinical calves. The number of γδ T cells continuing to reduce in clinical and non-clinical calves to 9 dpi, to proportions of 55.2% and 62.2% respectively however the numbers of T cells, B cells and monocytes stayed steady or rose towards pre-challenge levels at day 9, with the exception of monocyte numbers in clinical calves. At 9 dpi there was a sharp divergence between clinical and non-clinical animals, with non-clinical animal monocyte numbers increasing but clinical animal monocyte numbers continuing to drop. This divergence was not significantly different according to a mixed-effects analysis.

Overall, these cell subpopulation dynamic analyses indicate that infection by LSDV causes a B, T and γδ T cell lymphopenia in all treatment groups. This lymphopenia is first detected at 3 dpi, which is 24 h before pyrexia was detected in the clinical calves (Figure 5.8) and 2-4 days before skin nodules developed (Figure 5.11). The lymphopenia was more marked at

7 dpi. Additionally, the most rapid changes were seen in the circulating monocyte populations, with an obvious reduction in all three groups as early as 3 dpi. No significant difference between the three groups in any cell subpopulation dynamics were detected. There was also surprisingly little difference in number of leukocyte subpopulations present in the blood when comparing clinical and non-clinical animals across the three groups, with the exception of a trend for continued reduction in circulating monocytes at 9 dpi in clinical animals. This study of the cell subpopulation dynamics of the calves did not reveal an obvious reason for the difference in disease phenotype between the three groups. Furthermore, cell subpopulation dynamics did not shed light on the factors determining clinical or nonclinical disease outcomes.

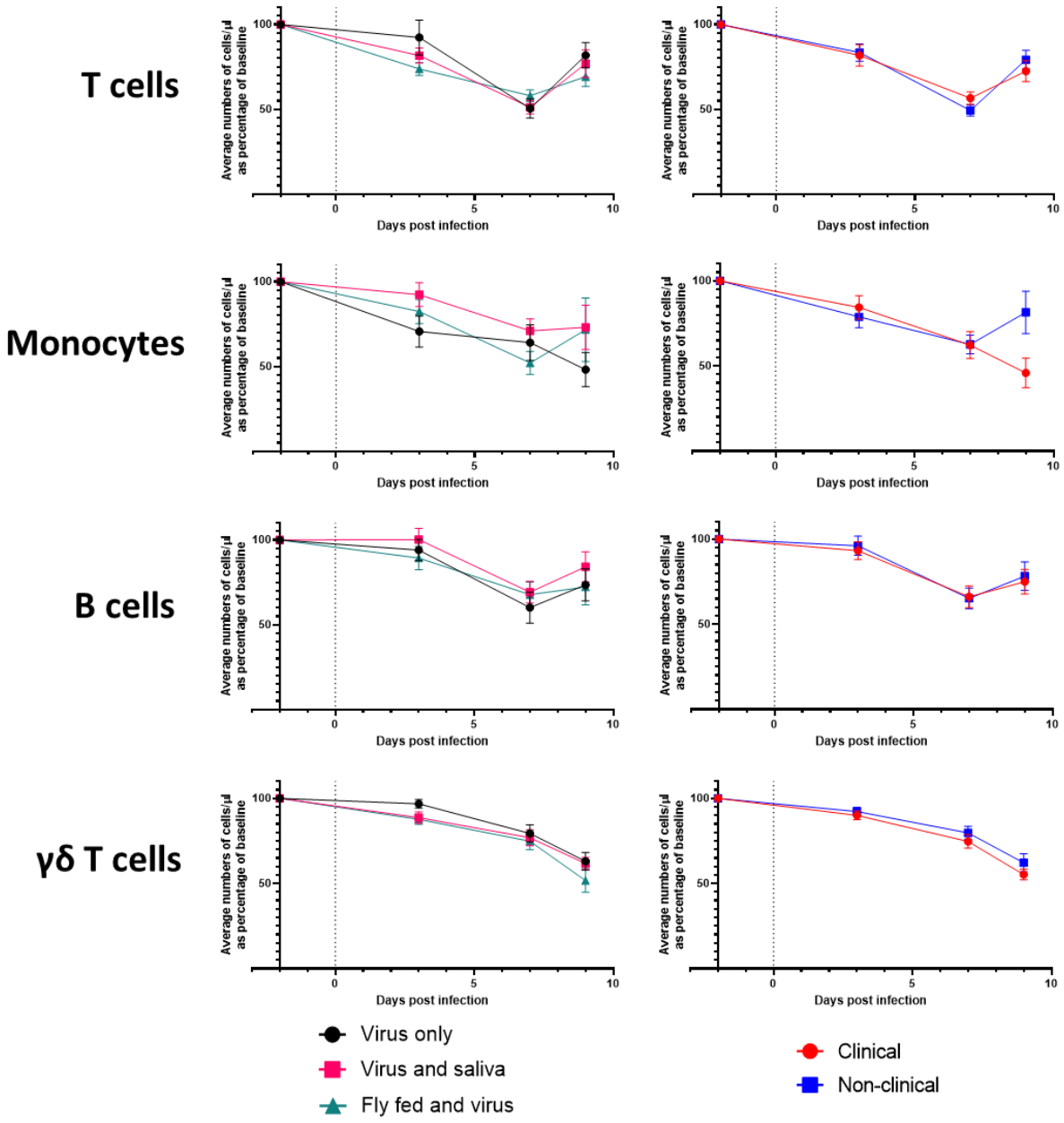


Figure 6.3 – LSDV infection of cattle induces a lymphopenia in clinical and non-clinical animals

The counts of cells/µl for each animal were converted to be a percentage of the cell count at -2 dpi for each animal, for each cell type. These proportions were then pooled into the treatment groups for each cell type and averaged. The dashed line indicates the day of challenge. Animals in black were only inoculated with virus, animals in pink were inoculated with saliva and virus, and animals in blue were spot fed with flies then inoculated with virus. The groups were then pooled and were split into clinical and non-clinical outcomes. Animals that became clinical are shown in red, and those that remained non-clinical are shown in blue. Data shown as mean ± SEM.

6.2.2 Inoculation route and clinical outcome are not correlated with a cell-mediated IFN-γ dependent immune response, as measured by a whole blood interferon-gamma assay

Interferon gamma (IFN-γ) is produced by activated T cells in response to infection. Quantification of the amount of IFN-γ produced in response to stimulation with an antigen, often called a recall assay or a cytokine release assay, measures the level of T-cell immune potential.

To assess the production of IFN-γ in response to challenge by LSDV, heparinised blood samples were collected from all challenged calves and stimulated on the day of sampling with live attenuated LSDV strain Neethling or controls. PBS was used as the negative control stimulus and pokeweed mitogen was the positive control. After incubation overnight the plasma was collected and the IFN-γ produced quantified using an ELISA. The mock stimulation of the blood with PBS produced negligible amounts of IFN-γ at any of the timepoints demonstrating very minimal pre-existing or non-specific production of IFN-γ, and production of IFN-γ was detected in response to PWM for all the timepoints for all calves in every treatment group, though not at consistent levels (Figure 6.4). The peak of IFN-γ release in response to LSDV Neethling was 11 dpi for the majority of animals, with a maximum response of 206 IU/ml in calf 8 of the fly-fed and virus inoculated group (Figure 6.5A and B). When the results are compiled into the clinical outcomes for each treatment group (Figure 6.5C) there is a trend towards non-clinical animals in the virus only and virus plus spot feeding groups having higher production of IFN-γ in response to stimulation with LSDV Neethling than the clinical animals, a trend that is reversed for the saliva and virus group (Figure 6.5C). However, the amount of IFN-γ produced in response to LSDV Neethling stimulation varied greatly from animal to animal. When the data for day 11 is plotted as

individual data points (Figure 6.5D), one animal in each group has a very strong response to incubation with LSDV Neethling, with low to trace amounts detected in the other calves. Therefore, no firm conclusions can be made from this data about the role of arthropods in the development of a cell-mediated immune response in response to LSDV inoculation.

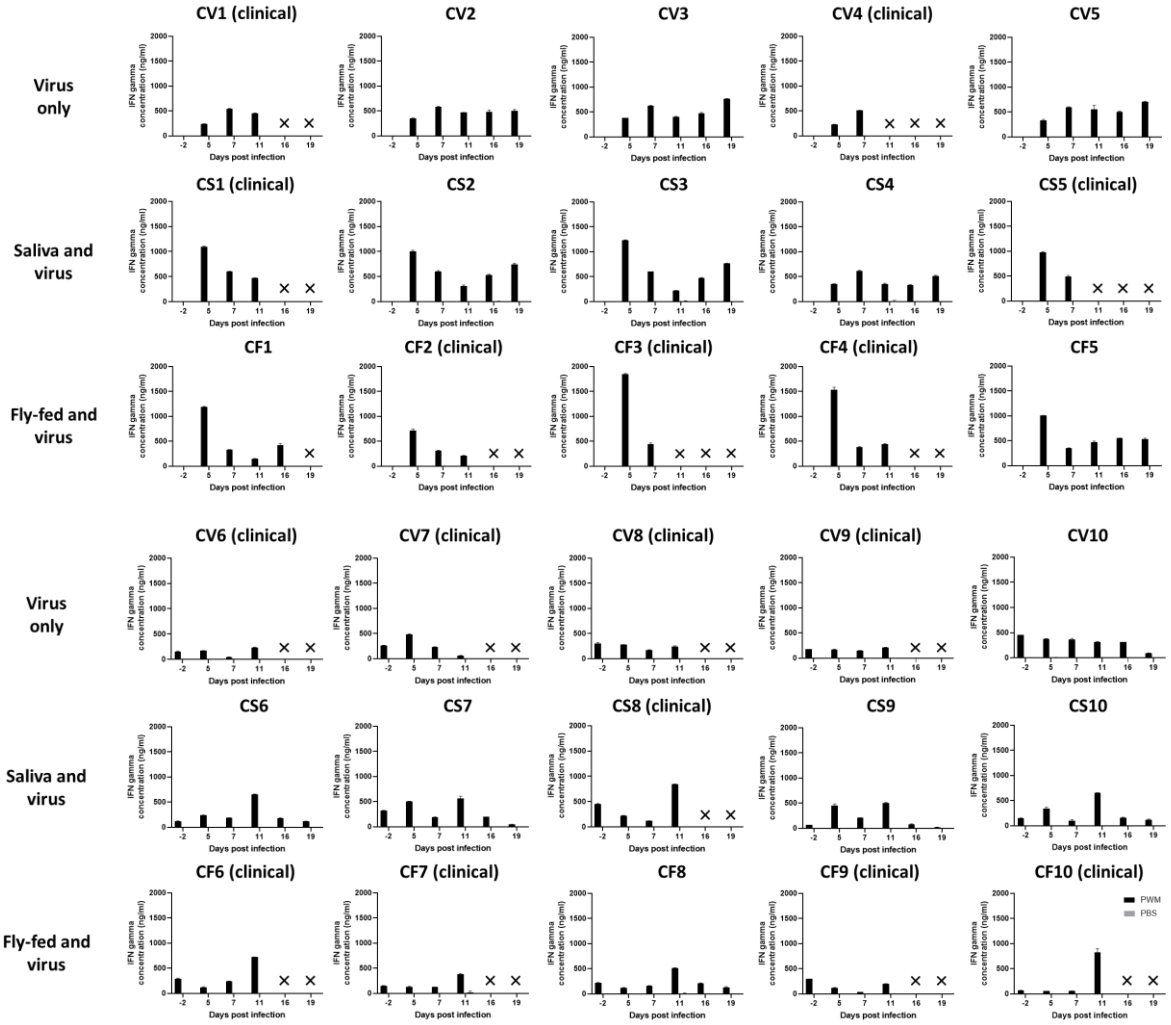


Figure 6.4 – The positive and negative controls for the interferon gamma release assay

The positive control (pokeweed mitogen) and the negative control (phosphate buffered saline) were used to stimulate IFN-γ production by cell in whole blood overnight followed by the collection of supernatants which were used to perform IFN-γ ELISAs to quantify the concentration of IFN-γ produced. The positive control (black bars) is on the left of each timepoint tick, and the negative control (grey bars if present) are on the right of each timepoint tick. Each condition was performed in two technical repeats and the error bars represent the standard error of the mean. The '×' symbol shows that the animal had been euthanised at that sampling point.

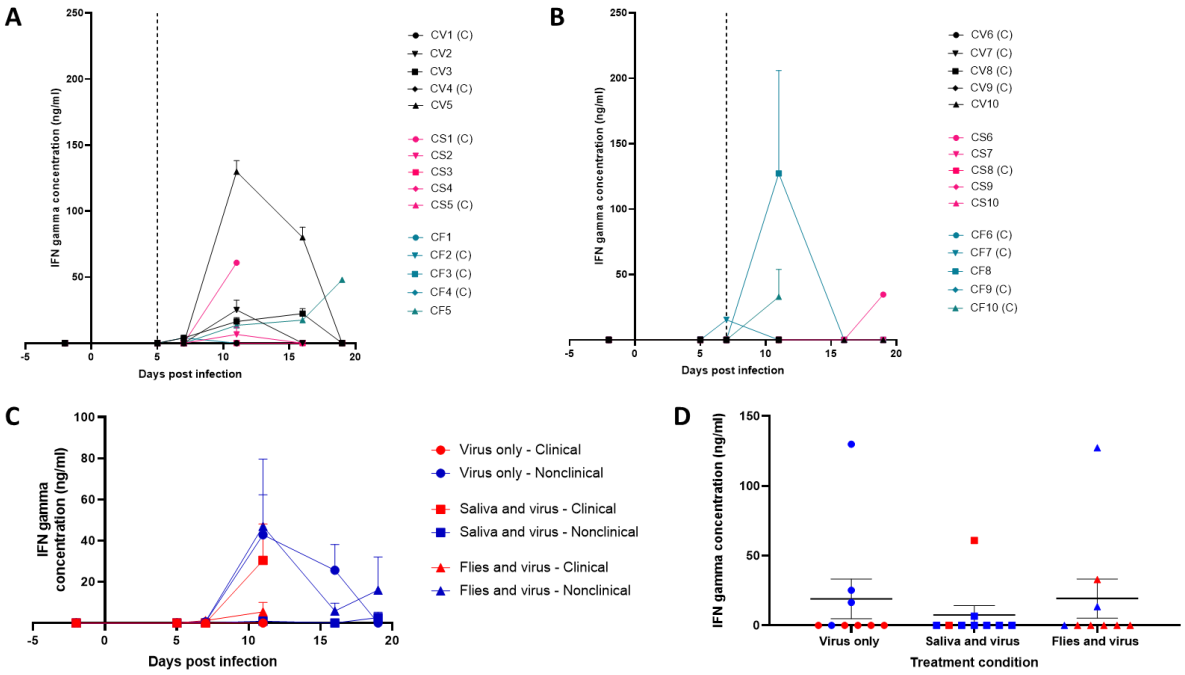


Figure 6.5 – Interferon-gamma release by immune cells in stimulated whole blood is not associated with clinical outcome or inoculation route

Blood samples from challenged animals were stimulated on the day of sampling with LSDV Neethling. Each sample was processed in duplicate on an ELISA to measure the IFN-γ released. IFN-γ concentrations released by blood cells from cattle in the first (A) and second (B) LSDV infection experiment were averaged and plotted; samples in black were from the virus inoculated group, in pink for the virus and saliva inoculated group, and in blue for the fly fed and virus inoculated group. C in the graph legend indicates that the individual animal had a clinical outcome. The results of all clinical and non-clinical animals in each inoculation group were combined to compare the outcomes (C). Graph shows data collected from -2 dpi to 19 dpi. Results from day 11 post challenge were shown individually to demonstrate the distribution (D). Data shown as mean ± SEM. Dotted line shows when nodules first appeared.

6.2.3 LSDV antibody production by LSDV challenged animals does not pass threshold levels

To explore if the production of anti-LSDV antibodies by the cattle was a factor in the clinical outcome of disease, or in the pathogenesis of disease in the different treatment groups, serum was harvested from each animal and then tested on a commercial capripoxvirus enzyme-linked immunosorbent assay (ELISA) kit (IDVet, ID Screen® Capripox Double Antigen Multi-species). Animals challenged only with LSDV, and those fly-fed then challenged with LSDV had only one animal in each of the respective groups that reached

the positive threshold for the test (Figure 6.6.A and C). In the saliva and virus challenged group, three animals crossed the threshold for positivity, with one animal (CS6), reaching a very high, and replicable, S/P% (Figure 6.6.B) (where S/P is a semi-titration calculated by the comparison of a samples colour change to that of a positive standard). However, when the animals were pooled into their treatment groups and compared (with animal CS6 being excluded as an unusual outlier), there was not a substantial difference between the groups (Figure 6.6.D). Overall, these data suggest that the antibody response to LSDV challenge, as measured by ELISA, rises to only low levels over the initial 28 days. Furthermore, no correlation with inoculation method or disease outcome was detectable.

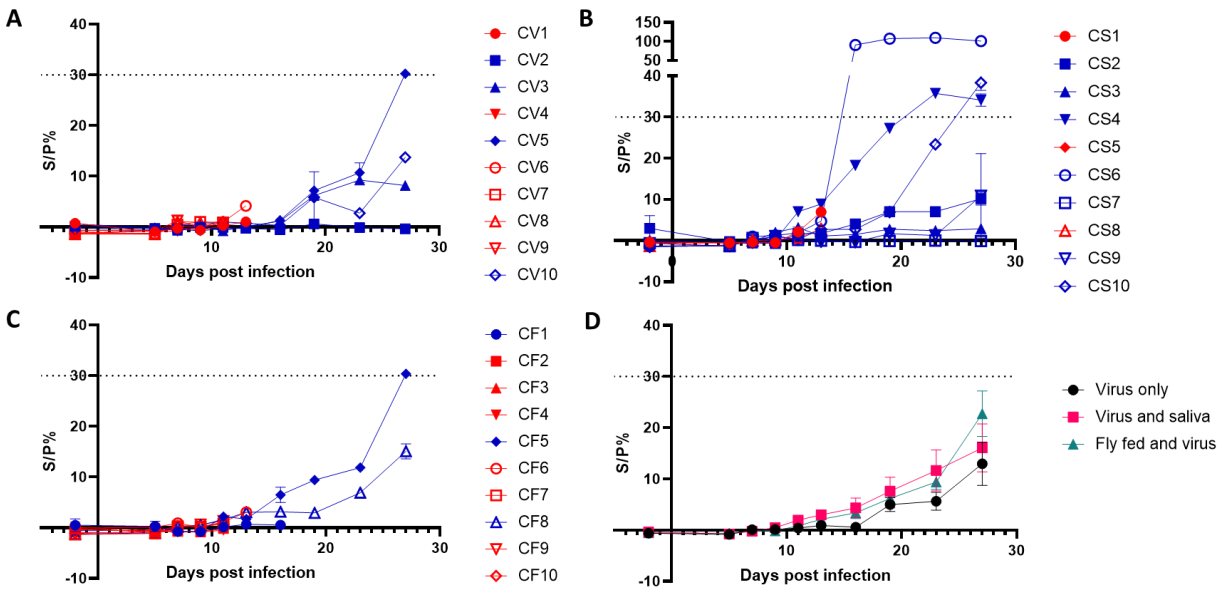


Figure 6.6 – Production of antibodies by cattle challenged with LSDV via three methodologies

Serum was collected from each animal and processed in duplicate on the IDVet ID Screen Capripox Double-Antigen Multi species ELISA kit, according to manufacturer's instructions. OD for each sample was collected and interpreted by calculating the S/P%. Samples with an S/P% greater than or equal to 30% (as shown by the dotted line) are considered positive. Samples were separated according to their route of challenge: viral inoculation only (A), viral and saliva inoculation (B), fly spot-fed and viral inoculation (C). The samples were then combined (excluding animal CS6) and plotted (D). Graphs show data collected from -2 dpi to 19 dpi. Data shown as mean ± SEM.

6.2.4 Fly-fed and inoculation animals produced antibodies much more rapidly

The ELISA was not able to detect differences between groups or between clinical outcomes. Virus neutralisation assays (VNT's) are more sensitive and therefore more able to detect lower levels of antibody at earlier timepoints (Samojlovic et al., 2019, Fay et al., 2022b). Using a fluorescent virus neutralisation test (FVNT), serum was analysed to quantify complete neutralisation of LSDV by sera collected at -2, 7, 11, 16 and 27 dpi (Table 6.1). Animals that developed a clinical outcome are highlighted in red. Once the plates were assessed for absence of foci, the total neutralisation of virus in each animal mirrored the pattern of antibody production seen in the ELISA. Most interestingly, complete neutralisation is seen in 78% (7/9) of the fly-fed and virus inoculated (CF) animals by 11 dpi, more animals than the other two inoculation groups at that timepoint (though not significantly).

Interestingly, the non-clinical calf in the saliva and virus inoculated group (CS) which had a very high ELISA titre from 14 dpi onwards (calf CS6) also showed a very strong neutralisation titre, greater than a dilution of 1280, at 16 and 27 dpi. These data suggest that the interaction of flies alongside virus inoculation provokes a more rapid production of antibodies.

Table 6.1 – Complete neutralisation by anti-LSDV antibodies in LSDV challenged cattle

CIVS 1	Complete Neutralisation ($FVNT_{100}$) Days Post Infection				
	-2	7	11	16	27
CV1	neg	neg	neg		
CV2	neg	neg	neg	15	40
CV3	neg	neg	neg	80	80
CV4	neg	neg			
CV5	neg	neg	neg	80	320
CS1	neg	neg	neg		
CS2	neg	neg	neg	320	320
CS3	neg	neg	neg	40	80
CS4	neg	neg	10	320	320
CS5	neg	neg			
CF1	neg	neg	10	40	
CF2	neg	neg	10		
CF3	neg	neg			
CF4	neg	neg	neg		
CF5	neg	neg	10	320	>1280*

CIVS 2	Complete Neutralisation ($FVNT_{100}$) Days Post Infection				
	-2	7	11	16	27
CV6	neg	neg	neg		
CV7	neg	neg	10		
CV8	neg	neg	neg		
CV9	neg	neg	neg		
CV10	neg	neg	neg	80	240
CS6	neg	neg	neg	>1280*	>1280*
CS7	neg	neg	neg	neg	15
CS8	neg	neg	30		
CS9	neg	neg	neg	neg	10
CS10	neg	neg	neg	480	>1280*
CF6	neg	neg	neg		
CF7	neg	neg	60		
CF8	neg	neg	10	120	640
CF9	neg	neg	40		
CF10	neg	neg	20		

The table shows the dilution and timepoint at which complete neutralisation of EGFP tagged LSDV by anti-LSDV antibodies in calf serum occurred. Calves highlighted in red developed clinical disease during the experiment. Black boxes denote that the animal had been euthanised at this timepoint.

6.3 Discussion

The *in vivo* LSDV infection experiment described in chapters 4 and 5 used three different methods of virus inoculation to explore if the pathogenesis of LSDV was affected by the vector *S. calcitrans*. Chapter 4 described how the saliva of the stable flies reduced the number of cattle with clinical disease, while fly feeding ahead of virus inoculation resulted in an earlier, higher viraemia and faster disease development. Specific aspects of either cellular mediated or humoral antibody responses of the LSDV-challenged cattle in the three groups were examined in a variety of ways to ascertain if any association between the responses and the clinical outcome of the animals could be drawn.

Changes in blood cell subpopulation dynamics throughout the course of LSDV infection were investigated by designing a flow cytometry panel. The absolute numbers of lymphocytes and monocytes in the blood of all calves at day 0 was within normal limits for bovine leukocytes (Roland et al., 2014). Following inoculation with LSDV, a very similar response for the population dynamics of each cell sub-type was seen across clinical and non-clinical animals. All the calves responded to inoculation by developing a lymphopenia in B and T cells at 7 dpi, before rebounding at 9 dpi. Lymphopenia has been documented before in animals infected with poxviruses (De et al., 2020, Niemeyer et al., 2013, Rehfeld et al., 2013), and in cattle infected with LSDV in the field naturally (Neamat-Allah, 2015). Most lymphocytes live for a few weeks, although there is considerable variation in lifespan amongst lymphocyte subtype (Gossel et al., 2017, Westera et al., 2013). A reduction in circulating lymphocytes can be caused by decreased production, increased tissue demand (movement of lymphocytes from the circulating blood to tissues), or increased consumption. Specific conditions that are known to cause bovine lymphopenia include acute stress, viral or bacterial infection, immune suppression, chronic renal insufficiency,

and application of corticosteroids (Roland et al., 2014). The mechanisms by which DNA viruses induce lymphopenia are poorly understood, but African swine fever virus (another large DNA virus) causes lymphopenia by inducing apoptosis in T lymphocytes (del Moral et al., 1999). Variola virus inoculation of cynomolgus macaques also caused lymphocyte apoptosis (Jahrling et al., 2004). The cause of the lymphopenia in the LSDV-inoculated calves seen in this study could therefore be a combination of increased tissue demand, as lymphocytes are recruited to the site of virus in the skin or lymph nodes, and increased consumption as a possible direct effect of LSDV-induced apoptosis.

Monocytes and gamma delta T cells reduced as proportions of pre-challenge cell numbers over the course of infection. Monocytes did not show a clear pattern across the three groups, whereas gamma delta T cells reduced consistently in every inoculation condition and did not exhibit any suggestion of return to pre-challenge levels. Gamma delta T cells are considered to be a component of the innate immune response, but also are able to act as part of the adaptive immune response, possessing memory-like qualities (Lalor and McLoughlin, 2016). They migrate to barrier organs such as the skin early in their development, and also act as immune sentinels (Nielsen et al., 2017). The continued reduction in γδ T cells seen over time after LSDV inoculation could be due to redistribution of cells to the skin, as seen in a subset of γδ T cells in human psoriasis patients with perturbed skin (Laggner et al., 2011). Once there, they could be taking part in wound healing, which would be required for both clinical and non-clinical animals as a result of inoculation (Toulon et al., 2009).

There was a divergence in monocyte cell numbers at the last time point, with non-clinical animals showing an increase in cell number proportions. This could indicate that the tissue demand for these cells is waning and/or that there is a reduction of cell consumption,

enabling the efforts by the animal to replenish the cells (either by release from storage pools or by increased production) to have an effect. The continued reduction in monocyte numbers in clinical animals could indicate the continued employment of these cells via redeployment to lesions in the skin. Quantification of monocytes at later timepoints by using flow cytometry could help determine if these trends continue and if non-clinical animals' monocyte numbers return faster to pre-challenge levels.

The contribution of IFN-γ secreting cells to the cell-mediated immune (CMI) response to LSDV inoculation and vector interaction was examined by stimulating whole blood with live-attenuated LSDV Neethling for 24h, then measuring the IFN-γ release. The release of IFN-γ in most calves in response to LSDV antigen was detected, indicating activation of the CMI response in both clinical and nonclinical calves. The amount of IFN-γ released was highly variable between animals but appeared to peak at 11 days post challenge. This is 1-2 days after the peak in temperature in infected animals and 4-5 days after the appearance of skin nodules. More recent work in the Beard lab (Fay et al., 2022b) has shown that stimulation of purified PBMCs, rather than whole blood, and stimulation with UV-inactivated LSDV rather than live virus, gives more consistent results when measuring the CMI response of calves inoculated with LSDV. Whole blood would have contained additional factors such as neutralising antibodies which could have interfered with the ability of the viral antigen to stimulate the T cells in the recall assay. Using live virus also allowed for direct effects of the virus on the PBMCs, such as infection and/or apoptosis, which may have influenced the result of the assay. Future studies should follow the optimised protocol for measuring CMI response in LSDV-inoculated calves (using purified PBMCs and UV-inactivated virus as a stimulant). Additional assays for measuring the CMI

response, such as an ELISpot, could also be carried out to provide more information on this component of the immune response.

The humoral immune response to LSDV inoculation was also studied. A number of studies in the literature have revealed the presence of anti-LSDV antibodies post-challenge (Haegeman et al., 2020), (Milovanovic et al., 2019, Kresic et al., 2020) however there has been no research published on the impact of vectors on the humoral response to challenge with virus. A commercially available ELISA was used to measure the anti-LSDV antibody response in the challenged animals in the three treatment groups, and an FVNT was conducted to study neutralisation titres. The results from the ELISA revealed that the induction of LSDV specific antibodies was very variable between cattle. Very few animals reached the assay-specific threshold to be classed as a positive for the presence of LSDV specific antibodies, which is consistent with previous LSD challenge studies which also showed a low but rising titre at 21 and 28 dpi (Sanz-Bernardo et al., 2021, Fay et al., 2022b) and it was unclear why some animals developed a higher peak than others. It could not be determined if higher antibody production was related to clinical outcome, as the levels of antibody in the serum of clinical animals were unable to be explored fully due to all clinical animals being euthanised before the later timepoints, where levels began to rise in non-clinical cattle. The response by non-clinical animals in the three inoculation groups could however be compared, and there was little difference between them. In order to help unpick potential differences between clinical and non-clinical animals, a methodology able to detect virus at earlier timepoints was needed. VNTs have a greater sensitivity (Samojlovic et al., 2019), and therefore might detect lower antibody concentrations at earlier timepoints. The results from this assay were clearer, showing that complete neutralisation of LSDV was achieved by sera collected at 11 dpi. Complete neutralisation

was reached in more animals in the fly-fed and virus inoculated group than the other groups. The FVNT did not reveal a clear pattern relating antibody neutralisation to clinical outcome. Non-clinical animals in each group also showed a varied neutralisation response that did not correlate to any inoculation method. In the future, rather than measuring the amount of antibody present, assays that quantify B cell numbers such as a B cell ELISpot could be used, in order to measure early humoral immune response activation.

6.4 Summary

In the previous chapter, the effect of inoculation methodology on the pathogenesis of lumpy skin disease was discussed, but it was unknown what these differences in nodule development and viraemia could be attributed to. Here, the role of selected cell-mediated and humoral immune responses in the development of clinical disease or lack thereof in the three treatment groups were investigated. A lymphopenia was seen in clinical and non-clinical animals across the three inoculation groups, as well as detection of a systemic cell mediated immune response (via a recall assay on whole blood) and humoral immune response (via an antigen ELISA and a FVNT on serum). A more rapid antibody response was seen in the group that were fed on by flies before virus inoculation, but otherwise little correlation between immune response and disease outcome was detected, suggesting more sensitive and discriminatory assays are required, possibly focusing on the local or regional, rather than the systemic immune response.

7

Conclusions

Lumpy skin disease virus is mechanically transmitted by haematophagous arthropods. Previous work has suggested that the stable fly, *Stomoxys calcitrans*, is an important mechanical vector of the virus. Mechanical vectors are commonly thought to be mere "dirty needles" that carry a pathogen from one host to the next, having no impact on the pathogen or the pathogenesis of disease that arises. In contrast biological vectors, in addition to playing host to part of some pathogens' replication cycle, have been found to have an impact on the pathogenesis of viruses through interactions with the host. These interactions included arthropod biting trauma and immunomodulatory proteins in saliva. Previous work showed that *S. calcitrans* salivary gland extract contained immunomodulatory proteins. Additionally, the telmophagous life history of these flies means that during feeding they lacerate the physical barrier of the skin. The hypothesis of this thesis was that the pathogenesis of LSD was affected by the interactions between the stable fly, the virus and the bovine host.

One way that vectors interact with their hosts is through secretion of saliva during the biting process. Secreted saliva was collected from *S. calcitrans* flies in useable concentrations and quantities using a modified artificial feeding system. Analysis of the secreted saliva validated previous work on the stable fly sialome, confirming the abundant presence of the protein Antigen-5. The collection of the secreted saliva allowed more

detailed investigation of the impact of vector interaction on LSDV infection in primary bovine cells.

Primary bovine fibroblast cell cultures were developed and their infection by LSDV characterised. It was discovered that the cells produced actin tails, which suggests that they might be a more representative model for the study of LSDV replication than the continuous cell cultures typically used in vitro. To further explore the role of skin cells in viral establishment, bovine primary keratinocytes were isolated and infected, with the lack of productive replication suggesting that these cells play a different role from BPFs in LSDV infection.

When primary bovine fibroblasts were inoculated with LSDV mixed with secreted saliva the viral replication kinetics did not change, suggesting that *S. calcitrans* saliva did not impact the virus directly. Therefore, a novel LSDV in vivo experimental model was developed to study the influence of *S. calcitrans* on LSDV in vivo. The model used intradermal microinoculations of virus to mimic the vector-borne route of infection. Comparisons of different inoculation methods revealed that vector interaction can affect the pathogenesis of LSD. Fly feeding preceding virus inoculation resulted in a higher and earlier viraemia, and a more severe disease than virus inoculated alone. In contrast, 10µg of secreted *S. calcitrans* saliva inoculated with virus appeared to suppress disease. These results indicated that *S. calcitrans* was more than just a “dirty needle”.

A detailed exploration of the immune response to inoculation was undertaken in order to unpick the differences seen in disease pathogenesis. A lymphopenia was seen in both clinical and non-clinical animals across the three inoculation groups, as well as detection of a systemic cell mediated immune response (via a recall assay on whole blood) and humoral immune response (via an antigen ELISA and FVNT on serum). Though an earlier antibody

response was detected in fly fed cattle, little other correlation between immune response and disease outcome was detected, suggesting more sensitive and discriminatory assays are required, possibly focusing on the local or regional, rather than the systemic immune response.

LSD is still a neglected transboundary pathogen, despite its rapid spread across most of Asia and threat to Australia, areas that have some of the world's largest cattle inventories. With the economic threat it represents, it is essential that research continues into this virus, using the best experimental models possible. In the past, experimental LSD models have not consistently produced disease, or taken the role of the vector into account. The successful development of a more reliable and representative infection methodology was not only useful for exploring the role of the vector in this work, but has also been utilised already in other LSDV animal experiments. Publication of this method will enable more consistent and representative LSDV studies, whilst reducing the number of animals required for powerful studies. Additionally, the transmission and impact of the vector on pathogenesis of disease was poorly understood. The finding that the mechanical vector *S. calcitrans* has an impact on the pathogenesis of LSD is the first example of this effect in the literature. This could have wider implications for the understanding and characterisation of transmission of other mechanically transmitted poxviruses such as myxoma virus and fowlpox virus. *S. calcitrans* are a vector for many important and impactful pathogens including but not limited to, equine infectious anaemia virus, West Nile virus and Rift Valley Fever virus. There is an opportunity for the mechanical transmission of EIAV and RVFV by stable flies to be more deeply explored, catalysed by the findings of this thesis. Finally, the discovery of actin tails as a method of LSDV cellular exit is a completely novel finding for this virus, and further advances understanding of LSDV replication.

Though much has been uncovered about this important stage of the disease cycle, it has also left many questions unanswered. By treating mechanical vectors less as “dirty needles” and more as crucial components of disease pathogenesis, these questions can be framed in a way that takes the vector into account in the crucial early stages of interaction between the bovine host, lumpy skin disease virus, and vector.

8

Appendix

Table 8.1 – Ages and weights of challenged animals

Experimental identifier	Age at challenge (days)	Arrival weight (kg)
CV1	179	140
CV2	179	148
CV3	175	154
CV4	178	164
CV5	172	164
CV6	136	133
CV7	155	136
CV8	126	154
CV9	144	156
CV10	174	163
CS1	174	142
CS2	177	148
CS3	173	150
CS4	188	158
CS5	184	166
CS6	144	133
CS7	142	150
CS8	185	152
CS9	145	156
CS10	164	167
CF1	174	139

CF2	174	144
CF3	190	150
CF4	172	160
CF5	180	166
CF6	143	125
CF7	120	145
CF8	148	152
CF9	156	157
CF10	138	164

Table 8.2: Treatments administered to experimental animals

		Treatment										
Eartag	Animal	Nuflor 450 mg/ml, IM	Imaverol 100 mg/ml, topical wash	Metacam 20mg/ml SC	Terramycin 200mg/ml, IM	Baytril 100mg/ml, SC	Draxxin 100mg/ml, SC	Naxcel 200mg/ml, SC	Bisolvon (in feed)	Ventipulmin 30ug/ml, IV	Dexadreson 2mg/ml, IM	Orbenin (ointment)
960	CV1	07May2021, 6.22ml	From 11May2021, 3x a day, every 3 days									
957	CV2	07May2021, 6.58ml	From 11May2021, 3x a day, every 3 days	04June2021, 4ml		04June2021, 2 x 6mls						
950	CV3	07May2021, 6.84ml	From 11May2021, 3x a day, every 3 days									
935	CV4	07May2021, 7.29ml	From 11May2021, 3x a day, every 3 days									
996	CV5	07May2021, 7.29ml	From 11May2021, 3x a day, every 3 days									
792	CV6	14June2021, 5.91ml		02July2021, 3.3ml								
				04July2021, 3.3ml								
644	CV7	14June2021, 6.04ml		02July2021, 3.4ml	20June2021, 13.5ml							20June2021, 0.25-0.5 tube
				04July2021, 3.4ml								22June2021, 0.25-0.5 tube
147	CV8	14June2021, 6.84ml		02July2021, 3.8ml								
				04July2021, 3.8ml								
318	CV9	14June2021, 6.93ml		02July2021, 3.9ml								
				04July2021, 3.9ml								
167	CV10	14June2021, 7.24ml										
970	CS1	07May2021, 6.31ml	From 11May2021, 3x a day, every 3 days		30May2021, 8.5ml x 2							
944	CS2	07May2021, 6.58ml	From 11May2021, 3x a day, every 3 days									
988	CS3	07May2021, 6.67ml	From 11May2021, 3x a day, every 3 days	25May2021, 3.5ml								
804	CS4	07May2021, 7.02ml	From 11May2021, 3x a day, every 3 days									
829	CS5	07May2021, 7.38ml	From 11May2021, 3x a day, every 3 days									
316	CS6	14June2021, 5.91ml		02July2021, 3.3ml		02July2021, 9.9ml	06July2021, 3.3ml					
				04July2021, 3.3ml		03July2021, 9.9ml	08July2021, 3.3ml					
						04July2021, 9.9ml	10July2021. 3.3ml					
427	CS7	14June2021, 6.67ml										
54	CS8	14June2021, 6.76ml		02July2021, 3.8ml		02July2021, 11.4ml						
				04July2021, 3.8ml		03July2021, 11.4ml						
						04July2021, 11.4ml						
438	CS9	14June2021, 6.93ml		02July2021, 3.9ml		02July2021, 11.4ml	06July2021, 3.9ml					
				04July2021, 3.9ml		03July2021, 11.4ml	08July2021, 3.9ml					
						04July2021, 11.4ml	10July2021, 3.9ml					
620	CS10	14June2021, 7.42ml		02July2021, 4.2ml		02July2021, 11.4ml	06July2021, 4.2ml					
				04July2021, 4.2ml		03July2021, 11.4ml	08July2021, 4.2ml					
						04July2021, 11.4ml	10July2021, 4.2ml					
971	CF1	07May2021, 6.18ml	From 11May2021, 3x a day, every 3 days	13May2021, 3.5ml	14May2021, 14ml	15May2021, 7ml	26May2021, 4ml	26May2021, 5ml	27May2021, 1.5 sachet	27May2021, 3.8ml, 2x daily	27May2021, 4.5ml	
		13May2021, 12.4ml (SC)		15May2021, 3.5ml		16May2021, 7ml	28May2021, 4ml	28May2021, 5ml	28May2021, 1.5 sachet	28May2021, 3.8ml, 2x daily	28May2021, 4.5ml	
				23May2021, 3.5ml		17May2021, 7ml	30May2021, 4ml	30May2021, 5ml	29May2021, 1.5 sachet			
				25May2021, 3.5ml		18May2021, 7ml	01June2021, 4ml	01June2021, 5ml	30May2021, 1.5 sachet			
						19May2021, 7ml			31May2021, 1.5 sachet			
983	CF2	07May2021, 6.40ml	From 11May2021, 3x a day, every 3 days	28May2021, 3.6ml		28May2021, 7ml						
						29May2021, 7ml						
						30May2021, 7ml						
848	CF3	07May2021, 6.67ml	From 11May2021, 3x a day, every 3 days									
974	CF4	07May2021, 7.11ml	From 11May2021, 3x a day, every 3 days	28May2021								
927	CF5	07May2021, 7.38ml	From 11May2021, 3x a day, every 3 days	28May2021, 4.1ml		28May2021, 8ml						
						29May2021, 8ml						
						30May2021, 8ml						
320	CF6	14June2021, 5.56ml		02July2021, 3.1ml								
				04July2021, 3.1ml								
966	CF7	14June2021, 6.44ml		02July2021, 3.6ml								
				04July2021, 3.6ml								
314	CF8	14June2021, 6.76ml										
641	CF9	14June2021, 6.98ml		02July2021, 3.9ml								
				04July2021, 3.9ml								
212	CF10	14June2021, 7.29ml		02July2021, 4.1ml								
				04July2021, 4.1ml								

Bibliography

AASEN, T. & BELMONTE, J. C. I. 2010. Isolation and cultivation of human keratinocytes from skin or plucked hair for the generation of induced pluripotent stem cells. *Nature Protocols,* 5**,** 371-382.

AERTS, L., HAEGEMAN, A., DE LEEUW, I., PHILIPS, W., VAN CAMPE, W., BEHAEGHEL, I., MOSTIN, L. & DE CLERCQ, K. 2021. Detection of Clinical and Subclinical Lumpy Skin Disease Using Ear Notch Testing and Skin Biopsies. *Microorganisms,* 9.

AFONSO, C. L., DELHON, G., TULMAN, E. R., LU, Z., ZSAK, A., BECERRA, V. M., ZSAK, L., KUTISH, G. F. & ROCK, D. L. 2005. Genome of deerpox virus. *Journal of Virology,* 79**,** 966-977.

AGARWAL, A., JOSHI, G., NAGAR, D. P., SHARMA, A. K., SUKUMARAN, D., PANT, S. C., PARIDA, M. M. & DASH, P. K. 2016. Mosquito saliva induced cutaneous events augment Chikungunya virus replication and disease progression. *Infection Genetics and Evolution,* 40**,** 126-135.

ALCAMI, A. & SMITH, G. L. 1996. Soluble interferon-gamma receptors encoded by poxviruses. *Comparative Immunology Microbiology and Infectious Diseases,* 19**,** 305-317.

ALEKSANDR, K., OLGA, B., DAVID, W. B., PAVEL, P., YANA, P., SVETLANA, K., ALEXANDER, N., VLADIMIR, R., DMITRIY, L. & ALEXANDER, S. 2020. Non-vector-borne transmission of lumpy skin disease virus. *Scientific Reports,* 10.

ALI, B. H. & OBEID, H. M. 1977. INVESTIGATION OF 1ST OUTBREAKS OF LUMPY SKIN-DISEASE IN SUDAN. *British Veterinary Journal,* 133**,** 184-189.

ALJABR, W., ARMSTRONG, S., RICKETT, N. Y., POLLAKIS, G., TOUZELET, O., CLOUTMAN-GREEN, E., MATTHEWS, D. A. & HISCOX, J. A. 2019. High Resolution Analysis of Respiratory Syncytial Virus Infection In Vivo. *Viruses-Basel,* 11.

ALKHAMIS, M. A. & VANDERWAAL, K. 2016. Spatial and Temporal Epidemiology of Lumpy Skin Disease in the Middle East, 2012-2015. *Frontiers in Veterinary Science,* 3.

AMERI, M., WANG, X., WILKERSON, M. J., KANOST, M. R. & BROCE, A. B. 2008. An immunoglobulin binding protein (Antigen 5) of the stable fly (Diptera : Muscidae) salivary gland stimulates bovine immune responses. *Journal of Medical Entomology,* 45**,** 94-101.

ANDERSON, S. L., RICHARDS, S. L. & SMARTT, C. T. 2010. A SIMPLE METHOD FOR DETERMINING ARBOVIRUS TRANSMISSION IN MOSQUITOES. *Journal of the American Mosquito Control Association,* 26**,** 108-111.

ARCA, B., LOMBARDO, F., FRANCISCHETTI, I. M. B., PHAM, V. M., MESTRES-SIMON, M., ANDERSEN, J. F. & RIBEIRO, J. M. C. 2007. An insight into the sialome of the adult female mosquito Aedes albopictus. *Insect Biochemistry and Molecular Biology,* 37**,** 107-127.

AREND, W. P., PALMER, G. & GABAY, C. 2008. IL-1, IL-18, and IL-33 families of cytokines. *Immunological Reviews,* 223**,** 20-38.

ASCOLI-CHRISTENSEN, A., SUTCLIFFE, J. & STRATON, C. 2008. Feeding response of the stable fly, Stomoxys calcitrant L., to blood fractions and adenine nucleotides. *Physiological Entomology,* 15**,** 249-259.

ASSUMPCAO, T. C. F., MA, D. Y., SCHWARZ, A., REITER, K., SANTANA, J. M., ANDERSEN, J. F., RIBEIRO, J. M. C., NARDONE, G., YU, L. L. & FRANCISCHETTI, I. M. B. 2013. Salivary Antigen-5/CAP Family Members Are Cu2+-dependent Antioxidant Enzymes That Scavenge O-2(radical anion) and Inhibit Collagen-induced Platelet Aggregation and Neutrophil Oxidative Burst. *Journal of Biological Chemistry,* 288**,** 14341-14361.

BABIUK, S., BOWDEN, T. R., PARKYN, G., DALMAN, B., MANNING, L., NEUFELD, J., EMBURY-HYATT, C., COPPS, J. & BOYLE, D. B. 2008. Quantification of lumpy skin disease virus following experimental infection in cattle. *Transboundary and Emerging Diseases,* 55**,** 299-307.

BABIUK, S., PARKYN, G., COPPS, J., LARENCE, J. E., SABARA, M. I., BOWDEN, T. R., BOYLE, D. B. & KITCHING, R. P. 2007. Evaluation of an ovine testis cell line (OA3.Ts) for propagation of capripoxvirus isolates and development of an immunostaining technique for viral plaque visualization. *Journal of Veterinary Diagnostic Investigation,* 19**,** 486-491.

BARNARD, B. J. H. 1997. Antibodies against some viruses of domestic animals in southern African wild animals. *Onderstepoort Journal of Veterinary Research,* 64**,** 95-110.

BEARD, P. M. 2016. Lumpy skin disease: a direct threat to Europe. *Veterinary Record,* 178**,** 557-558.

BELON, L., SKIDMORE, P., MEHRA, R. & WALTER, E. 2021. Effect of a fever in viral infections - the 'Goldilocks' phenomenon? *World Journal of Clinical Cases,* 9**,** 296-307.

BERNARD, J., HUTET, E., PABOEUF, F., RANDRIAMPARANY, T., HOLZMULLER, P., LANCELOT, R., RODRIGUES, V., VIAL, L. & LE POTIER, M. F. 2016. Effect of O. porcinus Tick Salivary Gland Extract on the African Swine Fever Virus Infection in Domestic Pig. *Plos One,* 11.

BIDGOOD, S. R. & MERCER, J. 2015. Cloak and Dagger: Alternative Immune Evasion and Modulation Strategies of Poxviruses. *Viruses-Basel,* 7**,** 4800-4825.

BINEPAL, Y. S., ONGADI, F. A. & CHEPKWONY, J. C. 2001. Alternative cell lines for the propagation of lumpy skin disease virus. *Onderstepoort Journal of Veterinary Research,* 68**,** 151-153.

BISSONNETTE, E. Y., ROSSIGNOL, P. A. & BEFUS, A. D. 1993. EXTRACTS OF MOSQUITO SALIVARY-GLAND INHIBIT TUMOR-NECROSIS-FACTOR-ALPHA RELEASE FROM MAST-CELLS. *Parasite Immunology,* 15**,** 27-33.

BISWAS, S., NOYCE, R. S., BABIUK, L. A., LUNG, O., BULACH, D. M., BOWDEN, T. R., BOYLE, D. B., BABIUK, S. & EVANS, D. H. 2020. Extended sequencing of vaccine and wild-type capripoxvirus isolates provides insights into genes modulating virulence and host range. *Transboundary and Emerging Diseases,* 67**,** 80-97.

BLANK, S., BAZON, M. L., GROSCH, J., SCHMIDT-WEBER, C. B., BROCHETTO-BRAGA, M. R., BILO, M. B. & JAKOB, T. 2020. Antigen 5 Allergens of Hymenoptera Venoms and Their Role in Diagnosis and Therapy of Venom Allergy. *Current Allergy and Asthma Reports,* 20.

BREIJO, M., ESTEVES, E., BIZZARRO, B., LARA, P. G., ASSIS, J. B., ROCHA, S., PASTRO, L., FERNANDEZ, C., MEIKLE, A. & SA-NUNES, A. 2018. Hematobin is a novel immunomodulatory protein from the saliva of the horn fly Haematobia irritans that inhibits the inflammatory response in murine macrophages. *Parasites & Vectors,* 11.

BROGNA, S., SATO, T. A. & ROSBASH, M. 2002. Ribosome components are associated with sites of transcription. *Molecular Cell,* 10**,** 93-104.

BRUGMAN, V. A., HERNANDEZ-TRIANA, L. M., PROSSER, S. W. J., WELAND, C., WESTCOTT, D. G., FOOKS, A. R. & JOHNSON, N. 2015. Molecular species identification, host preference and detection of myxoma virus in the Anopheles maculipennis complex (Diptera: Culicidae) in southern England, UK. *Parasites & Vectors,* 8**,** 8.

CALISTRI, P., DE CLERCQ, K., GUBBINS, S., KLEMENT, E., STEGEMAN, A., ABRAHANTES, J. C., MAROJEVIC, D., ANTONIOU, S. E., BROGLIA, A. & EFSA 2020. Lumpy skin disease epidemiological report IV: data collection and analysis. *Efsa Journal,* 18**,** 36.

CALJON, G., BROOS, K., DE GOEYSE, I., DE RIDDER, K., STERNBERG, J. M., COOSEMANS, M., DE BAETSELIER, P., GUISEZ, Y. & VAN DEN ABBEELE, J. 2009. Identification of a functional Antigen5-related allergen in the saliva of a blood feeding insect, the tsetse fly. *Insect Biochemistry and Molecular Biology,* 39**,** 332-341.

CALVO, E. & RIBEIRO, J. M. C. 2006. A novel secreted endonuclease from Culex quinquefasciatus salivary glands. *Journal of Experimental Biology,* 209**,** 2651-2659.

CANTU, F., CAO, S., HERNANDEZ, C., DHUNGEL, P., SPRADLIN, J. & YANG, Z. L. 2020. Poxvirus-encoded decapping enzymes promote selective translation of viral mRNAs. *Plos Pathogens,* 16.

CARN, V. M. & KITCHING, R. P. 1995a. AN INVESTIGATION OF POSSIBLE ROUTES OF TRANSMISSION OF LUMPY SKIN-DISEASE VIRUS (NEETHLING). *Epidemiology and Infection,* 114**,** 219-226.

CARN, V. M. & KITCHING, R. P. 1995b. THE CLINICAL-RESPONSE OF CATTLE EXPERIMENTALLY INFECTED WITH LUMPY SKIN-DISEASE (NEETHLING) VIRUS. *Archives of Virology,* 140**,** 503-513.

CASAL, J., ALLEPUZ, A., MITEVA, A., PITE, L., TABAKOVSKY, B., TERZIEVSKI, D., ALEXANDROV, T. & BELTRAN-ALCRUDO, D. 2018. Economic cost of lumpy skin disease outbreaks in three Balkan countries: Albania, Bulgaria and the Former Yugoslav Republic of Macedonia (2016-2017). *Transboundary and Emerging Diseases,* 65**,** 1680-1688.

CAVALCANTE, R. R., PEREIRA, M. H. & GONTIJO, N. F. 2003. Anti-complement activity in the saliva of phlebotomine sand flies and other haematophagous insects. *Parasitology,* 127**,** 87-93.
CHAGAS, A. C., OLIVEIRA, F., DEBRABANT, A., VALENZUELA, J. G., RIBEIRO, J. M. C. & CALVO, E. 2014. Lundep, a Sand Fly Salivary Endonuclease Increases Leishmania Parasite Survival in Neutrophils and Inhibits XIIa Contact Activation in Human Plasma. *Plos Pathogens,* 10.
CHELIKANI, V., RANJAN, T. & KONDABAGIL, K. 2014. Revisiting the genome packaging in viruses with lessons from the "Giants". *Virology,* 466**,** 15-26.
CHEN, Q., FISHER, D. T., CLANCY, K. A., GAUGUET, J. M. M., WANG, W. C., UNGER, E., ROSE-JOHN, S., VON ANDRIAN, U. H., BAUMANN, H. & EVANS, S. S. 2006. Fever-range thermal stress promotes lymphocyte trafficking across high endothelial venules via an interieukin 6 trans-signaling mechanism. *Nature Immunology,* 7**,** 1299-1308.
CHIBSSA, T. R., KANGETHE, R. T., BERGUIDO, F. J., SETTYPALLI, T. B. K., LIU, Y., GRABHERR, R., LOITSCH, A., SASSU, E. L., PICHLER, R., CATTOLI, G., DIALLO, A., WIJEWARDANA, V. & LAMIEN, C. E. 2021. Innate Immune Responses to Wildtype and Attenuated Sheeppox Virus Mediated Through RIG-1 Sensing in PBMC In-Vitro. *Frontiers in Immunology,* 12.
CHIHOTA, C. M., RENNIE, L. F., KITCHING, R. P. & MELLOR, P. S. 2001. Mechanical transmission of lumpy skin disease virus by Aedes aegypti (Diptera : Culicidae). *Epidemiology and Infection,* 126**,** 317-321.
CHOUMET, V., ATTOUT, T., CHARTIER, L., KHUN, H., SAUTEREAU, J., ROBBE-VINCENT, A., BREY, P., HUERRE, M. & BAIN, O. 2012. Visualizing Non Infectious and Infectious Anopheles gambiae Blood Feedings in Naive and Saliva-Immunized Mice. *Plos One,* 7.
CLAYTON, K., VALLEJO, A. F., DAVIES, J., SIRVENT, S. & POLAK, M. E. 2017. Langerhans Cells-Programmed by the Epidermis. *Frontiers in Immunology,* 8**,** 14.
CONWAY, M. J., WATSON, A. M., COLPITTS, T. M., DRAGOVIC, S. M., LI, Z. Y., WANG, P. H., FEITOSA, F., SHEPHERD, D. T., RYMAN, K. D., KLIMSTRA, W. B., ANDERSON, J. F. & FIKRIG, E. 2014. Mosquito Saliva Serine Protease Enhances Dissemination of Dengue Virus into the Mammalian Host. *Journal of Virology,* 88**,** 164-175.
COOKE, L. 2018. *Understanding the effects of Culicoides saliva on Bluetongue virus infection of bovine monocytes.* University of Surrey.
COUNCIL DIRECTIVE 17 December 1992. introducing general Community measures for the control of certain animal disease and specific measures relating to swine vesicular disease. *In:* COMMUNITIES, C. O. T. E. (ed.) *92/119/EEC.* OJ L 62.
COX, J., MOTA, J., SUKUPOLVI-PETTY, S., DIAMOND, M. S. & RICO-HESSE, R. 2012. Mosquito Bite Delivery of Dengue Virus Enhances Immunogenicity and Pathogenesis in Humanized Mice. *Journal of Virology,* 86**,** 7637-7649.
CUDMORE, S., COSSART, P., GRIFFITHS, G. & WAY, M. 1995. ACTIN-BASED MOTILITY OF VACCINIA VIRUS. *Nature,* 378**,** 636-638.
DA LAGE, J. L. 2018. The Amylases of Insects. *Int J Insect Sci,* 10**,** 1179543318804783.
DAN, A., PEREIRA, M. H., PESQUERO, J. L., DIOTAIUTI, L. & BEIRAO, P. S. L. 1999. Action of the saliva of Triatoma infestans (Heteroptera : Reduviidae) on sodium channels. *Journal of Medical Entomology,* 36**,** 875-879.
DAO, T. D., TRAN, L. H., NGUYEN, H. D., HOANG, T. T., NGUYEN, G. H., TRAN, K. V. D., NGUYEN, H. X., DONG, H. V., BUI, A. N. & BUI, V. N. Characterization of Lumpy skin disease virus isolated from a giraffe in Vietnam. *Transboundary and Emerging Diseases*.
DARPEL, K. E., LANGNER, K. F. A., NIMTZ, M., ANTHONY, S. J., BROWNLIE, J., TAKAMATSU, H. H., MELLOR, P. S. & MERTENS, P. P. C. 2011. Saliva Proteins of Vector Culicoides Modify Structure and Infectivity of Bluetongue Virus Particles. *Plos One,* 6.
DAVIES, F. G. 1982. OBSERVATIONS ON THE EPIDEMIOLOGY OF LUMPY SKIN-DISEASE IN KENYA. *Journal of Hygiene,* 88**,** 95-102.
DE, U. K., CHANDER, V., AKHILESH, MAHAJAN, S., SHARMA, G. K., NANDI, S., SING, K. P. & GUPTA, V. K. 2020. Alterations of hemogram, serum biochemistry, oxidative/nitrosative balance, and copper/zinc homeostasis in dromedary camels naturally infected with poxvirus. *Tropical Animal Health and Production,* 52**,** 2997-3003.

DEFRA. 2014. *Notifiable diseases in animals* [Online]. Available: https://www.gov.uk/government/collections/notifiable-diseases-in-animals [Accessed 23 February 2021].
DEL MORAL, M. G., ORTUNO, E., FERNANDEZ-ZAPATERO, P., ALONSO, F., ALONSO, C., EZQUERRA, A. & DOMINGUEZ, J. 1999. African swine fever virus infection induces tumor necrosis factor alpha production: Implications in pathogenesis. *Journal of Virology,* 73**,** 2173-2180.
DENGLER, B., MENDOZA-KUZNETSOVA, E., NIKOLAEVA, L., RIEGER, A. & MUELLER, R. S. 2021. Evaluation of a clinical scoring system for canine demodicosis. *Veterinary Dermatology,* 32**,** 311-+.
DODDING, M. P. & WAY, M. 2009. Nck- and N-WASP-Dependent Actin-Based Motility Is Conserved in Divergent Vertebrate Poxviruses. *Cell Host & Microbe,* 6**,** 536-550.
DOEBEL, T., VOISIN, B. & NAGAO, K. 2017. Langerhans Cells - The Macrophage in Dendritic Cell Clothing. *Trends in Immunology,* 38**,** 817-828.
DOMS, R. W., BLUMENTHAL, R. & MOSS, B. 1990. FUSION OF INTRACELLULAR AND EXTRACELLULAR FORMS OF VACCINIA VIRUS WITH THE CELL-MEMBRANE. *Journal of Virology,* 64**,** 4884-4892.
DONNELLY, S. K., WEISSWANGE, I., ZETTL, M. & WAY, M. 2013. WIP Provides an Essential Link between Nck and N-WASP during Arp2/3-Dependent Actin Polymerization. *Current Biology,* 23**,** 999-1006.
DOYLE, M. S., SWOPE, B. N., HOGSETTE, J. A., BURKHALTER, K. L., SAVAGE, H. M. & NASCI, R. S. 2011. Vector Competence of the Stable Fly (Diptera: Muscidae) for West Nile Virus. *Journal of Medical Entomology,* 48**,** 656-668.
DROLET, B. S., REISTER, L. M., LEHIY, C. J., VAN RIJN, P. A. & BOWEN, R. A. 2015. Effect of Culicoides sonorensis salivary proteins on clinical disease outcome in experimental Bluetongue virus serotype 8 infection of Dorset sheep. *Veterinaria Italiana,* 51**,** 379-384.
DUDLEY, D. M., NEWMAN, C. M., LALLI, J., STEWART, L. M., KOENIG, M. R., WEILER, A. M., SEMLER, M. R., BARRY, G. L., ZARBOCK, K. R., MOHNS, M. S., BREITBACH, M. E., SCHULTZ-DARKEN, N., PETERSON, E., NEWTON, W., MOHR, E. L., CAPUANO, S., OSORIO, J. E., O'CONNOR, S. L., O'CONNOR, D. H., FRIEDRICH, T. C. & ALIOTA, M. T. 2017. Infection via mosquito bite alters Zika virus tissue tropism and replication kinetics in rhesus macaques. *Nature Communications,* 8.
DUNCAN, M. L., HORSINGTON, J., ELDI, P., AL RUMAIH, Z., KARUPIAH, G. & NEWSOME, T. P. 2018. Loss of Actin-Based Motility Impairs Ectromelia Virus Release In Vitro but Is Not Critical to Spread In Vivo. *Viruses,* 10.
EGAWA, N., EGAWA, K., GRIFFIN, H. & DOORBAR, J. 2015. Human Papillomaviruses; Epithelial Tropisms, and the Development of Neoplasia. *Viruses-Basel,* 7**,** 3863-3890.
ELDE, N. C., CHILD, S. J., EICKBUSH, M. T., KITZMAN, J. O., ROGERS, K. S., SHENDURE, J., GEBALLE, A. P. & MALIK, H. S. 2012. Poxviruses Deploy Genomic Accordions to Adapt Rapidly against Host Antiviral Defenses. *Cell,* 150**,** 831-841.
EUROPEAN FOOD SAFETY AUTHORITY 2017. Lumpy skin disease: I. Data collection and analysis. *EFSA Journal,* 15.
EVANS, N. J., BROWN, J. M., SCHOLEY, R., MURRAY, R. D., BIRTLES, R. J., HART, C. A. & CARTER, S. D. 2014. Differential inflammatory responses of bovine foot skin fibroblasts and keratinocytes to digital dermatitis treponemes. *Veterinary Immunology and Immunopathology,* 161**,** 12-20.
FAO 2003. World agriculture: towards 2015/2030 AN FAO PERSPECTIVE. *In:* BRUINSMA, J. (ed.). London.
FAO, IFAD, UNICEF, WFP & WHO 2022. The State of Food Security and Nutrition in the World 2022. Rome: FAO.
FAY, P., LIMON, G., ULZIIBAT, G., KHANUI, B., MYAGMARSUREN, O., TORE, G., KHISHGEE, B., FLANNERY, J., SANDAG, B., DAMDINJAV, B. & BEARD, P. M. 2022a. A field study evaluating the humoral immune response in Mongolian sheep vaccinated against sheeppox virus. *Transboundary and Emerging Diseases,* 69**,** 1837-1846.

FAY, P. C., COOK, C. G., WIJESIRIWARDANA, N., TORE, G., COMTET, L., CARPENTIER, A., SHIH, B., FREIMANIS, G., HAGA, I. R. & BEARD, P. M. 2020. Madin-Darby bovine kidney (MDBK) cells are a suitable cell line for the propagation and study of the bovine poxvirus lumpy skin disease virus. *Journal of Virological Methods,* 285**,** 113943.

FAY, P. C., WIJESIRIWARDANA, N., MUNYANDUKI, H., SANZ-BERNARDO, B., LEWIS, I., HAGA, I. R., MOFFAT, K., VAN VLIET, A. H. M., HOPE, J., GRAHAM, S. & BEARD, P. 2022b. The immune response to lumpy skin disease virus in cattle is influenced by inoculation route. *bioRxiv***,** 2022.09.22.509006.

FENNER, F., BACHMANN, P. A., GIBBS, E. P. J., MURPHY, F. A., STUDDERT, M. J. & WHITE, D. O. 1987. Pathogenesis: Infection and the Spread of Viruses in the Body. *Veterinary Virology***,** 133.

FENNER, F. & WOODROOFE, G. M. 1953. THE PATHOGENESIS OF INFECTIOUS MYXOMATOSIS - THE MECHANISM OF INFECTION AND THE IMMUNOLOGICAL RESPONSE IN THE EUROPEAN RABBIT (ORYCTOLAGUS-CUNICULUS). *British Journal of Experimental Pathology,* 34**,** 400-&.

FINE, N., TASEVSKI, N., MCCULLOCH, C. A., TENENBAUM, H. C. & GLOGAUER, M. 2020. The Neutrophil: Constant Defender and First Responder. *Frontiers in Immunology,* 11.

FLANNERY, J., SHIH, B., HAGA, I. R., ASHBY, M., CORLA, A., KING, S., FREIMANIS, G., POLO, N., TSE, A. C. N., BRACKMAN, C. J., CHAN, J., PUN, P., FERGUSON, A. D., LAW, A., LYCETT, S., BATTEN, C. & BEARD, P. M. A novel strain of lumpy skin disease virus causes clinical disease in cattle in Hong Kong. *Transboundary and Emerging Diseases*.

FOIL, L. D. & HOGSETTE, J. A. 1994. BIOLOGY AND CONTROL OF TABANIDS, STABLE FLIES AND HORN FLIES. *Revue Scientifique Et Technique De L Office International Des Epizooties,* 13**,** 1125-1158.

FONTAINE, A., DIOUF, I., BAKKALI, N., MISSE, D., PAGES, F., FUSAI, T., ROGIER, C. & ALMERAS, L. 2011. Implication of haematophagous arthropod salivary proteins in host-vector interactions. *Parasites & Vectors,* 4.

FRISCHKNECHT, F., MOREAU, V., ROTTGER, S., GONFLONI, S., RECKMANN, I., SUPERTI-FURGA, G. & WAY, M. 1999. Actin-based motility of vaccinia virus mimics receptor tyrosine kinase signalling. *Nature,* 401**,** 926-929.

GADHAVE, K. R., GAUTAM, S., RASMUSSEN, D. A. & SRINIVASAN, R. 2020. Aphid transmission of Potyvirus: the largest plant-infecting RNA virus genus. *Viruses,* 12**,** 773.

GAO, X. A., SHI, L., ZHOU, Y. Z., CAO, J., ZHANG, H. S. & ZHOU, J. L. 2011. Characterization of the anticoagulant protein Rhipilin-1 from the Rhipicephalus haemaphysaloides tick. *Journal of Insect Physiology,* 57**,** 339-343.

GARCIA, M., ALOUT, H., DIOP, F., DAMOUR, A., BENGUE, M., WEILL, M., MISSE, D., LEVEQUE, N. & BODET, C. 2018. Innate Immune Response of Primary Human Keratinocytes to West Nile Virus Infection and Its Modulation by Mosquito Saliva. *Frontiers in Cellular and Infection Microbiology,* 8**,** 13.

GARI, G., WARET-SZKUTA, A., GROSBOIS, V., JACQUIET, P. & ROGER, F. 2010. Risk factors associated with observed clinical lumpy skin disease in Ethiopia. *Epidemiology and Infection,* 138**,** 1657-1666.

GEISER, D. L. & WINZERLING, J. J. 2012. Insect transferrins: Multifunctional proteins. *Biochimica Et Biophysica Acta-General Subjects,* 1820**,** 437-451.

GERSHON, P. D., ANSELL, D. M. & BLACK, D. N. 1989a. A COMPARISON OF THE GENOME ORGANIZATION OF CAPRIPOXVIRUS WITH THAT OF THE ORTHOPOXVIRUSES. *Journal of Virology,* 63**,** 4703-4708.

GERSHON, P. D., KITCHING, R. P., HAMMOND, J. M. & BLACK, D. N. 1989b. POXVIRUS GENETIC-RECOMBINATION DURING NATURAL VIRUS TRANSMISSION. *Journal of General Virology,* 70**,** 485-489.

GIBBS, E. P. J., JOHNSON, R. H. & OSBORNE, A. D. 1973. EXPERIMENTAL STUDIES OF EPIDEMIOLOGY OF BOVINE HERPES MAMMILLITIS. *Research in Veterinary Science,* 14**,** 139-144.

GOSSEL, G., HOGAN, T., COWNDEN, D., SEDDON, B. & YATES, A. J. 2017. Memory CD4 T cell subsets are kinetically heterogeneous and replenished from naive T cells at high levels. *Elife,* 6.

GRESETH, M. D., CARTER, D. C., TERHUNE, S. S. & TRAKTMAN, P. 2017. Proteomic Screen for Cellular Targets of the Vaccinia Virus F10 Protein Kinase Reveals that Phosphorylation of mDia Regulates Stress Fiber Formation. *Molecular & Cellular Proteomics,* 16**,** S124-S143.

GUBBINS, S. 2019. Using the basic reproduction number to assess the risk of transmission of lumpy skin disease virus by biting insects. *Transboundary and Emerging Diseases,* 66**,** 1873-1883.

GUZMAN, E., HOPE, J., TAYLOR, G., SMITH, A. L., CUBILLOS-ZAPATA, C. & CHARLESTON, B. 2014. Bovine gamma delta T Cells Are a Major Regulatory T Cell Subset. *Journal of Immunology,* 193**,** 208-222.

GWAKISA, P., YOSHIHARA, K., TO, T. L., GOTOH, H., AMANO, F. & MOMOTANI, E. 2001. Salivary gland extract of Rhipicephalus appendiculatus ticks inhibits in vitro transcription and secretion of cytokines and production of nitric oxide by LPS-stimulated JA-4 cells. *Veterinary Parasitology,* 99**,** 53-61.

HAEGEMAN, A., DE LEEUW, I., MOSTIN, L., VAN CAMPE, W., AERTS, L., VASTAG, M. & DE CLERCQ, K. 2020. An Immunoperoxidase Monolayer Assay (IPMA) for the detection of lumpy skin disease antibodies. *Journal of Virological Methods,* 277.

HAEGEMAN, A., DE LEEUW, I., MOSTIN, L., VAN CAMPE, W., AERTS, L., VENTER, E., TUPPURAINEN, E., SAEGERMAN, C. & DE CLERCQ, K. 2021. Comparative Evaluation of Lumpy Skin Disease Virus-Based Live Attenuated Vaccines. *Vaccines,* 9.

HATTORI, M., KOMATSU, S., NODA, H. & MATSUMOTO, Y. 2015. Proteome Analysis of Watery Saliva Secreted by Green Rice Leafhopper, Nephotettix cincticeps. *Plos One,* 10.

HE, Y., FISHER, R., CHOWDHURY, S., SULTANA, I., PEREIRA, C. P., BRAY, M. & REED, J. L. 2014. Vaccinia Virus Induces Rapid Necrosis in Keratinocytes by a STAT3-Dependent Mechanism. *Plos One,* 9**,** 21.

HERMANCE, M. E. & THANGAMANI, S. 2015. Tick Saliva Enhances Powassan Virus Transmission to the Host, Influencing Its Dissemination and the Course of Disease. *Journal of Virology,* 89**,** 7852-7860.

HOCH, A. L., GARGAN, T. P. & BAILEY, C. L. 1985. MECHANICAL TRANSMISSION OF RIFT-VALLEY FEVER VIRUS BY HEMATOPHAGOUS DIPTERA. *American Journal of Tropical Medicine and Hygiene,* 34**,** 188-193.

HODGE, K., TEN HAVE, S., HUTTON, L. & LAMOND, A. I. 2013. Cleaning up the masses: Exclusion lists to reduce contamination with HPLC-MS/MS. *Journal of Proteomics,* 88**,** 92-103.

HOGSETTE, J. A. & RUFF, J. P. 1985. STABLE FLY (DIPTERA, MUSCIDAE) MIGRATION IN NORTHWEST FLORIDA. *Environmental Entomology,* 14**,** 170-175.

HOUSE, J. A., WILSON, T. M., EL NAKASHLY, S., KARIM, I. A., ISMAIL, I., EL DANAF, N., MOUSSA, A. M. & AYOUB, N. M. 1990. The isolation of lumpy skin disease virus and bovine herpesvirus - from cattle in Egypt. *Journal of Veterinary Diagnostic Investigation***,** 111-115.

ICPALD 2013. The Contribution of Livestock to the Ethiopian Economy. *Policy Brief Series.* IGAD Centre for Pastoral Areas and Livestock Development.

INSPECTOR GENERAL OF BIOSECURITY 2022. Assurance review for arrangements to import live lumpy skin disease virus to CSIRO's Australian Centre for Disease Preparedness. Canberra: Department of Agriculture, Fisheries and Forestry.

IRONS, P. C., TUPPURAINEN, E. S. M. & VENTER, E. H. 2005. Excretion of lumpy skin disease virus in bull semen. *Theriogenology,* 63**,** 1290-1297.

ISSEL, C. J., RUSHLOW, K., FOIL, L. D. & MONTELARO, R. C. 1988. A PERSPECTIVE ON EQUINE INFECTIOUS-ANEMIA WITH AN EMPHASIS ON VECTOR TRANSMISSION AND GENETIC-ANALYSIS. *Veterinary Microbiology,* 17**,** 251-286.

ISSIMOV, A., KUTUMBETOV, L., ORYNBAYEV, M. B., KHAIRULLIN, B., MYRZAKHMETOVA, B., SULTANKULOVA, K. & WHITE, P. J. 2020. Mechanical Transmission of Lumpy Skin Disease

Virus by Stomoxys spp. (Stomoxys calsitrans, Stomoxys sitiens, Stomoxys indica), Diptera: Muscidae. *Animals,* 10**,** 11.

JAHRLING, P. B., HENSLEY, L. E., MARTINEZ, M. J., LEDUC, J. W., RUBINS, K. H., RELMAN, D. A. & HUGGINS, J. W. 2004. Exploring the potential of variola virus infection of cynomolgus macaques as a model for human smallpox. *Proceedings of the National Academy of Sciences of the United States of America,* 101**,** 15196-15200.

JAMES, M. T. & HARWOOD, R. F. 1970. Herms's medical entomology.

JEANBOURQUIN, P. & GUERIN, P. M. 2007. Sensory and behavioural responses of the stable fly Stomoxys calcitrans to rumen volatiles. *Medical and Veterinary Entomology,* 21**,** 217-224.

JEKLOVA, E., LEVA, L., MATIASOVIC, J., KOVARCIK, K., KUDLACKOVA, H., NEVORANKOVA, Z., PSIKAL, I. & FALDYNA, M. 2008. Characterisation of immunosuppression in rabbits after infection with myxoma virus. *Veterinary Microbiology,* 129**,** 117-130.

JHA, S., ROLLINS, M. G., FUCHS, G., PROCTER, D. J., HALL, E. A., COZZOLINO, K., SARNOW, P., SAVAS, J. N. & WALSH, D. 2017. Trans-kingdom mimicry underlies ribosome customization by a poxvirus kinase. *Nature,* 546**,** 651-+.

KAHANA-SUTIN, E., KLEMENT, E., LENSKY, I. & GOTTLIEB, Y. 2017. High relative abundance of the stable fly Stomoxys calcitrans is associated with lumpy skin disease outbreaks in Israeli dairy farms. *Medical and Veterinary Entomology,* 31**,** 150-160.

KARA, P. D., MATHER, A. S., PRETORIUS, A., CHETTY, T., BABIUK, S. & WALLACE, D. B. 2018. Characterisation of putative immunomodulatory gene knockouts of lumpy skin disease virus in cattle towards an improved vaccine. *Vaccine,* 36**,** 4708-4715.

KAUR, G. & DUFOUR, J. M. 2012. Cell lines: Valuable Tools or Useless Artifacts. *Spermatogenesis,* 2**,** 1-5.

KAWAHORI, S., SEKI, C., MIZUSHIMA, D., TABBABI, A., YAMAMOTO, D. S. & KATO, H. 2022. Ayaconin, a novel inhibitor of the plasma contact system from the sand fly Lutzomyia ayacuchensis, a vector of Andean-type cutaneous leishmaniasis. *Acta Tropica,* 234.

KITCHING, R. P., BHAT, P. P. & BLACK, D. N. 1989. THE CHARACTERIZATION OF AFRICAN STRAINS OF CAPRIPOXVIRUS. *Epidemiology and Infection,* 102**,** 335-343.

KITCHING, R. P., HAMMOND, J. M. & TAYLOR, W. P. 1987. A SINGLE VACCINE FOR THE CONTROL OF CAPRIPOX INFECTION IN SHEEP AND GOATS. *Research in Veterinary Science,* 42**,** 53-60.

KITCHING, R. P. & MELLOR, P. S. 1986. INSECT TRANSMISSION OF CAPRIPOXVIRUS. *Research in Veterinary Science,* 40**,** 255-258.

KLECHEVSKY, E. 2015. Functional Diversity of Human Dendritic Cells. *Crossroads between Innate and Adaptive Immunity V,* 850**,** 43-54.

KLUN, J. A., KRAMER, M. & DEBBOUN, M. 2013. Four simple stimuli that induce host-seeking and blood-feeding behaviors in two mosquito species, with a clue to DEET's mode of action. *Journal of Vector Ecology,* 38**,** 143-153.

KOGAME, T., KABASHIMA, K. & EGAWA, G. 2021. Putative Immunological Functions of Inducible Skin-Associated Lymphoid Tissue in the Context of Mucosa-Associated Lymphoid Tissue. *Frontiers in Immunology,* 12.

KOVACS, L., JURKOVICH, V., BAKONY, M., SZENCI, O., POTI, P. & TOZSER, J. 2014. Welfare implication of measuring heart rate and heart rate variability in dairy cattle: literature review and conclusions for future research. *Animal,* 8**,** 316-330.

KRESIC, N., SIMIC, I., BEDEKOVIC, T., ACINGER-ROGIC, Z. & LOJKIC, I. 2020. Evaluation of Serological Tests for Detection of Antibodies against Lumpy Skin Disease Virus. *Journal of Clinical Microbiology,* 58.

LAGGNER, U., DI MEGLIO, P., PERERA, G. K., HUNDHAUSEN, C., LACY, K. E., ALI, N., SMITH, C. H., HAYDAY, A. C., NICKOLOFF, B. J. & NESTLE, F. O. 2011. Identification of a Novel Proinflammatory Human Skin-Homing V gamma 9V delta 2 T Cell Subset with a Potential Role in Psoriasis. *Journal of Immunology,* 187**,** 2783-2793.

LAI, Y. & GALLO, R. L. 2008. Toll-like receptors in skin infections and inflammatory diseases. *Infectious Disorders-Drug Targets (Formerly Current Drug Targets-Infectious Disorders),* 8**,** 144-155.

LALOR, S. J. & MCLOUGHLIN, R. M. 2016. Memory gamma delta T Cells-Newly Appreciated Protagonists in Infection and Immunity. *Trends in Immunology,* 37**,** 690-702.

LANGNER, K. F. A., DARPEL, K. E., DENISON, E., DROLET, B. S., LEIBOLD, W., MELLOR, P. S., MERTENS, P. P. C., NIMTZ, M. & GREISER-WILKE, I. 2007. Collection and analysis of salivary proteins from the biting midge Culicoides nubeculosus (Diptera : Ceratopogonidae). *Journal of Medical Entomology,* 44**,** 238-248.

LAVOIPIERRE, M. M. 1965. FEEDING MECHANISM OF BLOOD-SUCKING ARTHROPODS. *Nature,* 208**,** 302-+.

LAW, M., CARTER, G. C., ROBERTS, K. L., HOLLINSHEAD, M. & SMITH, G. L. 2006. Ligand-induced and nonfusogenic dissolution of a viral membrane. *Proceedings of the National Academy of Sciences of the United States of America,* 103**,** 5989-5994.

LAZAREVIC, J. & JANKOVIC-TOMANIC, M. 2015. Dietary and phylogenetic correlates of digestive trypsin activity in insect pests. *Entomologia Experimentalis Et Applicata,* 157**,** 123-151.

LE COUPANEC, A., BABIN, D., FIETTE, L., JOUVION, G., AVE, P., MISSE, D., BOULOY, M. & CHOUMET, V. 2013. Aedes Mosquito Saliva Modulates Rift Valley Fever Virus Pathogenicity. *Plos Neglected Tropical Diseases,* 7.

LEFTERI, D., A., BRYDEN, S., R., PINGEN, M., TERRY, S., MCCAFFERTY, A., BESWICK, E., F., GEORGIEV, G., VAN DER LAAN, M., MASTRULLO, V., CAMPAGNOLO, P., WATERHOUSE, R., M., VARJAK, M., MERITS, A., FRAGKOUDIS, R., GRIFFIN, S., SHAMS, K., PONDEVILLE, E. & MCKIMMIE, C., S. 2022. Mosquito saliva enhances virus infection through sialokinin-dependent vascular leakage. *Proceedings of the National Academy of Sciences,* 119**,** e2114309119.

LEHIY, C. J. & DROLET, B. S. 2014. The salivary secretome of the biting midge, Culicoides sonorensis. *Peerj,* 2.

LERNER, E. A., RIBEIRO, J. M. C., NELSON, R. J. & LERNER, M. R. 1991. ISOLATION OF MAXADILAN, A POTENT VASODILATORY PEPTIDE FROM THE SALIVARY-GLANDS OF THE SAND FLY LUTZOMYIA-LONGIPALPIS. *Journal of Biological Chemistry,* 266**,** 11234-11236.

LESTINOVA, T., ROHOUSOVA, I., SIMA, M., DE OLIVEIRA, C. I. & VOLF, P. 2017. Insights into the sand fly saliva: Blood-feeding and immune interactions between sand flies, hosts, and Leishmania. *Plos Neglected Tropical Diseases,* 11.

LIU, L., ZHONG, Q., TIAN, T., DUBIN, K., ATHALE, S. K. & KUPPER, T. S. 2010. Physical disruption of skin during poxvirus immunization is critical for the generation of highly protective T cell-mediated immunity. *Nature medicine,* 16**,** 224.

LIU, L. Z., XU, Z., FUHLBRIGGE, R. C., PENA-CRUZ, V., LIEBERMAN, J. & KUPPER, T. S. 2005. Vaccinia virus induces strong immunoregulatory cytokine production in healthy human epidermal keratinocytes: a novel strategy for immune evasion. *Journal of Virology,* 79**,** 7363-7370.

LIU, S. W., KATSAFANAS, G. C., LIU, R. K., WYATT, L. S. & MOSS, B. 2015. Poxvirus Decapping Enzymes Enhance Virulence by Preventing the Accumulation of dsRNA and the Induction of Innate Antiviral Responses. *Cell Host & Microbe,* 17**,** 320-331.

LU, G., XIE, J. X., LUO, J. L., SHAO, R., JIA, K. & LI, S. J. 2021. Lumpy skin disease outbreaks in China, since 3 August 2019. *Transboundary and Emerging Diseases,* 68**,** 216-219.

LUBINGA, J. C., TUPPURAINEN, E. S. M., MAHLARE, R., COETZER, J. A. W., STOLTSZ, W. H. & VENTER, E. H. 2015. Evidence of Transstadial and Mechanical Transmission of Lumpy Skin Disease Virus by Amblyomma hebraeum Ticks. *Transboundary and Emerging Diseases,* 62**,** 174-182.

LUO, Y. P. 2014. A novel multiple membrane blood-feeding system for investigating and maintaining Aedes aegypti and Aedes albopictus mosquitoes. *Journal of Vector Ecology,* 39**,** 271-277.

LYSYK, T. J. 1993. SEASONAL ABUNDANCE OF STABLE FLIES AND HOUSE-FLIES (DIPTERA, MUSCIDAE) IN DAIRIES IN ALBERTA, CANADA. *Journal of Medical Entomology,* 30**,** 888-895.

MA, B., ZHANG, K. Z., HENDRIE, C., LIANG, C. Z., LI, M., DOHERTY-KIRBY, A. & LAJOIE, G. 2003. PEAKS: powerful software for peptide de novo sequencing by tandem mass spectrometry. *Rapid Communications in Mass Spectrometry,* 17**,** 2337-2342.

MA, D., LI, Y., DONG, J., AN, S., WANG, Y., LIU, C., YANG, X., YANG, H., XU, X., LIN, D. & LAI, R. 2011. Purification and characterization of two new allergens from the salivary glands of the horsefly, Tabanus yao. *Allergy,* 66**,** 101-109.

MAGORI-COHEN, R., LOUZOUN, Y., HERZIGER, Y., ORON, E., ARAZI, A., TUPPURAINEN, E., SHPIGEL, N. Y. & KLEMENT, E. 2012. Mathematical modelling and evaluation of the different routes of transmission of lumpy skin disease virus. *Veterinary Research,* 43.

MAIER, G. U., ROWE, J. D., LEHENBAUER, T. W., KARLE, B. M., WILLIAMS, D. R., CHAMPAGNE, J. D. & ALY, S. S. 2019. Development of a clinical scoring system for bovine respiratory disease in weaned dairy calves. *Journal of Dairy Science,* 102**,** 7329-7344.

MALISSEN, B., TAMOUTOUNOUR, S. & HENRI, S. 2014. The origins and functions of dendritic cells and macrophages in the skin. *Nature Reviews Immunology,* 14**,** 417-428.

MANTOVANI, A., CASSATELLA, M. A., COSTANTINI, C. & JAILLON, S. 2011. Neutrophils in the activation and regulation of innate and adaptive immunity. *Nature Reviews Immunology,* 11**,** 519-531.

MARTIN-MARTIN, I., LEON, P. C. V., AMO, L., SHRIVASTAVA, G., INIGUEZ, E., ARYAN, A., BROOKS, S., KOJIN, B. B., WILLIAMS, A. E., BOLLAND, S., ACKERMAN, H., ADELMAN, Z. N. & CALVO, E. 2022. Aedes aegypti sialokinin facilitates mosquito blood feeding and modulates host immunity and vascular biology. *Cell Reports,* 39.

MATHEWOS, M., DULO, F., TANGA, Z. & SOMBO, M. 2022. Clinicopathological and molecular studies on cattle naturally infected with lumpy skin diseases in selected districts of Wolaita Zone, Southern Ethiopia. *Bmc Veterinary Research,* 18.

MCCRACKEN, M. K., GROMOWSKI, G. D., GARVER, L. S., GOUPIL, B. A., WALKER, K. D., FRIBERG, H., CURRIER, J. R., RUTVISUTTINUNT, W., HINTON, K. L., CHRISTOFFERSON, R. C., MORES, C. N., VANLOUBBEECK, Y., LORIN, C., MALICE, M. P., THOMAS, S. J., JARMAN, R. G., VAUGHN, D. W., PUTNAK, J. R. & WARTER, L. 2020. Route of inoculation and mosquito vector exposure modulate dengue virus replication kinetics and immune responses in rhesus macaques. *Plos Neglected Tropical Diseases,* 14.

MCFADDEN, G. 2005. Poxvirus tropism. *Nature Reviews Microbiology,* 3**,** 201-213.

MEAD-BRIGGS, A. R. & VAUGHAN, J. A. 1975. The differential transmissibility of Myxoma virus strains of differing virulence grades by the rabbit flea Spilopsyllus cuniculi (Dale). *J Hyg (Lond),* 75**,** 237-47.

MEADE, N., FUREY, C., LI, H., VERMA, R., CHAI, Q. Q., ROLLINS, M. G., DIGIUSEPPE, S., NAGHAVI, M. H. & WALSH, D. 2018. Poxviruses Evade Cytosolic Sensing through Disruption of an mTORC1-mTORC2 Regulatory Circuit. *Cell,* 174**,** 1143-+.

MELLOR, P. S., KITCHING, R. P. & WILKINSON, P. J. 1987. MECHANICAL TRANSMISSION OF CAPRIPOX VIRUS AND AFRICAN SWINE FEVER VIRUS BY STOMOXYS-CALCITRANS. *Research in Veterinary Science,* 43**,** 109-112.

MESCHER, M. F., CURTSINGER, J. M., AGARWAL, P., CASEY, K. A., GEMER, M., HAMMERBECK, C. D., POPESCU, F. & XIAO, Z. G. 2006. Signals required for programming effector and memory development by CD8(+) T cells. *Immunological Reviews,* 211**,** 81-92.

MILOVANOVIC, M., DIETZE, K., MILICEVIC, V., RADOJICIC, S., VALCIC, M., MORITZ, T. & HOFFMANN, B. 2019. Humoral immune response to repeated lumpy skin disease virus vaccination and performance of serological tests. *Bmc Veterinary Research,* 15.

MIRANDA, M. A., STEGEMAN, J. A., BICOUT, D., BOTNER, A., BUTTERWORTH, A., CALISTRI, P., DEPNER, K., EDWARDS, S., GARIN-BASTUJI, B., GOOD, M., SCHMIDT, C. G., MICHEL, V., MORE, S., RAJ, M., NIELSEN, S. S., SIHVONEN, L., SPOOLDER, H., THULKE, H. H., VELARDE, A., WILLEBERG, P., WINCKLER, C. & WELF, E. P. A. H. 2016. Urgent advice on lumpy skin disease EFSA Panel on Animal Health and Welfare. *Efsa Journal,* 14**,** 27.

MOLINI, U., BOSHOFF, E., NIEL, A. P., PHILLIPS, J., KHAISEB, S., SETTYPALLI, T. B. K., DUNDON, W. G., CATTOLI, G. & LAMIEN, C. E. 2021. Detection of Lumpy Skin Disease Virus in an

Asymptomatic Eland (Taurotragus oryx) in Namibia. *Journal of Wildlife Diseases,* 57**,** 708-711.
MOLLA, W., DE JONG, M. C. M., GARI, G. & FRANKENA, K. 2017. Economic impact of lumpy skin disease and cost effectiveness of vaccination for the control of outbreaks in Ethiopia. *Preventive Veterinary Medicine,* 147**,** 100-107.
MOSS, B. 2012. Poxvirus Cell Entry: How Many Proteins Does it Take? *Viruses-Basel,* 4**,** 688-707.
MOSS, B. 2016. Membrane fusion during poxvirus entry. *Seminars in Cell & Developmental Biology,* 60**,** 89-96.
MUELLER, S. N. & ROUSE, B. T. 2008. Immune responses to viruses. *Clinical Immunology.* Copyright © 2008 Elsevier Ltd. All rights reserved.
MULLENS, B. A. & MEYER, J. A. 1987. SEASONAL ABUNDANCE OF STABLE FLIES (DIPTERA, MUSCIDAE) ON CALIFORNIA DAIRIES. *Journal of Economic Entomology,* 80**,** 1039-1043.
MULLENS, B. A. & PETERSON, N. G. 2005. Relationship between rainfall and stable fly (Diptera : Muscidae) abundance on California dairies. *Journal of Medical Entomology,* 42**,** 705-708.
MULLER, J., MORITZ, T., SCHLOTTAU, K., KRSTEVSKI, K., HOFFMANN, D., BEER, M. & HOFFMANN, B. 2019. Experimental lumpy skin disease virus infection of cattle: comparison of a field strain and a vaccine strain. *Archives of Virology,* 164**,** 2931-2941.
NEAMAT-ALLAH, A. N. F. 2015. Immunological, hematological, biochemical, and histopathological studies on cows naturally infected with lumpy skin disease. *Veterinary World,* 8**,** 1131-1136.
NESTLE, F. O., DI MEGLIO, P., QIN, J. Z. & NICKOLOFF, B. J. 2009. Skin immune sentinels in health and disease. *Nature Reviews Immunology,* 9**,** 679-691.
NEWSOME, T. P., WEISSWANGE, I., FRISCHKNECHT, F. & WAY, M. 2006. Abl collaborates with Src family kinases to stimulate actin-based motility of vaccinia virus. *Cellular Microbiology,* 8**,** 233-241.
NEWTON, K. & DIXIT, V. M. 2012. Signaling in Innate Immunity and Inflammation. *Cold Spring Harbor Perspectives in Biology,* 4.
NICOLA, A. V., HOU, J., MAJOR, E. O. & STRAUS, S. E. 2005. Herpes simplex virus type 1 enters human epidermal keratinocytes, but not neurons, via a pH-dependent endocytic pathway. *Journal of Virology,* 79**,** 7609-7616.
NIELSEN, M. M., WITHERDEN, D. A. & HAVRAN, W. L. 2017. gamma delta T cells in homeostasis and host defence of epithelial barrier tissues. *Nature Reviews Immunology,* 17**,** 733-745.
NIEMEYER, C., FAVERO, C. M., KOLESNIKOVAS, C. K. M., BHERING, R. C. C., BRANDAO, P. & CATAO-DIAS, J. L. 2013. Two different avipoxviruses associated with pox disease in Magellanic penguins (Spheniscus magellanicus) along the Brazilian coast. *Avian Pathology,* 42**,** 546-551.
ODENIRAN, P. O., MACLEOD, E. T., ADEMOLA, I. O. & WELBURN, S. C. 2019. Molecular identification of bloodmeal sources and trypanosomes in Glossina spp., Tabanus spp. and Stomoxys spp. trapped on cattle farm settlements in southwest Nigeria. *Medical and Veterinary Entomology,* 33**,** 269-281.
OIE. 2017a. Lumpy Skin Disease. *Technical Disease Cards* [Online].
OIE 2017b. Lumpy Skin Disease. *Manual of Diagnostic Tests and Vaccines for Terrestrial Animals.* World Organisation for Animal Health.
OIE 2018. Infection with Lumpy Skin Disease Virus. *In:* OIE (ed.) *Terrestrial Animal Health Code.* 27th ed. Paris: OIE.
OIE. 2021. *OIE-Listed diseases, infections and infestations in force in 2021* [Online]. Available: https://www.oie.int/en/animal-health-in-the-world/oie-listed-diseases-2021/ [Accessed 2021].
OLAFSON, P. U., AKSOY, S., ATTARDO, G. M., BUCKMEIER, G., CHEN, X. T., COATES, C. J., DAVIS, M., DYKEMA, J., EMRICH, S. J., FRIEDRICH, M., HOLMES, C. J., IOANNIDIS, P., JANSEN, E. N., JENNINGS, E. C., LAWSON, D., MARTINSON, E. O., MASLEN, G. L., MEISEL, R. P., MURPHY, T. D., NAYDUCH, D., NELSON, D. R., OYEN, K. J., RASZICK, T. J., RIBEIRO, J. M. C., ROBERTSON, H. M., ROSENDALE, A. J., SACKTON, T. B., SAELAO, P., SWIGER, S. L., SZE, S.

H., TARONE, A. M., TAYLOR, D. B., WARREN, W. C., WATERHOUSE, R. M., WEIRAUCH, M. T., WERREN, J. H., WILSON, R. K., ZDOBNOV, E. M. & BENOIT, J. B. 2021. The genome of the stable fly, Stomoxys calcitrans, reveals potential mechanisms underlying reproduction, host interactions, and novel targets for pest control (vol 19, 41, 2021). *Bmc Biology,* 19.

PAGES, N., BREARD, E., URIEN, C., TALAVERA, S., VIAROUGE, C., LORCA-ORO, C., JOUNEAU, L., CHARLEY, B., ZIENTARA, S., BENSAID, A., SOLANES, D., PUJOLS, J. & SCHWARTZ-CORNIL, I. 2014. Culicoides Midge Bites Modulate the Host Response and Impact on Bluetongue Virus Infection in Sheep. *Plos One,* 9.

PARRAVANI, A., CHIVERS, C. A., BELL, N., LONG, S., BURDEN, F. & WALL, R. 2019. Seasonal abundance of the stable fly Stomoxys calcitrans in southwest England. *Medical and Veterinary Entomology,* 33**,** 485-490.

PETERS, N. E., FERGUSON, B. J., MAZZON, M., FAHY, A. S., KRYSZTOFINSKA, E., ARRIBAS-BOSACOMA, R., PEARL, L. H., REN, H. W. & SMITH, G. L. 2013. A Mechanism for the Inhibition of DNA-PK-Mediated DNA Sensing by a Virus. *Plos Pathogens,* 9.

PINGEN, M., BRYDEN, S. R., PONDEVILLE, E., SCHNETTLER, E., KOHL, A., MERITS, A., FAZAKERLEY, J. K., GRAHAM, G. J. & MCKIMMIE, C. S. 2016. Host Inflammatory Response to Mosquito Bites Enhances the Severity of Arbovirus Infection. *Immunity,* 44**,** 1455-1469.

PINGEN, M., SCHMID, M. A., HARRIS, E. & MCKIMMIE, C. S. 2017. Mosquito Biting Modulates Skin Response to Virus Infection. *Trends in Parasitology,* 33**,** 645-657.

PROZESKY, L. & BARNARD, B. J. H. 1982. A STUDY OF THE PATHOLOGY OF LUMPY SKIN-DISEASE IN CATTLE. *Onderstepoort Journal of Veterinary Research,* 49**,** 167-175.

QUARESMA, J. A. S. 2019. Organization of the Skin Immune System and Compartmentalized Immune Responses in Infectious Diseases. *Clinical Microbiology Reviews,* 32.

RADONJIC-HOESLI, S., BRUGGEN, M. C., FELDMEYER, L., SIMON, H. U. & SIMON, D. 2021. Eosinophils in skin diseases. *Seminars in Immunopathology,* 43**,** 393-409.

REHFELD, I. S., GUEDES, M., MATOS, A. C. D., DE OLIVEIRA, T. M. L., RIVETTI, A. V., MOURA, A. C. J., PAES, P. R. O., DO LAGO, L. A., KROON, E. G. & LOBATO, Z. I. P. 2013. Clinical, hematological and biochemical parameters of dairy cows experimentally infected with Vaccinia virus. *Research in Veterinary Science,* 95**,** 752-757.

REINKE, J. M. & SORG, H. 2012. Wound Repair and Regeneration. *European Surgical Research,* 49**,** 35-43.

RIBEIRO, J. M. C., SARKIS, J. J. F., ROSSIGNOL, P. A. & SPIELMAN, A. 1984. SALIVARY APYRASE OF AEDES-AEGYPTI - CHARACTERIZATION AND SECRETORY FATE. *Comparative Biochemistry and Physiology B-Biochemistry & Molecular Biology,* 79**,** 81-86.

RICE, A. D., ADAMS, M. M., LINDSEY, S. F., SWETNAM, D. M., MANNING, B. R., SMITH, A. J., BURRAGE, A. M., WALLACE, G., MACNEILL, A. L. & MOYER, R. W. 2014. Protective Properties of Vaccinia Virus-Based Vaccines: Skin Scarification Promotes a Nonspecific Immune Response That Protects against Orthopoxvirus Disease. *Journal of Virology,* 88**,** 7753-7763.

RICE, P., MARTIN, E., HE, J., FRANK, M., DETOLLA, L., HESTER, L., O'NEILL, T., MANKA, C., BENJAMIN, I., NAGARSEKAR, A., SINGH, I. & HASDAY, J. D. 2005. Febrile-range hyperthermia augments neutrophil accumulation and enhances lung injury in experimental gram-negative bacterial pneumonia. *Journal of Immunology,* 174**,** 3676-3685.

RICHTER, D., MATUSCHKA, F. R., SPIELMAN, A. & MAHADEVAN, L. 2013. How ticks get under your skin: insertion mechanics of the feeding apparatus of Ixodes ricinus ticks. *Proceedings of the Royal Society B-Biological Sciences,* 280.

ROBERTS, K. L. & SMITH, G. L. 2008. Vaccinia virus morphogenesis and dissemination. *Trends in Microbiology,* 16**,** 472-479.

ROCHE, X., ROZSTALNYY, A., TAGOPACHECO, D., PITTIGLIO, C., KAMATA, A., BELTRAN ALCRUDO, D., BISHT, K., KARKI, S., KAYAMORI, J. & LARFAOUI, F. 2021. *Introduction and spread of*

lumpy skin disease in South, East and Southeast Asia: qualitative risk assessment and management, Food & Agriculture Org.
ROLAND, L., DRILLICH, M. & IWERSEN, M. 2014. Hematology as a diagnostic tool in bovine medicine. *Journal of Veterinary Diagnostic Investigation,* 26**,** 592-598.
ROMANO, P. R., ZHANG, F., TAN, S. L., GARCIA-BARRIO, M. T., KATZE, M. G., DEVER, T. E. & HINNEBUSCH, A. G. 1998. Inhibition of double-stranded RNA-dependent protein kinase PKR by vaccinia virus E3: Role of complex formation and the E3 N-terminal domain. *Molecular and Cellular Biology,* 18**,** 7304-7316.
SAMOJLOVIC, M., POLACEK, V., GURJANOV, V., LUPULOVIC, D., LAZIC, G., PETROVIC, T. & LAZIC, S. 2019. DETECTION OF ANTIBODIES AGAINST LUMPY SKIN DISEASE VIRUS BY VIRUS NEUTRALIZATION TEST AND ELISA METHODS. *Acta Veterinaria-Beograd,* 69**,** 47-60.
SANTOS, R. I., HERMANCE, M. E., REYNOLDS, E. S. & THANGAMANI, S. 2021. Salivary gland extract from the deer tick, Ixodes scapularis, facilitates neuroinvasion by Powassan virus in BALB/c mice. *Scientific Reports,* 11.
SANZ-BERNARDO, B., HAGA, I. R., WIJESIRIWARDANA, N., BASU, S., LARNER, W., DIAZ, A. V., LANGLANDS, Z., DENISON, E., STONER, J., WHITE, M., SANDERS, C., HAWES, P. C., WILSON, A. J., ATKINSON, J., BATTEN, C., ALPHEY, L., DARPEL, K. E., GUBBINS, S. & BEARD, P. M. 2021. Quantifying and Modeling the Acquisition and Retention of Lumpy Skin Disease Virus by Hematophagus Insects Reveals Clinically but Not Subclinically Affected Cattle Are Promoters of Viral Transmission and Key Targets for Control of Disease Outbreaks. *Journal of Virology,* 95.
SANZ-BERNARDO, B., HAGA, I. R., WIJESIRIWARDANA, N., HAWES, P. C., SIMPSON, J., MORRISON, L. R., MACINTYRE, N., BROCCHI, E., ATKINSON, J., HAEGEMAN, A., DE CLERCQ, K., DARPEL, K. E. & BEARD, P. M. 2020. Lumpy Skin Disease Is Characterized by Severe Multifocal Dermatitis With Necrotizing Fibrinoid Vasculitis Following Experimental Infection. *Veterinary Pathology,* 57**,** 388-396.
SANZ-BERNARDO, B., SUCKOO, R., HAGA, I. R., WIJESIRIWARDANA, N., HARVEY, A., BASU, S., LARNER, W., ROONEY, S., SY, V., LANGLANDS, Z., DENISON, E., SANDERS, C., ATKINSON, J., BATTEN, C., ALPHEY, L., DARPEL, K. E., GUBBINS, S. & BEARD, P. M. 2022. The Acquisition and Retention of Lumpy Skin Disease Virus by Blood-Feeding Insects Is Influenced by the Source of Virus, the Insect Body Part, and the Time since Feeding. *Journal of Virology,* 96.
SCAPLEHORN, N., HOLMSTROM, A., MOREAU, V., FRISCHKNECHT, F., RECKMANN, I. & WAY, M. 2002. Grb2 and Nck act cooperatively to promote actin-based motility of vaccinia virus. *Current Biology,* 12**,** 740-745.
SCHLEGER, A. V. & LINCOLN, D. T. 1976. BOOPHILUS-MICROPLUS - CHARACTERIZATION OF ENZYMES INTRODUCED INTO HOST. *Australian Journal of Biological Sciences,* 29**,** 487-497.
SCHMID, M. A., GLASNER, D. R., SHAH, S., MICHLMAYR, D., KRAMER, L. D. & HARRIS, E. 2016. Mosquito Saliva Increases Endothelial Permeability in the Skin, Immune Cell Migration, and Dengue Pathogenesis during Antibody-Dependent Enhancement. *Plos Pathogens,* 12.
SCHMIDT, F. I., BLECK, C. K. E., HELENIUS, A. & MERCER, J. 2011. Vaccinia extracellular virions enter cells by macropinocytosis and acid-activated membrane rupture. *Embo Journal,* 30**,** 3647-3661.
SCHNEIDER, B. S., SOONG, L., COFFEY, L. L., STEVENSON, H. L., MCGEE, C. E. & HIGGS, S. 2010. Aedes aegypti Saliva Alters Leukocyte Recruitment and Cytokine Signaling by Antigen-Presenting Cells during West Nile Virus Infection. *Plos One,* 5.
SCHNEIDER, B. S., SOONG, L., GIRARD, Y. A., CAMPBELL, G., MASON, P. & HIGGS, S. 2006. Potentiation of West Nile encephalitis by mosquito feeding. *Viral Immunology,* 19**,** 74-82.
SEVIK, M. & DOGAN, M. 2017. ` Epidemiological and Molecular Studies on Lumpy Skin Disease Outbreaks in Turkey during 2014-2015. *Transboundary and Emerging Diseases,* 64**,** 1268-1279.
SHAVA, S. & MASUKU, S. 2019. Living currency: The multiple roles of livestock in livelihood sustenance and exchange in the context of rural indigenous communities in southern Africa. *Southern African Journal of Environmental Education,* 35.

SHEVCHENKO, A., TOMAS, H., HAVLIS, J., OLSEN, J. V. & MANN, M. 2006. In-gel digestion for mass spectrometric characterization of proteins and proteomes. *Nature Protocols,* 1**,** 2856-2860.

SHI, J. S., AONO, S., LU, W. Y., OUELLETTE, A. J., HU, X. Y., JI, Y. B., WANG, L., LENZ, S., VAN GINKEL, F. W., LILES, M., DYKSTRA, C., MORRISON, E. E. & ELSON, C. O. 2007. A novel role for defensins in intestinal homeostasis: Regulation of IL-1 beta secretion. *Journal of Immunology,* 179**,** 1245-1253.

SHOWLER, A. T. & OSBRINK, W. L. 2015. Stable fly, Stomoxys calcitrans (L.), dispersal and governing factors. *International journal of insect science,* 7**,** IJIS. S21647.

SIGAL, L. J. 2016. The Pathogenesis and Immunobiology of Mousepox. *Advances in Immunology, Vol 129,* 129**,** 251-276.

SMITH, G. L. & LAW, M. 2004. The exit of Vaccinia virus from infected cells. *Virus Research,* 106**,** 189-197.

SMITH, G. L., VANDERPLASSCHEN, A. & LAW, M. 2002. The formation and function of extracellular enveloped vaccinia virus. *Journal of General Virology,* 83**,** 2915-2931.

SMITH, J., SONES, K., GRACE, D., MACMILLAN, S., TARAWALI, S. & HERRERO, M. 2013. Beyond milk, meat, and eggs: Role of livestock in food and nutrition security. *Animal Frontiers,* 3**,** 6-13.

SOHIER, C., HAEGEMAN, A., MOSTIN, L., DE LEEUW, I., VAN CAMPE, W., DE VLEESCHAUWER, A., TUPPURAINEN, E. S. M., VAN DEN BERG, T., DE REGGE, N. & DE CLERCQ, K. 2019. Experimental evidence of mechanical lumpy skin disease virus transmission by Stomoxys calcitrans biting flies and Haematopota spp. horseflies. *Scientific Reports,* 9**,** 10.

SPRYGIN, A., ARTYUCHOVA, E., BABIN, Y., PRUTNIKOV, P., KOSTROVA, E., BYADOVSKAYA, O. & KONONOV, A. 2018a. Epidemiological characterization of lumpy skin disease outbreaks in Russia in 2016. *Transboundary and Emerging Diseases,* 65**,** 1514-1521.

SPRYGIN, A., BABIN, Y., PESTOVA, Y., KONONOVA, S., WALLACE, D. B., VAN SCHALKWYK, A., BYADOVSKAYAL, O., DIEVL, V., LOZOVOYL, D. & KONONOV, A. 2018b. Analysis and insights into recombination signals in lumpy skin disease virus recovered in the field. *Plos One,* 13**,** 19.

STENN, K. S., LINK, R., MOELLMANN, G., MADRI, J. & KUKLINSKA, E. 1989. DISPASE, A NEUTRAL PROTEASE FROM BACILLUS-POLYMYXA, IS A POWERFUL FIBRONECTINASE AND TYPE-IV COLLAGENASE. *Journal of Investigative Dermatology,* 93**,** 287-290.

STYER, L. M., LIM, P. Y., LOUIE, K. L., ALBRIGHT, R. G., KRAMER, L. D. & BERNARD, K. A. 2011. Mosquito Saliva Causes Enhancement of West Nile Virus Infection in Mice. *Journal of Virology,* 85**,** 1517-1527.

SUN, P., NIE, K. X., ZHU, Y. B., LIU, Y., WU, P., LIU, Z. W., DU, S. Y., FAN, H. H., CHEN, C. H., ZHANG, R. L., WANG, P. H. & CHENG, G. 2020. A mosquito salivary protein promotes flavivirus transmission by activation of autophagy. *Nature Communications,* 11.

SWIST, S. L., WILKERSON, M. J., WYATT, C. R., BROCE, A. B. & KANOST, M. R. 2002. Modulation of bovine lymphocyte response by salivary gland extracts of the stable fly, Stomoxys calcitrans (Diptera : Muscidae). *Journal of Medical Entomology,* 39**,** 900-907.

TAICHMAN, L. B., REILLY, S. S. & LAPORTA, R. F. 1983. THE ROLE OF KERATINOCYTE DIFFERENTIATION IN THE EXPRESSION OF EPITHELIOTROPIC VIRUSES. *Journal of Investigative Dermatology,* 81**,** S137-S140.

TASIOUDI, K. E., ANTONIOU, S. E., ILIADOU, P., SACHPATZIDIS, A., PLEVRAKI, E., AGIANNIOTAKI, E. I., FOUKI, C., MANGANA-VOUGIOUKA, O., CHONDROKOUKI, E. & DILE, C. 2016. Emergence of Lumpy Skin Disease in Greece, 2015. *Transboundary and Emerging Diseases,* 63**,** 260-265.

TECLE, T., WHITE, M. R., GANTZ, D., CROUCH, E. C. & HARTSHORN, K. L. 2007. Human neutrophil defensins increase neutrophil uptake of influenza A virus and bacteria and modify virus-induced respiratory burst responses. *Journal of Immunology,* 178**,** 8046-8052.

THE WORLD BANK. 2020. *Ethiopia* [Online]. Available: https://data.worldbank.org/country/ethiopia [Accessed May 25, 2020].

THEODOS, C. M. & TITUS, R. G. 1993. SALIVARY-GLAND MATERIAL FROM THE SAND FLY LUTZOMYIA-LONGIPALPIS HAS AN INHIBITORY EFFECT ON MACROPHAGE FUNCTION IN-VITRO. *Parasite Immunology,* 15**,** 481-487.

THOMAS, A. N., RIAZANSKAIA, S., CHEUNG, W., XU, Y., GOODACRE, R., THOMAS, C. L. P., BAGUNEID, M. S. & BAYAT, A. 2010. Novel noninvasive identification of biomarkers by analytical profiling of chronic wounds using volatile organic compounds. *Wound Repair and Regeneration,* 18**,** 391-400.

TOLONEN, N., DOGLIO, L., SCHLEICH, S. & LOCKER, J. K. 2001. Vaccinia virus DNA replication occurs in endoplasmic reticulum-enclosed cytoplasmic mini-nuclei. *Molecular Biology of the Cell,* 12**,** 2031-2046.

TONA, G. O. 2021. Impact of Beef and Milk Sourced from Cattle Production on Global Food Security. *Bovine Science-Challenges and Advances.* IntechOpen.

TOULON, A., BRETON, L., TAYLOR, K. R., TENENHAUS, M., BHAVSAR, D., LANIGAN, C., RUDOLPH, R., JAMESON, J. & HAVRAN, W. L. 2009. A role for human skin-resident T cells in wound healing. *Journal of Experimental Medicine,* 206**,** 743-750.

TUFAIL, S., BADREALAM, K. F., SHERWANI, A., GUPTA, U. D. & OWAIS, M. 2013. Tissue specific heterogeneity in effector immune cell response. *Frontiers in Immunology,* 4.

TULMAN, E. R., AFONSO, C. L., LU, Z., ZSAK, L., KUTISH, G. F. & ROCK, D. L. 2001. Genome of lumpy skin disease virus. *Journal of Virology,* 75**,** 7122-7130.

TULMAN, E. R., AFONSO, C. L., LU, Z., ZSAK, L., SUR, J. H., SANDYBAEV, N. T., KEREMBEKOVA, U. Z., ZAITSEV, V. L., KUTISH, G. F. & ROCK, D. L. 2002. The genomes of sheeppox and goatpox viruses. *Journal of Virology,* 76**,** 6054-6061.

TUPPURAINEN, E., ALEXANDROV, T. & BELTRÁN-ALCRUDO, D. 2017. Lumpy skin disease field manual–A manual for veterinarians. FAO Animal Production and Health Manual No. 20 (pp. 1–60). Rome: Food and Agriculture Organization of the United Nations (FAO).

TUPPURAINEN, E. S. M., LUBINGA, J. C., STOLTSZ, W. H., TROSKIE, M., CARPENTER, S. T., COETZER, J. A. W., VENTER, E. H. & OURA, C. A. L. 2013. Mechanical transmission of lumpy skin disease virus by Rhipicephalus appendiculatus male ticks. *Epidemiology and Infection,* 141**,** 425-430.

VALENZUELA, J. G., PHAM, V. M., GARFIELD, M. K., FRANCISCHETTI, I. M. B. & RIBEIRO, J. M. C. 2002. Toward a description of the sialome of the adult female mosquito Aedes aegypti. *Insect Biochemistry and Molecular Biology,* 32**,** 1101-1122.

VAN EIJL, H., HOLLINSHEAD, M. & SMITH, G. L. 2000. The vaccinia virus A36R protein is a type Ib membrane protein present on intracellular but not extracellular enveloped virus particles. *Virology,* 271**,** 26-36.

VAN LINTHOUT, S., MITEVA, K. & TSCHOPE, C. 2014. Crosstalk between fibroblasts and inflammatory cells. *Cardiovascular Research,* 102**,** 258-269.

VANDENBUSSCHE, F., MATHIJS, E., PHILIPS, W., SADUAKASSOVA, M., DE LEEUW, I., SULTANOV, A., HAEGEMAN, A. & DE CLERCQ, K. 2022. Recombinant LSDV Strains in Asia: Vaccine Spillover or Natural Emergence? *Viruses-Basel,* 14.

VIDANOVIC, D., SEKLER, M., PETROVIC, T., DEBELJAK, Z., VASKOVIC, N., MATOVIC, K. & HOFFMANN, B. 2016. REAL-TIME PCR ASSAYS FOR THE SPECIFIC DETECTION OF FIELD BALKAN STRAINS OF LUMPY SKIN DISEASE VIRUS. *Acta Veterinaria-Beograd,* 66**,** 444-454.

VON BACKSTROM, U. 1945. NGAMILAND CATTLE DISEASE. PRELIMINARY REPORT ON A NEW DISEASE, THE ETIOLOGICAL AGENT BEING PROBABLY OF AN INFECTIOUS NATURE. *Journal of the South African Veterinary Medical Association***,** 29-35.

WAHIS. 2022. *https://wahis.woah.org/#/home* [Online]. WOAH. [Accessed Sept 2022 2022].

WAINWRIGHT, S., EL IDRISSI, A., MATTIOLI, R., TIBBO, M., NJEUMI, F. & RAIZMAN, E. 2013. Emergence of lumpy skin disease in the Eastern Mediterranean Basin countries. *FAO Empres Watch,* 29**,** 1-6.

WALSH, D. 2017. Poxviruses: Slipping and sliding through transcription and translation. *Plos Pathogens,* 13.

WANG, H. & NUTTALL, P. A. 1994. EXCRETION OF HOST IMMUNOGLOBULIN IN TICK SALIVA AND DETECTION OF IGG-BINDING PROTEINS IN TICK HEMOLYMPH AND SALIVARY-GLANDS. *Parasitology,* 109**,** 525-530.

WANG, X. Y., RIBEIRO, J. M. C., BROCE, A. B., WILKERSON, M. J. & KANOST, M. R. 2009. An insight into the transcriptome and proteome of the salivary gland of the stable fly, Stomoxys calcitrans. *Insect Biochemistry and Molecular Biology,* 39**,** 607-614.

WANG, Z. P., LAI, Y. P., BERNARD, J. J., MACLEOD, D. T., COGEN, A. L., MOSS, B. & DI NARDO, A. 2012. Skin Mast Cells Protect Mice against Vaccinia Virus by Triggering Mast Cell Receptor S1PR2 and Releasing Antimicrobial Peptides. *Journal of Immunology,* 188**,** 345-357.

WASSERMAN, H. A., SINGH, S. & CHAMPAGNE, D. E. 2004. Saliva of the Yellow Fever mosquito, Aedes aegypti, modulates murine lymphocyte function. *Parasite Immunology,* 26**,** 295-306.

WESTERA, L., DRYLEWICZ, J., DEN BRABER, I., MUGWAGWA, T., VAN DER MAAS, I., KWAST, L., VOLMAN, T., VAN DE WEG-SCHRIJVER, E. H. R., BARTHA, I., SPIERENBURG, G., GAISER, K., ACKERMANS, M. T., ASQUITH, B., DE BOER, R. J., TESSELAAR, K. & BORGHANS, J. A. M. 2013. Closing the gap between T-cell life span estimates from stable isotope-labeling studies in mice and humans. *Blood,* 122**,** 2205-2212.

WICHIT, S., DIOP, F., HAMEL, R., TALIGNANI, L., FERRARIS, P., CORNELIE, S., LIEGEOIS, F., THOMAS, F., YSSEL, H. & MISSE, D. 2017. Aedes Aegypti saliva enhances chikungunya virus replication in human skin fibroblasts via inhibition of the type I interferon signaling pathway. *Infection Genetics and Evolution,* 55**,** 68-70.

WOLFF, J., KRSTEVSKI, K., BEER, M. & HOFFMANN, B. 2020. Minimum Infective Dose of a Lumpy Skin Disease Virus Field Strain from North Macedonia. *Viruses-Basel,* 12.

WOLFF, J., MORITZ, T., SCHLOTTAU, K., HOFFMANN, D., BEER, M. & HOFFMANN, B. 2021. Development of a Safe and Highly Efficient Inactivated Vaccine Candidate against Lumpy Skin Disease Virus. *Vaccines,* 9.

WORLD TRADE ORGANISATION 2021. G/SPS/N/THA/370. *In:* MEASURES, C. O. S. A. P. (ed.) *Notification of Emergency Measures.*

XU, X. Q., YANG, H. L., MA, D. Y., WU, J., WANG, Y. P., SONG, Y. Z., WANG, X., LU, Y., YANG, J. X. & LAI, R. 2008. Toward an understanding of the molecular mechanism for successful blood feeding by coupling proteomics analysis with pharmacological testing of horsefly salivary glands. *Molecular & Cellular Proteomics,* 7**,** 582-590.

YAO, C., OH, J. H., LEE, D. H., BAE, J. S., JIN, C. L., PARK, C. H. & CHUNG, J. H. 2015. Toll-like receptor family members in skin fibroblasts are functional and have a higher expression compared to skin keratinocytes. *International Journal of Molecular Medicine,* 35**,** 1443-1450.

YEO, G., WANG, Y. F., CHONG, S. M., HUMAIDI, M., LIM, X. F., MAIEPESSOV, D., CHAN, S., HOW, C. B., LIN, Y. N., HUANGFU, T. Q., FERNANDEZ, C. J., HAPUARACHCHI, H. C. & YAP, G. 2019. Characterization of Fowlpox virus in chickens and bird-biting mosquitoes: a molecular approach to investigating Avipoxvirus transmission. *Journal of General Virology,* 100**,** 838-850.

YERUHAM, I., NIR, O., BRAVERMAN, Y., DAVIDSON, M., GRINSTEIN, H., HAYMOVITCH, M. & ZAMIR, O. 1995. SPREAD OF LUMPY SKIN-DISEASE IN ISRAELI DAIRY HERDS. *Veterinary Record,* 137**,** 91-93.

YOUNG-SPEIRS, M., DROUIN, D., CAVALCANTE, P. A., BARKEMA, H. W. & COBO, E. R. 2018. Host defense cathelicidins in cattle: types, production, bioactive functions and potential therapeutic and diagnostic applications. *International Journal of Antimicrobial Agents,* 51**,** 813-821.

ZHANG, Y. F. & MOSS, B. 1991. VACCINIA VIRUS MORPHOGENESIS IS INTERRUPTED WHEN EXPRESSION OF THE GENE ENCODING AN 11-KILODALTON PHOSPHORYLATED PROTEIN IS PREVENTED BY THE ESCHERICHIA-COLI LAC REPRESSOR. *Journal of Virology,* 65**,** 6101-6110.

ZUMPT, F. 1973. *The Stomoxyine biting flies of the world. Diptera: Muscidae. Taxonomy, biology, economic importance and control measures*.